

University of Dundee

DOCTOR OF PHILOSOPHY

Characterisation of transgenic mouse models of Alzheimer's disease

Graham, Lindsay

*Award date:*  
2011

*Awarding institution:*  
University of Dundee

[Link to publication](#)

**General rights**

Copyright and moral rights for the publications made accessible in the public portal are retained by the authors and/or other copyright owners and it is a condition of accessing publications that users recognise and abide by the legal requirements associated with these rights.

- Users may download and print one copy of any publication from the public portal for the purpose of private study or research.
- You may not further distribute the material or use it for any profit-making activity or commercial gain
- You may freely distribute the URL identifying the publication in the public portal

**Take down policy**

If you believe that this document breaches copyright please contact us providing details, and we will remove access to the work immediately and investigate your claim.

DOCTOR OF PHILOSOPHY

# Characterisation of transgenic mouse models of Alzheimer's disease

Lindsay Graham

2011

University of Dundee

## Conditions for Use and Duplication

Copyright of this work belongs to the author unless otherwise identified in the body of the thesis. It is permitted to use and duplicate this work only for personal and non-commercial research, study or criticism/review. You must obtain prior written consent from the author for any other use. Any quotation from this thesis must be acknowledged using the normal academic conventions. It is not permitted to supply the whole or part of this thesis to any other person or to post the same on any website or other online location without the prior written consent of the author. Contact the Discovery team ([discovery@dundee.ac.uk](mailto:discovery@dundee.ac.uk)) with any queries about the use or acknowledgement of this work.

**Characterisation of transgenic mouse  
models of Alzheimer's disease**

**by**

**Lindsay Graham**

**A thesis submitted to the University of Dundee for the  
degree of Doctor of Philosophy**

**August 2011**

# Contents

<b>Contents .....</b>	<b>ii</b>
<b>List of figures .....</b>	<b>viii</b>
<b>List of tables.....</b>	<b>xi</b>
<b>Acknowledgements.....</b>	<b>xii</b>
<b>Declarations .....</b>	<b>xiii</b>
<b>Abstract.....</b>	<b>xiv</b>
<b>List of abbreviations .....</b>	<b>xvi</b>
<b>Chapter 1: Introduction.....</b>	<b>19</b>
<b>1.1 Alzheimer’s disease .....</b>	<b>20</b>
1.1.1: Risk factors in AD .....	20
1.1.2: Genetic risk factors in AD .....	23
1.1.3: Diagnosis of AD .....	25
1.1.4: Treatment of AD .....	26
<b>1.2: Proteins involved in AD.....</b>	<b>27</b>
1.2.1: Amyloid precursor protein (APP).....	28
1.2.1.1: Physiological functions of APP.....	28
1.2.1.2: Cleavage of APP .....	29
1.2.1.3: Familial APP mutations .....	32
1.2.2: Tau .....	34
1.2.2.1: Phosphorylation of tau .....	34
1.2.2.2: Familial tau mutations.....	35
1.2.3: Presenilins .....	36
1.2.3.1: Familial presenilin mutations.....	37
<b>1.3: Molecular pathways of AD .....</b>	<b>38</b>
1.3.1: The amyloid cascade hypothesis.....	39
1.3.1.1: The role of oligomeric A $\beta$ .....	39
1.3.1.2: A $\beta$ and synaptic dysfunction.....	41
1.3.2: Neuronal dysfunction and death in AD.....	45
1.3.3: Protein kinases in AD .....	46
1.3.4: The role of tau .....	50
<b>1.4: Transgenic mouse models of AD .....</b>	<b>52</b>
1.4.1: Single transgenic models: APP .....	56
1.4.2: Single transgenic models: tau .....	59
1.4.3: Single transgenic models: presenilin.....	60
1.4.4: Double transgenic models.....	61
1.4.5: The triple transgenic (3xTg) mouse.....	67
1.4.5.1: Pathological features of the 3xTg mouse: amyloid pathology.....	67
1.4.5.2: Pathological features of the 3xTg mouse: tau pathology .....	67
1.4.5.3: Pathological features of the 3xTg mouse: other alterations .....	68

1.4.5.4: Behavioural phenotype of the 3xTg mouse.....	69
1.4.5.5: Cognitive testing of 3xTg mice.....	70
<b>1.5: The hippocampus.....</b>	<b>72</b>
1.5.1: Structure and anatomy of the hippocampus.....	72
1.5.2: Function of the human hippocampus.....	74
1.5.3: Synaptic plasticity in the hippocampus.....	77
1.5.3.1: Paired-pulse facilitation (PPF).....	77
1.5.3.2: Induction of LTP.....	78
1.5.3.3: Post-tetanic (PTP) and short-term (STP) potentiation.....	79
1.5.3.4: Early phase LTP (E-LTP).....	80
1.5.3.5: Postsynaptic expression mechanisms.....	82
1.5.3.6: Late phase LTP (L-LTP).....	83
1.5.3.7: LTP and memory.....	84
<b>1.6: Aims and objectives of this thesis.....</b>	<b>86</b>
1.6.1: Background.....	87
1.6.2: Aims.....	88
1.6.3: Summary.....	89
<b>Chapter 2: Materials and Methods.....</b>	<b>89</b>
<b>2.1: Materials.....</b>	<b>90</b>
2.1.1: Antibodies.....	90
2.1.2: Buffer composition.....	90
2.1.3: Chemicals.....	90
2.1.4: Transgenic mice.....	91
<b>2.2: Methods.....</b>	<b>93</b>
2.2.1: Electrophysiology methods.....	93
2.2.1.1: Hippocampal slice preparation.....	93
2.2.1.2: Extracellular recording.....	93
2.2.1.3: Measurement of the fEPSP.....	96
2.2.1.4: Input-output function.....	98
2.2.1.5: Paired-pulse facilitation.....	99
2.2.1.6: Stimulation protocols for the induction of LTP.....	99
2.2.1.7: Measurement of LTP.....	100
2.2.1.8: Statistics and analysis.....	101
2.2.2: Biochemical methods.....	104
2.2.2.1: Brain lysate preparation.....	104
2.2.2.2: Sodium dodecyl sulphate polyacrylamide gel electrophoresis.....	105
2.2.2.3: Western blotting.....	106
2.2.2.4: Densitometry and analysis.....	107
2.2.3: Behavioural methods.....	108
2.2.3.1: Rewarded alternation T-maze.....	108
2.2.3.2: Activity box.....	109
2.2.3.3: Statistical analysis.....	110

<b>Chapter 3: Electrophysiology .....</b>	<b>111</b>
<b>3.1: Introduction.....</b>	<b>112</b>
<b>3.2: Results .....</b>	<b>113</b>
3.2.1: Control data.....	114
3.2.2: Electrophysiological characterisation of 2 month old 3xTg mice .....	114
3.2.2.1: Input-output function.....	114
3.2.2.2: Paired-pulse facilitation.....	115
3.2.2.3: Long-term potentiation.....	116
3.2.2.4: Non-normalised long-term potentiation .....	117
3.2.2.4: Summary .....	118
3.2.3: Electrophysiological characterisation of 6 month old 3xTg mice .....	126
3.2.3.1: Input-output function.....	126
3.2.3.2: Paired-pulse facilitation.....	127
3.2.3.3: Long-term potentiation.....	128
3.2.3.4: Non-normalised long-term potentiation .....	129
3.2.3.5: Summary .....	130
3.2.4: Electrophysiological characterisation of 12 month old 3xTg mice .....	138
3.2.4.1: Input-output function.....	138
3.2.4.2: Paired-pulse facilitation.....	139
3.2.4.3: Long-term potentiation.....	140
3.2.4.4: Non-normalised long-term potentiation .....	141
3.2.4.5: Summary .....	142
3.2.5: Electrophysiological characterisation of 17 month old 3xTg mice .....	150
3.2.5.1: Input-output function.....	150
3.2.5.2: Paired-pulse facilitation.....	151
3.2.5.3: Long-term potentiation.....	151
3.2.5.4: Non-normalised long-term potentiation .....	153
3.2.5.5: Summary .....	153
3.2.6: Comparison of results obtained in 3xTg and control mice by age.....	159
3.2.6.1: Input-output function.....	159
3.2.6.2: Maximum fEPSP slope and amplitude.....	160
3.2.6.3: Paired-pulse facilitation.....	160
3.2.6.4: Long-term potentiation.....	161
3.2.6.5: Non-normalised long-term potentiation .....	162
3.2.6.6: Summary .....	163
3.2.7: Electrophysiological characterisation of 2 month old TASTPM mice .....	169
3.2.7.1: Input-output function.....	169
3.2.7.2: Paired-pulse facilitation.....	170
3.2.7.3: Long-term potentiation.....	170
3.2.7.4: Summary .....	171
3.2.8: Electrophysiological characterisation of 6 month old TASTPM mice .....	174
3.2.9: Treatment of 6 month TASTPM slices with kynurenic acid .....	177
3.2.9.1: Introduction .....	177
3.2.9.2: Methods .....	178
3.2.9.3: fEPSP measurements.....	179
3.2.9.4: Long-term potentiation.....	179
3.2.10: Treatment of 12 month 3xTg slices with kynurenic acid.....	183
3.2.10.1: fEPSP measurements.....	183

3.2.10.2: Input-output function.....	184
3.2.10.3: Paired-pulse facilitation.....	185
3.2.10.4: Long-term potentiation.....	185
3.2.10.5: Summary .....	186
<b>3.3: Discussion .....</b>	<b>192</b>
3.3.1: Technical aspects .....	192
3.3.2: Characterisation of the 3xTg mouse .....	194
3.3.2.1: Paired-pulse facilitation in the 3xTg model.....	194
3.3.2.2: Basal synaptic transmission in the 3xTg model.....	195
3.3.2.3: Long-term potentiation in the 3xTg model .....	197
3.3.2.4: Effects of the individual transgenes on synaptic plasticity .....	200
3.3.2.5: Calcium regulation in the 3xTg model.....	203
3.3.2.6: The network dysfunction hypothesis.....	205
3.3.2.7: Excitotoxicity and its mechanisms.....	207
3.3.2.8: Summary of electrophysiological findings in 3xTg mice .....	212
3.3.3: TASTPM mouse .....	213
3.3.2.1: Synaptic function in 2 month TASTPM mice.....	213
3.3.2.2: Synaptic function in 6 month TASTPM mice.....	214
3.3.3: Summary .....	216
<b>Chapter 4: Biochemistry .....</b>	<b>218</b>
<b>4.1: Introduction.....</b>	<b>219</b>
<b>4.2: Results .....</b>	<b>223</b>
4.2.1: Age dependent effects on cortical expression of AD-related proteins in 3xTg mice.....	223
4.2.1.1: APP.....	224
4.2.1.2: CRMP2 (total and phosphorylated).....	224
4.2.1.3: Tau (total and phosphorylated) .....	224
4.2.1.4: Other proteins .....	226
4.2.1.5: Summary .....	226
4.2.2: Analysis of cortical expression of AD-related proteins in aged 3xTg mice.....	233
4.2.2.1: APP.....	234
4.2.2.2: CRMP2 (total and phosphorylated).....	234
4.2.2.3: Tau (total and phosphorylated) .....	234
4.2.2.4: Other proteins .....	235
4.2.2.5: Summary .....	235
4.2.3: AD related protein expression and phosphorylation in different brain regions in 17 month mice .....	239
4.2.3.1: APP.....	240
4.2.3.2: CRMP2 (total and phosphorylated).....	240
4.2.3.3: Tau (total and phosphorylated) in 3xTg mice .....	241
4.2.3.4: Tau (total and phosphorylated) in control mice .....	241
4.2.3.5: Other proteins .....	242
4.2.3.6: Summary .....	242
4.2.4: Correlations between APP, tau and electrophysiology in 3xTg mice.....	247
4.2.5: Biochemical profiles in 2 month old TASTPM mice .....	249

4.2.5.1: Overview .....	249
4.2.5.2: APP.....	250
4.2.5.3: CRMP2 (total and phosphorylated).....	250
4.2.5.4: Tau (total and phosphorylated) .....	250
4.2.5.5: Other proteins .....	251
4.2.5.6: Summary .....	251
4.2.6: Biochemical profiles in 6 month old TASTPM mice .....	255
4.2.6.1: APP.....	255
4.2.6.2: CRMP2 (total and phosphorylated).....	255
4.2.6.3: Tau (total and phosphorylated) .....	256
4.2.6.4: Other proteins .....	256
4.2.6.5: Summary .....	256
4.2.7: AD related protein expression and phosphorylation in different brain regions of TASTPM mice .....	261
4.2.7.1: APP.....	261
4.2.7.2: CRMP2 (total and phosphorylated).....	261
4.2.7.3: Tau (total and phosphorylated) .....	262
4.2.7.4: Other proteins .....	262
4.2.7.5: Summary .....	263
4.2.8: Kynurenic acid treatment .....	267
<b>4.3: Discussion .....</b>	<b>269</b>
4.3.1: Technical aspects .....	269
4.3.2: Analysis of cortical expression of AD-related proteins in 3xTg mice.....	269
4.3.2.1: APP expression in 3xTg mice .....	270
4.3.2.2: Tau expression in 3xTg mice .....	272
4.3.2.3: Tau phosphorylation in 3xTg mice .....	274
4.3.2.4: CRMP2 phosphorylation in 3xTg mice .....	276
4.3.2.5: p35/p25 in 3xTg mice .....	277
4.3.2.6: Synaptophysin in 3xTg mice.....	278
4.3.2.7: Summary .....	279
4.3.3: AD related protein expression and phosphorylation in different brain regions of 3xTg .....	280
4.3.4: Correlations between biochemical changes and electrophysiology in 3xTg mice .....	283
4.3.5: Analysis of cortical expression of AD-related proteins in TASTPM mice .....	284
4.3.5.1: APP expression in TASTPM mice.....	285
4.3.5.2: Tau expression and phosphorylation in TASTPM mice .....	285
4.3.5.3: CRMP2 phosphorylation in TASTPM mice .....	287
4.3.5.4: p35/p25 in TASTPM mice .....	287
4.3.5.5: Synaptophysin in TASTPM mice .....	288
4.3.5.6: Summary .....	289
4.3.6: AD related protein expression and phosphorylation in different brain regions of TASTPM mice .....	290
4.3.7: Effects of kynurenic acid .....	290
4.3.7.1: Technical aspects.....	292

<b>Chapter 5: Behaviour .....</b>	<b>295</b>
<b>5.1: Introduction.....</b>	<b>296</b>
<b>5.2: Results .....</b>	<b>297</b>
5.2.1: Activity box in 6 month 3xTg males .....	297
5.2.1.1: Mobile counts .....	297
5.2.1.2: Total mobile time .....	298
5.2.1.3: Other measures .....	299
5.2.1.4: Summary .....	299
5.2.2: T-maze performance in 6 month 3xTg male mice.....	302
5.2.2.1: T-maze results (delay).....	302
5.2.2.2: Summary .....	303
<b>5.3: Discussion .....</b>	<b>306</b>
5.3.1: Activity box .....	306
5.3.2: T-maze performance .....	309
<b>Chapter 6: Conclusions and Perspectives.....</b>	<b>313</b>
6.1: Electrophysiology .....	316
6.2: Biochemistry .....	319
6.3: Behaviour .....	321
6.4: Final conclusions.....	322
<b>References .....</b>	<b>325</b>

## List of Figures

### Chapter 1: Introduction

1.1: Prevalence of dementia/ pathological features of AD .....	22
1.2: APP processing .....	31
1.3: Amino acid sequence of the A $\beta$ peptide .....	33
1.4: The amyloid cascade hypothesis.....	40
1.5: Protein kinases and phosphorylation in AD.....	48
1.6: Sagittal section of the rodent hippocampus .....	73
1.7: Mechanisms of LTP .....	81

### Chapter 2: Materials and Methods

2.1: Diagram of the electrophysiology setup .....	95
2.2: A field extracellular postsynaptic potential (fEPSP) .....	97
2.3: Long-term potentiation .....	103

### Chapter 3: Electrophysiology

3.1: Normalised input-output curves obtained from 2 month old male and female 3xTg and control mice. ....	119
3.2: Normalised and non-normalised input-output curves obtained from 2 month old 3xTg and control mice. ....	120
3.3: Paired-pulse facilitation determined in 2 month old male and female 3xTg and control mice.....	121
3.4: Paired-pulse facilitation determined in 2 month old 3xTg and control mice... ..	122
3.5: The influence of gender on long-term potentiation recorded from 2 month old 3xTg and control mice. ....	123
3.6: Long-term potentiation in 2 month old 3xTg and control mice.....	124
3.7: A comparison of long-term potentiation in 2 month old 3xTg and control mice (non-normalised).....	125
3.8: Normalised input-output curves obtained from 6 month old male and female 3xTg and control mice... ..	131
3.9: Normalised and non-normalised input-output curves obtained from 6 month old 3xTg and control mice... ..	132
3.10: Paired-pulse facilitation determined in 6 month old male and female 3xTg and control mice.....	133
3.11: Paired-pulse facilitation determined in 6 month old 3xTg and control mice. ....	134
3.12: The influence of gender on long-term potentiation recorded from 6 month old 3xTg and control mice.....	135
3.13: Long-term potentiation in 6 month old 3xTg mice and control.....	136
3.14: A comparison of long-term potentiation in 6 month old 3xTg and control mice (non-normalised). ....	137
3.15: Normalised input-output curves obtained from 12 month old male and female 3xTg and control mice. ....	143

3.16: Normalised and non-normalised input-output curves obtained from 12 month old 3xTg and control mice.....	144
3.17: Paired-pulse facilitation determined in 12 month old male and female 3xTg and control mice.....	145
3.18: Paired-pulse facilitation determined in 12 month old 3xTg and control mice. ....	146
3.19: The influence of gender on long-term potentiation recorded from 12 month old 3xTg mice and control mice.. ....	147
3.20: Long-term potentiation in 12 month old 3xTg mice and control.....	148
3.21: A comparison of long-term potentiation in 12 month old 3xTg and control mice (non-normalised) .....	149
3.22: Normalised and non-normalised input-output curves obtained from 17 month old 3xTg and control mice. ....	154
3.23: Paired-pulse facilitation determined for 17 month old 3xTg and control mice. ....	155
3.24: Normalised input-output curves obtained from 2 month old male and female 3xTg and control mice. ....	156
3.25: Long-term potentiation in 17 month old 3xTg and control mice.....	157
3.26: A comparison of long-term potentiation in 17 month old 3xTg and control mice (non-normalised) .....	158
3.27: Non-normalised input-output curve for slope obtained at all ages in 3xTg and control mice.....	164
3.28: Average maximum fEPSP slope in 3xTg and control at different ages.....	165
3.29: Paired-pulse facilitation determined at all ages in 3xTg and control mice	166
3.30: A comparison of normalised and non-normalised LTP in control mice from 2-17 months. ....	167
3.31: A comparison of normalised and non-normalised LTP in 3xTg mice from 2-17 months.....	168
3.32: Normalised and non-normalised input-output curves obtained from 2 month old TASTPM and control mice.....	172
3.33: Paired-pulse facilitation determined in 2 month old TASTPM and control mice.....	173
3.34: Long-term potentiation in 2 month TASTPM and control mice. ....	174
3.35: Long-term potentiation in 6 month TASTPM and control mice. ....	176
3.36: Maximum fEPSP amplitude and percentage of successful fEPSPs obtained from slices in 6 month old TASTPM mice treated with 1mM kynurenic acid. ....	181
3.37: Long term potentiation in 6 month TASTPM mice, with and without treatment with 1mM kynurenic acid, and control mice. ....	182
3.38: A comparison of fEPSP amplitude in 12 month 3xTg and control mice with and without treatment with 1mM kynurenic acid.....	187
3.39: Normalised and non-normalised input-output curves obtained from 12 month old male and female 3xTg and control mice treated with 1mM kynurenic acid. ....	188
3.40: Non-normalised input-output curves obtained from 12 month old male and female 3xTg and control mice treated with 1mM kynurenic acid.....	189
3.41: Paired-pulse facilitation determined in 12 month 3xTg and control treated with 1mM kynurenic acid. ....	190
3.42: Long term potentiation in 12 month 3xTg and control with and without 1mM kynurenic acid. ....	191

## Chapter 4: Biochemistry

4.1: Synaptic and biochemical alterations in mouse models of AD. ....	222
4.2: APP, total and phosphorylated CRMP2 in 2 and 12 month male 3xTg and control mice. ....	227
4.3: APP, total and phosphorylated CRMP2 in 2 and 12 month female 3xTg and control mice. ....	228
4.4: Total and phosphorylated tau in 2 and 12 month male 3xTg and control mice. ....	229
4.5: Total and phosphorylated tau in 2 and 12 month female 3xTg and control mice. ....	230
4.6: Synaptophysin, p35 and p25 in 2 and 12 month male 3xTg and control mice. ....	231
4.7: Synaptophysin, p35 and p25 in 2 and 12 month female 3xTg and control mice. ....	232
4.8: APP, total and phosphorylated CRMP2 in 17 month 3xTg and control mice. ....	236
4.9: Total and phosphorylated tau in 17 month 3xTg and control mice. ....	237
4.10: Synaptophysin, p35 and p25 in 17 month 3xTg and control mice. ....	238
4.11: APP, total and phosphorylated CRMP2 in 17 month 3xTg hippocampus, cortex and cerebellum. ....	243
4.12: Total and phosphorylated tau in 17 month 3xTg hippocampus, cortex and cerebellum. ....	244
4.13: Total and phosphorylated tau in 17 month control hippocampus, cortex and cerebellum. ....	245
4.14: Synaptophysin, p35 and p25 in 17 month 3xTg hippocampus, cortex and cerebellum. ....	246
4.15: Biochemical and electrophysiological measurements in individual 3xTg mice. ....	248
4.16: APP, total and phosphorylated CRMP2 in 2 month TASTPM male and female mice. ....	252
4.17: Total and phosphorylated tau in 2 month TASTPM male and female mice. ....	253
4.18: Synaptophysin, p35 and p25 in 2 month TASTPM male and female mice. ....	254
4.19: APP, total and phosphorylated CRMP2 in 6 month TASTPM male and female mice. ....	258
4.20: Total and phosphorylated tau in 6 month TASTPM male and female mice. ....	259
4.21: Synaptophysin, p35 and p25 in 6 month TASTPM male and female mice. ....	260
4.22: APP, total and phosphorylated CRMP2 in 6 month TASTPM hippocampus, cortex and cerebellum. ....	264
4.23: Total and phosphorylated tau in 6 month TASTPM hippocampus, cortex and cerebellum. ....	265
4.24: Synaptophysin, p35 and p25 in 6 month TASTPM hippocampus, cortex and cerebellum. ....	266
4.25: Kynurenic acid treatment of slices from 12 month old 3xTg and control mice. ....	268

## **Chapter 5: Behaviour**

5.1: Fast and slow mobile counts measured in the activity box.....	300
5.2: Total mobile counts measured in the activity box. ....	301
5.3: Percentage of correct entries in 3xTg and control. ....	304
5.4: Mean percentage of correct entries for all trials .....	305

## **List of Tables**

### **Chapter 1: Introduction**

1.1: Genetic risk factors for AD.....	24
1.2: Selected single transgenic mouse models of AD.....	56
1.3: Selected double/triple transgenic mouse models of AD.....	62

### **Chapter 2: Materials and Methods**

2.1.1: Antibodies .....	90
2.1.2: Buffer composition .....	90
2.1.3: Chemicals.....	91

### **Chapter 3: Electrophysiology**

3.1: Technical variables in hippocampal slice recordings .....	193
--	-----

### **Chapter 6: Conclusions and perspectives**

6.1: Summary of main findings in 3xTg mice.....	314
6.2: Summary of main findings in TASTPM mice.....	315

## Acknowledgements

Firstly, I would like to thank my supervisors David Balfour, Delia Belelli, Jeremy Lambert and Calum Sutherland for their guidance and advice throughout the time of my PhD studies. Thanks in particular go to my principal supervisor Calum for his invaluable feedback during the writing of this thesis.

Special thanks to Lori-An Etherington, for teaching me the electrophysiology techniques with unending patience and good humour, and to Ritchie Williamson for sharing his knowledge and troubleshooting advice for my biochemistry experiments. Alison McNeilly also provided useful advice during the behavioural work.

Thanks to my Mum whose job at the University of Edinburgh proved incredibly useful for extending my access to scientific journals required for this thesis. I am very grateful for the time you spent finding those papers!

All my friends in the Lambert, Sutherland and Ashford labs, thank you for being a great bunch of people and making every day in the lab enjoyable. Particular thanks go to my movie night buddies Amy and Fiona – we finished the list! Everyone in the Neurosciences corridor – it's been a privilege working with you all.

Jane, thank you for your wonderful meals and the many hours of horse riding we have shared. Sky – you give me freedom. Teddy – we're going on an adventure!

I would like to dedicate this thesis to my parents for their unconditional love and support. You have given me the strength to achieve my goals.

## **Declarations**

I hereby declare that the following thesis is based on the results of investigations conducted by myself and that this thesis is of my own composition. Work other than my own is stated with reference to the researcher or their publications. This body of work has not previously been presented for a higher degree.

Lindsay Graham

I certify that Lindsay Graham has spent the equivalent of nine terms in research work in the Biomedical Research Institute, University of Dundee. She has fulfilled the conditions of the Ordinance General No. 14 of the University of Dundee and is qualified to submit this thesis in application for the degree of Doctor of Philosophy.

Dr. Calum Sutherland

## Abstract

A number of transgenic mouse models have been developed to study the molecular and pathological alterations associated with Alzheimer's disease (AD). The 3xTg mouse is widely used as a research tool and carries mutations in the amyloid precursor protein (Swedish APP<sub>K670N/M671L</sub>), presenilin 1 (PS1<sub>M146V</sub>) and tau (Tau<sub>P301L</sub>) which results in the development of pathological features similar to the plaques and tangles observed in human AD. The TASTPM mouse carries both the APP<sub>K670N/M671L</sub> and PS1<sub>M146V</sub> mutations but does not possess a tau transgene, so develops only plaque-like structures in the brain.

This thesis aims to systematically characterise biochemical, electrophysiological and behavioural changes present in the 3xTg and TASTPM mouse models of AD. The widely studied amyloid cascade hypothesis proposes that the generation of A $\beta$  through abnormal APP processing is a key initiating process in AD, and so molecular or electrophysiological changes which are observed in both models could represent a common pathway of disease development. In addition, comparison between the two models could help to elucidate the role of the tau transgene in early phenotypic changes.

The studies of hippocampal electrophysiology presented in this thesis show that the marked deficits in long-term potentiation (LTP) originally reported at the age of 6 months (Oddo *et al.*, 2003) are not present in our colony of 3xTg mice. In support of this, although these mice do overexpress APP and tau the expected hyperphosphorylation of tau is not observed even at the advanced ages of 12-17 months. This suggests that some of the processes associated with the development

of pathological features are occurring more slowly in our colony. In addition, studies using a T-maze paradigm in 6 month 3xTg mice suggest that major cognitive deficits are not present at this age. This suggests that drift of the phenotype has occurred in the 3xTg mouse and has implications for further studies using this model.

The 3xTg mouse does, however, present a deficit in basal synaptic transmission which is progressive with increasing age from 6-17 months. Similarly, hippocampal synaptic function is normal in TASTPM mice studied at 2 months, when no biochemical changes are present, but is markedly reduced at the age of 6 months when it proved difficult to make any electrophysiological recordings. The data in this thesis shows that treatment with 1mM kynurenic acid during the slicing process markedly improved baseline synaptic transmission to the level observed in control mice. This shows that kynurenic acid can improve the viability of the slices, and as the compound is a glutamate receptor antagonist, suggests that reduction of glutamate-induced excitotoxicity during the slicing process results in its neuroprotective effects. This data suggests that alterations common to the 3xTg and TASTPM models, and therefore due to the presence of the APP or PS1 transgenes, may result in an increased susceptibility of hippocampal neurons to cellular stressors such as excitotoxicity.

To summarise, this thesis presents data which characterises in detail aspects of the electrophysiological, biochemical and behavioural phenotype of the 3xTg and TASTPM mouse models of AD, with the aim of observing early changes which may be associated with the mechanisms of AD development.

## List of abbreviations

3xTg	triple transgenic mouse (APP <sub>Swe</sub> , PS1 <sub>M146V</sub> , tau <sub>P301L</sub> )
3R	3 repeat
4R	4 repeat
A $\beta$	$\beta$ -amyloid peptide
ACh	acetylcholine
AChE	acetylcholinesterase
aCSF	artificial cerebrospinal fluid
AD	Alzheimer's disease
AICD	APP intracellular domain
AMPA	$\alpha$ -amino-3-hydroxy-5-methyl-4-isoxazole propionic acid
ANOVA	analysis of variance
ApoE	apolipoprotein E
APP	amyloid precursor protein
APP <sub>Swe</sub>	APP with the 'Swedish' K670N, M671L double mutation
Ca <sup>2+</sup>	calcium
CA1	cornu ammonis 1
CA3	cornu ammonis 3
CaMKII	Ca <sup>2+</sup> /calmodulin-dependent protein kinase II
Cdk5	cyclin-dependent kinase 5
CICR	calcium-induced calcium release
CREB	cAMP response element binding protein

CRMP2	collapsin response mediator protein 2
DG	dentate gyrus
DTT	dithiothreitol
EAAT	excitatory amino acid transporter
EC	entorhinal cortex
ECL	enhanced chemiluminescence
E-LTP	early long-term potentiation
EPSC	excitatory postsynaptic current
ER	endoplasmic reticulum
fEPSP	field excitatory postsynaptic potential
FTDP-17	frontotemporal dementia and parkinsonism linked to chromosome 17
GABA	$\gamma$ -aminobutyric acid
GSK3	glycogen synthase kinase 3
HFS	high-frequency stimulation
IPSC	inhibitory postsynaptic current
HRP	horseradish peroxidase
L-LTP	late long-term potentiation
LDS	lithium dodecyl sulphate
LTD	long-term depression
LTP	long-term potentiation
MAPK	mitogen-activated protein kinase
MWM	Morris water maze
NMDA	<i>N</i> -methyl-D-aspartate

PAGE	polyacrylamide gel electrophoresis
PDGF- $\beta$	platelet-derived growth factor $\beta$
PI3K	phosphoinositide 3-kinase
PKA	protein kinase A
PKB	protein kinase B
PKC	protein kinase C
PPF	paired-pulse facilitation
PrP	prion protein
PS1	presenilin 1
PS2	presenilin 2
PTP	post-tetanic potentiation
RIPA buffer	radioimmunoprecipitation buffer
ROS	reactive oxygen species
RyR	ryanodine receptor
SDS	sodium dodecyl sulphate
SOD	superoxide dismutase
STP	short-term potentiation
TASTPM	<b>Thy-1 APP<sub>695</sub> Swedish</b> (K670N, M671L) <b>Thy-1 PS1</b> (M146V)
TBOA	DL-threo- $\beta$ -benzyloxyaspartic acid
TBS	theta-burst stimulation
TBS-T	tris buffered saline with Tween

# **Chapter 1**

## **Introduction**

## **1.1 Alzheimer's disease**

Alzheimer's disease (AD) is a progressive form of dementia which is becoming increasingly common in today's aging population. Dementia is classed as an impairment of memory, particularly in the learning of new information. It may also include other cognitive symptoms such as deterioration in judgement, planning, and information processing of a severity that causes impairment in daily living. In addition, dementia often causes alterations in emotional behaviour, such as apathy or emotional lability, or difficulties with social functioning (ICD-10, World Health Organisation). Dementia progresses over a number of years from mild memory loss to a condition where the individual affected is completely reliant on others for their care.

In the UK, 820 000 individuals suffer from dementia with the cost to the economy reaching £23 billion per year. The majority of dementia sufferers (61%) are 80 years or older, but 8% of sufferers are under 65 years of age. There is currently no conclusive test for AD: a definitive diagnosis can only be obtained post mortem so the exact number of sufferers of the condition is unknown. However, it is the most common form of dementia, making up 50-60% of all cases (Dementia 2010, Alzheimer's Research Trust).

### **1.1.1: Risk factors in AD**

The majority of cases of AD are sporadic and occur in individuals without a family history of the disease. The causes of AD are currently unknown and it can be considered a multifactorial condition. However, a number of non-genetic risk

factors are associated with the development of AD. Clearly, the most important is age, as the prevalence of AD increases exponentially from the age of 65 onwards (Fig. 1.1A). This suggests that mechanisms occur within the ageing brain which make it more susceptible to neurodegeneration. However, due to the difficulties of studying the intact human brain, the effects of ageing are not well understood although they are hypothesised to include alterations in gene transcription, neurotransmitter release and neuronal plasticity, with a reduction in brain weight and loss of grey matter associated with increasing age (Good *et al.*, 2001). However, the age-dependent mechanisms which promote the increased formation and aggregation of proteins such as A $\beta$  or tau are not currently well understood.

There are many lifestyle and environmental factors which have been associated with AD risk but scientific studies into many of these factors have given mixed and often inconclusive results. One of the most significant correlations is with education, as individuals with a low education level are at increased risk of developing AD; it is suggested that mentally stimulating activities have a preventative effect (Gatz *et al.*, 2007). Another major risk factor is previous neuronal damage due to traumatic head injury; this has been shown to result in a transient increase in brain amyloid levels and may have long-term effects (Hartman *et al.*, 2002). Cardiovascular risk factors, such as hyperlipidaemia, hypercholesterolaemia, high blood pressure and smoking markedly increase the risk of vascular forms of dementia such as multi-infarct dementia. However, there is evidence to suggest these factors may also be associated with AD (Altman and Rutledge, 2010), and other medical conditions such as hyperinsulinaemia and type II diabetes also increase the risk of AD (Cole *et al.*, 2007a).

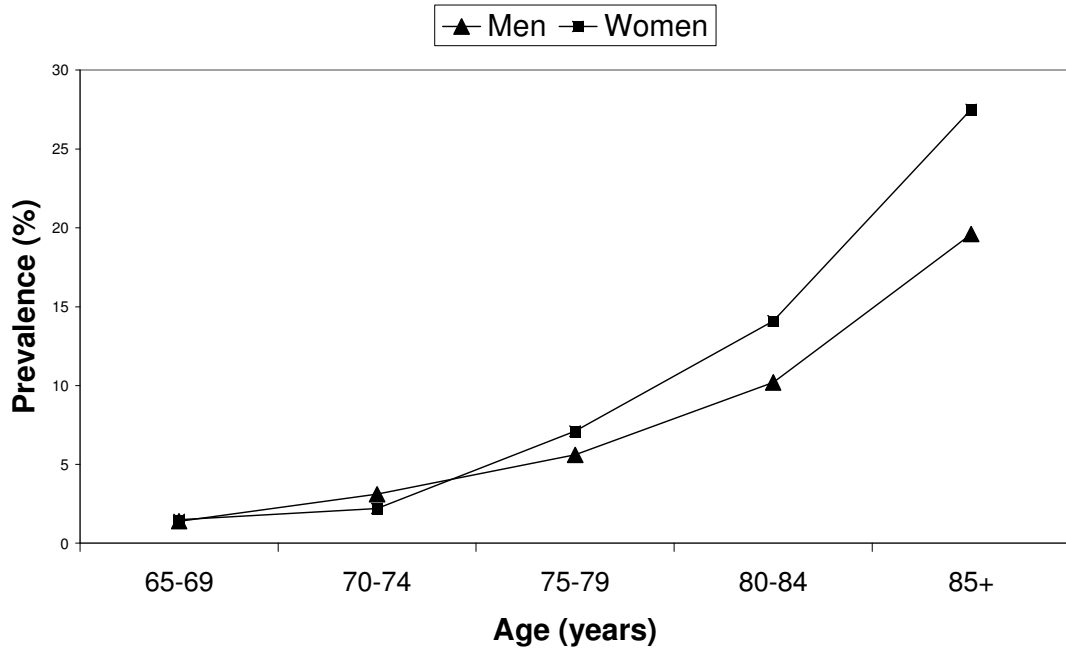


**Figure 1.1A: Prevalence of dementia by age and gender.** Data from the MRC CFAS study of England and Wales (1998).

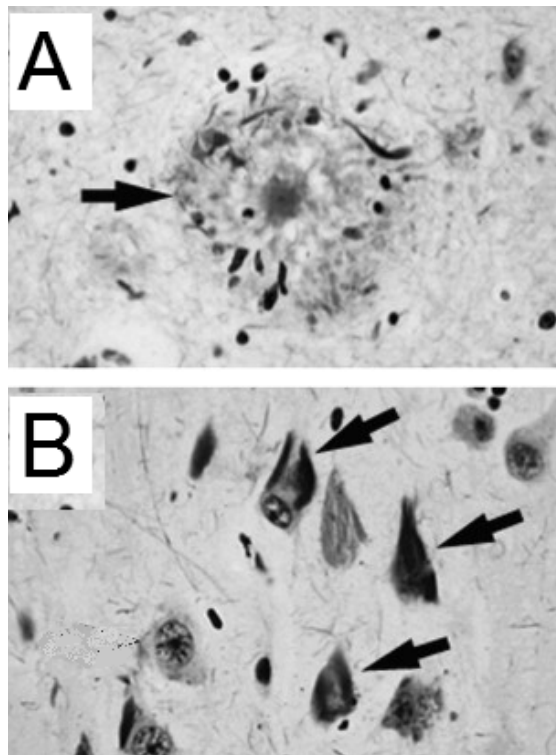


**Figure 1.1B: Pathological features of AD.** Amyloid plaque (A, black arrow) and neurofibrillary tangles (B, black arrows) in human brain tissue visualised with silver staining. Image from Gorrie *et al.* 2007.

Finally, multiple other variables such as diet, exercise, and psychological factors such as stress and depression may also influence susceptibility. It is likely that a number of diverse and overlapping genetic, biological and environmental factors play a role in the likelihood of an individual developing AD in later life.

### **1.1.2: Genetic risk factors in AD**

The second greatest risk factor for AD, following age, is the apolipoprotein E (ApoE) genotype carried by an individual. ApoE can bind to A $\beta$  to regulate its clearance and degradation (Jiang *et al.*, 2008). The protein has three alleles,  $\epsilon$ 2,  $\epsilon$ 3 and  $\epsilon$ 4; carriers of the ApoE  $\epsilon$ 4 allele have an increased probability of developing AD with a lower age of onset (Corder *et al.*, 1993).

A number of other genes have been implicated in susceptibility to AD using genome-wide association studies and are shown in Table 1.1. The most frequently observed associations are with the CLU and PICALM genes, encoding clusterin/apolipoprotein J protein and phosphatidylinositol-binding clathrin assembly protein respectively. Clusterin is a protein upregulated in states of cellular stress and is involved in pro- and anti-apoptotic events and protein clearance, while PICALM is involved in clathrin-mediated endocytosis (Harold *et al.*, 2009). Other genes implicated in AD can be broadly divided into proteins mediating synaptic vesicle fusion or protein endocytosis, and those involved in immune responses or the breakdown and clearance of cellular products. This suggests that mechanisms which are not yet fully understood such as cellular protein trafficking may have an important role in the pathogenesis of AD.

**Table 1.1: Genetic risk factors for AD**

<i>Gene</i>	<i>Protein</i>	<i>Odds ratio</i>	<i>Function</i>	<i>Reference</i>
ApoE	Apolipoprotein E ( $\epsilon$ 4 allele)	4.1	Lipoprotein and cholesterol transport, enhances proteolytic breakdown of A $\beta$ peptide	Bertram <i>et al.</i> 2007
CLU	Clusterin/ apolipoprotein J	0.86	Regulates apoptotic mechanisms, involved in the clearance of cellular proteins including A $\beta$ peptide	Harold <i>et al.</i> 2009
PICALM	Phosphatidylinositol-binding clathrin assembly protein	0.85	Involved in clathrin-mediated endocytosis. Directs the trafficking of synaptic vesicle fusion proteins	Harold <i>et al.</i> 2009
CR1	Complement receptor 1	1.21	Processing and clearance of immune complexes	Lambert <i>et al.</i> 2009
BIN1	Bridging integrator 1	1.18	Involved in synaptic vesicle endocytosis	Hollingworth <i>et al.</i> 2011
EPHA1	Epherin receptor A1	0.85	Influences cell morphology and motility	Naj <i>et al.</i> 2011
CD33	Myeloid cell surface antigen CD33	0.88	Involved in immune responses, mediates endocytosis through a clathrin-independent mechanism	Naj <i>et al.</i> 2011
CD2AP	CD2-associated protein	1.14	Scaffold adaptor protein	Naj <i>et al.</i> 2011
ABCA7	ATP-binding cassette, subfamily A, member 7	1.22	Involved in lipid transport across membranes, regulates APP processing, modulates phagocytosis of apoptotic cells	Hollingworth <i>et al.</i> 2011

A small proportion of cases of AD are familial with a clear monogenetic link, however these affect only an estimated 1% of sufferers. The majority of these cases result from genetic mutations (discussed in section 1.2) which cause an early-onset form of the disease, affecting individuals in their 60s and younger. The most common cause of familial AD are mutations in the presenilin genes, primarily PS1, with over 170 different mutations recorded to date and new mutations still being discovered (Antonell *et al.*, 2011). In addition, over 20 mutations have been reported in the APP gene (Basun *et al.*, 2008). Tau mutations are not associated with AD but with other neurodegenerative conditions such as frontotemporal dementia (Hutton *et al.*, 1998). It is these familial genetic mutations that have been used to generate transgenic animal models which develop features of AD.

### **1.1.3: Diagnosis of AD**

AD is usually diagnosed based on a detailed clinical history and the presence of memory impairment in structured tests. Neuronal loss is a prominent feature of the disease with an average loss of 8% of total brain weight (Terry *et al.*, 1981) and cortical atrophy is often observable on a brain scan. However, a definitive diagnosis of AD can only be obtained post mortem, and relies on the presence of two main pathological features within the brain: the extracellular deposition of amyloid plaques, and intraneuronal neurofibrillary tangles (Fig. 1.1B). Neurofibrillary tangles are a feature of other forms of dementia, such as frontotemporal dementia, but plaques are only found in AD. However, the presence of some plaques and tangles is common in the brain of cognitively normal individuals (Fukumoto *et al.*, 1996). Variation between pathological

features in individuals with AD is often apparent, with amyloid plaques being diffuse or focal and tangles present in the cell body, axon or dendrites. These may be present in cortical regions as well as subcortical areas such as the hippocampus and can be graded according to severity (Braak and Braak, 1991). The progression of tangle pathology is used as the grading scale for post-mortem analysis of AD brain tissue, and this follows severity of clinical symptoms more closely than plaque deposition.

#### **1.1.4: Treatment of AD**

The current treatments available for AD are able to slow the progression of the disease in some cases but do not cure or reverse it. Two types of medication are currently available: acetylcholinesterase (AChE) inhibitors (donepezil, galantamine, rivastigmine) and memantine, a glutamate receptor antagonist.

In AD, one of the earliest pathological events is a loss of cholinergic basal forebrain neurons and a reduction in cortical acetylcholine (ACh) (Perez *et al.*, 2007). AChE inhibitors such as donepezil prevent the breakdown of ACh by these enzymes, leading to an increased level of the neurotransmitter within the synaptic cleft. This may result in an improvement of some of the cognitive symptoms and behavioural alterations associated with AD, such as apathy and attention, which involve cortical circuits (Rockwood *et al.*, 2004).

Memantine is a NMDA receptor channel blocker which is used therapeutically to prevent glutamate-induced neuronal death. It has been shown to act preferentially at extrasynaptic NMDA receptors (Bordji *et al.*, 2010), which are activated by synaptic glutamate spillover and play a role in excitotoxicity (Frasca *et al.*, 2011).

In addition, the modulation of glutamatergic synaptic transmission may have an important role in memory processes. Treatment with memantine, as well as prolonging neuronal survival, may therefore also enhance cognitive function in AD.

Unfortunately, despite a number of new treatments aimed at preventing or disrupting amyloid pathology showing potential in animal models none of these have translated into clinical progress. An initial trial of anti-A $\beta$  immunisation, which stimulated plaque clearance and improved cognitive function in mice (Schenk *et al.*, 1999), was halted due to the development of meningoencephalitis in several patients (Vellas *et al.*, 2009). Work continues into the development of other A $\beta$  peptide vaccines along with novel strategies such as  $\gamma$ -secretase inhibition (Basi *et al.*, 2010), although the first phase III trial of a  $\gamma$ -secretase inhibitor was recently halted with the finding that it *worsened* the symptoms of AD (Eli Lilly, press release, August 2010). It is clear that a better understanding of the initiation and progression of AD is needed to allow future treatments to be developed against novel drug targets.

## **1.2: Proteins involved in AD**

Analysis of the familial forms of AD has identified several proteins crucial to the disease process, with the most important being amyloid precursor protein (APP), presenilin 1 (PS1) and tau. APP is cleaved to form a small peptide, A $\beta$ , which forms the amyloid plaques characteristic of the disease. Also mutated in some cases of familial AD are the presenilins, a component of the  $\gamma$ -secretase complex

involved in the processing of APP. Tau is the major protein constituent of neurofibrillary tangles and its abnormal aggregation is crucial for tangle generation. Mutated and overexpressed forms of these three proteins have been used to develop the majority of mouse models for the study of AD. The role of these proteins in normal function and the effects of their mutation are discussed below.

### **1.2.1: Amyloid precursor protein (APP)**

Amyloid precursor protein (APP) is a type I transmembrane protein with an intracellular cytoplasmic C-terminal, an extracellular N-terminal and a single alpha-helical transmembrane domain. The gene for APP is located on chromosome 21 and contains 19 exons, with alternative splicing creating three major human isoforms of APP of 695, 751 and 770 amino acids; the isoform of 695 amino acids is the most abundant in neuronal tissue (Konig *et al.*, 1992).

#### **1.2.1.1: Physiological functions of APP**

The normal cellular function of APP is not clear, although there is most evidence for its role as a trophic factor as APP has been shown to stimulate neural outgrowth (Qiu *et al.*, 1995). APP knockout mice show reactive gliosis and locomotor deficits (Zheng *et al.*, 1995), along with abnormal neuronal morphology, impairments in long-term potentiation (LTP) and cognitive deficits (Seabrook *et al.*, 1999, Dawson *et al.*, 1999). There is evidence to suggest APP may have a role as a modulator of synaptic function through Ca<sup>2+</sup> channel regulation and alterations in GABAergic short term plasticity (Yang *et al.*, 2009),

or by the promotion of NMDA receptor activity (Hoe *et al.*, 2009). APP possesses a heparin binding domain which allows binding to proteoglycans in the extracellular matrix (Small *et al.*, 1994). Consistent with this finding, it has been suggested that APP may act as a synaptic adhesion molecule through studies of the mouse neuromuscular junction (Wang *et al.*, 2009) and also mediate cell-cell and cell-surface adhesion (Breen *et al.*, 1991).

#### **1.2.1.2: Cleavage of APP**

APP undergoes a two-step process known as regulated intramembrane proteolysis, with an extracellular N-terminal cleavage step followed by cleavage within the transmembrane domain of the protein and the release of an intracellular C-terminal fragment. APP can be cleaved through one of two pathways: the amyloidogenic and non-amyloidogenic pathways (Fig. 1.2). Although it is thought that the non-amyloidogenic pathway is regulated in part by protein kinase C (PKC) (Hung *et al.*, 1993), the reason for the cellular choice between the two pathways is not fully understood. In familial AD, increased levels of the peptide A $\beta$  are caused by a shift to processing through the amyloidogenic pathway.

The initial enzymatic processing step, which determines the final cleavage products, is mediated by  $\alpha$  or  $\beta$ -secretase and releases the majority of the N-terminal domain. This produces either the soluble APP- $\alpha$  or  $\beta$  protein fragments, and leaves the C-terminal domain attached to the membrane, either as the  $\alpha$  (C83) C-terminal fragment (if cleaved by  $\alpha$ -secretase) or  $\beta$  (C99) C-terminal fragment (if cleaved by  $\beta$ -secretase). The  $\alpha$ -secretase zinc metalloproteinase enzymes

mediate the non-amyloidogenic pathway by cleavage within the A $\beta$  sequence, preventing the generation of A $\beta$  (Allinson *et al.*, 2003). Processing by the aspartic-acid protease  $\beta$ -secretase (BACE1) generates the longer N-terminal extension of A $\beta$  within the  $\beta$  C-terminal fragment and thus mediates the amyloidogenic pathway.

The second enzymatic processing step involves the cleavage of either the  $\alpha$  or  $\beta$  C-terminal fragment by an enzyme complex known as  $\gamma$ -secretase. This complex consists of four proteins: presenilin, nicastrin, APH-1 (anterior pharynx defective-1) and PEN2 (presenilin enhancer 2). The catalytic subunit is the presenilin protein, which can be either the PS1 or PS2 isoform (DeStrooper *et al.*, 1995, Francis *et al.*, 2002). Cleavage of the  $\alpha$  C-terminal fragment results in the generation of the cytoplasmic APP intracellular domain (AICD) and a small peptide known as p3, while cleavage of the  $\beta$  C-terminal fragment results in the generation of AICD and A $\beta$ . Dependent on the cleavage site several forms of A $\beta$  can be generated, ranging from 39-43 amino acids in length. Although the 40 amino acid (A $\beta_{40}$ ) is the most commonly produced form of the peptide, the 42 amino acid (A $\beta_{42}$ ) is thought to be the more 'toxic' form of A $\beta$ ; it has a tendency to aggregate more readily than A $\beta_{40}$  and is the predominant form deposited in human amyloid plaques (Gravina *et al.*, 1995). The role of A $\beta$  in the pathogenesis of AD is discussed in more detail in section **1.3**.

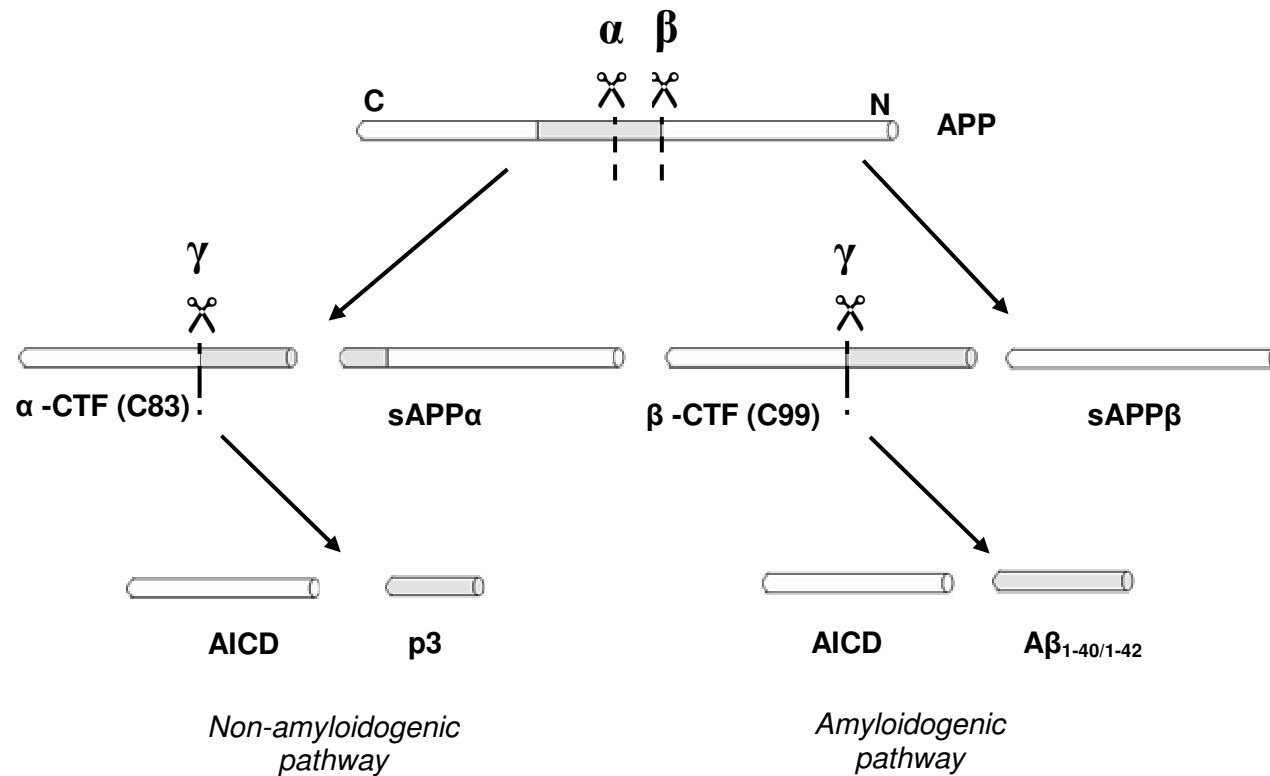


**Figure 1.2: APP processing.** APP can be cleaved by  $\alpha$ -secretase to progress down the non-amyloidogenic pathway or by  $\beta$ -secretase in the amyloidogenic pathway. Processing of APP by  $\alpha$ -secretase results in the generation of the  $\alpha$ -CTF and sAPP $\alpha$ , with further processing by  $\gamma$ -secretase generating AICD and a small fragment p3. Processing of APP by  $\beta$ -secretase results in the generation of the  $\beta$ -CTF and sAPP $\beta$ , while further processing by  $\gamma$ -secretase generates AICD and the A $\beta$  peptide. The most common forms of A $\beta$  are 40 and 42 amino acids in length, with the 42 amino acid form most prone to aggregation.

Abbreviations: APP (amyloid precursor protein),  $\alpha$ -CTF (alpha C-terminal fragment), sAPP $\alpha$  (soluble APP alpha), sAPP $\beta$  (soluble APP beta) AICD (APP intracellular domain), A $\beta$  (beta amyloid).

### 1.2.1.3: Familial APP mutations

There are around 20 known APP mutations, each named after the country (or region) in which they were discovered (Fig. 1.3). For example, the K670N/M671L mutation was first observed in two large Swedish families with early-onset AD (Mullan *et al.*, 1992), while the Indiana mutation (V717F) was observed in an American family with markedly early-onset AD beginning in the mid to late- thirties (Murrell *et al.*, 2000). The common feature of all APP mutations is that they increase brain levels of the A $\beta$ <sub>42</sub> form of the peptide, either through an overall increase in A $\beta$  production or an alteration in the ratio of A $\beta$ <sub>40</sub> to A $\beta$ <sub>42</sub> generated. For example, the Swedish mutation lies within the N-terminal sequence of A $\beta$  (Fig. 1.3) and results in an alteration of the cellular location of  $\beta$ -secretase cleavage, putting it in direct competition with  $\alpha$ -secretase and resulting in a three to six-time increased production of A $\beta$  (Haass *et al.*, 1995). Multiple mutations are also clustered round the C-terminal  $\gamma$ -secretase site (e.g. Florida, London, Indiana), where they result in a selective increase of A $\beta$ <sub>42</sub> generation (De *et al.*, 2001). Finally, several mutations near the  $\alpha$ -secretase site (Dutch, Flemish, Arctic) result in the generation of forms of A $\beta$  which show an enhanced propensity to form fibrils and a resistance to proteolytic degradation (Walsh *et al.*, 2001, Tsubuki *et al.*, 2003).



#### Selected familial APP mutations

K670N + M671L	Swedish
A673T	
H677R	
D678N	Tottori
A692G	Flemish
E693Q / E693G	Dutch / Arctic
D694N	Iowa
A713T	
T714I / T714A	Austrian / Iranian
V715A / V715M	German / French
I716V	Florida
V717I / V717F	London / Indiana
T719P	

**Figure 1.3: Amino acid sequence of the Aβ<sub>42</sub> peptide.** Residues mutated in familial AD are shown in bold. The majority of familial AD mutations, shown in the table on the left, are clustered around the two terminals of the protein at the β- and γ-secretase cleavage sites. Some mutations also occur at the α-secretase cleavage site. These mutations all increase the levels of Aβ generated within the neuron.

## 1.2.2: Tau

Tau is a microtubule-stabilising protein generated from the MAPT (microtubule-associated protein tau) gene present on chromosome 17. In humans, there are six tau isoforms generated by alternative splicing of this gene. At the N-terminus, zero, one or two 28 amino-acid inserts can be present through the alternative splicing of exons 2 and 3, while at the C-terminus, three or four 31-35 amino-acid microtubule-binding inserts can be present, giving rise to 3R (3 repeat) or 4R tau (4 repeat) tau. Functionally, the ability of 4R tau to stabilise and prevent microtubule shortening is greater than 3R tau due to the presence of the additional insert (Panda *et al.*, 2003). There are species-dependent differences in isoform expression, as adult humans express approximately equal ratios of 3R and 4R tau (Takuma *et al.*, 2003), while adult mice and rats express only the three 4R forms (Kampers *et al.*, 1999).

Although it would be expected that tau is critical for neuronal function, tau knockout mice are viable and show only minor changes in neuronal maturation and outgrowth in culture (Dawson *et al.*, 2001). This suggests that compensatory mechanisms such as the expression of other microtubule-associated proteins (MAP1/MAP2) can maintain microtubule function in the absence of tau.

### 1.2.2.1: Phosphorylation of tau

The primary role of tau is to bind and stabilise tubulin within microtubules and help maintain cellular structure and axonal transport. The phosphorylation of tau is an important mechanism to regulate this interaction with microtubules, with its

biological activity dependent on the degree of phosphorylation. There are over 40 different phosphorylation sites on tau, with multiple sites in the microtubule-binding domains. These are a mixture of serine, threonine and tyrosine residues which can be phosphorylated by a number of kinases, including glycogen synthase kinase 3 (GSK3), cyclin-dependent kinase 5 (Cdk5), protein kinase A (PKA) and casein kinase 1 (CK1) (Hanger *et al.*, 2009a). The regulation of tau phosphorylation is a complex process and the role of individual phosphorylation sites on tau function is not fully established.

Tau can be transiently hyperphosphorylated in a number of states such as hypothermia (Planel *et al.*, 2007). However, long-term hyperphosphorylation of tau at a number of sites is a characteristic feature of AD and a subset of diseases known as tauopathies (Grundke-Iqbal *et al.*, 1986). This hyperphosphorylation results in the disruption of microtubule function and the formation of insoluble tau aggregates, resulting in the characteristic tangle pathology observed in AD. This is discussed further in section **1.3.4**.

#### **1.2.2.2: Familial tau mutations**

There are around 25 mutations which have been discovered in the tau protein. However, these are not associated with AD but with a rare form of dementia, frontotemporal dementia with parkinsonism linked to chromosome 17 (FTDP-17). Individuals with FTDP-17 show behavioural and personality changes, with symptoms of dementia and motor difficulties such as frequent falls, bradykinesia and rigidity (Wszolek *et al.*, 2006). Pathologically, this is accompanied by

progressive cortical atrophy and the presence of tau-positive inclusions containing both 3R and 4R tau (Cairns *et al.*, 2007).

Familial tau mutations consist of missense, silent or deletion mutations in the coding region of the gene, with several intronic mutations also discovered (Spillantini and Goedert, 2000). All tau mutations are autosomal dominant, and it has been suggested that this is due to the production of tau with altered conformational states and a tendency for hyperphosphorylation which can sequester normal tau into fibrils, causing a toxic gain of function (Alonso *et al.*, 2004). The coding region mutations generally result in a reduced ability of tau to bind to and stabilise microtubules, or the generation of forms of tau with an increased propensity to form fibrils. Several coding region mutations and all those observed in the intron region of the gene influence alternative splicing, resulting in the overproduction of 4R tau and an alteration of the 3R:4R ratio. As 4R tau has an enhanced ability to bind to microtubules, it displaces the 3R tau, resulting in an alteration of microtubule binding kinetics and the formation of fibrillar tau aggregates (Lu and Kosik, 2001).

### **1.2.3: Presenilins**

The presenilin proteins, presenilin 1 (PS1) and presenilin 2 (PS2), are encoded by the PSEN1 and PSEN2 genes present on chromosome 14. They are the main catalytic component of the  $\gamma$ -secretase enzyme complex which is involved in the second enzymatic cleavage step of APP, resulting in the generation of A $\beta$  (see section 1.2.1.2). PS1 and PS2 show a high degree of structural similarity (~65%), with both proteins highly expressed in the neuronal population (Lee *et al.*, 1996).

Although widely known for its role in APP processing, the  $\gamma$ -secretase complex has a number of type I membrane protein substrates, including the Notch receptor (De *et al.*, 1999). Notch is a protein which is critical for the control of cellular differentiation during embryonic development, (Ables *et al.*, 2011) and likely due to disruption of this signalling pathway PS1 knockout mice die shortly after birth with a phenotype of marked skeletal deformities, cerebral haemorrhage and neuronal loss (Shen *et al.*, 1997). In contrast, PS2 knockout mice are viable and show only mild pulmonary haemorrhage and fibrosis with age, suggesting that its role in development can be compensated for by PS1 (Herreman *et al.*, 1999). However, mice in which PS1 knockout is conditionally restricted to postnatal cortex show reduced A $\beta$  accumulation and mild impairments of spatial memory (Yu *et al.*, 2001). In addition to its role in APP processing, PS1 has been suggested to be involved in the regulation of intracellular Ca<sup>2+</sup> homeostasis and synaptic plasticity (discussed in detail in Chapter 3).

### **1.2.3.1: Familial presenilin mutations**

The majority of known familial AD mutations are associated with presenilin function. Over 170 mutations in PS1 and over 10 mutations in PS2 have been reported which are all autosomal dominant. In general, PS1 mutations result in an earlier age of onset and more rapid disease progression than PS2 mutations (Bertram and Tanzi, 2004). PS1 is an eight-pass transmembrane protein, and the majority of mutations are clustered within the transmembrane domain, although some are also observed in the cytoplasmic or extracellular regions. Almost all of these are single amino acid point mutations, suggesting that minor sequence

changes within the structure of the protein may have a major effect on its function.

The majority of known PS1 mutations result in an overall increase in A $\beta$ <sub>42</sub> generation through an influence on  $\gamma$ -secretase cleavage of the  $\beta$  C-terminal fragment. As different mutations widely spread throughout the protein can cause a similar phenotype it has been suggested that these result in similar conformational changes. Several mutations result in alterations in the distance between the N and C-termini in the tertiary structure of the protein, which may alter interactions with APP and favour generation of the A $\beta$ <sub>42</sub> peptide (Berezovska et al., 2005). Some PS1 mutations also cause a concomitant reduction in A $\beta$ <sub>40</sub> levels, which is not simply a result of a shift in substrate preference but rather appears to be a distinct inhibition of A $\beta$ <sub>40</sub> generation (Shen and Kelleher, III, 2007). However, the precise effect of PS1 mutations on  $\gamma$ -secretase activity is not currently fully understood. PS2 mutations have been shown to alter the ratio of A $\beta$ <sub>40</sub>/ A $\beta$ <sub>42</sub> in a similar manner to PS1. Familial PS2 mutations must result in a dramatic alteration of PS2 function to produce an observable effect, due to the predominant role of PS1 in A $\beta$  generation (Walker et al., 2005).

### **1.3: Molecular pathways of AD**

AD is a complex disorder and all of the molecular mechanisms which lead to disease progression are not yet fully understood. The predominant hypothesis in the field is the 'amyloid cascade hypothesis' in which elevated levels of A $\beta$  form soluble aggregates followed by insoluble plaques. This leads to synaptic

dysfunction and eventually neurodegeneration through a number of downstream mechanisms such as inflammation and oxidative damage (Fig 1.4). AD is also characterised by the activation of a number of protein kinases which result in hyperphosphorylation of cellular proteins such as tau, leading to the generation of neurofibrillary tangles. An overview of the main events involved in AD pathogenesis is given in the following sections.

### **1.3.1: The amyloid cascade hypothesis**

This hypothesis proposes that the primary event in the progression of AD is the deposition of A $\beta$ , with tau phosphorylation and neuronal death occurring subsequent to this event (Hardy and Allsop, 1991). Evidence for the amyloid cascade hypothesis comes from the numerous familial mutations in APP and PS1/PS2 which increase A $\beta$  generation and subsequently lead to AD (see section 1.2.1, 1.2.3), while animal models have been generated which overexpress A $\beta$  and subsequently develop memory deficits (see section 1.4.1).

However, the initiating event in sporadic forms of AD is not yet known. It has been suggested that a failure of A $\beta$  clearance mechanisms may result in a gradually increasing concentration of the peptide in the brain until it reaches a level at which it becomes harmful to neuronal function (Mawuenyega et al., 2010). Alternatively, an increase in  $\beta$ -secretase activity is associated with ageing, and so changes in the function of this enzyme could enhance A $\beta$  formation (Cole and Vassar, 2007).

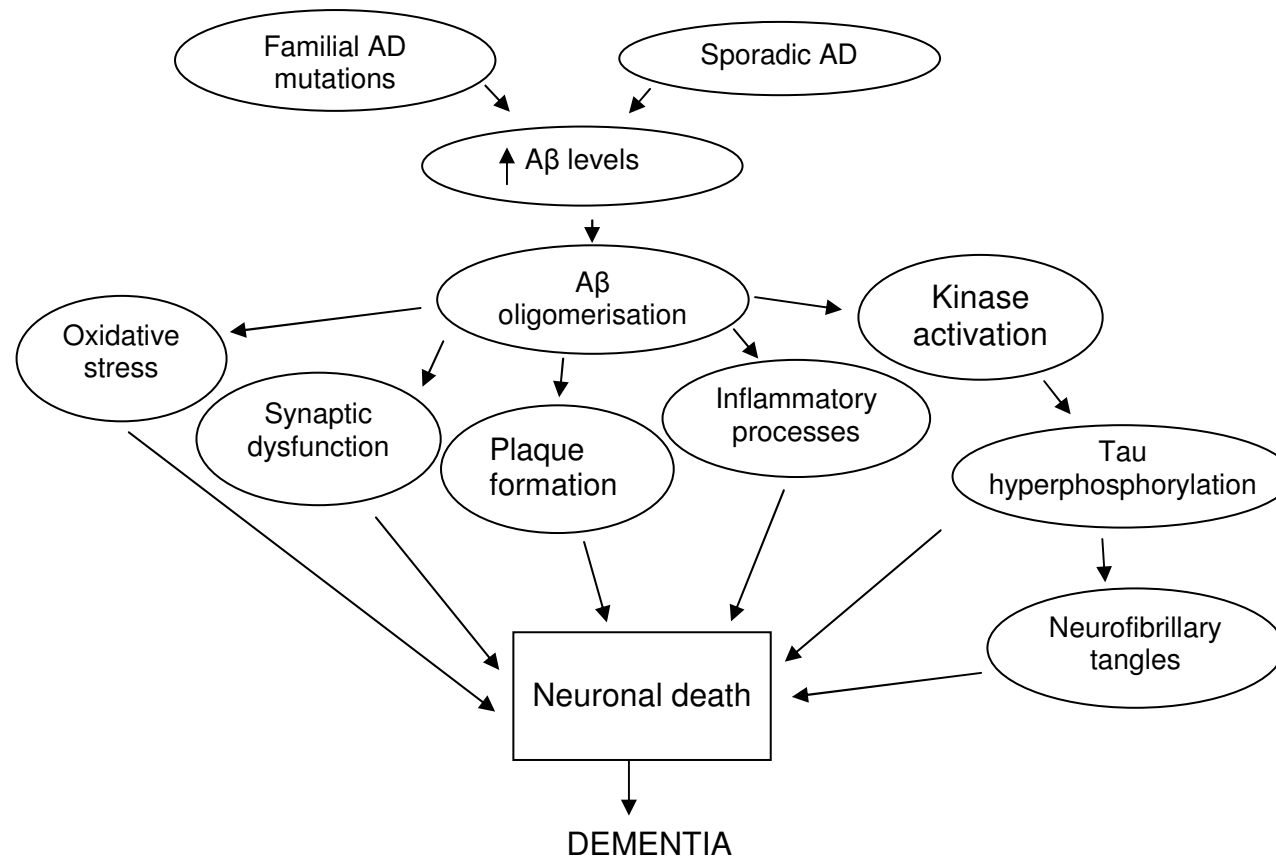


**Figure 1.4: The amyloid cascade hypothesis.** Increased levels of the peptide A $\beta$ , in particular A $\beta_{42}$ , occur both in sporadic and familial forms of AD. This leads to oligomerisation and aggregation of A $\beta$  and subsequent amyloid plaque formation. A number of harmful downstream effects include synaptic dysfunction and loss, the initiation of inflammatory processes and oxidative damage. In addition, hyperphosphorylation of tau results in its aggregation and the formation of neurofibrillary tangles. A combination of these factors leads to eventual neuronal death which is a contributing factor to dementia. (Modified from Hardy and Allsop, 1991).

### 1.3.1.1: The role of oligomeric A $\beta$

There is ongoing debate about the form of A $\beta$  responsible for its toxic downstream events. Initially, it was proposed that insoluble plaques were the main cause of toxicity but this idea has fallen out of favour as plaque load has been shown to correlate poorly with dementia (Giannakopoulos et al., 2003). Attention has therefore turned to the role of intraneuronal, oligomeric forms of A $\beta$  as the toxic moiety.

Treatment with oligomeric and fibrillar forms of A $\beta$  causes toxicity in neuronal culture (Deshpande et al., 2006) and significantly inhibits the magnitude of long-term potentiation (LTP) in hippocampal slice preparation (Townsend et al., 2006). The field is complicated in this respect by the wide variety of oligomeric preparations of A $\beta$  which have been used, including A $\beta$ -derived diffusible ligands (ADDLs), dimers/trimers and protofibrils. However, it has been suggested that all these forms share conformational similarities which may result in a common mechanism of toxicity (Glabe and Kaye, 2006). In addition, a number of transgenic mouse models exhibit deficits in memory and reduction in LTP well before the development of plaques (see section 1.4). This suggests a role for oligomeric A $\beta$  in the production of early cognitive deficits. The exact conformation of these oligomers is unknown, but in the Tg2576 model a 56 kDa soluble protein known as A $\beta$ \*56 has been suggested to impair memory function independent of the generation of amyloid plaques (Lesne *et al.*, 2006).

### **1.3.2: Early events in AD progression**

There are a number of findings which are associated with the early stages of AD in human studies and mouse models. One of the major features thought to contribute to the early cognitive deficits in AD is synaptic loss and alterations in neuronal synaptic transmission. Other changes observed include mitochondrial dysfunction, which contributes to metabolic abnormalities and enhanced oxidative stress, and the initiation of low-grade inflammatory processes.

#### **1.3.2.1: A $\beta$ and synaptic dysfunction**

It is thought that many of the early symptoms in AD may result not from overt neuronal death but by more subtle effects of A $\beta$  on synaptic transmission and function. Again, a large body of evidence comes from APP transgenic mice which show alterations in synaptic plasticity and basal synaptic transmission, suggesting that this may be an important mediator of cognitive deficits in models of AD. In hippocampal slices from APP<sub>Swe</sub> mice the processing and secretion of A $\beta$  is activity-dependent with the secreted A $\beta$  acting to depress excitatory synaptic transmission through an NMDA receptor-dependent mechanism (Kamenetz et al., 2003). In support of this, A $\beta$  has been shown to regulate NMDA receptor surface expression (Snyder et al., 2005). This suggests that there may be a feedback loop between the processing of neuronal A $\beta$  and hippocampal excitatory transmission. Hippocampal slice studies have shown that the exogenous application of A $\beta$  oligomers results in an impairment of not only LTP but also forms of long-term depression (LTD) (Li et al., 2009) which may occur through activation of mitogen-activated protein kinase (MAPK) resulting in

AMPA receptor phosphorylation and endocytosis (Hsieh et al., 2006). Alteration of different forms of synaptic plasticity through regulation of receptor expression may underlie the effects of A $\beta$  on excitatory neuronal transmission.

Synaptic loss is a common feature of AD and synaptic density within the brain may correlate with the severity of cognitive symptoms (Scheff et al., 2006). A $\beta$  has been shown to cause a loss of dendritic spines and reduction in synaptic number in both slice preparations (Wei et al., 2010) and transgenic mouse models (Bittner et al., 2010). This is thought to occur through an NMDA receptor and Ca<sup>2+</sup>-mediated pathway in a mechanism similar to that involved in the induction of LTD (Shankar et al., 2007). It is likely that a reduction in synapse number in AD within regions of the brain such as the hippocampus is associated with memory deficits, particularly in the early stages of the disease. Therefore, A $\beta$  can affect multiple synaptic mechanisms resulting in a reduction of excitatory transmission and structural alterations such as a loss of spine density.

### **1.3.2.2: Glucose hypometabolism**

Metabolic dysfunction is associated with the early stages of AD, and this has been shown in a number of studies in which glucose uptake is regionally reduced, particularly in cortical areas, in AD patients (Foster *et al.*, 1984). This glucose hypometabolism has marked effects on brain function, as the brain relies on glucose as its primary energy source and utilises 20% of the body's total supply (Murray *et al.*, 2011). It has been suggested that this feature occurs prior to disease onset in high-risk individuals such as those with mild cognitive

impairment (MCI) which may progress to AD, and presymptomatic individuals with familial AD mutations (Mosconi *et al.*, 2008), and that it may be prognostic of further cognitive decline (Silverman *et al.*, 2001). The major determinant of glucose utilisation in the brain is synaptic function, and so it has been suggested that synaptic loss, combined with alterations in cerebral blood flow and glucose transport, may underlie the observed hypometabolism (Pierr *et al.*, 1996).

### **1.3.2.3: Oxidative stress**

The major risk factors for AD include increasing age, cardiovascular disease and diabetes, and these are all associated with elevated reactive oxygen species (ROS), oxidative and inflammatory stress.

One hypothesis is that the endogenous systems for protection against ROS and oxidative stress are somehow compromised or insufficient in early AD. In support of this, an increased level of lipid peroxidation, a marker of oxidative stress, has been observed in human AD brain (Pratico 2008), while key anti-oxidant enzymes such as glutathione peroxidase and superoxide dismutase (SOD) are depleted in animal models of AD (Resende *et al.*, 2008). Reduction of manganese SOD enhances the pathological phenotype of an APP transgenic mouse model (Li *et al.*, 2004), which strongly supports the notion that impairment of anti-oxidant defence systems enhances AD pathology. In addition, a mouse has been generated with reduced levels of nitric oxide (NO) due to the knockout of nitric oxide synthase 2 (NOS2), with the expression of the Swedish mutant form of APP ( $APP_{swe}/NOS2^{-/-}$ ). Nitric oxide is a molecule which is involved in neuroinflammation and is also an effective antioxidant. The double

transgenic  $APP_{swe}/NOS2^{-/-}$  mouse exhibits more severe amyloid and tau pathology compared to the single  $APP_{swe}$  model and has evidence of neuronal loss and behavioural deficits characteristic of AD (Colton *et al.*, 2008).

There is also evidence for mitochondrial dysfunction in AD, which can lead to oxidative stress.  $A\beta$  can enter mitochondria to cause deficits in mitochondrial respiration and energy production, and the generation of harmful ROS (Pagani and Eckert, 2011). It has been shown that increased ROS production can enhance APP processing,  $A\beta$  levels and tau phosphorylation. These data suggest that the oxidant or anti-/pro-inflammatory balance in the brain modifies AD-like pathology.

### **1.3.3: Neuronal death in AD**

In more advanced cases of AD marked neuronal loss is observed in regions of the hippocampus and cortex. This feature is not observed in transgenic mouse models of the disease and it is unclear why the human brain is particularly vulnerable to age-related neuronal death. This is thought to occur primarily through activation of apoptotic pathways and the continued contribution of oxidative stress, mitochondrial dysfunction and inflammatory processes.

$A\beta$  has been shown to interact, either directly or indirectly, with a number of cellular signalling proteins. These include components of the apoptotic signalling pathway, such as activation of c-Jun N-terminal kinase (JNK) which results in downregulation of anti-apoptotic proteins (Yao *et al.*, 2005a), and the activation of calpain and caspase-3 through an increase in intracellular  $Ca^{2+}$  concentration (Kuwako *et al.*, 2002).

Also important in the progression of AD are inflammatory processes, with elevated levels of astrocytes and microglia associated with areas of plaque deposition. Activation of microglia results in the clearance of A $\beta$  deposits, but with the simultaneous release of ROS and proinflammatory mediators such as cytokines, chemokines and complement factors (Heneka et al., 2010). This perpetuates a cycle resulting in the promotion of further inflammation and ultimately leading to cell death.

The relative contribution of each of these complex factors in the promotion of neuronal apoptosis is not currently known. Therefore, it is likely that a number of overlapping and interacting factors, each increasing susceptibility to apoptosis, are involved in the mechanisms of neuronal cell loss in AD.

#### **1.3.4: Protein kinases in AD**

Another feature of AD is an alteration of protein kinase activity. A $\beta$  causes the aberrant activation of neuronal signalling pathways, which leads to the dysregulation of kinase activity and altered phosphorylation of downstream target proteins. For example, an increase in phosphorylation of the microtubule associated protein tau is a characteristic feature of AD which is discussed in section **1.2.2.1**. Studies have implicated a number of kinases including glycogen synthase kinase 3 (GSK3), cyclin-dependent kinase 5 (Cdk5) and MAPK in the pathogenesis of AD.

The serine-threonine kinase GSK3 is thought to contribute to A $\beta$ -induced neurotoxicity and is one of the major contributors to tau hyperphosphorylation in AD. Studies of GSK3 levels in human AD have given mixed results, with some

reporting an increase in GSK3 activity and some no change, likely due to the technical difficulties of measuring enzyme activity in post mortem brain tissue (Hooper *et al.*, 2008). In cell models, the activity of GSK3 is increased by A $\beta$ , contributing to neurotoxicity (Koh *et al.*, 2008), and in turn GSK3 facilitates the processing of A $\beta$  peptides (Phiel *et al.*, 2003). Further evidence for the role of GSK3 comes from transgenic mouse models where conditional overexpression results in hyperphosphorylation of tau and neuronal death (Lucas *et al.*, 2001). Currently, interest is growing in the use of GSK3 inhibitors such as lithium and more selective synthetic compounds as treatments for AD, as GSK3 inhibition in transgenic mouse models reduces tau phosphorylation and appears to be neuroprotective (Noble *et al.*, 2005).

In addition to its role in the hyperphosphorylation of tau, GSK3 is involved in the phosphorylation of other cellular proteins. For example, phosphorylation of the GSK3 target collapsin response mediator protein 2 (CRMP2) has been observed in transgenic models of AD and may be one of the early biochemical changes associated with the disease (Cole *et al.*, 2007b). This protein plays a role in neuronal polarity and axon guidance and promotes the association of tubulin into microtubule filaments (Soutar *et al.*, 2009). Therefore, hyperphosphorylation of CRMP2 could alter its functional properties and contribute to neurodegeneration.

Other kinases such as Cdk5 have been suggested to play a role in AD-associated neurodegeneration. For example, an increased level of the Cdk5 cofactor protein p25 has been reported in AD brain tissue, which results in the prolonged activation and altered cellular localisation of Cdk5 (Tseng *et al.*, 2002).

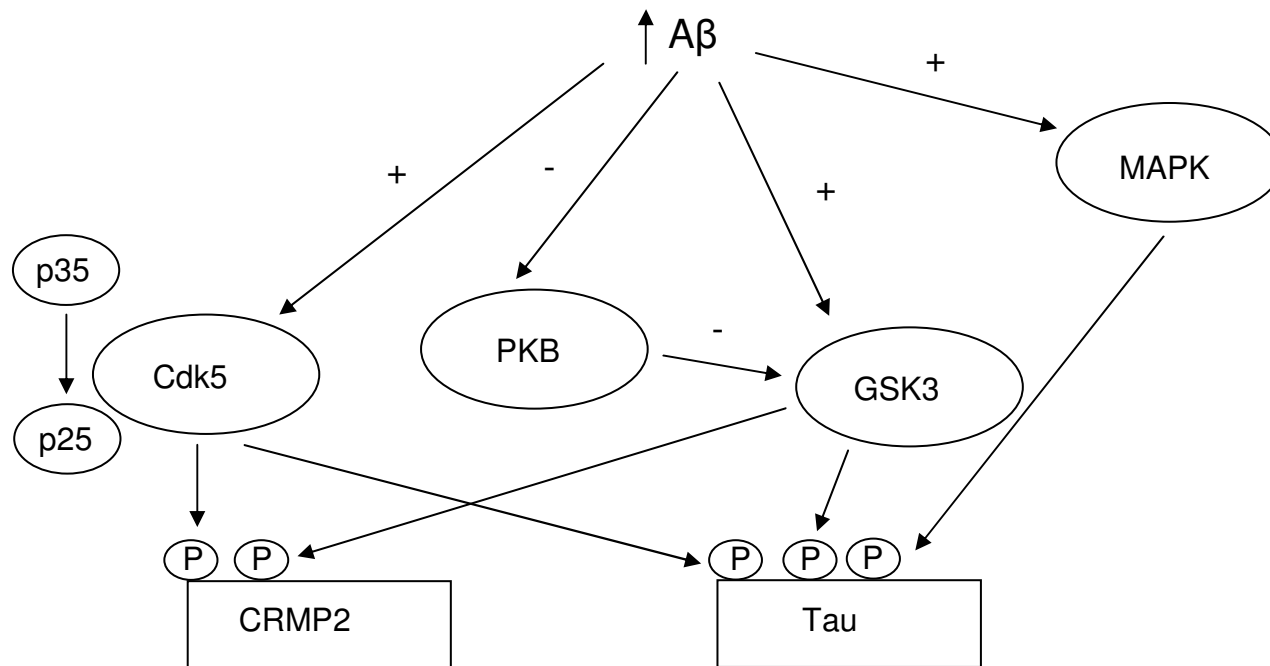


**Figure 1.5: Protein kinases and phosphorylation in AD.** In AD the regulation of a number of protein kinases is altered. The activity of GSK3 may be increased; one mechanism by which this occurs is through downregulation of the PI3K-PKB pathway by A $\beta$ , resulting in a decrease of the inhibitory phosphorylation of GSK3 at Ser9. Another feature of AD is an increase in levels of the p25 cofactor of Cdk5 which results in altered localisation and increased activation of the enzyme. Cdk5 can phosphorylate substrates such as CRMP2 and tau, while acting as a priming kinase for further phosphorylation of these proteins by GSK3. Other signalling cascades such as the MAPK cascade may also be activated and associated with tau phosphorylation. The result is a hyperphosphorylation of these cellular proteins which is a characteristic feature of AD.

Abbreviations: P = phosphorylation. For others, see main text.

Overexpression of p25 in transgenic mice results in phosphorylation and aggregation of tau, associated with neuronal toxicity (Cruz *et al.*, 2003).

Also implicated in the pathogenesis of AD are members of the MAPK cascades. Activation of p38 MAPK in AD has been suggested to contribute to inflammatory processes in microglia and astrocytes (Munoz and Ammit, 2010) and to be involved in tau phosphorylation (Hanger *et al.*, 2009b).

Protein kinases have an important role in the regulation of synaptic plasticity (see section 1.5.3.4). A $\beta$  treatment of cells reduces the activity of Ca<sup>2+</sup>/calmodulin-dependent protein kinase II (CaMKII) and the phosphoinositide 3-kinase/protein kinase B (PI3K/PKB) pathway (Townsend *et al.*, 2007) and in this way A $\beta$  can indirectly modulate LTP. The reduction in the activity of PKB prevents the inhibitory phosphorylation of GSK3 leading to its activation (Hernandez *et al.*, 2010). Recently, GSK3 has been shown to play an important role in synaptic plasticity with inhibition of the kinase necessary for the induction of LTP (Hooper *et al.*, 2007) and activation required for LTD (Peineau *et al.*, 2007). In this way, GSK3 may contribute to the alterations in hippocampal synaptic plasticity and subsequent memory deficits which are a feature of mouse models of AD.

### **1.3.5: Insulin signalling in AD**

Insulin receptors are expressed in many parts of the brain and physiological roles for insulin action on the brain are starting to be more clearly defined. In addition, exposing primary neuronal cultures to low levels of insulin can be neuroprotective, reducing vulnerability to oxidative stress and ischaemic damage

(Duarte *et al.*, 2008, Sun *et al.*, 2010), while culturing neurons in high insulin is neurotoxic (Noh *et al.*, 1999). This has led to the hypothesis that disrupted neuronal insulin action may underlie the link between diabetes and neurodegenerative disorders. There are three potential mechanisms proposed, firstly that lifestyle factors promote a decline in the insulin sensitivity of the brain, in line with the peripheral tissues, leading to loss of protective/vital actions of insulin on neurons/synapses (Steen *et al.*, 2005); secondly that the hyperinsulinemia that occurs due to insulin resistance reduces insulin transport across the blood brain barrier generating insulin deficiency in the brain (Urayama and Banks, 2008); and thirdly that hyperinsulinemia in the periphery generates hyperinsulinemia in the brain promoting neuronal damage (Cole *et al.*, 2007a). It remains to be seen which, if any, of these mechanisms contributes to the development of dementia.

### **1.3.6: The role of tau**

Although somewhat neglected due to the prominence of A $\beta$  in the study of AD, tau plays an important role in the progression of the disease. The best pathological correlation of the cognitive deficits present in AD is the extent of neurofibrillary tangle deposition within the brain (Giannakopoulos *et al.*, 2003). Familial mutations in the tau gene which cause an increase in tau filament formation do not result in AD, but in a form of dementia called frontotemporal dementia and parkinsonism linked to chromosome 17 (FTDP-17). In transgenic mouse models the expression of a familial tau transgene alone results in marked neuronal death (discussed in section **1.4.2**). This shows that the aggregation of

tau is a critical event in the progression of forms of dementia including AD, and so AD could be considered a specific form of tauopathy.

Oligomerisation of tau is enhanced by hyperphosphorylation of the protein which increases its propensity to form filaments. This results in not only a loss of the normal function of tau in stabilising microtubules but also a toxic gain of function as it sequesters normal tau and other microtubule-associated proteins to cause further disruption of microtubule function (Alonso et al., 1997). This results in compromised axonal function, synapse loss and neuronal degeneration (Alonso et al., 2010). It has been suggested that oligomeric tau may have a deleterious role on other cellular processes such as actin binding and cellular signalling, and cause mitochondrial dysfunction as a result of impaired intracellular transport (Gendron and Petrucelli, 2009). However, the exact mechanisms by which tau mediates its neurotoxic effects are not currently understood. The tau present in neurofibrillary tangles is relatively inert and does not appear to cause cellular death, and it is proposed that tangle formation may act as a neuroprotective mechanism by removing oligomeric tau forms (Lee et al., 2005).

Although tau pathology is widely thought to be downstream of amyloid pathology, it may still play a key role in the generation of the cognitive deficits observed in the disease. For example, clearance of soluble A $\beta$  by immunization does not improve cognitive deficits in the 3xTg mice, with reduction of both A $\beta$  and soluble tau required for improvement in performance on a memory task (Oddo et al., 2006b). Similarly, the reduction of tau levels in APP-overexpressing mice leads to an improvement in cognitive symptoms (Roberson

et al., 2007). Therefore, it is clear that the contributions of A $\beta$  and tau to the progression of AD are closely linked and both should be considered in models of the disease.

## **1.4: Transgenic mouse models of AD**

Multiple different mouse models have been generated using familial AD mutations as a basis (see Tables 1.2, 1.3). Although these models do not completely replicate all aspects of the disease, they have been useful in understanding some of the mechanisms involved in the progression of AD.

Mice are a particularly attractive model system due to their relatively easy genetic manipulation, short lifespan and ease of breeding. They can be engineered to develop specific pathological features which closely mimic aspects of human AD, and they perform well in cognitive tasks which involve areas of the brain affected by AD in humans, such as the hippocampus. However, there are a number of caveats and limitations which must be considered.

In the majority of mouse models of AD, including the 3xTg and TASTPM models, the transgene construct, comprising the gene of interest, enhancer and promoter regions, is microinjected into the nucleus of a mouse ovum and integrates randomly into the genome. Disadvantages of this approach include the insertion of the transgene into other gene sequences potentially altering regulation of those sequences, and the influence of surrounding sequence regions on transgene expression, with effects such as gene silencing. The insertion of multiple transgene copies is common, resulting in different levels of the gene

product being produced and the possibility of excessive overexpression (Nature Online, Cell Migration Gateway). For this reason, most models are generated using multiple founder lines which are individually characterized. Another approach, used in the generation of the PS1 M146V knock-in model (Guo *et al.*, 1999), is the targeted knockin approach. A culture of embryonic stem cells is exposed to the vector containing the gene of interest and a neomycin resistance gene. In some cells this gene will be taken up and inserted into the mouse genome by homologous recombination; these cells can be selected by the use of neomycin then injected into a mouse blastocyst. An advantage of this approach is the integration of the transgene at a known site, and of a single copy only. However, this method is more time consuming and technically difficult (Nature Online, Cell Migration Gateway).

When generating mouse models, the choice of promoter is important as it drives the regional expression of pathology. The commonly used promoters are Thy-1, platelet-derived growth factor  $\beta$  (PDGF- $\beta$ ) and the mouse or hamster prion protein (PrP) promoter which are considered neuron-specific. However, each has its own region-specific expression. For example, Thy-1 is expressed in the highest levels in the hippocampus and striatum, followed by the cortex and cerebellum (Seki *et al.*, 2002). For a model of AD, it is desirable that the promoter produces an expression pattern which mimics that of the protein in the human disease.

The background strain must also be carefully considered as there are biochemical and behavioural differences between a number of commonly used inbred mouse strains. For example, in the Morris water maze (MWM) task, C57BL/6 mice

perform better than DBA2 mice, and use a different search strategy which is associated with alterations in hippocampal gene expression (Sung *et al.*, 2008). Strain-dependent differences in a range of behavioural tasks, such as the elevated plus maze and object recognition tasks, are widely reported (Brooks *et al.*, 2005). Linked to this, electrophysiological studies show altered induction and maintenance of LTP between a number of commonly used strains such as C57BL/6 and 129/Sv (Nguyen 2006). Unfortunately, the use of one single strain is not without its difficulties, as C57BL/6 sub-strains with different genetic backgrounds also show behavioural differences (Matsuo *et al.*, 2010). Due to this, the choice of transgenic background strain must be carefully considered when choosing behavioural readouts, and reported in detail.

One of the difficulties with transgenic mouse models of this disease is that they do not fully replicate all aspects of AD. APP transgenic mice develop plaques, cognitive deficits and related pathological changes such as inflammation. However, one of the major features of human AD is marked neuronal loss resulting in atrophy of the brain (Terry *et al.*, 1981). So far, there is no convincing evidence for the presence of this feature in any transgenic models. In addition, the marked overexpression of human APP required for plaque formation does not result in the generation of tangle pathology in the mouse. Only with the presence of both an APP and tau mutation, as in the 3xTg mouse, are both plaques and tangles apparent (Oddo *et al.*, 2003).

All transgenic mouse models that have been generated have focused, by necessity, on the familial mutations associated with AD. It is possible that although the initiating mechanisms vary between sporadic and familial AD this

results in the same pathogenic endpoint. However, in studies designed to identify a treatment to prevent the early development of features of the disease there may be critical differences between sporadic and familial AD. For this reason, mouse models of the sporadic form of AD are desperately needed, along with a renewed focus on gene-environment interactions in transgenic mice, which look at the effects of stress, exercise and other ‘lifestyle’ factors on the development of pathology.

Despite their limitations, transgenic mouse models have provided much valuable information about the pathology of AD and greatly contributed to the advancement of the field. The models available can be broadly divided into three groups: single transgenic mice, expressing APP, PS1 or tau, double transgenic mice, expressing APP and PS1, and the triple transgenic mouse, expressing all three transgenes. The following sections will describe some of the most commonly used mouse models, their phenotype, and relevance to the disease. A summary table of single transgenic mouse models is presented in Table **1.2** and double/ triple transgenic models in Table **1.3**.

**Table 1.2: Selected single transgenic mouse models of AD**

<i>Model</i>	<i>Mutation</i>	<i>Promoter</i>	<i>Background</i>	<i>Pathology (age in months)</i>	<i>Behavioural phenotype (age in months)</i>	<i>Electrophysiology studies (age in months)</i>	<i>References</i>
Tg2576	APP695 K670N /M671L (Swedish)	Hamster prion	C57BL/6SJL x C57BL/6	Soluble A $\beta$ (6) Amyloid plaques (12-18)	Impairment in Y- maze(3) and MWM (9) *	Reduced basal transmission (5) * Reduced LTP (5) *	Hsiao et al 1996 Jacobsen <i>et al.</i> 2006 Lesne et al. 2006 Westerman et al. 2002
PDAPP	APP(all isoforms) V717F (Indiana)	PDGF- $\beta$	C57BL/6 x DBA2	Amyloid plaques (6-9) Hippocampal atrophy (3)	Impairment in MWM (6 – 18) Object recognition (6)	Reduced LTP (4) * Reduced basal transmission (8)	Chen <i>et al.</i> 2000 Dodart <i>et al.</i> 1999 Games <i>et al.</i> 1995
CRND8	APP695 K670N /M671L and V717F	Hamster prion	C3H/HeJ x C57BL/6	A $\beta$ deposition (3) Amyloid plaques (3-5)	Impairment in MWM (3) Reduced seizure threshold	Reduced basal transmission (5) Increased LTP (5) Increased synaptic excitability	Chishti et al. 2001 Del Vecchio et al. 2004 Jolas et al. 2002
PS1 knockin	PS1 M146V		129/Sv x C57BL/6	None	None	Reduced basal transmission (6) Increased LTP (6) Alterations in Ca <sup>2+</sup> signalling	Guo et al. 1999 Oddo et al. 2003 Stutzmann et al. 2006 Wang et al. 2004
JNPL3	Tau P301L	Mouse prion	C57BL/6 x DBA2 x SW	Neurofibrillary tangles (4-7)	Progressive motor disturbances		Gotz et al. 2001

\* Differences reported by other experimental groups (see text)

### 1.4.1: Single transgenic models: APP

Single transgenic APP mice express a human APP transgene with one of a number of familial AD mutations. There are a vast number of models now available using different mutations, promoters or strains; all develop plaque pathology and cognitive deficits, but the time course of these events is variable. Some of the most commonly studied models have subsequently been used in crosses with mice expressing other transgenic proteins in an attempt to replicate more fully the pathological features of AD.

The PDAPP mouse was the first model to be generated, which expresses the V717F (Indiana mutation) under the PDGF- $\beta$  promoter, resulting in a selective increase in A $\beta$ <sub>42</sub> levels. This mouse develops plaque pathology by 6-9 months in the hippocampus and, though it does not show neuronal loss, is one of the few models with hippocampal atrophy (Games *et al.*, 1995). It shows age-independent deficits in the Morris water maze (MWM), a spatial learning task which is thought to be hippocampal-dependent, and age-dependent deficits in object recognition memory from 6 months, which correlate with the development of amyloid plaque pathology (Dodart *et al.*, 1999, Chen *et al.*, 2000). Electrophysiological studies have shown a reduction in basal synaptic transmission from mice as young as 1 month suggesting there are age-independent deficits associated with the expression of the transgene (Hsia *et al.*, 1999). The same study found no impairment in LTP in the hippocampal cornu ammonis 1 (CA1) region at 8 months, in contrast with another study which found a more rapid decline in LTP from 4 months (Hsia *et al.*, 1999, Larson *et al.*, 1999). A lack of consensus, particularly in electrophysiological studies, between

research groups represents one of the difficulties in working with these transgenic models.

Another widely used model is the Tg2576 mouse, which expresses the APP695 isoform with the K670N/M671L (Swedish mutation) under the hamster PrP promoter. This results in overexpression of both A $\beta$ <sub>40</sub> and A $\beta$ <sub>42</sub> leading to plaque generation. The Tg2576 mouse develops plaques relatively late on in the lifespan, from between 12 and 18 months in the cortex and hippocampus (Hsiao *et al.*, 1996). The large number of studies using this mouse have resulted in a number of disparate findings which may in part be due to the use of different behavioural tests and electrophysiological protocols. For example, deficits were observed in the MWM at 9 months by one group, but this was not replicated in another study, although deficits were reported at 3 months in a Y-maze spatial task (Hsiao *et al.*, 1996, King *et al.*, 1999). In studies of synaptic plasticity, reduced basal synaptic transmission has been reported from 5 months, but this was not observed at 15 months in another study (Chapman *et al.*, 1999a, Jacobsen *et al.*, 2006), while LTP in aged mice (over 12 months) is reduced in several studies (Chapman *et al.*, 1999a, Mitchell *et al.*, 2009) but unimpaired in another (Fitzjohn *et al.*, 2001). In the Tg2576 mouse, the late onset of plaque deposition and the lack of correlation between memory deficits and insoluble amyloid (Westerman *et al.*, 2002) has been used to provide evidence for the toxicity of soluble, oligomeric forms of A $\beta$  in AD.

Finally, the CRND8 mouse model expresses the APP695 isoform with both the K670N/M671L (Swedish) and V717F (Indiana) mutations. Due to the combination of two familial mutations this mouse develops early and marked A $\beta$

deposition from the age of 3 months which is accompanied by premature mortality (Chishti *et al.*, 2001). In addition, cognitive deficits in the MWM are observed at this early age (McCool *et al.*, 2003). Interestingly, although reduced basal synaptic transmission is observed in these mice, LTP is increased in magnitude at 5 months of age. This has been linked to altered neuronal excitability, with a reduction in GABAergic and enhancement in glutamatergic function (Jolas *et al.*, 2002). In support of this, CRND8 mice show an enhanced susceptibility to seizures induced by pentylenetetrazole, a GABA receptor antagonist (Del Vecchio *et al.*, 2004). This suggests that changes in hippocampal network function and an alteration of the balance between excitatory and inhibitory transmission may occur in APP transgenic mice.

#### **1.4.2: Single transgenic models: tau**

There are several transgenic models developed which express familial tau mutations. However, mutations in tau are not observed in human AD, but in other forms of dementia such as frontotemporal dementia (Hutton *et al.*, 1998). In addition, tangle pathology is observed in a number of neurodegenerative conditions (classified as ‘tauopathies’) such as corticobasal degeneration and progressive supranuclear palsy which generally involve a component of movement disorder.

Tau mutant mice develop marked motor deficits, a feature characteristic of other tauopathies and not generally observed in AD. For example, the JNPL3 mouse, which expresses the tau P301L mutation under the mouse PrP promoter, shows degeneration of motor neurons in the spinal cord, neuropathy and muscular

atrophy. Neurofibrillary tangles are apparent in regions not widely affected in AD such as the brainstem and cerebellum (Lewis *et al.*, 2000). Severe motor impairments occur from the age of 6 months which progress rapidly to a terminal state within 4-5 weeks.

The JNPL3 mouse does however develop several features which mimic those observed in AD. Hyperphosphorylation of tau occurs at several AD-related epitopes, such as the AT8 epitope, and tau deposition is observed in the cortex, hippocampus and amygdala (Gotz *et al.*, 2001). This suggests that tau mutant mice might be useful for studying aspects of AD pathology; for example the JNPL3 mouse has been used in the study of tau filament formation (Sahara *et al.*, 2002).

The primary value of tau transgenic mice in AD research has been to study the interactions between A $\beta$  and tau. For example, injection of A $\beta$  fibrils exacerbates pathology in the JNPL3 mouse, resulting in a fivefold increase in tangles in the amygdala (Gotz *et al.*, 2001). In another study, a cross between Tg2576 and the JNPL3 mouse results in an enhancement of neurofibrillary tangle pathology when compared to the tau mutants alone (Lewis *et al.*, 2001), showing that A $\beta$  overexpression can interact with tau protein to cause an enhancement of tangle pathology.

### **1.4.3: Single transgenic models: presenilin**

Mouse models have been generated using a number of mutations in the PS1 gene such as M146V or M146L, PS1 $\Delta$ e9 (exon 9 deleted), and A246E. Although human mutant PS1 expression in mice causes a selective increase in the levels of

A $\beta$ <sub>42</sub> (Sudoh *et al.*, 1998), this does not result in the development of plaque or tangle pathology. The homozygous PS1 M146V knockin mouse shows no overt biochemical or cognitive phenotype (Guo *et al.*, 1999). However, these mice appear to have an enhanced susceptibility to excitotoxicity, with an increased vulnerability to seizure-induced neurodegeneration *in vivo* and glutamate-induced toxicity in hippocampal culture (Guo *et al.*, 1999). In addition to this, they have been shown to possess alterations in intracellular Ca<sup>2+</sup> signalling (Stutzmann *et al.*, 2006). Studies of synaptic function have shown a reduction in basal synaptic transmission at 6 months, but an enhancement in PPF and the initial phase of LTP, which involve Ca<sup>2+</sup>-mediated signalling (Oddo *et al.*, 2003). A similar phenotype of facilitated LTP and enhanced excitotoxicity is observed in another PS1 model, A246E (Schneider *et al.*, 2001). Therefore, PS1 mutant mice may be useful for studying the role of Ca<sup>2+</sup> in the pathogenesis of AD.

In addition to this PS1 transgenic mice have been used in the generation of multiple other models, including the 3xTg mouse, and these are discussed in the following sections.

#### **1.4.4: Double transgenic models**

The two most commonly used APP x PS1 mice are the PSAPP and the TASTPM models. Biochemical and electrophysiological characterisation of the TASTPM mouse is a focus of this thesis.

**Table 1.3: Selected double/triple transgenic mouse models of AD**

<i>Model</i>	<i>Mutation</i>	<i>Promoter</i>	<i>Background</i>	<i>Pathology (age in months)</i>	<i>Behavioural phenotype (age in months)</i>	<i>Electrophysiology studies (age in months)</i>	<i>References</i>
PSAPP	APP695 K670N/ M671L x PS1M146V	PDGF- $\beta$ / prion promoter	C57BL/6 x DBA2	Amyloid plaques (3-6)	Impairment in radial arm water maze (15)		Holcomb et al. 1998 Gordon et al. 2001 McGowan et al. 1999
TASTPM	APP695 K670N/ M671L (TAS10 line) x PS1 M146V	Thy-1	C57BL/6 x C3H backcrossed to C57BL/6	A $\beta$ deposition (3) Amyloid plaques (6)	Deficits in object recognition (6) Aggression Premature mortality	Alterations in intracellular Ca <sup>2+</sup> signalling	Goussakov et al. 2010 Howlett et al. 2004 Howlett et al. 2008 Pugh et al. 2006
3xTg	APP695 K670N/ M671L, TauP301L x PS1M146V	Thy-1	C57BL/6 x 129X1/SvJ x 129S1/Sv	Soluble A $\beta$ (3-9)* Amyloid plaques (6-12)* Tau hyperphosphory- lation (6-12)* Tangles (18)	Deficits in MWM (4-6)* Increased contextual fear conditioning (6)	Reduced basal transmission (6)* Reduced LTP (6)*	Billings et al. 2005 España et al. 2010 Hirata-Fukae et al. 2008 Mastrangelo et al. 2008 Oddo et al. 2003

\* Differences reported by other experimental groups (see text)

The cross of an APP and PS1 transgenic mouse results in the acceleration of A $\beta$  pathology. For example, the PSAPP mouse, generated by crossing the Tg2576 (APP<sub>Swe</sub>) with the PS1 M146V model, shows the onset of plaque deposition at 3 months in the cortex and hippocampus, with extensive deposition by 6 months, (McGowan *et al.*, 1999). This is markedly faster than in the single transgenic Tg2576, and the PSAPP mice show a four- to six-fold elevation of A $\beta$ <sub>42</sub> levels due to the presence of the PS1 mutation (Holcomb *et al.*, 1998).

The TASTPM mouse was generated by a cross of the PS1 M146V mouse with the previously generated TAS10 line, which expresses the APP695 K670N/M671L (Swedish) mutation under the Thy-1 promoter on a C57BL/6 background. The TAS10 mouse shows A $\beta$  deposition from the age of 12 months in hippocampus and cortex, which increases progressively to the age of 24 months. Cognitive deficits are present in the MWM from 6 months, when initial structural changes are observed such as dystrophic neurites and activated microglia (Richardson *et al.*, 2003). In electrophysiological studies at 12 months, these mice show impaired basal synaptic transmission but normal LTP induction, with altered synchronous activity suggesting a disruption of neuronal network function in the hippocampus (Brown *et al.*, 2005).

The development of A $\beta$  deposition occurs more rapidly in the TASTPM model than in the parent TAS10 line. At 3 months of age, amyloid deposition is apparent in the cortex, with mature plaques developing by 6 months; by 6-8 months the plaque levels are similar to those observed in 16 month TAS10 mice. There is a gender-dependent difference, with A $\beta$  load higher in female mice at all ages studied (Howlett *et al.*, 2004). Other pathological features include neuronal

loss in the vicinity of amyloid plaques and hyperphosphorylated tau associated with dystrophic neurons (Howlett *et al.*, 2008a); this shows that in mice overexpression of mutant APP in combination with mutant PS1 can induce biochemical changes in wild type tau.

In comparison to the widely studied 3xTg model there have been relatively few electrophysiological or behavioural studies of the TASTPM mice. These mice show a marked behavioural phenotype characterised in males by a high level of aggression which requires individual housing. They also exhibit weight loss, despite a higher food intake, and premature mortality which is particularly apparent in female mice. In addition, they show alterations in circadian rhythm, disinhibition and locomotor hypoactivity (Pugh *et al.*, 2007). This has been suggested to replicate some of the behavioural alterations in human AD, such as a fragmented sleep-wake cycle and personality changes such as irritability and aggression, however it is difficult to make correlations between mouse and human behaviour.

Studies of cognitive behaviour in the TASTPM mouse have shown deficits in the hippocampal and cortical-dependent novel object recognition task from the age of 6 months (Howlett *et al.*, 2004). At this age, there is marked amyloid deposition with mature plaque formation, suggesting these mice require a significant A $\beta$  load before cognitive deficits are observed in this task.

Electrophysiological studies have shown a marked reduction in basal synaptic transmission in the TASTPM mice at the age of 8 months (Spencer *et al.*, 2004) similar to that observed in the parent TAS10 line (Brown *et al.*, 2005). In addition, these mice show an alteration in intracellular Ca<sup>2+</sup> signalling, likely due

to the presence of the PS1 mutation (Goussakov *et al.*, 2010). This suggests that there are alterations in synaptic function in the TASTPM mice which have not been fully characterised.

#### **1.4.5: The triple transgenic (3xTg) mouse**

The triple transgenic (3xTg) mouse is the primary mouse model investigated in this thesis. It was generated at the University of California, Irvine, by a group led by Dr. Frank LaFerla. A homozygous PS1<sub>M146V</sub> mutant mouse was used which was developed from a hybrid C57BL/6 x 129/Sv strain. cDNA constructs containing an hAPP K670N/M671L Swedish mutation and a P301L tau mutation were microinjected into the embryos of these mice and expressed using the Thy1.2 neuronal-specific promoter to produce a triple APP<sub>K670N/M671L</sub>, Tau<sub>P301L</sub> and PS1<sub>M146V</sub> mouse. In the founder line, these integrated at the same locus, allowing co-transmission of the transgenes. The homozygous mouse shows a 3-4 fold increased steady state level of APP and a 6-8 fold increased level of tau above endogenous levels in the brain (Oddo *et al.*, 2003).

##### **1.4.5.1: Pathological features of the 3xTg mouse: amyloid pathology**

The pathology in these mice has been extensively characterised, but there are some discrepancies in the findings, in particular between studies from distinct groups. It was originally reported that intraneuronal A $\beta$  reactivity was present at 3-4 months in the cortex and by 6 months in the CA1 region of the hippocampus. Within the hippocampus the majority of neurons expressing intraneuronal A $\beta$  may be outside the pyramidal layer and instead within the stratum oriens,

subiculum and corpus callosum (Mastrangelo and Bowers, 2008). The intraneuronal A $\beta$  is monomeric until around 4-6 months of age, at which stage it may begin to oligomerise within the neurons (Oddo *et al.*, 2006a). However, a recent paper has suggested that the intraneuronal A $\beta$  is not present as a free peptide but as the uncleaved peptide within the APP protein, which the majority of antibodies are unable to distinguish between (Winton *et al.*, 2011), and that free A $\beta$  may not be required for pathogenesis in these mice. Extracellular plaques begin to develop at 6 months in the frontal cortex and are clearly apparent by 12 months, when plaques begin to develop in other regions of the cortex and hippocampus (Oddo *et al.*, 2003); plaque pathology initiates at the interface between the subiculum and CA1 region before spreading to involve the entire hippocampus (Mastrangelo and Bowers, 2008). España *et al.*, (2010) also observed intraneuronal A $\beta$  at 6 months in the cortex and hippocampus, with plaques present by 12 months. Interestingly, they highlight the importance of the basolateral amygdala in the pathological staging as this region shows the highest levels of intraneuronal A $\beta$  at 6 months. Intraneuronal A $\beta$  is also present within midbrain and brainstem regions from the age of 2 months (Overk *et al.*, 2009).

The development of pathology is reported by others to occur more slowly than originally reported. Hirata-Fukae *et al.* (2008) observed intraneuronal A $\beta$  at 6 months in the cortex and 9 months in the hippocampus, a full 3 months later than the original report. Mastrangelo *et al.* (2008) observed the early development of intraneuronal A $\beta$  from the age of 2 months but report no plaque pathology within the hippocampus until mice are older than 15 months of age, and none within the cortex until 18 months of age.

The late onset of plaques was also observed by Hirata-Fukae *et al.* (2008) who did not report their development until the age of at least 14 months, and initially only in female mice, in contrast with the original study by Oddo *et al.* (2003) who observed no gender-dependent differences in brain pathological features. More pronounced pathology in female mice has also been reported by Overk *et al.*, (2009) who observed plaques in the pons of female mice only at the age of 9 to 12 months. Hirata-Fukae *et al.* (2008) suggest that an upregulation of A $\beta$  production, as measured by soluble levels, and a reduction in the activity of the A $\beta$  degrading enzyme neprilysin may be the cause of the more severe pathological features in females.

Although the exact time course remains unclear, it is therefore evident that intraneuronal A $\beta$  accumulation precedes plaque deposition by a number of months with plaque formation a relatively late event in the lifespan of this model. In addition, the amyloid pathology shows a region-specific progression within the mouse brain, affecting the cortex first and followed by the hippocampus.

#### **1.4.5.2: Pathological features of the 3xTg mouse: tau pathology**

Tau pathology occurs initially with somato-dendritic accumulation (Clinton *et al.*, 2007) and sequential phosphorylation of multiple residues, which can be shown using antibodies raised against the different phosphorylatable sites on the tau protein. At 6 months, increased phosphorylation is present at sites recognised by the AT100 and 12E8 sites (Thr 212/Ser 214 and Ser262) but the AT8 (Ser 202, Thr 205) and AT180 (Thr 231) sites are not phosphorylated until 12-15 months, along with conformational changes detected by the MC1 antibody (Oddo *et al.*,

2003). Neurofibrillary tangles, to which the PHF-1 antibody reacts, are not evident until 12 - 18 months of age. In contrast to the APP pathology, which initiates in the cortex and then spreads to the hippocampus, the tau pathology is first apparent in the hippocampus, in particular the neurons of the CA1 region, and develops to involve the cortex (Oddo *et al.*, 2003, Oddo *et al.*, 2007). The development of biochemical changes in tau is not thought to show any gender-dependent differences (Hirata-Fukae *et al.*, 2008). It is generally accepted that tau hyperphosphorylation and tangle generation occurs much later than the development of amyloid pathology, but again there are some discrepancies between groups. Mastrangelo *et al.* (2008) observed AT180 staining suggesting phosphorylation of Thr231 as early as six months of age in the hippocampus, in contrast with Oddo *et al.* (2007) who observed such phosphorylation at 12 months. This group also failed to observe substantial tangle pathology until the late age of 23 months although they did detect some PHF-1 reactivity at 15 months within the hippocampus, a similar age to Oddo *et al.* (2007). One group has detected multiple phospho-tau isotopes, including AT180, as early as three weeks of age in the amygdala and cortex, although tangles do not appear until the age of 23 months (Oh *et al.*, 2010). There is a general consensus that the tangle pathology appears late in the lifespan of the mouse but the expression of phosphorylated tau epitopes may be time and brain-region specific and vary between individual colonies of 3xTg mice.

#### **1.4.5.3: Pathological features of the 3xTg mouse: other alterations**

An important feature that should be replicated in a mouse model of AD is the presence of an inflammatory response at sites adjacent to amyloid deposition.

Localised inflammation surrounding plaques is observed in AD and is characterised by the presence of activated microglia and astrocytes. In the 3xTg mouse there is a progressive increase in activated microglia with age, although this occurs relatively late in the lifespan from the age of 12 months (Kitazawa *et al.*, 2005). However, there is no alteration in the levels of activated astrocytes with age (Mastrangelo and Bowers, 2008). This shows that in the 3xTg model there is a limited inflammatory response; however, this may still mirror some aspects of this feature of human AD.

Alterations in adult neurogenesis (Rodriguez *et al.*, 2008, Hamilton *et al.*, 2010), serotonergic function (Noristani *et al.*, 2010), and the presence of dendritic spine loss (Bittner *et al.*, 2010) have also been observed in this model. However, further studies are required to understand the relevance of each of these features and how they relate to the cognitive and electrophysiological deficits observed. Also widely reported are alterations in neuronal  $\text{Ca}^{2+}$  homeostasis, with an increase in resting  $\text{Ca}^{2+}$  levels and enhanced ryanodine receptor (RyR)-mediated  $\text{Ca}^{2+}$  release (Stutzmann *et al.*, 2006, Lopez *et al.*, 2008). This may be due to the presence of the  $\text{PS1}_{\text{M146V}}$  mutation and may result in modulation of synaptic plasticity, which is discussed further in Chapter 3.

#### **1.4.5.4: Behavioural phenotype of the 3xTg mouse**

A number of studies have analysed the learning ability and general behaviour of 3xTg mice in an attempt to correlate deficits in these measures with the time course of the development of pathology.

3xTg mice, unlike the TASTPM strain, do not show abnormally aggressive behaviour and are reasonable docile and easy to handle. Young 3xTg mice appear healthy, with no apparent increase in premature mortality. At the age of 6 months, 3xTg mice have a significantly higher body weight than their control counterparts and this is accompanied by an increased food intake. In contrast, 12 month mice, despite an increased food intake, show reduced body weight and an increase in metabolic rate (Knight *et al.*, 2010). There are also circadian rhythm changes prior to 6 months of age, with both male and female mice showing decreased nocturnal behaviour compared with control. Males show greater locomotor activity during the day and females a decrease in activity levels during their normal active phase (Sterniczuk *et al.*, 2010b). These behavioural abnormalities occur at ages before the development of major plaque and tangle pathology.

#### **1.4.5.5: Cognitive testing of 3xTg mice**

3xTg mice show no impairment of performance in the MWM at 2 months but at 4 months show retention deficits from day to day during acquisition training and deficits in a 24 hour probe trial, showing impaired long-term memory. By 6 months the mice also have impairment in a 1.5 hour probe trial, showing that by this age they have marked deficits in spatial reference memory (Billings *et al.*, 2005). There is a gender-dependent effect on this task, with females showing poorer performance than males, possibly linked to an increased stress response and corticosterone levels (Clinton *et al.*, 2007). A further study has shown that previous experience of testing at 2, 6 and 9 months can markedly improve performance in the MWM of 12 month 3xTg mice, with experienced mice

showing a reduced plaque load at 12 months and decreased phosphorylation of tau compared with naïve mice (Billings *et al.*, 2007). In the novel object recognition task the 3xTg mice show impaired performance at the age of 12 months (Arsenault *et al.*, 2011), an age at which amyloid deposition should be well established within the hippocampus.

3xTg mice have also been tested in a contextual fear conditioning task, in which a freezing response is elicited from a tone or light which was previously paired with a footshock; this involves both the hippocampus and amygdala. At 6 months, 3xTg mice show improved performance when compared to control, characterised by an increased freezing response when tested 24 hours after the initial footshock. This may be associated with the increased anxiety behaviour observed in these mice (see Chapter 5), as they also show enhanced freezing behaviour when first placed in the test chamber (Espana *et al.*, 2010).

Finally, a recent study has used a five-choice serial reaction time test, which involves the mouse reacting to a light stimulus by pressing a touchscreen to subsequently receive a food reward (Romberg *et al.*, 2011). 9 month old 3xTg mice are impaired in this task and this may represent a deficit in attention, mediated by cholinergic inputs to the frontal cortex, as these effects are rescued by the cholinesterase donepezil. In addition, 3xTg mice show a higher rate of perseverative responses (i.e. the continued repetition of behaviour in the absence of the stimulus). It has been suggested that alterations in behavioural measures such as attention may also influence the performance of 3xTg mice on other cognitive tasks.

In summary, the behavioural phenotype of this model has been extensively examined but these studies did not attempt to link synaptic or electrophysiological deficits to the appearance of behavioural deficits.

## **1.5: The hippocampus**

The hippocampus is a region of the brain important in memory processes, including the retention of spatial information and memory for recent events. It is also one of the earliest regions to be affected by tau pathology in AD and is thought to contribute to the early memory deficits which are a symptom of the disease. Forms of synaptic plasticity such as long-term potentiation (LTP), thought to be a cellular correlate of memory, have been widely studied, with alterations in the magnitude of LTP associated with cognitive deficits in mouse models of AD. The following sections describe the anatomy of the hippocampus, its role in memory processes and the molecular mechanisms of synaptic plasticity.

### **1.5.1: Structure and anatomy of the hippocampus**

The hippocampus is a paired structure located within the medial temporal lobe of the brain. It has a curved appearance, resembling the body of a seahorse, which gives the region its name. This structure is unique within the brain as it possesses a mainly unidirectional neuronal circuit which lies within the same orientation, allowing the experimental preparation of hippocampal slices in which the synaptic contacts are largely preserved. A diagram of the hippocampus (sagittal orientation) is shown in Fig. **1.5**.

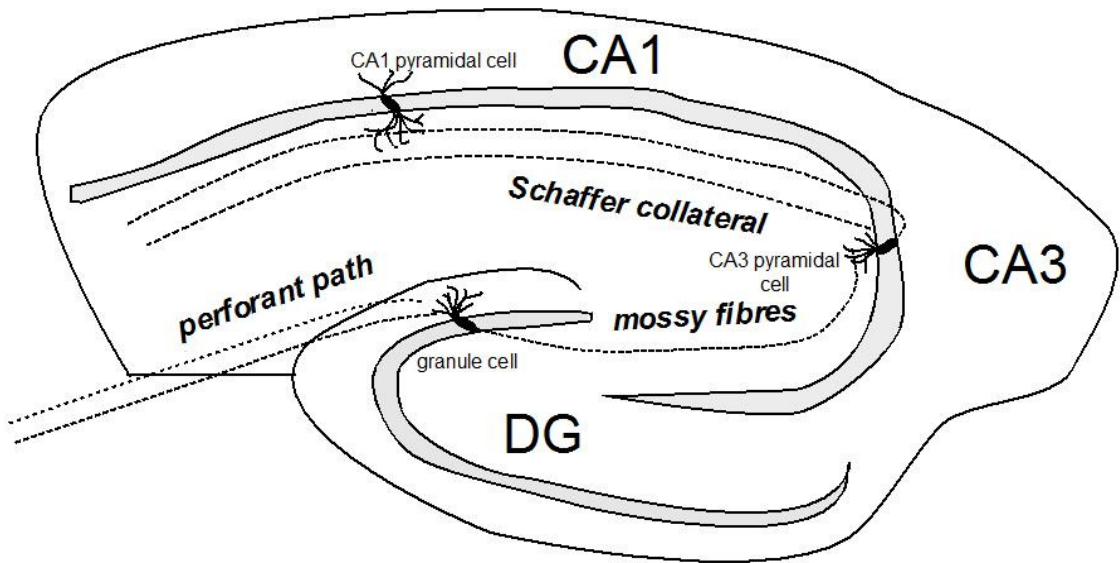


**Figure 1.6: Sagittal section of the rodent hippocampus.** Input comes from the EC via the perforant path where it synapses with DG granule cells. The granule cells project to the CA3 region via the mossy fibres and synapse with the pyramidal cells in this region. CA3 pyramidal cells then project to the CA1 pyramidal cells via the Schaffer collateral-commissural pathway. This pathway is primarily unidirectional and is so often called the ‘trisynaptic pathway’.

Abbreviations: EC (entorhinal cortex), DG (dentate gyrus), CA3 (cornu ammonis 3), CA1 (cornu ammonis 1).

The primary input pathway to the hippocampus occurs through the entorhinal cortex (EC) which projects to the dentate gyrus (DG) through the perforant pathway. In addition, the EC provides an output pathway for information leaving the hippocampus through the subiculum. The EC projects widely to a number of other cortical regions, including the piriform, temporal and frontal cortex (Burwell and Amaral, 1998) and also to other brain regions such as the amygdala and thalamus (Amaral and Lavenex, 2007).

From the DG to the CA1 region the pathway is unidirectional and is often called the 'trisynaptic circuit' i.e. EC to DG, DG to CA3, CA3 to CA1. The principal neurons of the DG, the granule cells, project via the mossy fibre pathway to the CA3 (cornu ammonis 3) region where they synapse with CA3 pyramidal neurons. From this region, the CA3 neurons project to the CA1 pyramidal neurons via the Schaffer-collateral commissural pathway. The CA1 region projects both to the hippocampal subiculum which is linked to the EC, and the EC directly to allow information to leave the hippocampus. Although the primary granule cells and pyramidal neurons are glutamatergic, the hippocampus also contains a network of GABAergic interneurons which modulate neuronal transmission (Amaral and Lavenex, 2007).

### **1.5.2: Function of the human hippocampus**

Studies involving patients with hippocampal lesions have shown unequivocally that the human hippocampus plays a critical role in aspects of memory. However, the concept of 'memory' is complex and can be divided into a number of subtypes, the most basic being the division between short-term and long-term

memory. Within the category of long-term memory are procedural memory (carrying out skills or motor tasks) and declarative memory (recollection of facts and events). It is in this latter process the hippocampus is thought primarily to be involved. This theory was first developed using the case of the famous patient H.M., who underwent bilateral removal of the medial temporal lobe as a treatment for intractable epilepsy. Following the procedure, he was unable to retain memory for new events (anterograde amnesia) or recent previous events (retrograde amnesia) although his short term and procedural memory were unaffected, along with his memory of early life events (Corkin *et al.*, 1997). Short-term memory and the prolonged storage of declarative memories are thought to involve regions of the brain distinct from the hippocampus, such as the cerebral cortex (Squire and Zola-Morgan, 1991). Similar amnesia is observed in a number of individuals who have experienced ischaemic damage to the hippocampal formation (Rempel-Clower *et al.*, 1996).

Overall, data supports the existence of a ‘medial temporal lobe memory system’ consisting of the hippocampus, EC and adjacent parahippocampal cortex, involved in the acquisition of facts (semantic memory) and events (episodic memory (Squire and Zola-Morgan, 1991)). Another widely studied function of the hippocampus is its role in spatial memory and processing. The existence of hippocampal place cells, which encode spatial location, has been demonstrated and widely studied in the mouse and rat. Performance in tasks such as the Morris water maze (MWM), in which the animal must form a spatial representation of a pool, is impaired in rats with hippocampal lesions (Morris *et al.*, 1990). In humans, a subset of neurons within the hippocampus fire in response to specific spatial locations (Ekstrom *et al.*, 2003) suggesting the existence of place cells

within this structure. However, it has been suggested that the role of the hippocampus in human spatial memory is more complex and involves the integration of aspects such as episodic memory and contextual information (Good *et al.* 2002).

The divergent roles of the hippocampus are consistent with damage in this region leading to some of the cognitive deficits observed in human AD. The EC and the hippocampus are one of the earliest regions to be affected by pathological changes such as tangle deposition (Braak and Braak, 1991). Early AD is primarily characterised by deficits in declarative memory, with an inability to learn new information and remember recent events, and this has been shown to correlate with the degree of hippocampal atrophy (Walker *et al.* 2007). Another early symptom is disorientation, with individuals 'getting lost' initially in unfamiliar environments but subsequently in their own homes. Damage to the hippocampal regions may result in an impaired memory for relevant places which may result in difficulties with spatial navigation. Therefore, neuronal damage and atrophy within the hippocampus and EC is likely to explain the impairments in spatial processing and anterograde amnesia in AD.

A number of other memory impairments are also reported in AD, and this is reflected in the varied cognitive tests required to form a preliminary diagnosis. An inability to recognise objects (visual agnosia), difficulties in performing tasks or movements (apraxia) and language difficulties may reflect increasing cortical involvement in the disease (Walker *et al.* 2007). This shows that, although the hippocampus plays a critical role in human memory, a number of other brain

regions are damaged in AD leading to the cognitive deficits observed, particularly in the later stages of the disease.

### **1.5.3: Synaptic plasticity in the hippocampus**

There are several activity-dependent forms of synaptic plasticity in the hippocampus which last from milliseconds to several hours, days or longer. Synaptic plasticity is an alteration of the efficiency of synaptic transmission, which may involve both increases and decreases in synaptic strength and is characterised by biochemical and morphological alterations of the synapse. Short-term forms of plasticity include paired-pulse facilitation (PPF) which occurs on the scale of several hundreds of milliseconds, and post-tetanic potentiation (PTP) which may last several minutes, while long-term potentiation (LTP) and depression (LTD) result in sustained changes in synaptic strength which may last for several hours or longer.

#### **1.5.3.1: Paired-pulse facilitation (PPF)**

Facilitation is a form of short-term synaptic enhancement which occurs over a period of several hundreds of milliseconds and results in an enhanced probability of neurotransmitter release. PPF occurs at CA1 hippocampal synapses when two stimuli are given within around 50 – 500ms of each other. The amplitude of the second synaptic response recorded is typically greater than that of the first stimulus. PPF is largely due to presynaptic mechanisms, in particular the transient increase in  $\text{Ca}^{2+}$  generated by an incoming action potential. The residual  $\text{Ca}^{2+}$  present in the terminal following the first stimulus is combined with the

$\text{Ca}^{2+}$  influx occurring from the second stimulus to cause an enhancement of the magnitude of the second synaptic response. It has been shown that the level of PPF is linearly related to the concentration of residual  $\text{Ca}^{2+}$  within the terminal (Wu and Saggau, 1994).

### **1.5.3.2: Induction of LTP**

Following an initial stimulus, an activity-dependent increase in the strength of synaptic transmission is observed which can be maintained for several hours or indeed many days *in vivo*. This was first observed in the anaesthetised rabbit, where brief high-frequency stimulation resulted in a long-lasting potentiation of the synaptic response obtained by stimulation of the perforant path (Bliss and Lomo, 1973). The clear laminar structure of the hippocampus lends itself well to such experiments, and over several decades the mechanisms of hippocampal LTP have been extensively studied. These are discussed in the following sections and summarised in Fig. 1.6.

In the two most commonly studied pathways, the Schaffer collateral-commissural pathway to CA1 pyramidal synapses and the perforant path to DG granule cell synapses, induction of LTP is dependent upon the activation of the NMDA receptor (Collingridge *et al.*, 1983). This receptor is subject to a voltage-dependent  $\text{Mg}^{2+}$  block under conditions of basal synaptic transmission. However, in the presence of enhanced glutamate release,  $\text{Na}^+$  influx through postsynaptic AMPA receptors results in a sustained depolarisation of the postsynaptic spine. This relieves the  $\text{Mg}^{2+}$  block of the NMDA receptor, allowing  $\text{Ca}^{2+}$  influx and the activation of  $\text{Ca}^{2+}$ -dependent enzymes. Inhibitory GABAergic interneurons

which act on the postsynaptic spine usually act to limit depolarisation, however sustained depolarisation (as delivered by a LTP induction protocol) results in the fatigue of these interneurons through the activation of inhibitory GABA<sub>B</sub> autoreceptors. For this reason stimulation protocols such as the theta burst have been developed which deliver stimuli at the time of maximal presynaptic GABA<sub>B</sub> autoreceptor activation, leading to a reduction in GABA-mediated hyperpolarisation of the postsynaptic cell (Davies and Collingridge, 1996).

### **1.5.3.3: Post-tetanic (PTP) and short-term (STP) potentiation**

Immediately following the induction stimulus there is an increase in synaptic strength which is often substantial and characteristic of PTP. This is a short term form of plasticity which declines within several minutes and, similar to PPF, is thought to depend upon the presynaptic Ca<sup>2+</sup> concentration. Following this, the amplitude of the synaptic response should become stable and elevated for at least 40-60 minutes to be considered as LTP. A return to basal synaptic strength prior to this period is usually considered STP, but the cutoff points vary between groups, as the two forms of plasticity overlap and cannot be distinguished without pharmacological means. STP can be generated by performing the stimulation protocol in the presence of broad spectrum protein kinase inhibitors which prevent the kinase activity necessary for LTP induction (Malenka *et al.*, 1989). It is thought to be a presynaptic phenomenon which decays in an activity-dependent manner (i.e. if the input stimulation is stopped for any period of time, STP will resume at the same magnitude when it is restarted) and the level of STP varies with the strength of induction protocol used (Volianskis and Jensen, 2003).

#### 1.5.3.4: Early phase LTP (E-LTP)

The initial phase of LTP occurs as a result of the marked rise in intracellular  $\text{Ca}^{2+}$  caused by influx through NMDA receptors and other mechanisms such as voltage-gated  $\text{Ca}^{2+}$  channel activation and release of  $\text{Ca}^{2+}$  from internal stores (Alford *et al.*, 1993). Studies of the molecular mechanisms of this process has been largely determined by the availability of selective inhibitors and transgenic models. A number of kinases have been implicated in this mechanism, although most play a regulatory rather than an essential role.

Thought to be most important in LTP expression is  $\text{Ca}^{2+}$ /calmodulin-dependent protein kinase (CaMKII) which undergoes autophosphorylation when associated with the  $\text{Ca}^{2+}$ -associated form of the protein calmodulin. This results in the persistent activation of the enzyme despite the reduction in intracellular  $\text{Ca}^{2+}$  which occurs subsequent to LTP induction. Evidence for the role of CaMKII comes from studies in which a peptide inhibitor blocks LTP induction (Malinow *et al.*, 1989). In addition, a transgenic mouse with a point mutation in which autophosphorylation of CaMKII is prevented shows a reduction of LTP in the CA1 region (Giese *et al.*, 1998). Activation of CaMKII results in a cascade of downstream events which allow the persistent expression of LTP and are discussed in the following section.

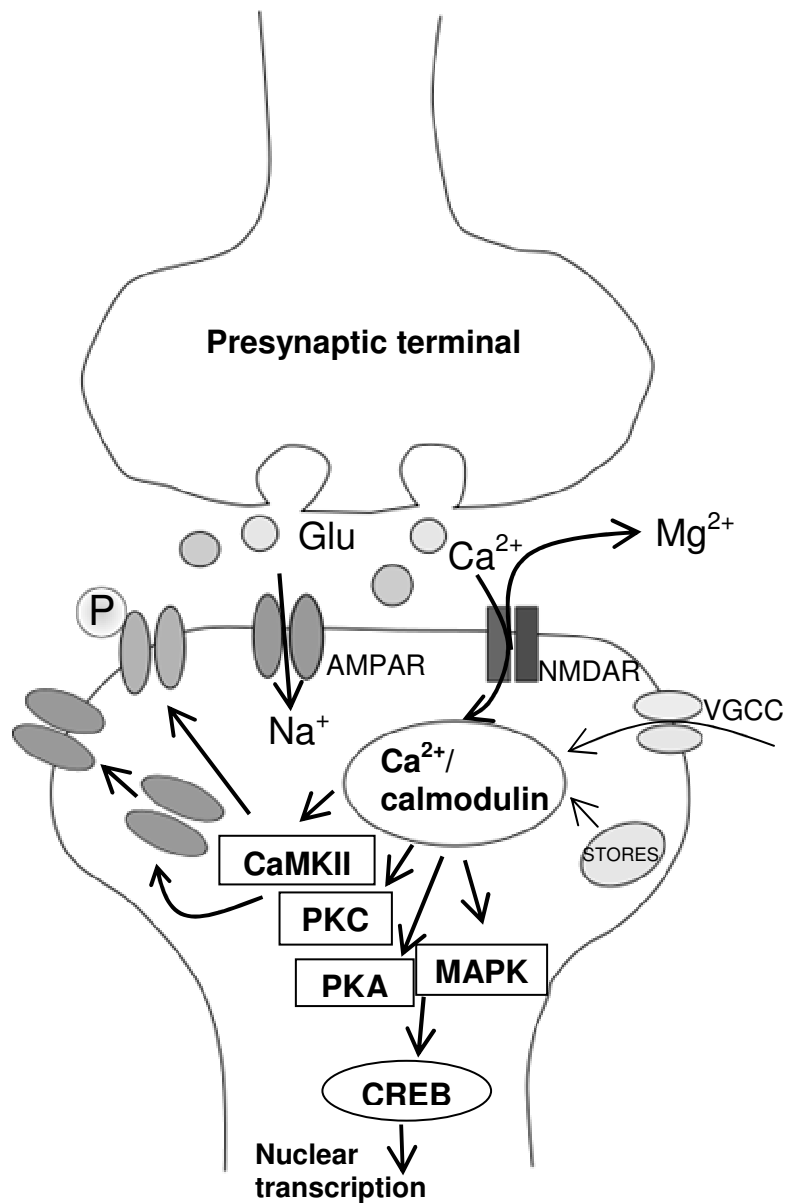


**Figure 1.7: Mechanisms of LTP.** Sustained glutamate release from the presynaptic terminal and depolarisation of the postsynaptic terminal mediated by AMPA receptor activation is sufficient to relieve the Mg<sup>2+</sup> block of the NMDA receptor and allow Ca<sup>2+</sup> influx. This is subsequently enhanced by the entry of Ca<sup>2+</sup> through voltage dependent Ca<sup>2+</sup> channels and release from intracellular stores. Ca<sup>2+</sup> bound to calmodulin activates the kinases CaMKII and PKC, which phosphorylate existing AMPA receptors and initiate the translocation of new receptors to the synapse. Activation of PKA and MAPK results in phosphorylation of the transcription factor CREB which translocates to the nucleus and initiates gene transcription, promoting the synthesis of new proteins essential for the maintenance of LTP.

Abbreviations: Glu (glutamate), AMPAR (AMPA receptor), NMDAR (NMDA receptor), VGCC (voltage gated Ca<sup>2+</sup> channels), P (phosphorylation).

A number of other kinases are thought to have a regulatory role in E-LTP. Protein kinase C (PKC), in particular the PKC $\gamma$  isoform, may be persistently activated following LTP induction and may initiate an alternative kinase cascade in parallel with CaMKII. Inhibitors of PKC applied into the postsynaptic neuron can inhibit both the induction and maintenance of LTP (Wang and Feng, 1992). Also implicated in LTP are protein tyrosine kinases such as fyn (Grant *et al.*, 1992), MAPK (English and Sweatt, 1997) and protein kinase A (PKA), although these are thought to have a greater role in L-LTP.

In conclusion, there are a number of protein kinases which modulate the expression of E-LTP. However, the exact role of each kinase and its downstream effects are not fully understood. It is likely that there are multiple and overlapping cascades which result in a number of downstream mechanisms allowing the prolonged maintenance of synaptic potentiation.

#### **1.5.3.5: Postsynaptic expression mechanisms**

The most important postsynaptic expression mechanisms in E-LTP involve the alteration of AMPA receptor function. This occurs both through the modification of existing receptors and the trafficking of new receptors into the synapse. Activation of CaMKII results in the phosphorylation of the GluR1 subunit membrane AMPA receptors at Ser831. This alters the single-channel conductance of the receptor to increase its permeability to Ca<sup>2+</sup> (Lee *et al.*, 2000). In addition, it has been suggested that there are alterations in the subunit composition of these AMPA receptors, with the transient expression of GluR2-lacking (Ca<sup>2+</sup>-permeable) receptors prolonging the rise in intracellular Ca<sup>2+</sup> (Plant

*et al.*, 2006). New AMPA receptors enter the synapse through two distinct mechanisms: trafficking from intracellular compartments and lateral diffusion from perisynaptic regions (Makino and Malinow, 2009). This may result in the activation of previously 'silent' synapses which lack functional AMPA receptors at resting membrane potential (Kullmann 2003). The subunit composition of these AMPA receptors varies and this may regulate the insertion or replacement of existing receptors through interactions with intracellular proteins (Shi *et al.*, 2001). The overall increase in cell surface AMPA receptor number as a result of these mechanisms is responsible for maintaining a sustained increase in synaptic strength.

#### **1.5.3.6: Late phase LTP (L-LTP)**

The second stage of LTP is known as late LTP (L-LTP) and commences from roughly one to five hours after LTP induction, although there is substantial overlap with E-LTP. L-LTP is protein-synthesis dependent and can be prevented by the application of protein synthesis or transcriptional inhibitors (Nguyen *et al.*, 1994). Activation of protein kinases initiate signalling cascades which result in the recruitment of nuclear transcription factors. Particularly important in this process is PKA, as inhibition of this kinase blocks L-LTP (Frey *et al.*, 1993) but the MAPK cascade is also involved in nuclear signalling (English and Sweatt, 1997). One of the most important downstream targets of PKA (and members of the MAPK family) are cAMP response element binding (CREB) proteins, which bind to cAMP response elements (CREs) in the regulatory region of genes to modulate transcription. This results in the activation of immediate early genes such as *zif268* and *arc* which encode proteins associated with synaptic

scaffolding complexes and influence receptor trafficking and cytoskeletal function. These and other newly synthesised proteins contribute to structural remodelling of dendritic spines and the enlargement and growth of new synapses (Okuno 2011). Such morphological alterations allow the prolonged maintenance of synaptic potentiation in hippocampal neurons.

#### **1.5.3.7: LTP and memory**

Although LTP has been primarily studied in the hippocampus, it is also apparent in other regions of the brain such as the cortex and cerebellum, and has been linked to motor learning in these areas (Rioult-Pedotti *et al.*, 2000, Coesmans *et al.*, 2004). It is hypothesised that LTP may be a cellular correlate of certain types of memory. A number of studies in mice have correlated deficits in spatial memory with reductions in LTP both *in vitro* and *in vivo*, including in transgenic models of AD (see section 1.4). These have attempted to link the induction and maintenance of LTP within individual neuronal populations more closely to particular behavioural tasks although this is technically challenging. Ideally, blocking LTP generation should impair the formation of new memories, and reversal of established LTP should induce amnesia. A pioneering study has shown the latter, as an inhibitor of the atypical PKC isoform PKM $\zeta$  that reverses established LTP results in the loss of previously obtained place-avoidance memory (Pastalkova *et al.*, 2006). This is consistent with LTP having a role in encoding subtypes of hippocampal-dependent memory. Overall, evidence suggests that it is valid to link alterations in LTP, such as those observed in transgenic models of AD, with observable memory deficits in hippocampal-

dependent tasks. It is also probable that LTP and other forms of synaptic plasticity occur in the human brain and interest is growing in how alterations in these processes may result in the cognitive symptoms of AD.

## 1.6: Aims and objectives of this thesis

### 1.6.1: Background

The 3xTg mouse is one of the most commonly used transgenic models of AD and is unique as it is the only available model to develop both plaque and tangle pathology, due to the presence of three transgenes: APP<sub>Swe</sub>, PS1<sub>M146V</sub> and Tau<sub>P301L</sub>. Previous studies of this mouse are described in detail in section 1.4.5, however in brief, the original paper by Oddo *et al.* described deficits in electrophysiological studies of LTP at the age of 6 months, accompanied by A $\beta$  accumulation (4-6 months) and subsequent plaque deposition (6-12 months). Tau hyperphosphorylation is present at the age of 6 months onwards, while tangle formation occurs later in the lifespan, from around 12 months of age. A number of published biochemical studies have replicated the presence of these pathological features in the model, although the time course of their development varies widely between reports. Behavioural studies of this mouse have shown the presence of cognitive deficits in a water-maze paradigm from 4 - 6 months, which may be linked to the rising intraneuronal A $\beta$  levels apparent with age (Billings *et al.*, 2005).

The TASTPM mouse, described in section 1.4.4, carries both the APP<sub>K670N/M671L</sub> and PS1<sub>M146V</sub> mutations but does not possess a tau transgene, so develops only plaque-like structures in the brain. This mouse possesses an earlier onset of the biochemical phenotype, with elevated A $\beta$  present at 3 months of age and plaque deposition at 6 months. Few electrophysiological studies have been carried out in these mice and LTP has not previously been characterised, however reduced basal synaptic transmission is reported at the age of 8 months (Spencer *et al.*,

2004). Behavioural studies have shown deficits in the novel object recognition test, along with a phenotype of markedly aggressive behaviour and premature death (Howlett *et al.*, 2004).

### **1.6.2: Aims**

Although there are a number of published studies of the 3xTg mouse, the majority have carried out biochemical analysis alone, or linked this to either electrophysiological or behavioural studies. In addition, there are a number of discrepancies between groups regarding the rate at which the pathological features develop in this model. One of the major aims of this thesis is to systematically characterise the time course of development of the phenotype using electrophysiological, behavioural and biochemical studies in the same colony of 3xTg mice, with a particular focus on any early phenotypic changes which could be relevant to the initial stages of AD development. There are fewer published studies on the TASTPM mouse, and in particular as LTP has not previously been reported in this model an aim of the thesis is to carry out electrophysiological studies to observe if, similar to the 3xTg mouse, reductions in synaptic plasticity or basal synaptic transmission become apparent with age.

Another primary aim of this thesis is the comparison of the 3xTg and TASTPM models. The predominant hypothesis in the field, the amyloid cascade hypothesis (see section 1.3.1) states that the generation of A $\beta$  through the abnormal processing of APP is a key initiating factor in the development of AD. Therefore, as both these models possess the human APP<sub>Swe</sub> transgene, any molecular or

electrophysiological changes which are observed in both could represent a common mechanism of disease progression.

The key difference between the 3xTg and TASTPM models is the presence of the Tau<sub>P301L</sub> transgene in the 3xTg mouse which results in tau hyperphosphorylation and subsequent tangle generation. An aim of this thesis is to observe the contribution of the tau transgene, and particularly early changes such as tau hyperphosphorylation, to the development of the phenotype in 3xTg mice. It is hoped that by comparison of the 3xTg and TASTPM mice the role of tau in early biochemical or electrophysiological deficits can be assessed.

### **1.6.3: Summary**

1. Characterise the development of any electrophysiological, biochemical or behavioural changes in the 3xTg or TASTPM mouse models of AD.
2. Link any observed alterations in synaptic function with the development of pathology in these models.
3. Observe any early features of these models that might be associated with the initial stages of AD.
4. Compare the 3xTg and TASTPM models to observe the role of tau in the development of AD pathology.

## **Chapter 2**

### **Materials and Methods**

## 2.1: Materials

### 2.1.1: Antibodies

Primary antibody	Source	Species
Actin	Sigma	Rabbit
6E10	Covance	Mouse
Total CRMP2	DSTT, University of Dundee	Sheep
CRMP2 pSer509/514	DSTT, University of Dundee	Sheep
CRMP2 pSer522	DSTT, University of Dundee	Sheep
Total GSK3 $\beta$	BD Biosciences	Mouse
GSK3 $\alpha/\beta$ pSer21/9	Cell Signalling	Rabbit
Total MAPK	Cell Signalling	Rabbit
MAPK pThr202/Tyr204	Cell Signalling	Rabbit
Total PKB	Cell Signalling	Rabbit
PKB pSer 473	Cell Signalling	Rabbit
Tau5	Millipore	Mouse
Tau AT8 (Ser202/Thr205)	Autogen Bioclear	Mouse
Tau pSer396	Cell Signalling	Mouse
Tau pSer404	Millipore	Rabbit
Synaptophysin	Abcam	Rabbit
p35	Cell Signalling	Rabbit

All primary antibodies were diluted 1/1000 in TBST containing 1% milk with the exception of actin which was diluted 1/5000.

**Secondary antibodies:** HRP-conjugated anti-mouse, rabbit and sheep (Pearce) were diluted 1/10 000. Infrared-dye conjugated anti-mouse (Rockland) was diluted 1/5000 while Infrared-dye conjugated anti-sheep (Rockland) was diluted 1/10 000.

### 2.1.2: Buffer composition

Buffer	Ingredients
aCSF	124mM NaCl, 3mM KCl, 26mM NaHCO <sub>3</sub> , 1.25mM NaH <sub>2</sub> PO <sub>4</sub> , 1mM MgSO <sub>4</sub> , 10mM D-glucose, 2mM CaCl <sub>2</sub>
RIPA buffer	50mM Tris base, 0.1mM EGTA, 1mM EDTA, 1% Triton-X 100, 1mM Na <sub>3</sub> VO <sub>4</sub> , 50mM NaF, 5mM Na <sub>4</sub> P <sub>2</sub> O <sub>7</sub> , 0.27M sucrose, 0.1% $\beta$ -mercaptoethanol, 1 Complete Protease Inhibitor Cocktail tablet (Roche)

NuPage LDS sample buffer (Invitrogen)	10% glycerol, 141mM Tris base, 2% LDS, 0.51mM EDTA, 0.22mM SERVA Blue G250, 0.175mM Phenol Red (pH 8.5)
NuPage MOPS SDS running buffer (Invitrogen)	50mM MOPS, 50mM Tris base, 0.1% SDS, 1mM EDTA (pH 7.7)
NuPage transfer buffer (Invitrogen)	25mM glycine, 50mM Tris base, 0.1% SDS, 1mM EDTA, 20% methanol
Tris-buffered saline with Tween (TBS-T)	50mM Tris base, 150mM NaCl, 0.1% v/v Tween 20
Laemmli sample buffer	63mM Tris base, 10% glycerol, 2% SDS, 0.0025% bromophenol blue (pH 6.8)
Running buffer	250mM Tris base, 1.92M glycine, 1% SDS, pH 8.3
Transfer buffer	48mM Tris base, 39mM glycine, 20% methanol

### 2.1.3: Chemicals

Chemical	Supplier
$\beta$ -mercaptoethanol, CaCl <sub>2</sub> , D-glucose, KCl, NaCl, NaHCO <sub>3</sub> , NaH <sub>2</sub> PO <sub>4</sub> , MgSO <sub>4</sub>	VWR
Bromophenol blue, EDTA, EGTA, kynurenic acid, NaF, Na <sub>4</sub> P <sub>2</sub> O <sub>7</sub> , Na <sub>3</sub> VO <sub>4</sub> , SDS, Tris base, Triton X, Tween	Sigma
Methanol, sucrose	Fisher
Glycine	Melford

### 2.1.4: Transgenic mice

3xTg mice were originally generated at the University of California (Irvine, USA) by the insertion of a transgene containing the human APP695 isoform with the Swedish (*K670M*, *N671L*) double mutation and human 4R0N tau with the P301L mutation, under the Thy1.2 promoter, into PS1<sub>M146V</sub> mice (Oddo *et al.*, 2003). The generation of PS1<sub>M146V</sub> mice from a C57BL/6 x 129/Sv background has

been previously described (Guo *et al.*, 1999). Male and female 3xTg founder mice for our colony were provided by Stuart Allan (Manchester). Additional female mice were provided by Karen Horsburgh (Edinburgh); these were maintained separately and not used for breeding purposes. Genotyping was carried out from ear punch biopsy in several 3xTg mice to confirm the presence of the transgenes (performed by Linda Gallacher). Control mice were generated from a mixed C57/BL6 x 129/Sv background and were initially provided by Stuart Allan (Manchester).

TASTPM mice were generated at GlaxoSmithKline (Harlow, UK) by the cross of two previously available lines, TAS10 and TPM (Howlett *et al.*, 2004). TAS10 mice were generated by the insertion of a transgene containing the human APP695 isoform with the Swedish (K670M, N671L) double mutation, under the Thy1 promoter, into C57BL/6 mice (Richardson *et al.*, 2003). TPM mice were generated by the insertion of a transgene containing the human PS1 gene with the M146V mutation, under the Thy1 promoter, into C57BL/6 mice (Howlett *et al.*, 2004). Following this, TAS10 mice were backcrossed onto a pure C57BL/6 line and then crossed with TPM to produce TASTPM mice with the double APP<sub>Swe</sub> and PS1<sub>M146V</sub> mutations.

All mice were maintained on a 12 hour light/dark schedule with free access to food (RM1, Special Diet Services) and water, and were group housed with the exception of a number of male TASTPM which had to be separated due to aggressive behaviour. All animal procedures were carried out under the Animals (Scientific Procedures) Act 1986.

## **2.2: Methods**

### **2.2.1: Electrophysiology methods**

#### **2.2.1.1: Hippocampal slice preparation**

Each mouse was killed by cervical dislocation under Schedule 1 of the Animals (Scientific Procedures) Act 1986, the brain was removed and placed in a dish of artificial cerebrospinal fluid (aCSF) at room temperature. The cerebellum and lateral portion of the temporal lobes were removed, and the brain was halved down the midline and glued by its flat edge to a metal plate with cyanoacrylate. 400 $\mu$ M thick sagittal brain sections were then cut using a Vibratome (Intracel, Herts, UK) with the brain submerged in room-temperature aCSF and oxygenated with a 95% O<sub>2</sub>/ 5% CO<sub>2</sub> mixture. Following sectioning the slices were placed on netting in a glass chamber containing oxygenated aCSF which was able to flow freely around the tissue. They were then allowed to recover for at least one hour before use in electrophysiological recording.

#### **2.2.1.2: Extracellular recording**

The slice was placed in an electrophysiological recording chamber (Scientific Systems Design, Mississauga, Ontario, Canada) which allowed extracellular submerged recording from the hippocampus. The aCSF within the chamber was maintained at 31-32°C using a temperature controller (Digitimer, Hertfordshire, UK) with an oxygenated water chamber which circulated the warmed water beneath the slice. The slice itself was oxygenated in the perfusion system with a 95% O<sub>2</sub>/ 5% CO<sub>2</sub> mixture at a flow rate of approximately 2ml/min.

Electrical stimulation was given using a stimulator box (Digitimer, Hertfordshire, UK) which was electrically isolated to prevent interference from mains electrical noise. A bipolar stimulating electrode either hand-made from twisted Teflon coated tungsten wire (Advent Research Materials, Oxford, UK) or a commercial electrode (World Precision Instruments, Florida, USA) with a resistance of 1 M $\Omega$  was used; responses were comparable using both types of electrode.

Recordings were made using an electrode made of borosilicate glass (King Precision Glass, California, USA) which had a resistance of 3-4 M $\Omega$  and was filled with aCSF. In the centre of the electrode was a silver wire (Advent Research Materials, Oxford, UK) and this, along with a ground electrode of silver wire, was attached to an isolated differential amplifier where the signal was amplified and filtered (Warner Instrument Corporation, Connecticut, USA). Both the stimulating and ground electrodes were electrically chlorided by immersion in 1M KCl solution. The output from the amplifier was fed through an oscilloscope (Tektronix, Oregon, USA) and digitised through an acquisition board (BNC-2090, National Instruments, Berkshire, UK). A schematic diagram of the setup is shown in Fig. **2.1**. The responses evoked from the slice were visualized using a computer running WinLTP software (v. 0.95b, Anderson, [www.winltp.com](http://www.winltp.com)).

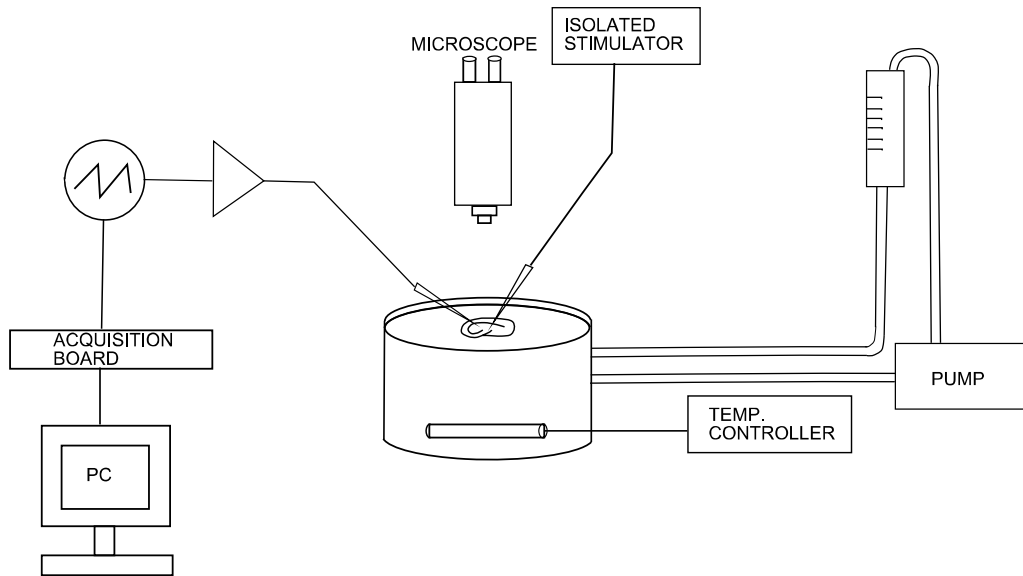


**Figure 2.1: Diagram of the electrophysiology setup.** The pump-controlled perfusion system provides oxygenated aCSF to the slice in the tissue bath, while a controller maintains the temperature at 32°C. A stimulating electrode is placed in the slice which is connected to an isolated stimulator unit to allow electrical pulses to be given to the tissue. The recording electrode is connected to an amplifier which enhances the output signal, then a data acquisition board via an oscilloscope. The acquisition board feeds into a PC running WinLTP software which allows visualisation of the evoked electrical responses from the tissue.

### 2.2.1.3: Measurement of the fEPSP

In the hippocampus, the presence of well-defined synaptic layers facilitates the measurements of field extracellular postsynaptic potentials (fEPSPs). These are generated by electrical stimulation of the Schaffer collateral fibres which project from the CA3 region to pyramidal neurons in the CA1 region. Stimulation of these presynaptic fibres results in glutamate release at the synapse between the axons of the CA3 region and dendrites of the CA1 neurons. This results in a synchronous postsynaptic depolarisation which occurs as a result of ionotropic receptor activation (primarily AMPA receptors) and influx of positive ions into the postsynaptic terminal. This can be detected by placing a recording electrode within the CA1 dendritic layer (stratum radiatum).

The WinLTP software provides a visual representation of the evoked fEPSP and can also be used to alter the stimulation protocol (e.g. the number or duration of pulses) or the parameters of the fEPSP recording (e.g. the length of recording or amplitude and slope detection values). All pulses given were 0.1ms in length. During the experiment stimulation was given at thirty second intervals to record dynamic changes in the fEPSP.

The fEPSP has a number of characteristic features (shown in Fig. 2.2). The two main measurements which are recorded are the amplitude and slope of the fEPSP which can be measured to give an indication of synaptic activity within the neuronal population. The slope is most commonly measured as it is less subject to interference by other sources of current flow such as feedforward GABAergic inhibition or action potential firing.

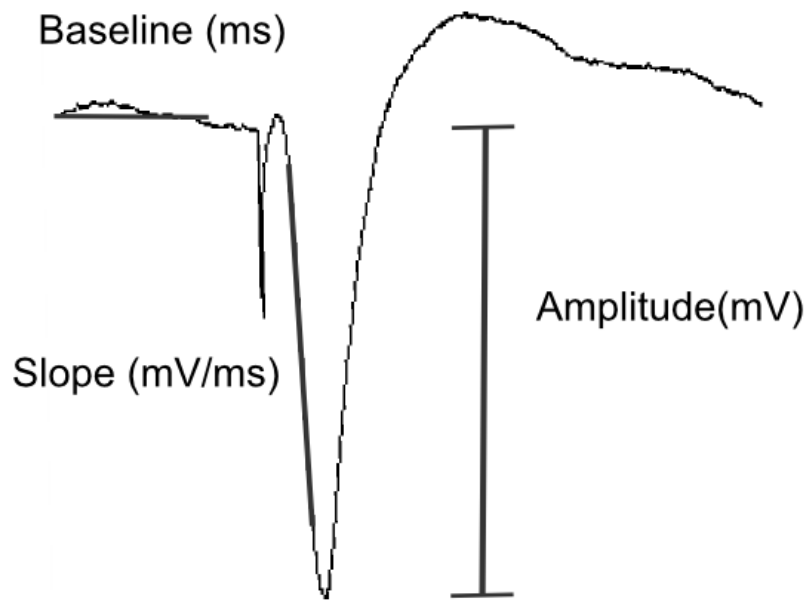


**Figure 2.2: A field extracellular postsynaptic potential (fEPSP).** The amplitude is calculated as the measurement from the baseline to the peak of the fEPSP while the slope is 20-80% of the initial phase. The stimulus artefact appears as a spike immediately before the fEPSP. An increase in the slope and amplitude values of the fEPSP is characteristic of LTP. The fEPSP represents the simultaneous depolarisation of a population of CA1 pyramidal neurons, which is recorded as a negative voltage deflection due to the flow of positive ions away from the recording electrode into the postsynaptic terminals.

The peak amplitude was usually measured 4-15 ms after the pulse and the slope was taken as 20-80% of the peak, with a baseline of at least 8-2ms before the pulse. An increase in the amplitude and slope is characteristic of LTP. However, the baseline fEPSP measurements can be used as a measure of the synaptic strength within the neuronal population. This is the likelihood of a synaptic response following an input stimulus and involves both presynaptic components (e.g. release probability, quantal size) and postsynaptic components (e.g. receptor function and density). For LTP experiments, a baseline fEPSP of approximately 40% of the maximum fEPSP was established to ensure that synaptic potentiation following theta burst was possible.

#### **2.2.1.4: Input-output function**

Basal synaptic transmission can be studied more systematically with an input-output curve. This is a measure of synaptic recruitment, which increases with the input stimulus due to the activation of a greater population of neurons. Input-output response can vary due to differences in synaptic density and the strength of individual synapses within the population (Usdin *et al.*, 1999). Curves were generated using an increasing stimulus intensity and recording the slope and amplitude of each evoked fEPSP. The intensity was initially set at 0.2mA and manually increased in 0.1mA increments which provided a sigmoidal shaped input-output response. Three slope and amplitude readings were recorded for each stimulation intensity at thirty second intervals and averaged. The slope of the fEPSP was then plotted as a function of stimulus strength. The curve was completed when a plateau phase was reached with the amplitude and slope of the

field remaining similar at several increasing stimulus intensities (usually 1-1.2mA).

### **2.2.1.5: Paired-pulse facilitation**

PPF was recorded at interstimulus intervals of 20ms, 50ms, 100ms, 200ms, 300ms, 400ms and 500ms. The optimum interstimulus interval was 50ms, with shorter intervals causing reduced PPF or even synaptic depression likely due to  $\text{Ca}^{2+}$  depletion, and longer stimulus intervals less effective at inducing PPF due to a gradually decreasing concentration of  $\text{Ca}^{2+}$  in the presynaptic terminal.

PPF was graphed using the paired pulse ratio, which is the amplitude of the second fEPSP divided by the amplitude of the first. Values of greater than 1.0 indicate facilitation.

### **2.2.1.6: Stimulation protocols for the induction of LTP**

There are a number of stimulation protocols which have been used to induce LTP in the hippocampal slice preparation. The appropriate choice of stimulation protocol is important as different protocols are thought to work through diverse cellular signalling mechanisms, which may be initiated by the dynamics of  $\text{Ca}^{2+}$  release (Smith *et al.*, 2009).

The theta burst protocol is characterised by an interburst interval of 200ms, and is thought to be relatively physiological as a hippocampal theta rhythm (6-10 Hz) is commonly observed in living animals. It is generally involved with states of

attention and movement but has also been associated with learning (Otto *et al.*, 1991).

The theta burst protocol used in these experiments was a four-pulse theta burst consisting of 4 pulses at a frequency of 100 Hz, repeated 10 times with an interburst interval of 200ms.

#### **2.2.1.7: Measurement of LTP**

A typical LTP experiment has several characteristic features (Fig. 2.3) which allows for several parameters to be compared between experiments. The measurement of LTP is complicated by the existence of several mechanisms of potentiation which superimpose and overlap. Following the theta-burst stimulation there is an immediate and often dramatic increase in both the slope and the amplitude of the fEPSP, which usually reaches its peak in the 30 seconds following LTP induction. This is related to an initial phase of post-tetanic potentiation (PTP) which decays rapidly, causing a steep decrease in the slope and amplitude of the fEPSP, typically over the first 10-15 minutes following theta burst. PTP is thought to be presynaptic and caused by an increase in the intra-terminal  $\text{Ca}^{2+}$  concentration causing enhanced neurotransmitter release (Delaney and Tank, 1994).

This initial phase is followed by a plateau phase in which the amplitude and slope of the fEPSP remain stable for at least 60 minutes following theta burst stimulation. Experiments which decay to baseline before this time (<5% of total) are described as showing short-term potentiation only and were discarded. The plateau phase corresponds to early LTP (E-LTP), characterised by protein-

synthesis independent mechanisms such as receptor phosphorylation and trafficking, and generally thought to persist over several hours (see Chapter 1). Late phase LTP (L-LTP), which involves gene transcription and protein synthesis, allows the prolonged expression of potentiation over many hours and shows overlap with early LTP (Frey and Morris, 1997). However, without using pharmacological treatments such as protein synthesis inhibitors, it is impossible to dissociate the phases of LTP; based on the time scale of these experiments it is likely that the majority of LTP recorded is E-LTP.

The peak potentiation following theta burst was used as a measure of PTP, and LTP was measured using the average potentiation of the plateau phase, taken as 50-60 minutes following theta burst stimulation. The mean value was calculated firstly for each individual mouse then for the group as a whole at all time points. The average potentiation of the graph during the complete experiment from 0-60 minutes was also used for statistical comparison between groups. LTP was plotted either conventionally using the normalised fEPSP slope values, which standardises differences in the size of the fEPSP between experiments, or as a non-normalised graph to show the actual recorded values of the fEPSP.

#### **2.2.1.8: Statistics and analysis**

All electrophysiology graphs were created using Origin software version 7 ([www.originlab.com](http://www.originlab.com)). Statistical analysis was carried out using SPSS version 17 ([www.spss.com](http://www.spss.com)). For input-output curves, an unpaired t-test was used to compare groups at each stimulus intensity. Paired-pulse facilitation was analysed using repeated measures ANOVA, followed by unpaired t-test at individual

interstimulus intervals to establish those which were statistically significant. LTP measurements were analysed using repeated measures ANOVA with strain as the between subjects factor and time as the within subjects factor. Post hoc analyses for time were only performed if the interaction between mouse strain and time was statistically significant. The analysis used for each experiment is indicated in the text where appropriate, and values are expressed as  $\pm$  standard error of the mean (s.e.m.). A  $p$  value of  $< 0.05$  was considered to be significant.

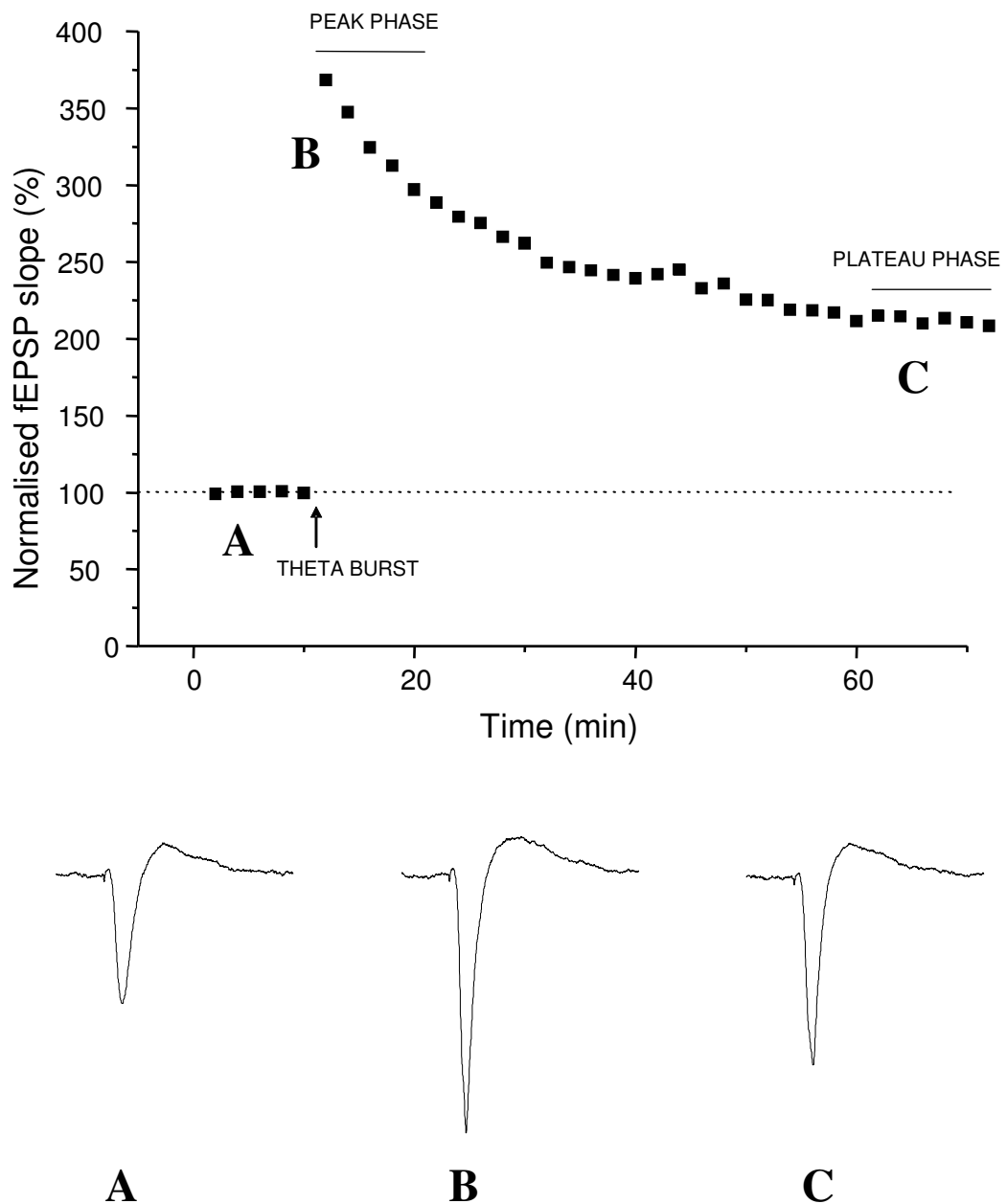


**Figure 2.3: Long-term potentiation.** Following at least ten minutes of stable baseline, a four-pulse theta burst stimulation is given. This causes a marked increase in the slope of the fEPSP which immediately reaches its peak and then declines to a sustained plateau phase. The peak value was used as a measure of PTP and the average from 50-60 minutes when the slope of the fEPSP has plateaued as a measure of LTP. Typical fEPSPs obtained at the labelled points of the experiment are represented below the graph.

## **2.2.2: Biochemical methods**

### **2.2.2.1: Brain lysate preparation**

Samples were prepared using a method to separate soluble and insoluble tissue. RIPA buffer was added at approximately double the volume of the sample and the tissue was homogenized using a pellet mixer. The lysate was then centrifuged in a chilled desktop centrifuge (Fisher Scientific, Leicestershire, UK) at 12 000 rpm for ten minutes and the supernatant removed and retained as the soluble protein fraction. Half the volume of RIPA buffer was then added to the pellet, the process repeated and the supernatants combined; the insoluble material was discarded. The soluble fraction was again centrifuged to remove any remaining insoluble material and then frozen at  $-80^{\circ}\text{C}$  for future use.

The concentration of protein in each brain lysate was determined using the Bradford method (Bradford 1976). This uses the Coomassie Blue G-250 dye, which shifts absorbance from 465nm to 595nm when bound to proteins within a sample. 980  $\mu\text{l}$  of reagent (Bio-Rad, California, USA) was added to 20 $\mu\text{l}$  of an appropriate dilution of brain lysate (e.g. 1/10, 1/20), triturated and incubated at room temperature for 10 minutes and the absorbance read using a spectrophotometer (Pharmacia Biotech, Uppsala, Sweden). The values obtained were compared against a standard curve generated using serial dilutions of bovine serum albumin to determine the protein concentration within each sample.

**2.2.2.2: Sodium dodecyl sulphate polyacrylamide gel electrophoresis (SDS-PAGE)**

Samples were diluted in RIPA buffer to a known concentration (i.e. 0.5 or 1mg/ml). Two methods were used for SDS-PAGE due to a change in laboratory protocol. NuPAGE SDS sample buffer (Invitrogen, California, USA) or LDS sample buffer was added to each sample; the negatively charged SDS/LDS within the sample buffer binds to the protein to provide a uniform charge density which allows each protein to migrate through the gel based solely on its molecular weight. The sample buffer also contained 10mM of the reducing agent dithiothreitol (DTT) to break up the native structure of the protein. As each sample was of known concentration an equal weight of protein could be loaded onto the gel. Samples were then loaded and run using either the Novex or BioRad systems.

Using the NuPage Novex system, (Invitrogen, California, USA) a current of 180V was applied for one hour through a graded 4-12% polyacrylamide gel, with a prestained molecular weight marker run alongside to provide bands of known molecular weight for comparison (SeeBlue, Invitrogen, California, USA). 0.5ml of antioxidant was added to the upper buffer chamber to prevent reoxidisation of the samples during electrophoresis.

Using the BioRad system, a current of 120V was applied for one and a half hours through a graded 4-15% polyacrylamide gel, with Plus Protein Dual Colour Standard, (BioRad, California, USA) used as the molecular weight marker.

### **2.2.2.3: Western blotting**

Following SDS-PAGE, a 0.45mm nitrocellulose membrane (Hybond-C, GE Healthcare, Buckinghamshire, UK) was placed on top of the gel to allow for protein transfer. The gel and membrane were then sandwiched between filter paper and placed in a transfer cassette containing nylon sponges soaked in transfer buffer (Invitrogen, California, USA), dehydrated with 20% methanol to allow for more efficient transfer. The cassette was placed in a chamber filled with transfer buffer and a current of 35V was applied for 2 hours, causing the proteins within the gel to migrate onto the nitrocellulose membrane.

Following transfer, the membrane was stained with the reversible protein dye Ponceau-S (Sigma-Aldrich, Missouri, USA), to assess efficiency of transfer and allow cutting of the membrane, and was then washed off.

For use with the enhanced chemiluminescence (ECL) development method, membranes were blocked with 5% milk powder in TBS-T for one hour to prevent non-specific binding of the primary antibody to the membrane. They were then incubated overnight at 5°C with the appropriate primary antibody. Following multiple washes, the membrane was incubated with a horseradish peroxidase (HRP)-conjugated secondary antibody for one hour at room temperature.

The membrane was then washed several times in TBS-T and 1ml of ECL reagent (GE Healthcare, Buckinghamshire, UK) was added to the surface of the membrane for one minute. This causes a chemiluminescent reaction with the secondary antibody that can be detected using photographic film. In a dark room,

either X-ray Film (CL-EXposure, Thermo Scientific, Illinois, USA) or high-sensitivity film (Hyperfilm, GE Healthcare, Buckinghamshire, UK) was used in a film cassette (Kodak, New York, USA) to develop multiple exposures of each membrane dependent on the strength of the signal.

For use with the Li-Cor Odyssey system, membranes were blocked in 3% bovine serum albumin for one hour and a primary antibody in 1% milk powder in TBS-T was then added overnight at 5°C. Following washing of the membrane, the infrared dye-conjugated secondary antibody was added for one hour at room temperature. Membranes were then developed using the Li-Cor Odyssey.

#### **2.2.2.4: Densitometry and analysis**

Densitometry of LiCor Odyssey-developed films was carried out using the Odyssey software (version 2.1). Actin was used as a loading control for each protein except the phosphorylated forms of tau and CRMP2 which were normalised to the total protein levels. All graphs were created using Origin software version 7 ([www.originlab.com](http://www.originlab.com)). Statistical analysis was carried out using SPSS version 17 ([www.spss.com](http://www.spss.com)) and consisted of unpaired t-test, one-way ANOVA and two-way ANOVA dependent on the number of groups and number of variables (detailed in results where appropriate). All values are expressed as  $\pm$  standard error of the mean (s.e.m.). Post-hoc analysis was carried out using Student-Newman-Keuls testing and a  $p$  value of  $< 0.05$  was considered to be significant.

### **2.2.3: Behavioural methods**

All behavioural experiments were carried out under license PPL 60/3766 from the Home Office under the Animals (Scientific Procedures) Act 1986.

#### **2.2.3.1: Rewarded alternation T-maze**

The T-maze consists of three arms: the start arm and two goal arms arranged in a T shape, with two removable doors that can be used to block the arms. A food reward is placed in a well at the end of each goal arm.

Mice were placed in the T-maze with their littermates for ten minutes on at least five days, with all arms open and a 1:1 solution of condensed milk (Carnation, Nestlé) placed within the food well at the end of each goal arm. At the same time, mice were provided with several drops of condensed milk in a food well overnight within their home cage to allow habituation to the apparatus and to the reward.

During the testing phase, mice were maintained at 85-90% free-feeding weight to increase motivation for the task. Mice were tested in squads of equal numbers (six to eight), with all mice having run the first trial before commencing the second trial which provided a similar inter-trial interval for each mouse. The apparatus was cleaned with 70% ethanol solution between individual mice. Four trials were carried out each day for nine or ten consecutive days.

The mouse was placed at the far end of the start arm, with access to the rest of the maze blocked by a removable door. After five seconds, the door was lifted and the mouse allowed to run down one of the goal arms and consume the

reward, with the other blocked by the second removable door. This forced direction was chosen in a pseudorandom manner, with no more than two consecutive left or right presentations to prevent the development of place preference. Following consumption of the condensed milk reward, the mouse was again placed in the start arm for five seconds. The doors blocking access to the rest of the start arm and to one of the goal arms were then lifted, allowing free access to all arms. The mouse was allowed to run down a goal arm; if the choice was correct it obtained another reward, if incorrect the door was lowered and it was ensured that the mouse had found the food well was empty before being removed from the maze. Each mouse was returned to its home cage between trials. Mice which were reluctant to run were encouraged initially by several drops of condensed milk placed in the start arm; if a mouse failed to complete the task within three minutes on either the forced or choice element of the trial they were returned to the home cage.

Where a delay was introduced, the mouse was placed in the start box for 0, 30 or 60 seconds following the forced element of the trial. The length of delay was varied and spread equally between left and right presentations. Trials in which the mouse failed to choose a goal arm within the first 30 seconds of the choice element were excluded from analysis.

### **2.2.3.2: Activity box**

The activity box used was a clear Perspex box of diameter 32 x 20 x 19 cm with a wire lid. An activity monitor (Benwick Electronics, Norfolk, UK) consisting of a 1 inch grid of infrared beams was used, with two sets of beams spaced 2cm vertically apart to measure both horizontal movement and rearing behaviour.

When the animal moved either horizontally or vertically the beam was broken and an activity count was recorded electronically. The break of two consecutive beams was considered a count to minimise the effect of static movements such as grooming. The parameters which were recorded were fast and slow mobile counts, fast and slow rearing counts and the percentage and time the mouse spent mobile.

Mice were placed in the box for fifteen minutes and allowed to explore freely, with measurements being recorded every five minutes. This was carried out on four consecutive days to allow both intra-trial and inter-trial habituation to be measured.

#### **2.2.3.3: Statistical analysis**

All behavioural graphs were created using Origin software version 7 ([www.originlab.com](http://www.originlab.com)). Statistical analysis was carried out using SPSS version 17 ([www.spss.com](http://www.spss.com)). The appropriate statistical test was carried out for each experiment and is noted in the results chapter. A  $p$  value of  $< 0.05$  was considered to be significant.

## **Chapter 3**

# **Electrophysiology**

### 3.1: Introduction

Studies using electrophysiological techniques have given an important insight into synaptic transmission and plasticity in mouse models of AD. In this chapter, I have used extracellular recording in the hippocampal slice preparation to examine basal synaptic function and LTP in the 3xTg and TASTPM mouse models.

It has previously been reported that the 3xTg mouse shows a reduction in basal transmission as shown by a smaller fEPSP, accompanied by deficits in LTP at the age of 6 months associated with an increase in intraneuronal A $\beta$  (Oddo *et al.*, 2003). For this reason, I studied measures of synaptic function in this model at a range of ages from 2 – 17 months when the pathological features such as A $\beta$  accumulation should be present in our colony of 3xTg mice. I have measured both LTP, basal synaptic transmission and other forms of short-term plasticity such as PPF.

There is currently no published hippocampal slice electrophysiology data on the TASTPM model. I therefore studied synaptic function in this model including basal transmission, PPF and LTP to observe any alterations in these measures that might be associated with the biochemical changes in these mice.

The final section of this chapter describes treatment of both 3xTg and TASTPM slices with the glutamate receptor antagonist kynurenic acid during slicing to reduce excitotoxicity and improve slice viability. It has previously been reported that deficits in fEPSP amplitude in APP-overexpressing mice can be reversed by incubation with this compound (Fitzjohn *et al.*, 2001). I have observed the effects

of kynurenic acid treatment in the 3xTg and TASTPM mice to determine whether an increased susceptibility to excitotoxicity is a feature of these models.

## 3.2: Results

In the 3xTg, TASTPM and control mice a number of parameters were measured to give a measure of synaptic function. These experimental approaches are discussed in more detail in the methods section (Section 2.2.1) and include: input-output function and fEPSP amplitude/slope measurements, PPF and LTP. Briefly, an input-output curve was generated by measuring the slope of the fEPSP at gradually increasing stimulus intensities to give a measure of basal synaptic transmission. PPF, a form of short-term plasticity, was also recorded to test presynaptic function. Finally, LTP was induced using a four pulse theta burst protocol, with the change in the slope of the fEPSP (quantified as mV/ms) used as a measure of synaptic plasticity.

The notation ( $n = x / y$ ) following a group indicates the number of brain slices used and the number of mice from which these slices came i.e. ( $n = 6/4$ ) denotes six slices obtained from four mice. All experiments were carried out on hippocampal slices from at least three individual mice in each group.

### 3.2.1: Control data

LTP was reliably obtained in slices from control mice at ages up to 17 months maintained for up to eight hours *in vitro* following initial slice preparation. LTP

could be induced and maintained for 60 minutes post-theta burst in control mice, and in some slices for up to 120 minutes (data not shown) although this was difficult due to technical limitations (e.g. the formation of air bubbles underneath the slice). This shows that the slices remain viable throughout the duration of the experiments reported in this thesis.

### **3.2.2: Electrophysiological characterisation of 2 month old 3xTg mice**

#### **3.2.2.1: Input-output function**

Input-output curves were generated and compared for 2 month old 3xTg mice and 2 month old control mice of both genders. A normalised input-output curve, where the maximum field slope is set to 100%, was generated, along with a non-normalised input-output curve using the actual values (mV/ms) obtained.

In 2 month old control mice, there is no significant difference ( $p > 0.05$ , unpaired t-test) between the normalised input-output curve of male ( $n = 5/3$ ) and female ( $n = 8/3$ ) mice (Fig. **3.1A**). Similarly, for the 2 month 3xTg mice, there is no significant difference ( $p > 0.05$ , unpaired t-test) between the normalised input-output curve for male ( $n = 5/3$ ) and female ( $n = 8/3$ ) mice (Fig. **3.1B**).

Given these findings the male and female data was pooled together. When the two groups are compared, there is no significant difference ( $p > 0.05$ , unpaired t-test) between the normalised input-output curve of the control mice ( $n = 12/7$ ) and the 3xTg mice ( $n = 13/8$ ) (Fig. **3.2A**).

For the non-normalised input-output curve, the control mice exhibit an fEPSP slope at 1 mA of  $0.46 \pm 0.11$  mV/ms, while the 3xTg mice exhibit an fEPSP slope at 1 mA of  $0.71 \pm 0.14$  mV/ms (Fig. **3.2B**). There is no significant difference ( $p > 0.05$ , unpaired t-test) between the two groups. The large error bars are due to the marked variability in the size of the fEPSP between individual slices, which occurs even in tissue from the same mouse.

### **3.2.2.2: Paired-pulse facilitation**

Paired-pulse facilitation was compared between 2 month old 3xTg mice and 2 month old control mice, and the effect of gender was also investigated. In all experiments the maximum facilitation was observed at an interstimulus interval of 50ms, which is in agreement with previously published work (Nathan *et al.*, 1990).

In control mice, the paired-pulse ratio at 50ms is  $2.0 \pm 0.06$  for males ( $n = 6/3$ ) and  $1.79 \pm 0.13$  for females ( $n = 5/3$ ) mice (Fig. **3.3A**). There is no significant difference ( $p > 0.05$ , repeated measures ANOVA) in the paired-pulse ratio in male or female control mice at interstimulus intervals ranging from 20 – 500ms.

In 3xTg mice, the paired-pulse ratio at 50ms is  $1.45 \pm 0.08$  for male ( $n = 5/3$ ) and  $1.57 \pm 0.06$  for female ( $n = 8/5$ ) mice (Fig. **3.3B**). There is no significant difference ( $p > 0.05$ , repeated measures ANOVA) in the paired-pulse ratio in male or female 3xTg mice at interstimulus intervals ranging from 20 – 500ms.

Given that gender did not influence the paired-pulse ratio for either genotype the data for male and female mice were combined. Collectively, the paired-pulse

ratio at 50ms is  $1.90 \pm 0.07$  for control ( $n = 11/6$ ) and  $1.52 \pm 0.05$  for 3xTg ( $n = 13/8$ ) mice (Fig. 3.4). There is a significant decrease in the paired-pulse ratio in 3xTg when compared to control mice ( $p < 0.05$ , repeated measures ANOVA, followed by unpaired t-test at individual intervals) at interstimulus intervals of 50, 100, 200, 300, 400 and 500 ms.

### 3.2.2.3: Long-term potentiation

LTP was measured in the CA1 region for 2 month 3xTg and control mice. These experiments were performed in both male and female mice and both normalised and non-normalised data were generated.

In all experiments a baseline fEPSP was recorded at 30 second intervals until the slope of the fEPSP was stabilised and constant over a 10 min period before delivery of the theta burst stimulus. In the following section the slope of the fEPSP is normalised to baseline (*i.e.* 100%) for each recording.

In 2 month old control male mice ( $n = 7/5$ ), the peak enhancement of the slope of the fEPSP is  $225 \pm 11\%$ , with a mean from 50-60 minutes following the theta burst stimulus of  $155 \pm 11\%$ . In 2 month old control female mice ( $n = 6/3$ ), the peak enhancement is  $185 \pm 28\%$ , with a mean from 50-60 minutes of  $131 \pm 7\%$  (Fig. 3.5A).

In 2 month old 3xTg male mice ( $n = 7/3$ ), the peak enhancement of the slope of the fEPSP is  $263 \pm 47\%$ , with a mean from 50-60 minutes following the theta burst stimulus of  $187 \pm 23\%$ . In 2 month 3xTg female mice ( $n = 9/5$ ), the peak

enhancement is  $191 \pm 17\%$ , with a mean from 50-60 minutes of  $146 \pm 4\%$  (Fig. **3.5B**).

There is no significant difference ( $p > 0.05$ , repeated measures ANOVA) between the magnitude of LTP in any of the four groups. There is a trend for enhanced LTP in the male 3xTg mice which reflects variability between the data obtained (at all times points determined), shown by the relatively large error bars associated with this group.

Combining the results obtained for each gender, a comparison was then made between the 3xTg and control mice. In 2 month control mice ( $n = 15/8$ ), the peak enhancement of the slope of the fEPSP is  $223 \pm 12\%$ , with a mean from 50-60 minutes following the theta burst stimulus of  $152 \pm 9\%$ . In 2 month old 3xTg mice ( $n = 17/8$ ), the peak enhancement is  $221 \pm 23\%$ , with a mean from 50-60 minutes of  $163 \pm 11\%$  (Fig. **3.6**).

There is no significant difference ( $p > 0.05$ , repeated measures ANOVA) between the magnitude of LTP in 2 month old 3xTg and control mice. This is the case for all phases of LTP, from the initial peak to the plateau phase.

#### **3.2.2.4: Non-normalised long-term potentiation**

When the slope of the fEPSP is not normalised to control and the actual values (mV/ms) are utilised, in 2 month control mice the mean baseline fEPSP is  $0.21 \pm 0.03$  mV/ms, the peak enhancement following theta burst is  $0.51 \pm 0.10$  mV/ms, and the mean from 50-60 minutes is  $0.32 \pm 0.05$  mV/ms. In 2 month 3xTg mice,

the mean baseline fEPSP is  $0.36 \pm 0.05$  mV/ms, the peak enhancement is  $0.87 \pm 0.16$  mV/ms, and the mean from 50-60 minutes is  $0.57 \pm 0.09$  mV/ms (Fig. 3.7).

There is a significant increase in the baseline fEPSP slope and the magnitude of LTP ( $p < 0.05$ , repeated measures ANOVA) in 2 month 3xTg mice when compared to control mice. This is present in all phases of LTP, from the initial peak to the plateau phase.

### 3.2.2.5: Summary

There are several differences in hippocampal CA1 synaptic function apparent in the 3xTg mice at 2 months old. No gender-dependent effects were observed on the magnitude of LTP in either 3xTg or control mice therefore both male and female data were pooled together. The 3xTg mice show a decrease in PPF, with no differences in input-output function, but a trend for an increased fEPSP at higher intensities. This is replicated in the non-normalised LTP graph with a baseline fEPSP slope value that is significantly greater than control. However, the normalised LTP graph shows that the magnitude of LTP is similar between the two groups. These data suggests that, although 2 months is an age prior to the intraneuronal accumulation of A $\beta$  observed by Oddo *et al.*, there are measurable electrophysiological changes in the 3xTg mice.

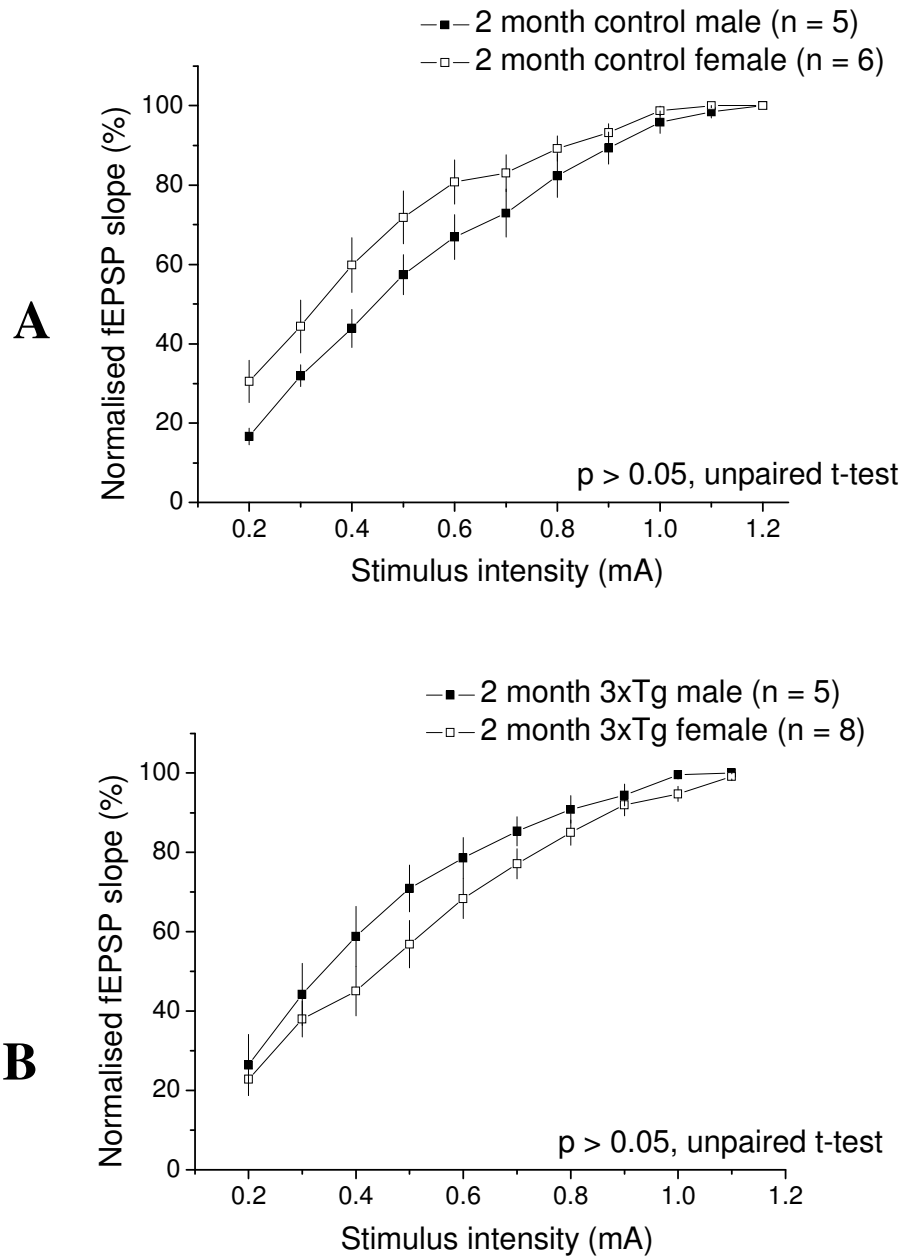


**Figure 3.1: Normalised input-output curves obtained from 2 month old male and female 3xTg and control mice.** The fEPSP slope was measured at a range of stimulus intensities and then normalised in male (n = 5/3) and female (n = 6/3) control mice (**A**) and male (n = 5/3) and female (n = 8/5) 3xTg mice (**B**).  $p > 0.05$ , unpaired t-test.

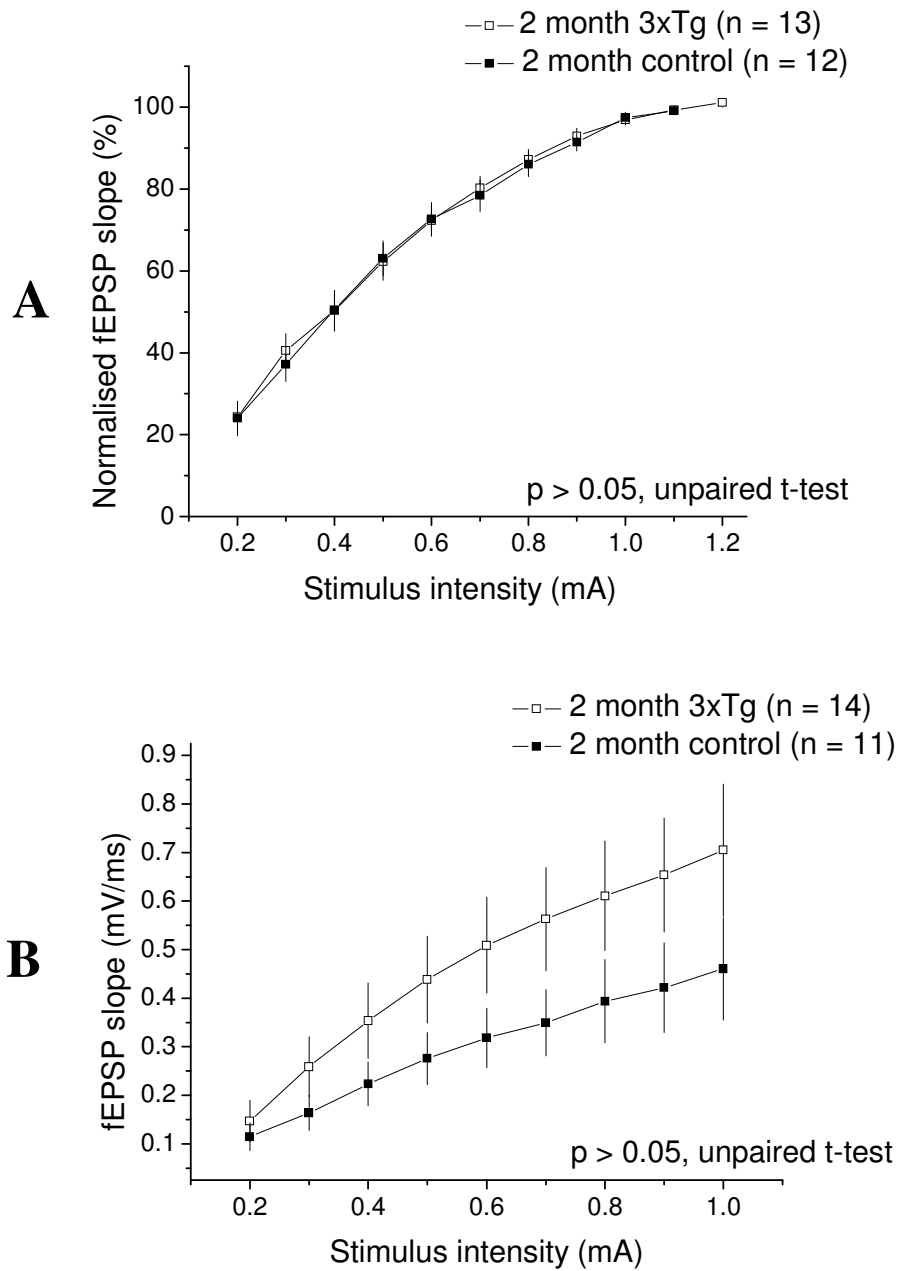


**Figure 3.2: Normalised and non-normalised input-output curves obtained from 2 month old 3xTg and control mice.** The fEPSP slope was measured at a range of stimulus intensities and then normalised in control (n = 12/7) and 3xTg mice (n = 13/8) (**A**). The non-normalised fEPSP slope measurement in control (n = 11/7) and 3xTg mice (n = 14/8) is shown in (**B**).  $p > 0.05$ , unpaired t-test.

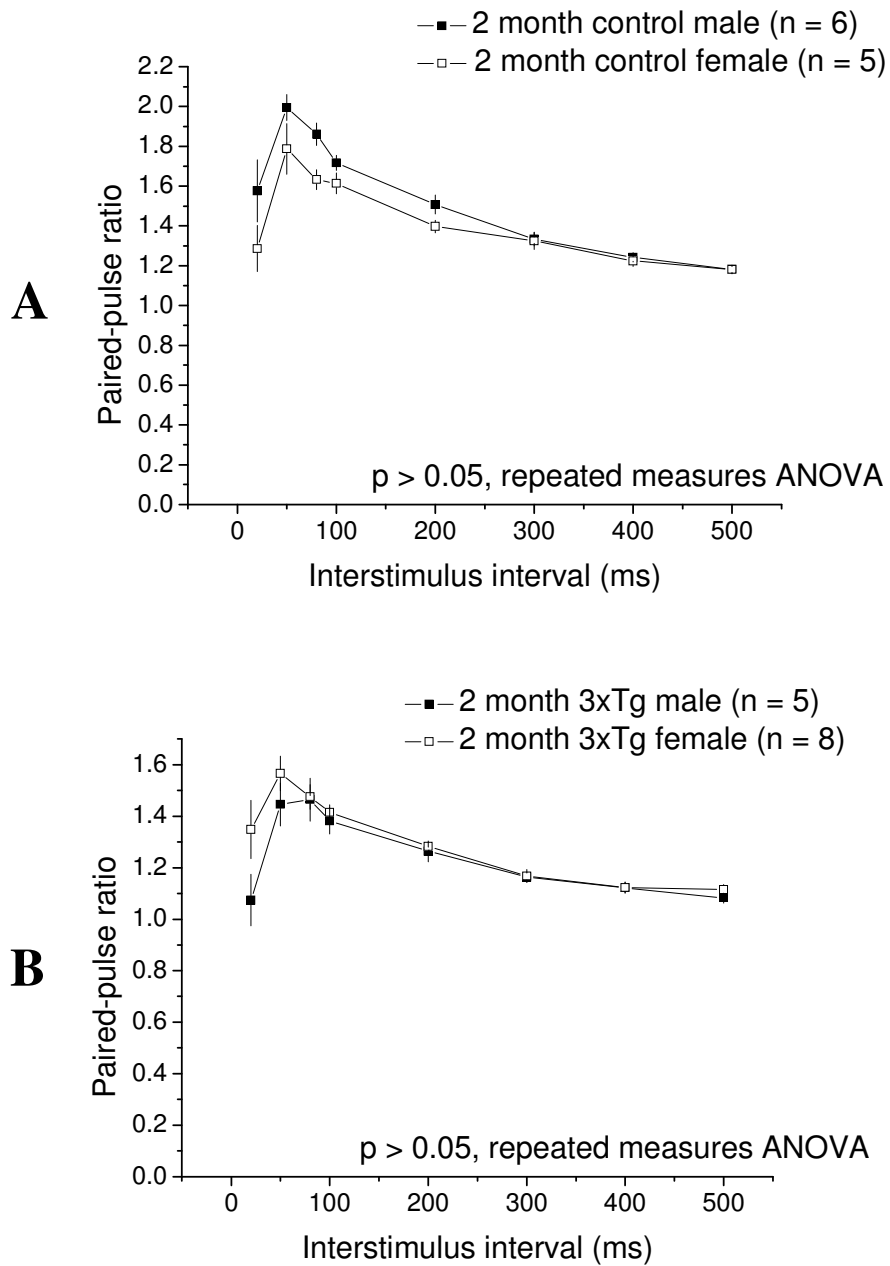


**Figure 3.3: Paired-pulse facilitation determined in 2 month old male and female 3xTg and control mice.** The paired-pulse ratio was calculated at a range of interstimulus intervals in (A) male (n = 6/3) and female (n = 5/3) control mice and (B) in male (n = 5/3) and female (n = 8/5) 3xTg mice.  $p > 0.05$ , repeated measures ANOVA.

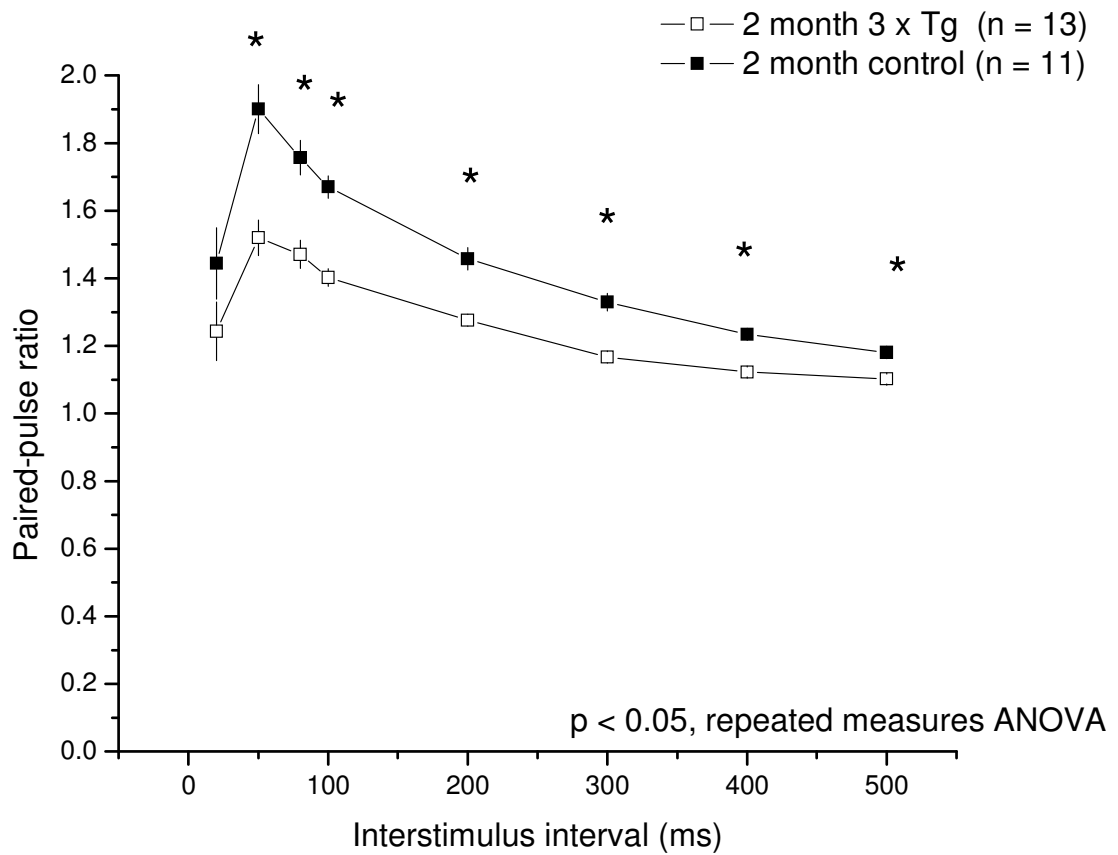


**Figure 3.4: Paired-pulse facilitation determined in 2 month old 3xTg and control mice.** The paired-pulse ratio was calculated at a range of interstimulus intervals in control mice (n = 11/6) and 3xTg mice (n = 13/8). \* =  $p < 0.05$ , repeated measures ANOVA followed by unpaired t-test at individual intervals.

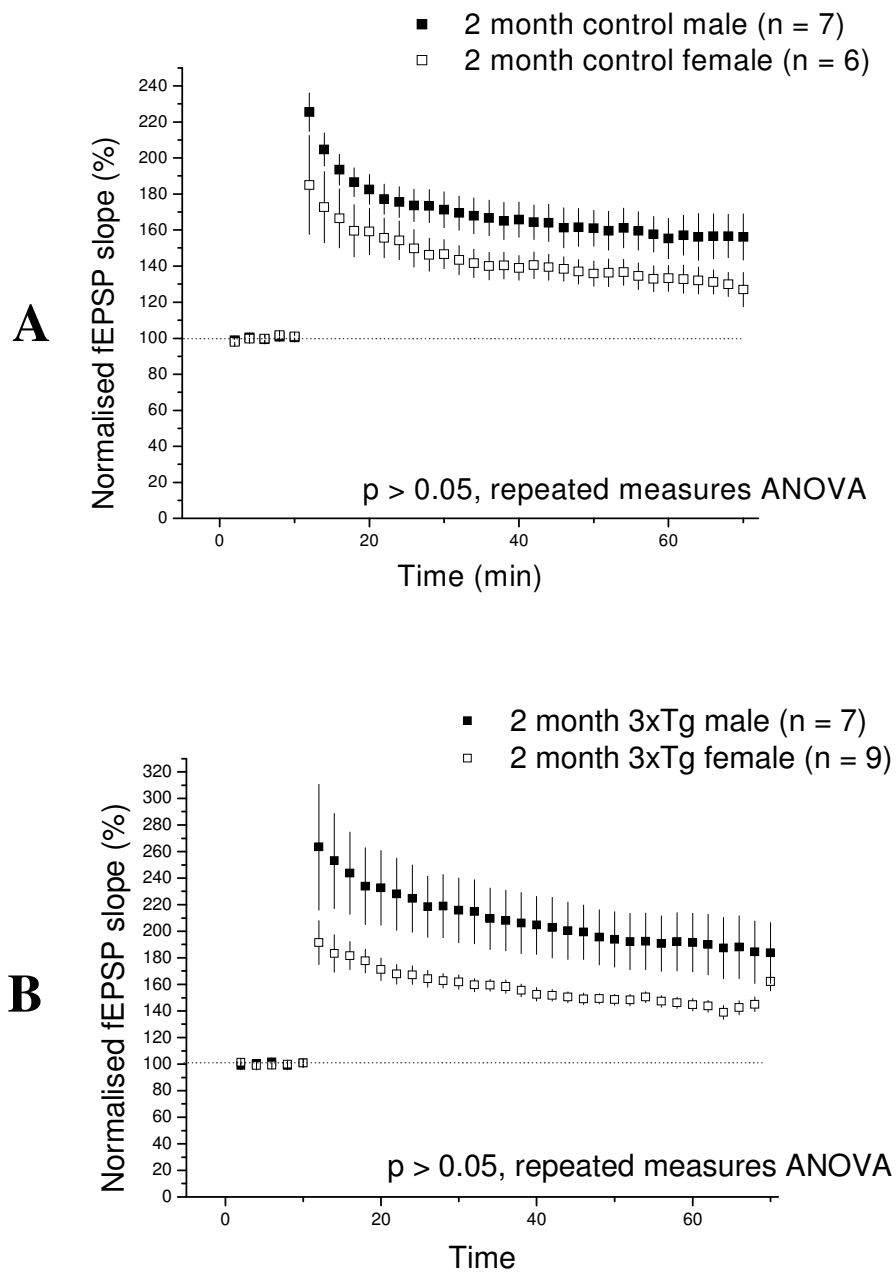


**Figure 3.5: The influence of gender on long-term potentiation recorded from 2 month old 3xTg and control mice.** The potentiation of the fEPSP slope obtained following four-pulse theta burst was measured in **(A)** control male (n = 7/5) and female mice (n = 6/3) and **(B)** 3xTg male (n = 7/3) and female mice (n = 9/5). All data are normalised to the average slope of the fEPSP for each genotype prior to delivery of the theta burst stimulus.  $p > 0.05$ , repeated measures ANOVA.

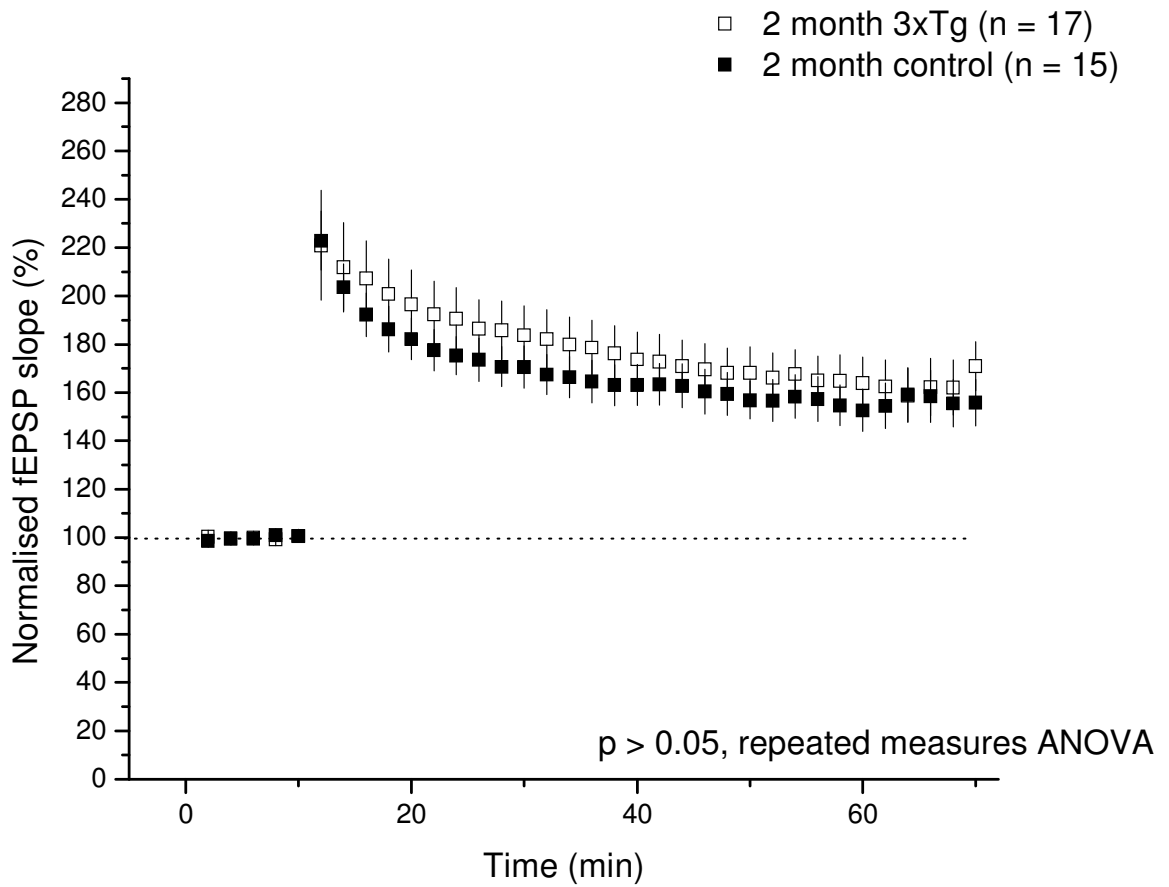


**Figure 3.6: Long-term potentiation in 2 month old 3xTg and control mice.** The enhancement of the fEPSP slope following a 4 pulse theta burst protocol was measured in control mice (n = 15/8) and 3xTg mice (n = 17/8). All data are normalised to the average slope of the fEPSP for each genotype prior to delivery of the theta burst stimulus.  $p > 0.05$ , repeated measures ANOVA.

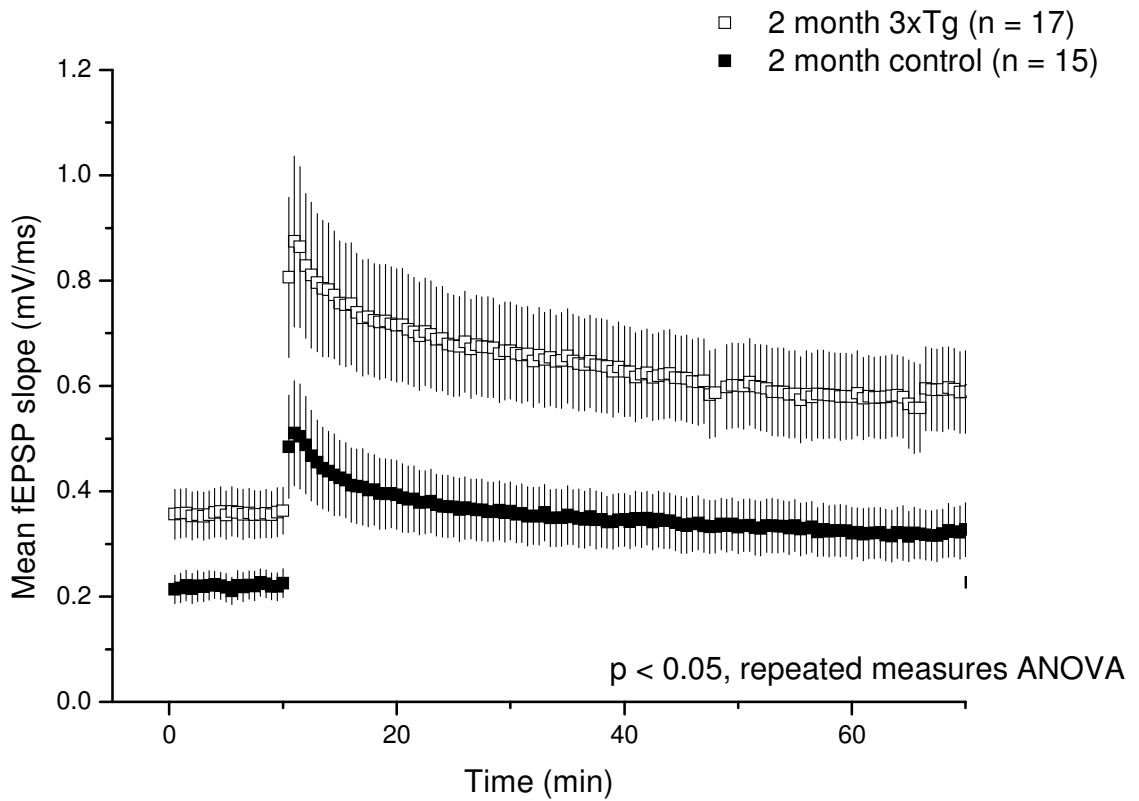


**Figure 3.7: A comparison of long-term potentiation in 2 month old 3xTg and control mice (non-normalised).** The enhancement of the fEPSP slope following 4 pulse theta burst was measured in control (n = 15/8) and 3xTg mice (n = 17/8) and is presented here as the actual values obtained in mV/ms.  $p < 0.05$ , repeated measures ANOVA.

### 3.2.3: Electrophysiological characterisation of 6 month old 3xTg mice

Following experiments with 2 month old 3xTg mice, another subset of mice were allowed to age to 6 months and studies were carried out to observe any differences between the transgenic and control mice.

#### 3.2.3.1: Input-output function

Input-output curves were generated and compared for 6 month old 3xTg mice and 6 month old control mice of both genders. A normalised input-output curve, where the maximum field slope is set to 100%, was generated, coupled with a non-normalised input-output curve using the actual values (mV/ms) obtained.

In 6 month control mice, there is no significant difference ( $p > 0.05$ , unpaired t-test) between the normalised input-output curve of male ( $n = 5/3$ ) and female ( $n = 9/4$ ) mice (Fig. **3.8A**). Similarly, in 6 month 3xTg mice, there is no significant difference ( $p > 0.05$ , unpaired t-test) between the normalised input-output curve of male ( $n = 5/3$ ) and female ( $n = 12/4$ ) mice (Fig. **3.8B**).

Given these findings the male and female data were pooled together. When the two groups are compared, there is no significant difference ( $p > 0.05$ , unpaired t-test) between the normalised input-output curve of the 3xTg ( $n = 15/7$ ) and control ( $n = 15/7$ ) mice (Fig. **3.9A**).

For the non-normalised input-output curve, the control mice exhibit an fEPSP slope at 1 mA of  $0.60 \pm 0.05$  mV/ms, while the 3xTg mice exhibit an fEPSP slope at 1 mA of  $0.41 \pm 0.05$  mV/ms. There is no significant difference ( $p > 0.05$ ,

unpaired t-test) between the two groups, although there is a trend for a reduced fEPSP slope at higher stimulus intensities in the 3xTg mice ( $p = 0.058$  at 1mA, unpaired t-test) (Fig. **3.9B**).

### **3.2.3.2: Paired-pulse facilitation**

Paired-pulse facilitation was compared between 6 month old 3xTg mice and control mice, and the effect of gender on both genotypes was determined. In all experiments the maximum facilitation was observed at an interstimulus interval of 50ms.

In control mice, the paired-pulse ratio at 50ms is  $1.47 \pm 0.05$  for male ( $n = 5/3$ ) and  $1.52 \pm 0.03$  for female ( $n = 8/4$ ) mice (Fig. **3.10A**). There is no significant difference ( $p > 0.05$ , repeated measures ANOVA) in the paired-pulse ratio in male or female control mice at interstimulus intervals from 20 – 500ms.

In the 3xTg mice, the paired-pulse ratio at 50ms is  $1.52 \pm 0.08$  for male ( $n = 6/3$ ) and  $1.60 \pm 0.12$  for female ( $n = 7/4$ ) mice (Fig. **3.10B**). There is no significant difference ( $p > 0.05$ , repeated measures ANOVA) in the paired-pulse ratio in male or female 3xTg mice at interstimulus intervals from 20 – 500ms.

Given that gender did not influence the paired-pulse ratio for either genotype, the data for male and female mice were combined. Collectively, the paired-pulse ratio at 50ms is  $1.49 \pm 0.03$  for control ( $n = 13/7$ ) and  $1.56 \pm 0.07$  for 3xTg ( $n = 13/7$ ) mice. There is no significant difference in the paired-pulse ratio between the 3xTg and control mice ( $p > 0.05$ , repeated measures ANOVA) at any interstimulus interval measured from 20-500 ms (Fig. **3.11**).

### 3.2.3.3: Long-term potentiation

LTP was measured in the CA1 region for 6 month 3xTg and control mice. These experiments were divided by gender and both normalised and non-normalised data was generated.

In all experiments a baseline fEPSP was recorded at 30 second intervals until the slope of the fEPSP was stabilised and constant over a 10 min period before delivery of the theta burst stimulus. In the following section the slope of the fEPSP is normalised to baseline (i.e. 100%) for each recording.

In 6 month control male mice ( $n = 6/5$ ), the peak enhancement of the slope of the fEPSP is  $222 \pm 14\%$ , with a mean from 50-60 minutes following the theta burst stimulus of  $165 \pm 6\%$ . In 6 month control female mice ( $n = 8/3$ ), the peak enhancement is  $229 \pm 29\%$ , with a mean from 50-60 minutes of  $178 \pm 10\%$  (Fig. **3.12A**).

In 6 month 3xTg male mice ( $n = 8/4$ ), the peak enhancement of the slope of the fEPSP is  $258 \pm 36\%$ , with a mean from 50-60 minutes following the theta burst of  $181 \pm 25\%$ . In 6 month 3xTg female mice ( $n = 12/4$ ), the peak enhancement is  $250 \pm 34\%$ , with a mean from 50-60 minutes of  $151 \pm 16\%$  (Fig. **3.12B**).

There is no significant difference ( $p > 0.05$ , repeated measures ANOVA) between the magnitude of LTP in any of the four groups.

Combining the results obtained for each gender, a comparison was then made between the 3xTg and control mice. In 6 month control mice ( $n = 14/8$ ), the peak enhancement of the slope of the fEPSP is  $225\% \pm 14\%$ , with a mean from 50-60 minutes following the theta burst stimulus of  $170 \pm 6\%$ . In 6 month 3xTg mice ( $n$

= 20/8), the peak enhancement is  $254 \pm 25\%$ , with a mean from 50-60 minutes of  $164 \pm 14\%$ .

There is no significant difference ( $p > 0.05$ , repeated measures ANOVA) between the magnitude of LTP in 6 month 3xTg and 6 month control mice (Fig. 3.13). This is the case for all phases of LTP, from the initial peak to the plateau phase.

#### 3.2.3.4: Non-normalised long-term potentiation

When the slope of the fEPSP is not normalised to control and the actual values (mV/ms) are utilised, in 6 month control mice the mean baseline fEPSP is  $0.23 \pm 0.04$  mV/ms, the peak enhancement following the theta burst stimulus is  $0.52 \pm 0.06$  mV/ms, and the mean from 50-60 minutes is  $0.41 \pm 0.07$  mV/ms. In 6 month 3xTg mice the mean baseline fEPSP is  $0.20 \pm 0.02$  mV/ms, the peak enhancement is  $0.52 \pm 0.07$  mV/ms, and the mean from 50-60 minutes is  $0.38 \pm 0.05$  mV/ms. (Fig. 3.14).

There is no significant difference ( $p > 0.05$ , repeated measures ANOVA) between LTP in the 6 month 3xTg and control mice using the non-normalised LTP values.

**3.2.3.5: Summary**

At 6 months of age there are no differences in hippocampal CA1 synaptic function apparent in the 3xTg mice. In addition, no gender-dependent effects were observed so both male and female data were pooled together. The 3xTg mice show no alterations in PPF, in input-output function or in normalised or non-normalised LTP values. These data show that in our colony of 3xTg mice there are no electrophysiological changes which could be linked to the reported development of pathological features at this age.

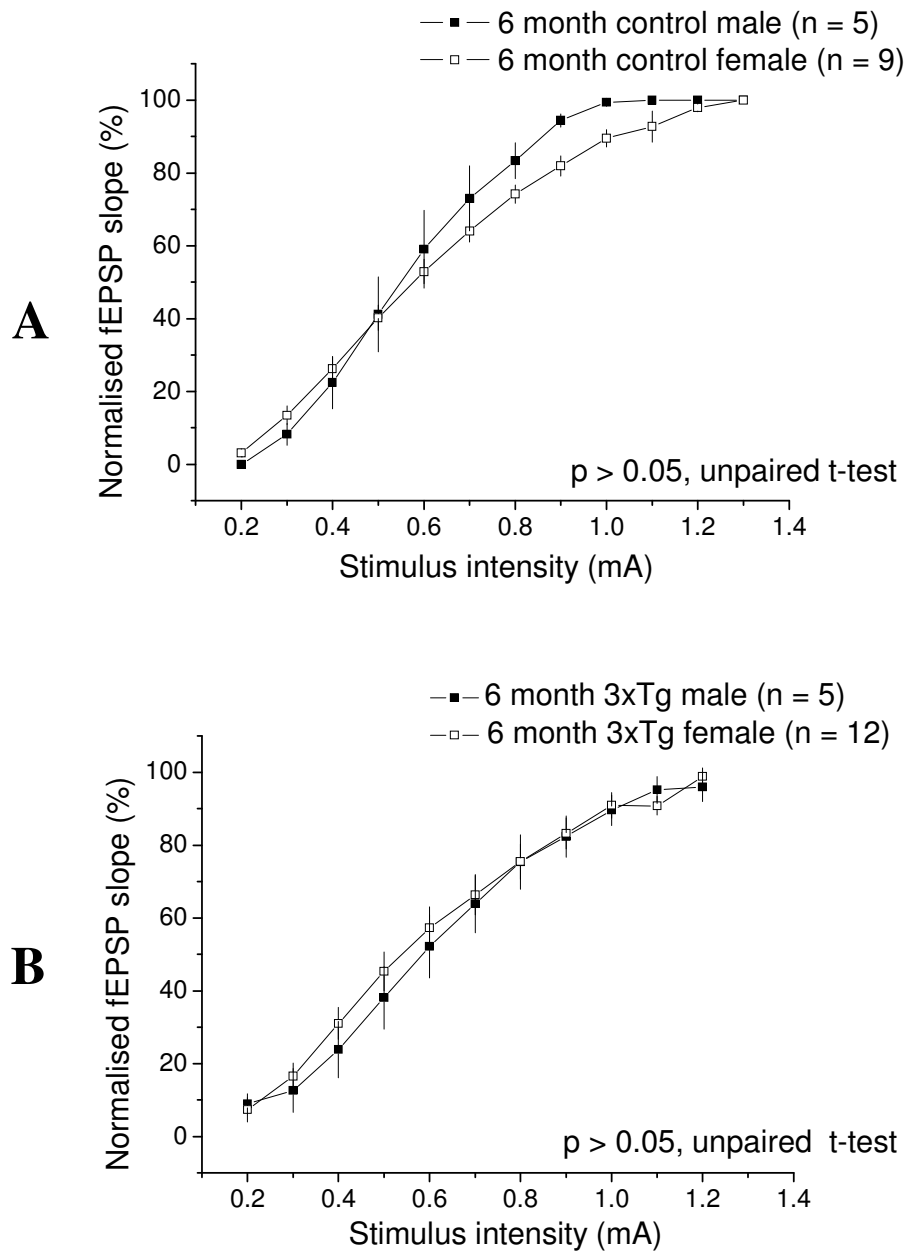


**Figure 3.8: Normalised input-output curves obtained from 6 month old male and female 3xTg and control mice.** The fEPSP slope was measured at a range of stimulus intensities and then normalised in **(A)** male (n = 5/3) and female (n = 9/4) control mice and **(B)** male (n = 5/3) and female (n = 12/4) 3xTg mice.  $p > 0.05$ , unpaired t-test.

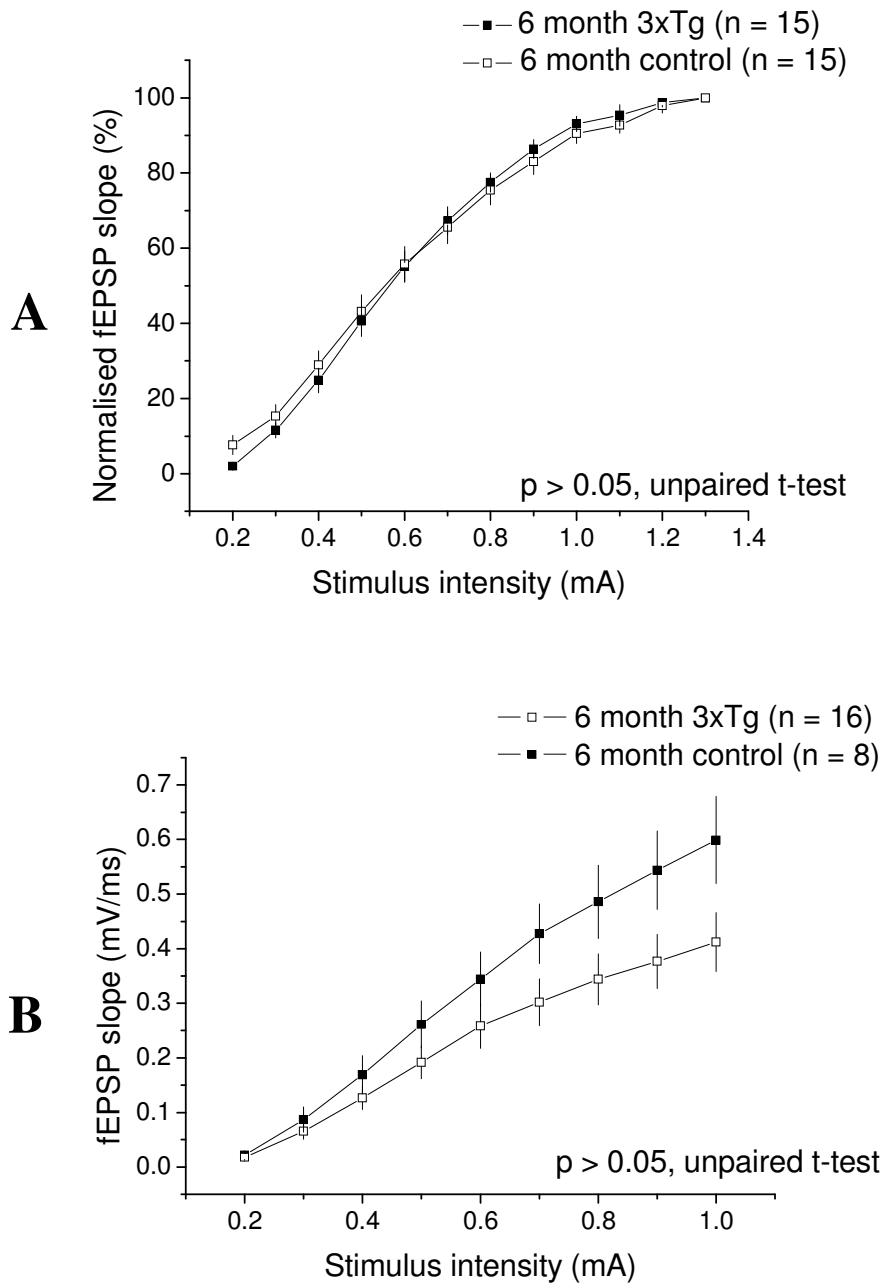


**Figure 3.9: Normalised and non-normalised input-output curves obtained from 6 month old 3xTg and control mice.** The fEPSP slope was measured at a range of stimulus intensities and then normalised in control (n = 15/7) and 3xTg mice (n = 15/7) (A). The non-normalised fEPSP slope measurement in control (n = 8/4) and 3xTg mice (n = 16/ 8) is shown in (B).  $p > 0.05$ , unpaired t-test.

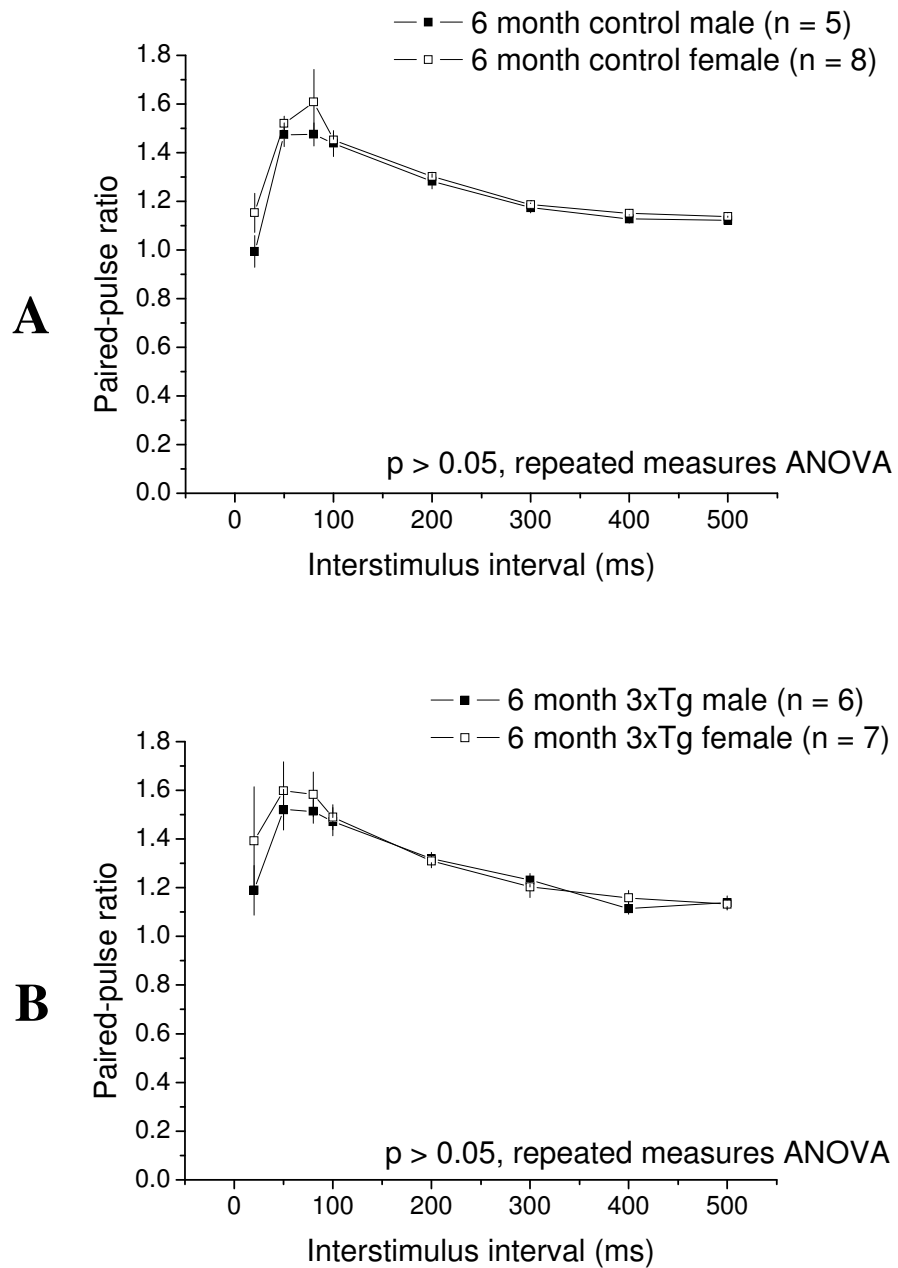


**Figure 3.10: Paired-pulse facilitation determined in 6 month old male and female 3xTg and control mice.** The paired-pulse ratio was calculated at a range of interstimulus intervals in (A) male (n = 5/3) and female (n = 8/4) control mice and (B) in male (n = 6/3) and female (n = 7/4) 3xTg mice.  $p > 0.05$ , repeated measures ANOVA.

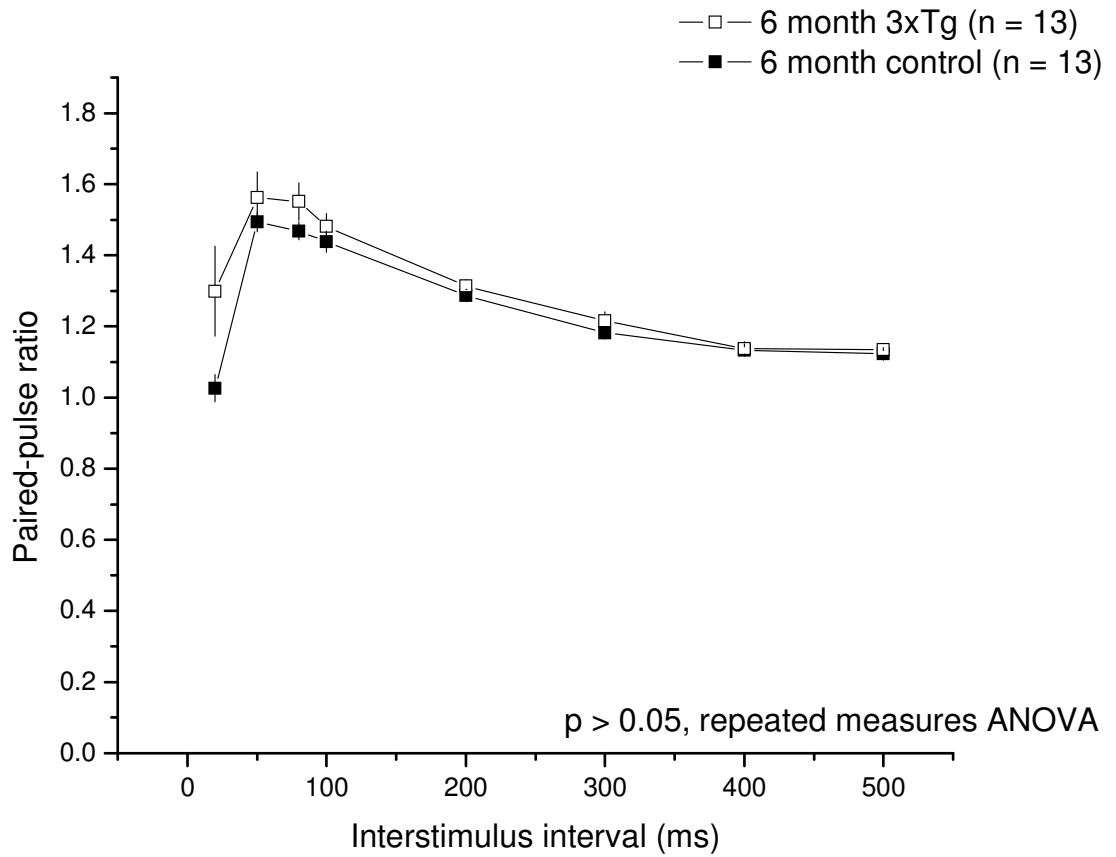


**Figure 3.11: Paired-pulse facilitation determined in 6 month old 3xTg and control mice.** The paired-pulse ratio was calculated at a range of interstimulus intervals in control mice (n = 13/7) and 3xTg mice (n = 13/7).  $p > 0.05$ , repeated measures ANOVA.

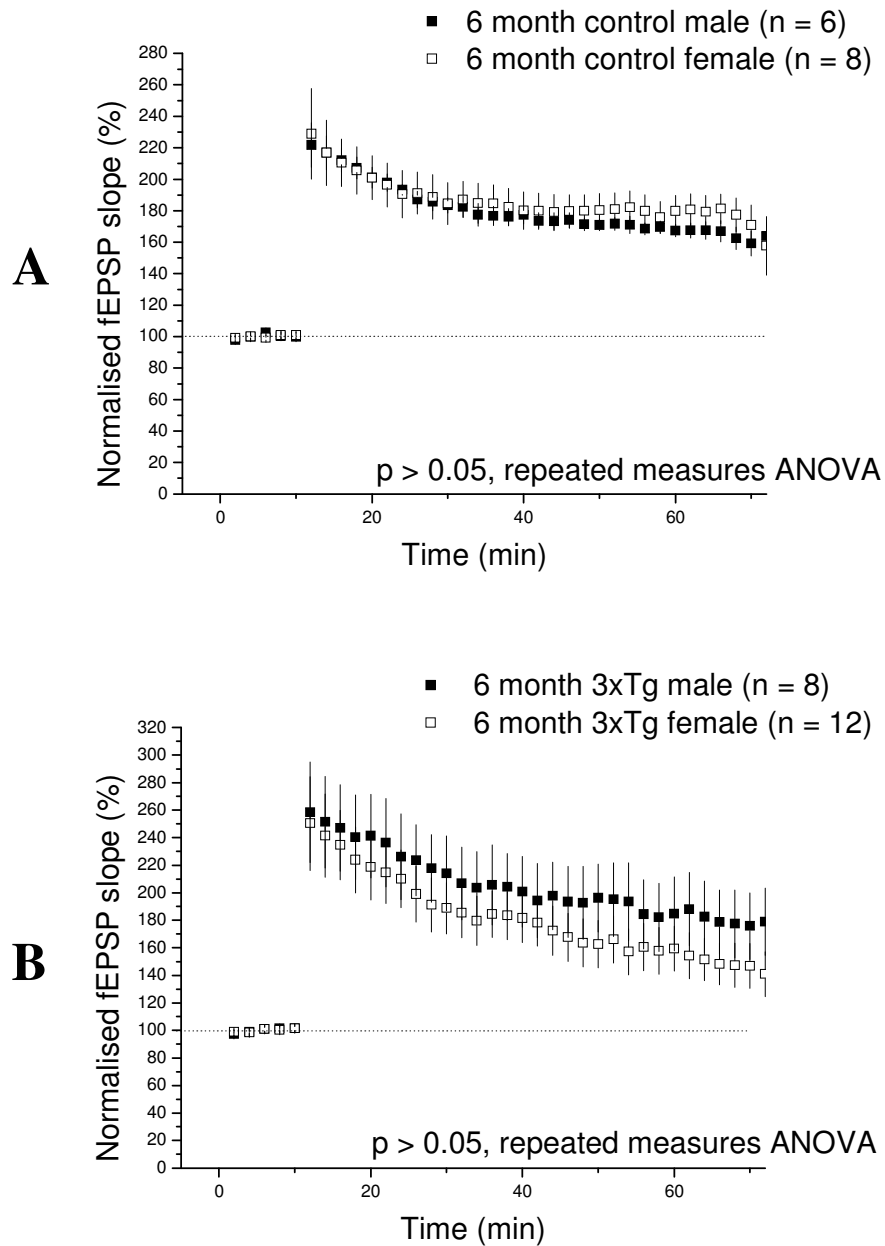


**Figure 3.12: The influence of gender on long-term potentiation recorded from 6 month old 3xTg and control mice.** The potentiation of the fEPSP slope obtained following four-pulse theta burst was measured in **(A)** control male (n = 6/5) and female mice (n = 8/3) and **(B)** 3xTg male (n = 8/4) and female mice (n = 12/4). All data are normalised to the average slope of the fEPSP for each genotype prior to delivery of the theta burst stimulus.  $p > 0.05$ , repeated measures ANOVA.

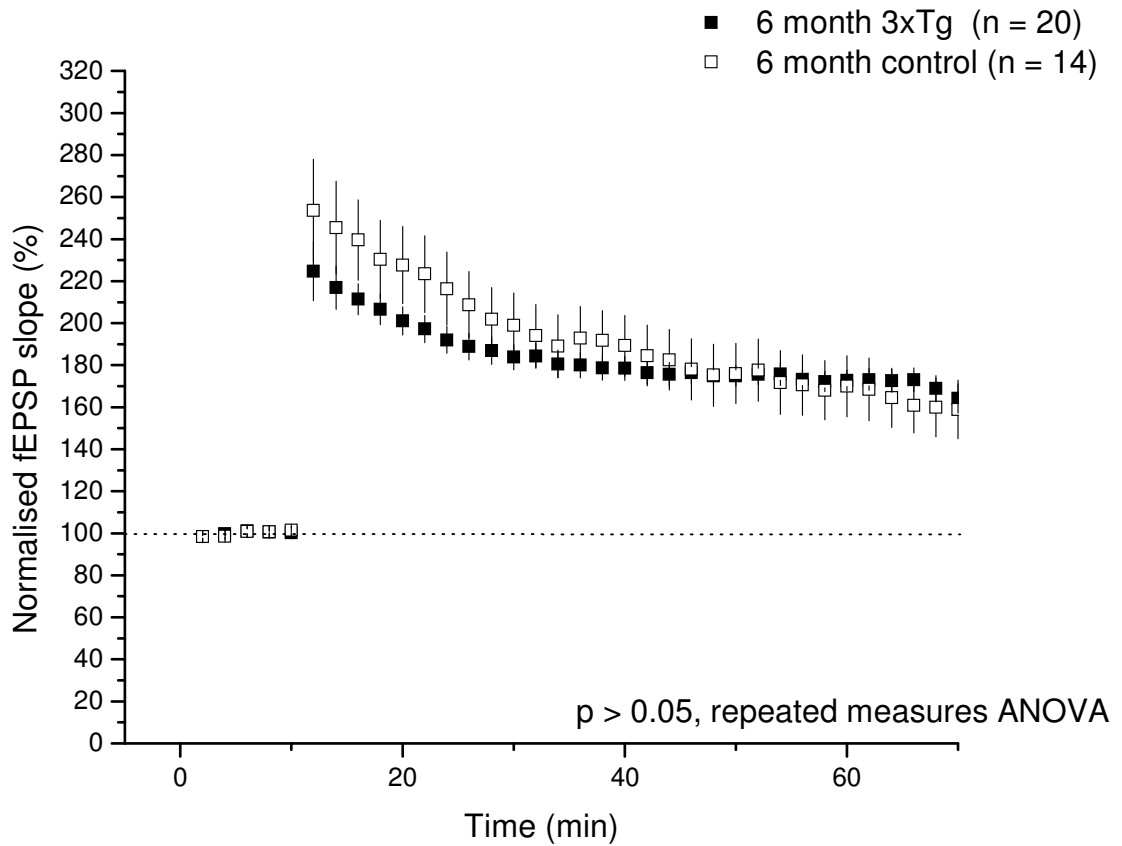


**Figure 3.13: Long-term potentiation in 6 month old 3xTg mice and control.**

The potentiation of the fEPSP slope following four pulse theta burst was measured in control mice (n = 14/8) and 3xTg mice (n = 20/8). All data are normalised to the average slope of the fEPSP for each genotype prior to delivery of the theta burst stimulus.  $p > 0.05$ , repeated measures ANOVA.

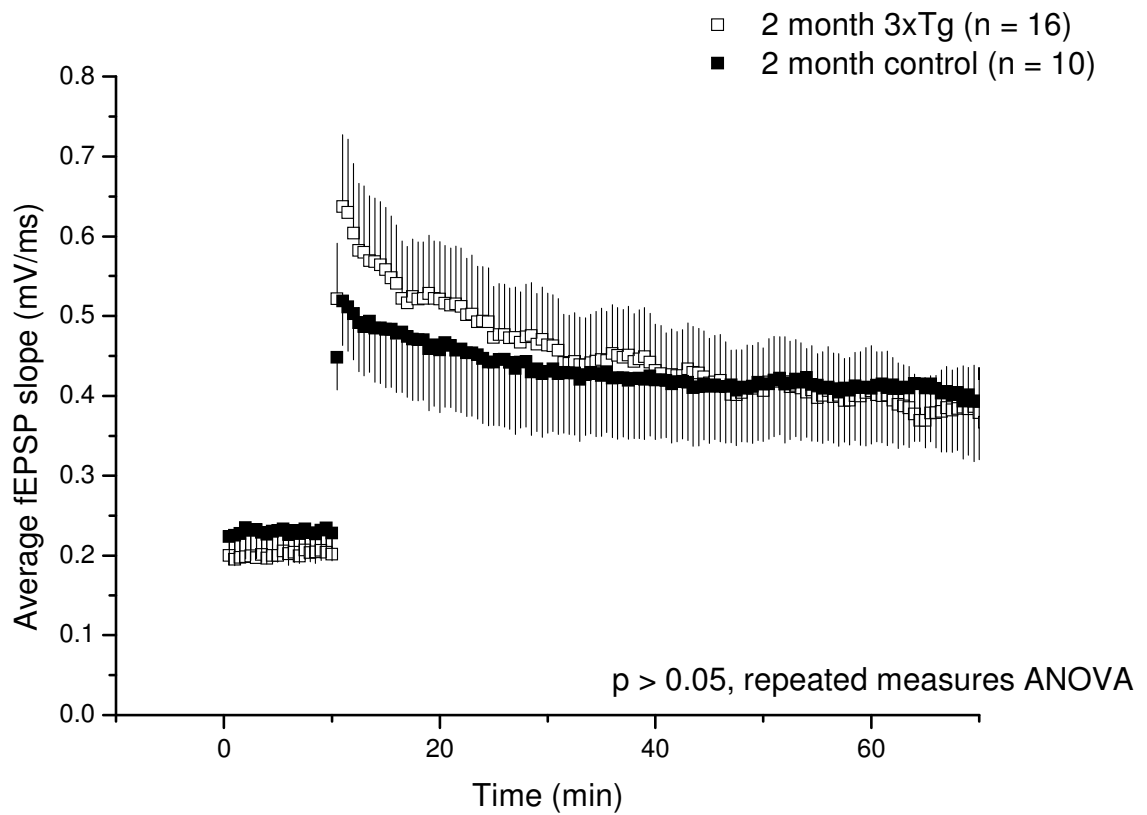


**Figure 3.14: A comparison of long-term potentiation in 6 month old 3xTg and control mice (non-normalised).** The potentiation of the fEPSP slope following four pulse theta burst was measured in control (n = 10/8) and 3xTg mice (n = 16/8) and is presented here as the actual values obtained.  $p > 0.05$ , repeated measures ANOVA.

### **3.2.4: Electrophysiological characterisation of 12 month old 3xTg mice**

#### **3.2.4.1: Input-output function**

As there was no difference in input-output function or LTP at 6 months of age in 3xTg mice, it was decided to use older mice for the study to see if the electrophysiological deficits previously reported (Oddo *et al.*, 2003) could be obtained. At 12 months 3xTg mice are reported to show not only intraneuronal amyloid accumulation, but the deposition of amyloid plaques in cortex and hippocampus (Oddo *et al.*, 2003). Electrophysiological measurements were therefore carried out at 12 months when the pathology was expected to be well established.

Input-output curves were generated and compared for 12 month old 3xTg mice and control mice of both genders. A normalised input-output curve, where the maximum field slope is set to 100%, was generated, along with a non-normalised input-output curve using the actual values obtained.

In 12 month old control mice, there is no significant difference ( $p > 0.05$ , unpaired t-test) between the normalised input-output curve of male ( $n = 6/3$ ) and female ( $n = 8/4$ ) mice (Fig. **3.15A**). Similarly for the 12 month old 3xTg mice there is no significant difference ( $p > 0.05$ , unpaired t-test) between the normalised input-output curve of male ( $n = 6/3$ ) and female ( $n = 5/4$ ) mice (Fig. **3.15B**).

The male and female data were pooled together, which resulted in a significant reduction ( $p < 0.05$ , unpaired t-test) in the normalised fEPSP slope in the 12 month 3xTg mice ( $n = 11/7$ ) compared with control mice ( $n = 14/7$ ) (Fig. **3.16A**).

For the non-normalised input-output curve, the control 12 month old mice exhibit an fEPSP slope at 1 mA of  $0.40 \pm 0.04$  mV/ms while the 3xTg mice exhibit a fEPSP slope at 1 mA of  $0.17 \pm 0.02$  mV/ms (Fig. **3.16B**). There is again a significant reduction ( $p < 0.05$ , unpaired t-test) in the fEPSP slope in the 12 month 3xTg mice compared with control.

#### **3.2.4.2: Paired-pulse facilitation**

Paired-pulse facilitation was compared between 12 month old 3xTg mice and 12 month old control mice, and the effect of gender was also investigated. In all experiments, the maximum facilitation was observed at an inter-stimulus interval of 50ms.

In control mice, the paired-pulse ratio at 50ms is  $1.70 \pm 0.07$  for male ( $n = 8/3$ ) and  $1.62 \pm 0.09$  for female ( $n = 6/3$ ) mice. There is no significant difference ( $p > 0.05$ , repeated measures ANOVA) in the paired-pulse ratio in male or female control mice at interstimulus intervals from 20 – 500ms (Fig. **3.17A**).

In the 3xTg mice, the paired-pulse ratio at 50ms is  $1.71 \pm 0.10$  for male ( $n = 7/3$ ) and  $1.65 \pm 0.11$  for female ( $n = 6/3$ ) mice. There is no significant difference ( $p > 0.05$ , repeated measures ANOVA) in the paired-pulse ratio in male, or female 3xTg mice at interstimulus intervals from 20 – 500ms (Fig. **3.17B**).

Given that gender did not influence the paired-pulse ratio for either genotype, the data for male and female mice were combined. Collectively, the paired-pulse ratio at 50ms is  $1.67 \pm 0.05$  for control (n = 14/6) and  $1.68 \pm 0.07$  for 3xTg (n = 13/6) mice. There is no significant difference in the paired-pulse ratio in 3xTg when compared to control mice ( $p > 0.05$ , repeated measures ANOVA) at any inter-stimulus interval measured from 20-500 ms (Fig. **3.18**).

### **3.2.4.3: Long-term potentiation**

LTP was measured in the CA1 region for 12 month old 3xTg and control mice. These experiments were divided by gender and both normalised and non-normalised data was generated.

In all experiments a baseline fEPSP was recorded at 30 second intervals until the slope of the fEPSP was stabilised and constant over a 10 min period before delivery of the 4 pulse theta burst stimulus. In the following section the slope of the fEPSP is normalised to baseline (i.e. 100%) for each recording.

In 12 month control male mice (n = 11/3), the peak enhancement of the slope of the fEPSP is  $252 \pm 24\%$ , with a mean from 50-60 minutes following the theta burst stimulus of  $184 \pm 12\%$ . In 12 month control female mice (n = 6/4), the peak enhancement is  $197 \pm 19\%$ , with a mean from 50-60 minutes of  $163 \pm 10\%$  (Fig. **3.19A**).

In 12 month 3xTg male mice (n = 6/3), the peak enhancement of the slope of the fEPSP is  $314 \pm 27\%$ , with a mean from 50-60 minutes following the theta burst stimulus of  $240 \pm 7\%$ . In 12 month 3xTg female mice (n = 5/3), the peak

enhancement is  $287 \pm 35\%$ , with an average from 50-60 minutes of  $155 \pm 13\%$  (Fig. **3.19B**).

There is a significant difference ( $p < 0.05$ , repeated measures ANOVA) between the magnitude of LTP in male and female 3xTg mice, with enhancement greater in males in the plateau phase following theta burst stimulation. There is no significant difference ( $p > 0.05$ , repeated measures ANOVA) between LTP in male and female control mice.

Combining the results for both genders, a comparison was then made between the 3xTg and control mice. In 12 month control mice ( $n = 17/7$ ), the peak enhancement of the fEPSP slope is  $233 \pm 18\%$ , with a mean from 50-60 minutes of  $177 \pm 8\%$ . In 12 month 3xTg mice ( $n = 11/6$ ), the peak enhancement is  $302 \pm 21\%$ , with a mean from 50-60 minutes of  $210 \pm 13\%$  (Fig **3.20**).

There is a significant difference ( $p < 0.05$ , repeated measures ANOVA) in the magnitude of LTP in the initial phase from 0-20 minutes following theta burst stimulation, with LTP greater in 3xTg mice than in control mice. This is caused by the increased potentiation observed in male 3xTg mice.

#### **3.2.4.4: Non-normalised long-term potentiation**

When the slope of the fEPSP is not normalised to control and the actual values (mV/ms) are utilised, in 12 month control mice, the mean baseline fEPSP is  $0.31 \pm 0.04$  mV/ms, the peak enhancement following four pulse theta burst is  $0.76 \pm 0.10$  mV/ms, and the mean from 50-60 minutes is  $0.55 \pm 0.07$  mV/ms. In 12 month 3xTg mice the mean baseline fEPSP is  $0.11 \pm 0.01$  mV/ms, the peak

enhancement is  $0.34 \pm 0.04$  mV/ms, and the mean from 50-60 minutes is  $0.24 \pm 0.04$  mV/ms.

There is a clear reduction in the magnitude of LTP in the 12 month old 3xTg mice compared with control which is statistically significant ( $p < 0.05$ , repeated measures ANOVA) (Fig. 3.21).

#### **3.2.4.5: Summary**

There are several differences in hippocampal CA1 synaptic function observed in 12 month 3xTg mice. Although there are no changes in PPF, there is a significant reduction in the fEPSP slope as measured in both the normalised and the non-normalised input-output curve. This is mirrored in the non-normalised LTP data where the values for 3xTg are significantly lower than control. However, the normalised LTP graph shows that the magnitude of LTP is slightly increased relative to baseline measurements. This data shows that an age-dependent reduction in basal synaptic transmission and alterations in LTP are apparent by 12 months in the 3xTg mice.

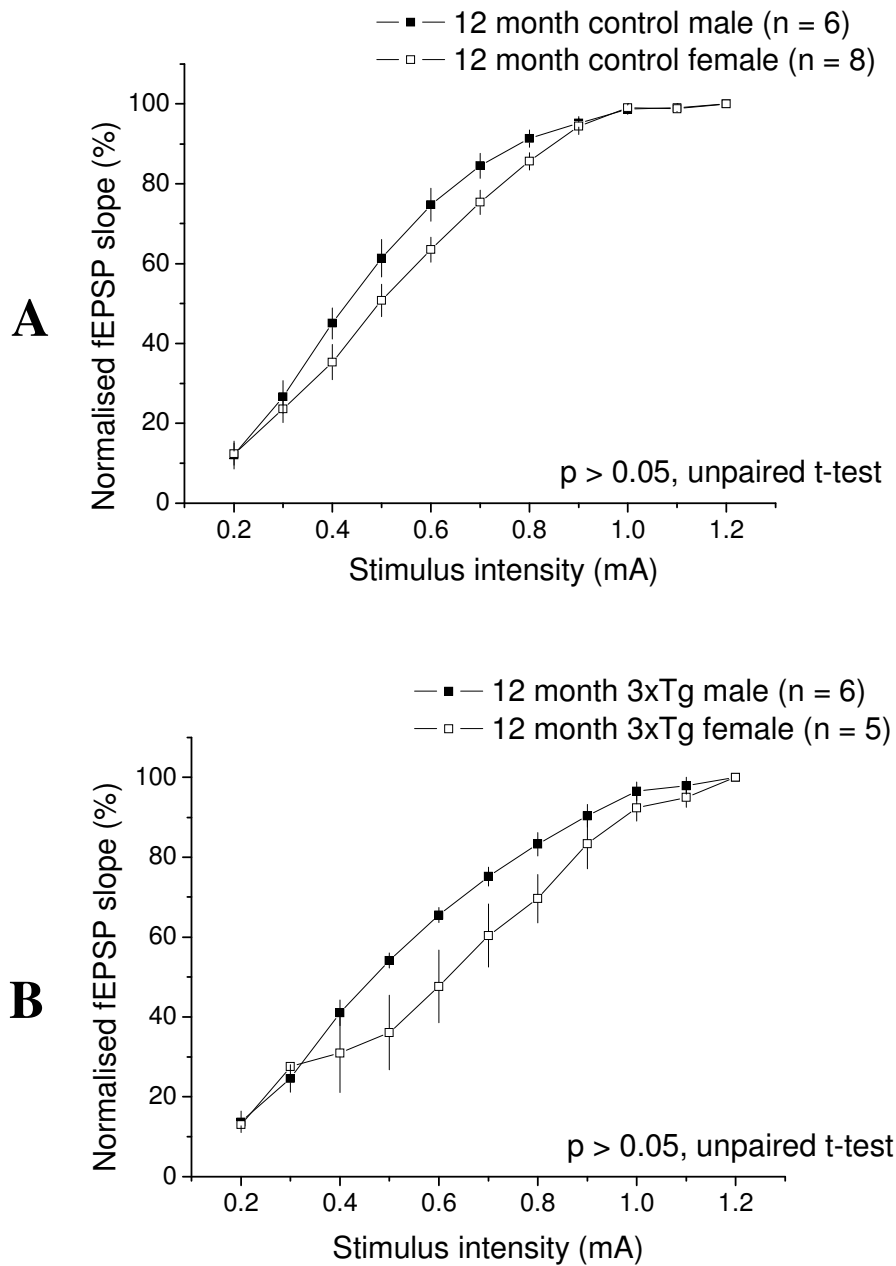


**Figure 3.15: Normalised input-output curves obtained from 12 month old male and female 3xTg and control mice.** The fEPSP slope was measured at a range of stimulus intensities and then normalised in (A) male (n = 5/3) and female (n = 8/4) control mice and (B) male (n = 6/3) and female (n = 5/4) 3xTg mice.  $p > 0.05$ , unpaired t-test.

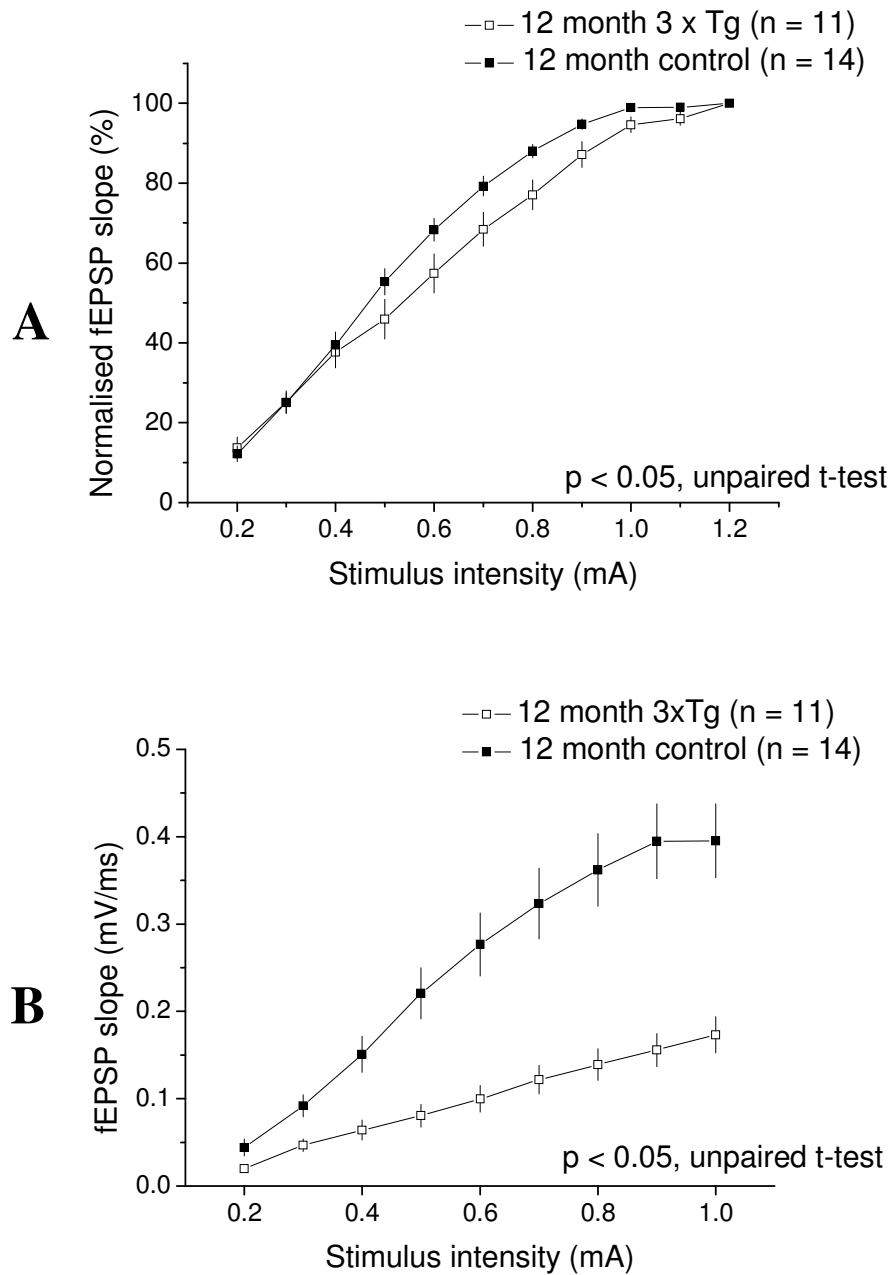


**Figure 3.16: Normalised and non-normalised input-output curves obtained from 12 month old 3xTg and control mice.** The fEPSP slope was measured at a range of stimulus intensities and then normalised for both the 3xTg mice (n = 11/6) and the control mice (n = 14/7) (**A**). The non-normalised fEPSP slope measurement in control (n = 14/7) and 3xTg mice (n = 11/6) is shown in (**B**).  $p < 0.05$ , unpaired t-test.

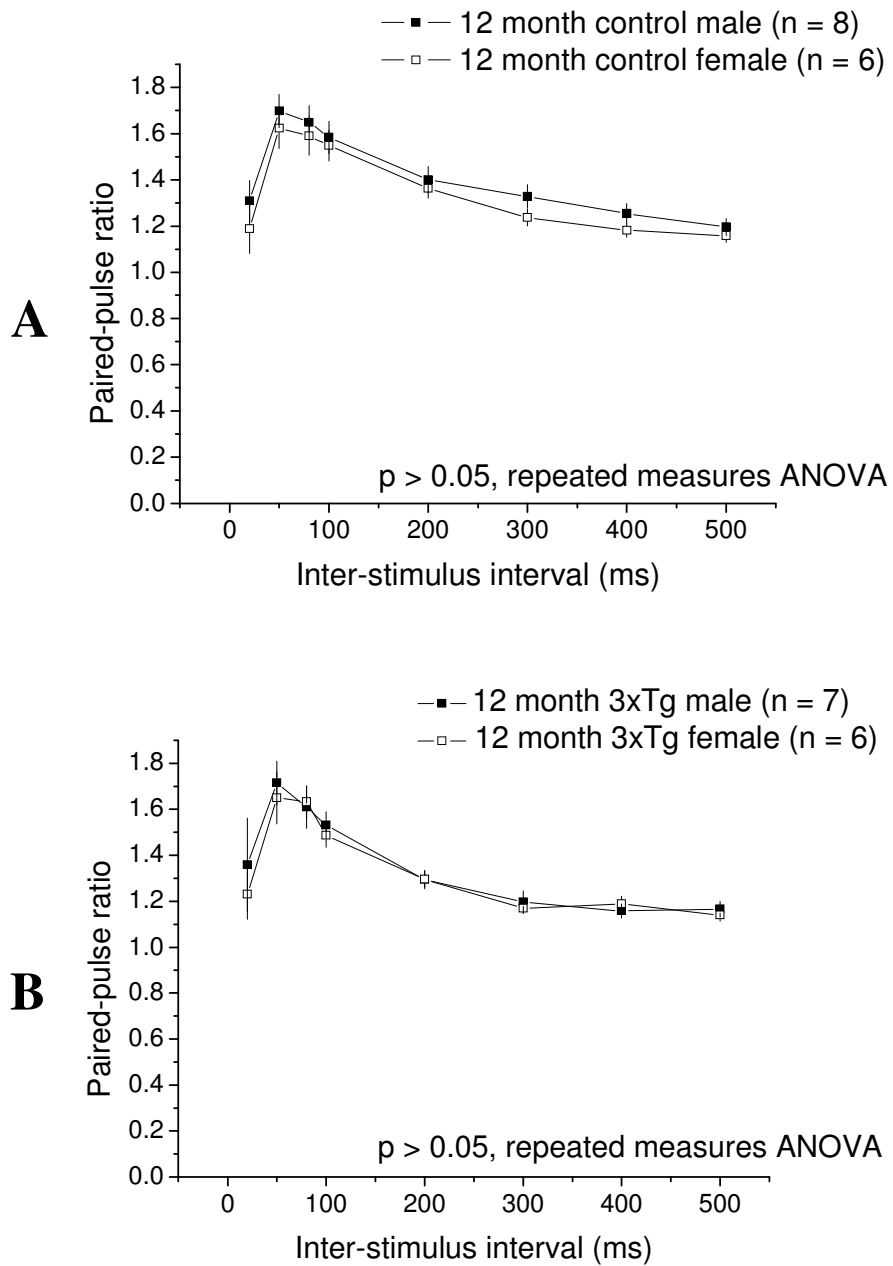


**Figure 3.17: Paired-pulse facilitation determined in 12 month old male and female 3xTg and control mice.** The paired-pulse ratio was calculated at a range of interstimulus intervals in (A) male (n = 8/3) and female (n = 6/3) control mice and (B) male (n = 7/3) and female (n = 6/3) 3xTg mice.  $p > 0.05$ , repeated measures ANOVA.

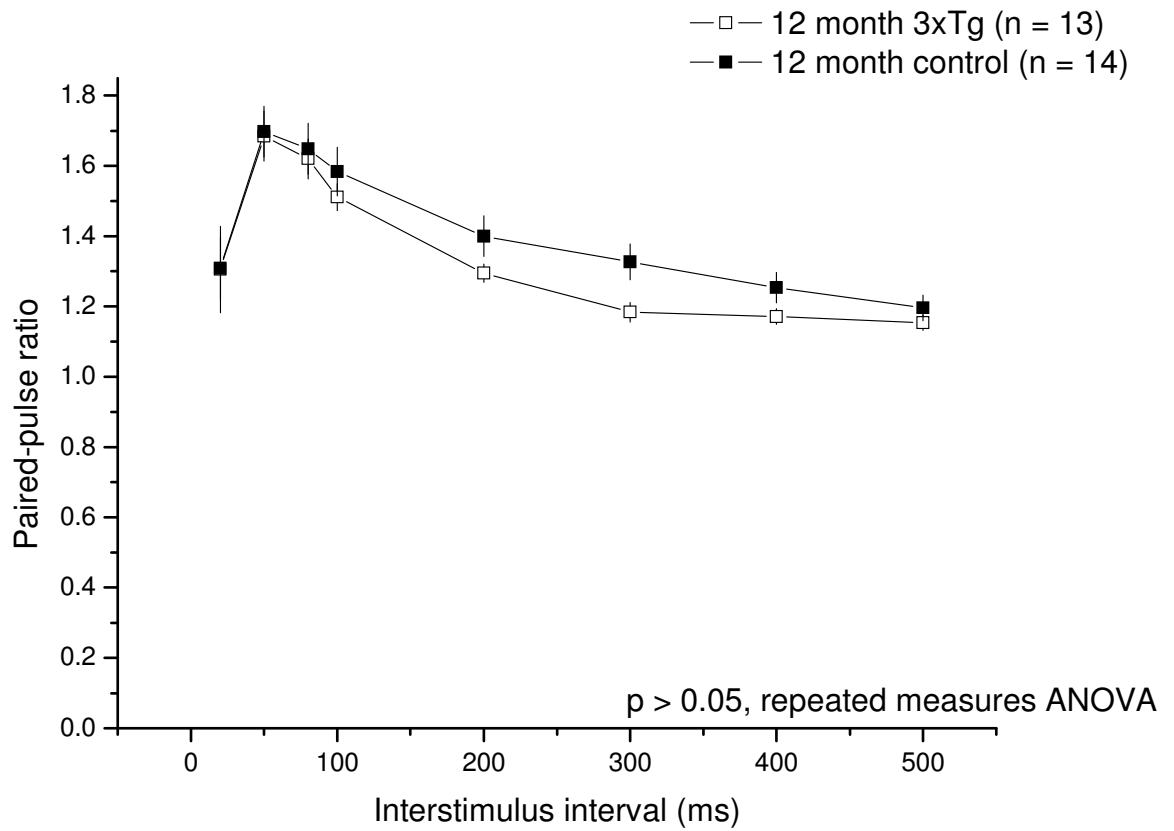


**Figure 3.18: Paired-pulse facilitation determined in 12 month old 3xTg and control mice.** The paired-pulse ratio was calculated at a range of interstimulus intervals in 3xTg mice (n = 13/6) and in control mice (n = 14/6).  $p > 0.05$ , repeated measures ANOVA.

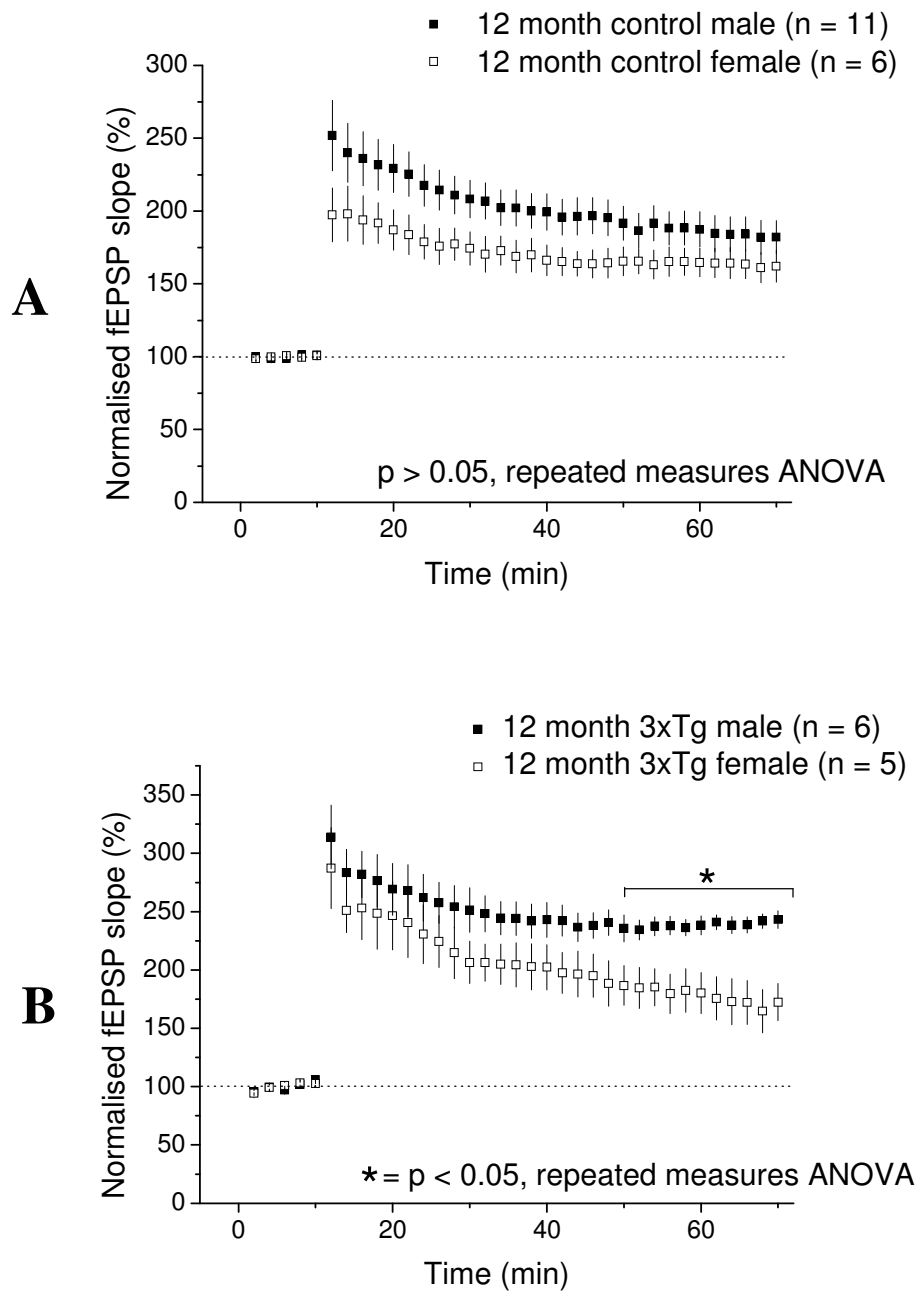


**Figure 3.19: The influence of gender on long-term potentiation recorded from 12 month old 3xTg mice and control mice.** The potentiation of the fEPSP slope obtained following four-pulse theta burst was measured in **(A)** control male (n = 11/3) and female mice (n = 6/4) and **(B)** 3xTg male (n = 6/3) and female mice (n = 5/3). All data are normalised to the average slope of the fEPSP for each genotype prior to delivery of the theta burst stimulus. \* =  $p < 0.05$ , repeated measures ANOVA.

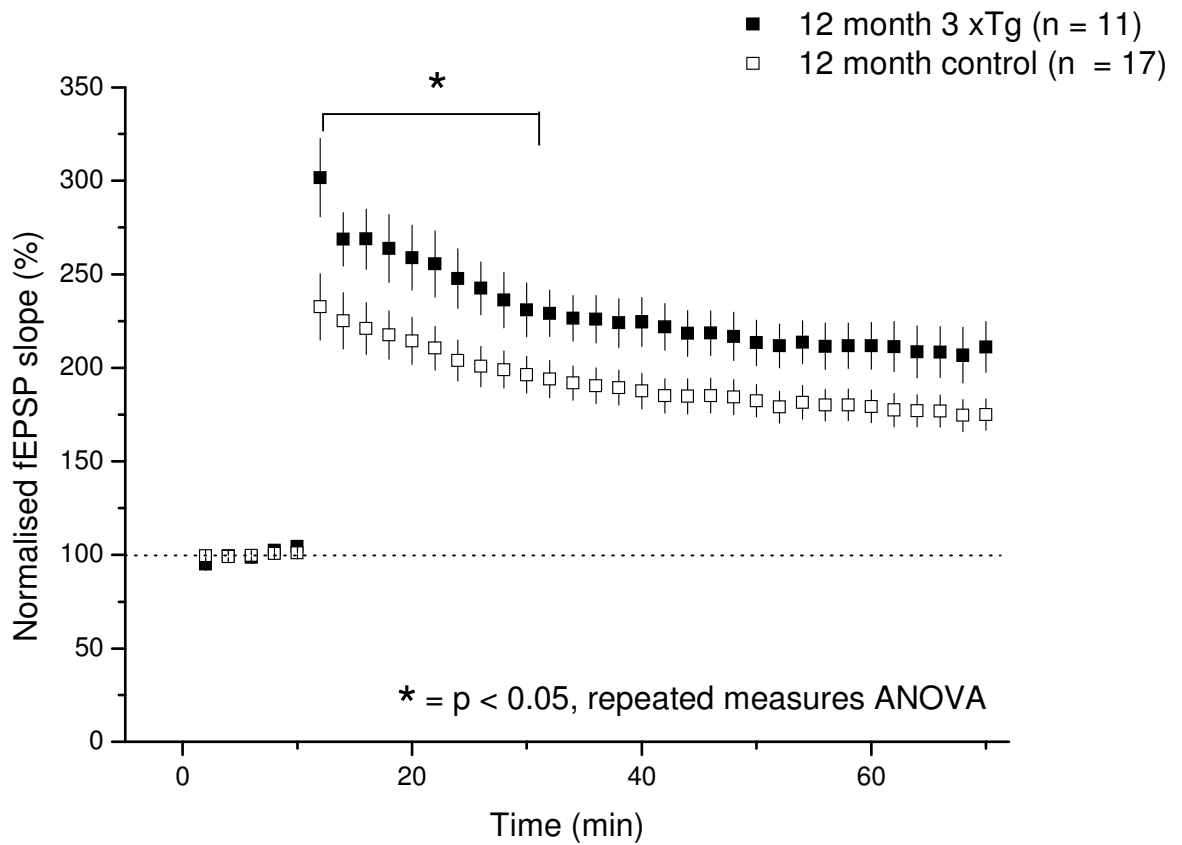


**Figure 3.20: Long-term potentiation in 12 month old 3xTg mice and control.** The potentiation of the fEPSP slope following four pulse theta burst was measured in control mice (n = 17/7) and 3xTg mice (n = 11/6). All data are normalised to the average slope of the fEPSP for each genotype prior to delivery of the theta burst stimulus.

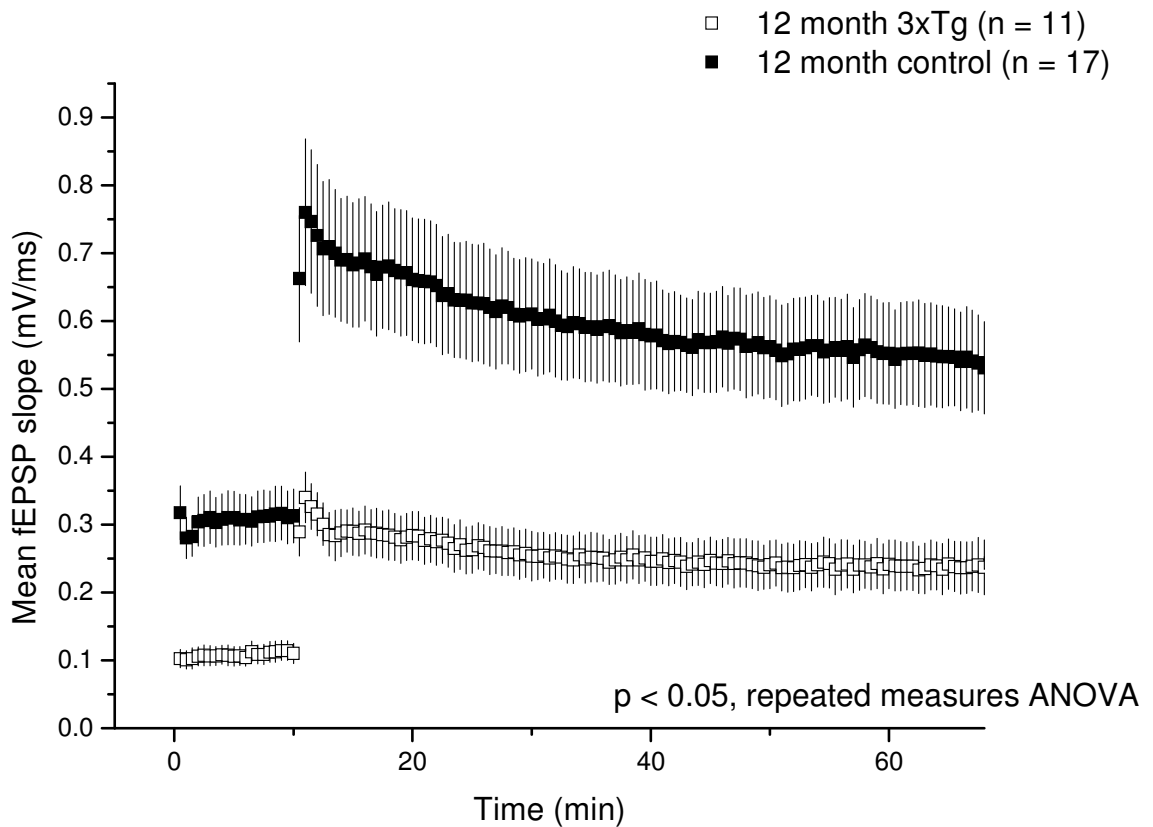


**Figure 3.21: A comparison of long-term potentiation in 12 month old 3xTg and control mice (non-normalised).** The potentiation of the fEPSP slope following four pulse theta burst was measured in control (n = 17/7) and 3xTg mice (n = 11/6) and is presented here as the actual values obtained.  $p < 0.05$ , repeated measures ANOVA.

### **3.2.5: Electrophysiological characterisation of 17 month old 3xTg mice**

#### **3.2.5.1: Input-output function**

17 month old 3xTg mice were used as the final group for electrophysiological measurements. Mice of this age have not previously been studied, but should fully express all the pathological features of the AD model, including extracellular amyloid plaques and intraneuronal tangle formation.

Input-output curves were generated and compared for 17 month old 3xTg mice and 17 month old control mice; due to the limited number of mice available it was not possible to divide these investigations by gender. A normalised input-output curve, where the maximum field slope is set to 100%, was generated, together with a non-normalised input-output curve using the actual values obtained.

There is a significant reduction ( $p < 0.05$ , unpaired t-test) in the normalised input-output curve values for 17 month old mice 3xTg mice ( $n = 6/3$ ) when compared to control mice ( $n = 11/6$ ). This difference is particularly apparent at low stimulus intensities (Fig. 3.22).

For the non-normalised input-output curve, the control mice exhibit an fEPSP slope at 1 mA of  $0.45 \pm 0.06$  mV/ms, while the 3xTg mice exhibit an fEPSP slope at 1 mA of  $0.15 \pm 0.04$  mV/ms. There is a significant reduction ( $p < 0.05$ , unpaired t-test) in the fEPSP slope in the 17 month old 3xTg mice when compared with control (Fig. 3.23).

### 3.2.5.2: Paired-pulse facilitation

Paired-pulse facilitation was compared between 17 month old 3xTg mice and 17 month old control mice. In all experiments, the maximum facilitation was observed at an interstimulus interval of 50ms.

In control mice ( $n = 13/6$ ), the paired-pulse ratio at 50ms is  $1.58 \pm 0.04$ , while in 3xTg mice ( $n = 11/6$ ) it is  $1.64 \pm 0.11$ . There is no significant difference ( $p > 0.05$ , repeated measures ANOVA) in the paired-pulse ratio in 3xTg when compared to control mice at any interstimulus interval measured from 20-500ms (Fig. 3.23).

### 3.2.5.3: Long-term potentiation

LTP was measured in the CA1 region for 17 month 3xTg and control mice. The results were separated by gender and both normalised and non-normalised data was generated.

In all experiments a baseline fEPSP was recorded at 30 second intervals until the slope of the fEPSP was stabilised and constant over a 10 min period before delivery of the theta burst stimulus. In the following section the slope of the fEPSP is normalised to baseline (i.e. 100%) for each recording.

In 17 month control male mice ( $n = 8/3$ ), the peak enhancement of the slope of the fEPSP is  $256 \pm 14\%$ , with a mean from 50-60 minutes following the theta burst stimulus of  $183 \pm 9\%$ . In 17 month old control female mice ( $n = 9/3$ ), the

peak enhancement is  $205 \pm 11\%$ , with a mean from 50-60 minutes of  $169 \pm 11\%$  (Fig. **3.24A**).

In 17 month 3xTg male mice ( $n = 7/3$ ), the peak enhancement of the slope of the fEPSP is  $300 \pm 79\%$ , with a mean from 50-60 minutes following the theta burst stimulus of  $211 \pm 23\%$ . In 17 month 3xTg female mice ( $n = 3/3$ ), the peak potentiation is  $277 \pm 84\%$ , with a mean from 50-60 minutes of  $230 \pm 35\%$  (Fig. **3.24B**). The large error bars are due to the limited number of female mice used in this experiment.

There is no significant difference ( $p > 0.05$ , repeated measures ANOVA) between the magnitude of potentiation in male and female control, or male and female 3xTg, in any phase of LTP.

Combining the results obtained for each gender, a comparison was then made between the 3xTg and control mice. For 17 month old control mice ( $n = 17/6$ ), the peak enhancement of the slope of the fEPSP is  $227 \pm 12\%$ , with a mean from 50-60 minutes following the theta burst stimulus of  $176 \pm 7\%$ . In 17 month 3xTg mice ( $n = 10/6$ ), the peak enhancement is  $294 \pm 58\%$ , with a mean from 50-60 minutes of  $217 \pm 18\%$ .

There is a significant difference ( $p < 0.05$ , repeated measures ANOVA) between the magnitude of LTP in 17 month 3xTg and control mice in the plateau phase from 40 minutes onwards following theta burst stimulation (Fig. **3.25**).

#### **3.2.5.4: Non-normalised long-term potentiation**

When the slope of the fEPSP is not normalised to control and the actual values (mV/ms) are utilised, in 17 month control mice the mean baseline fEPSP is  $0.24 \pm 0.03$  mV/ms, the peak enhancement following theta burst is  $0.57 \pm 0.06$  mV/ms, and the mean from 50-60 minutes is  $0.39 \pm 0.03$  mV/ms. In 17 month 3xTg mice the mean baseline fEPSP is  $0.11 \pm 0.02$  mV/ms, the peak enhancement is  $0.29 \pm 0.07$  mV/ms, and the mean from 50-60 minutes is  $0.23 \pm 0.05$  mV/ms.

There is a significant decrease ( $p < 0.05$ , repeated measures ANOVA) in the potentiation of the fEPSP slope in 17 month 3xTg mice when compared to control mice (Fig. **3.26**).

#### **3.2.5.5: Summary**

At 17 months, the oldest age group studied, there are a number of changes in hippocampal CA1 synaptic function in the 3xTg mice. There is no alteration in PPF, but a significant reduction in the slope of the fEPSP as measured by both the normalised and non-normalised input-output curves. Despite this, however, there is an increase in the magnitude of LTP when normalised to the baseline values, which becomes significant in the plateau phase. These electrophysiological changes may be related to the progressive nature of the pathology reported in these mice.

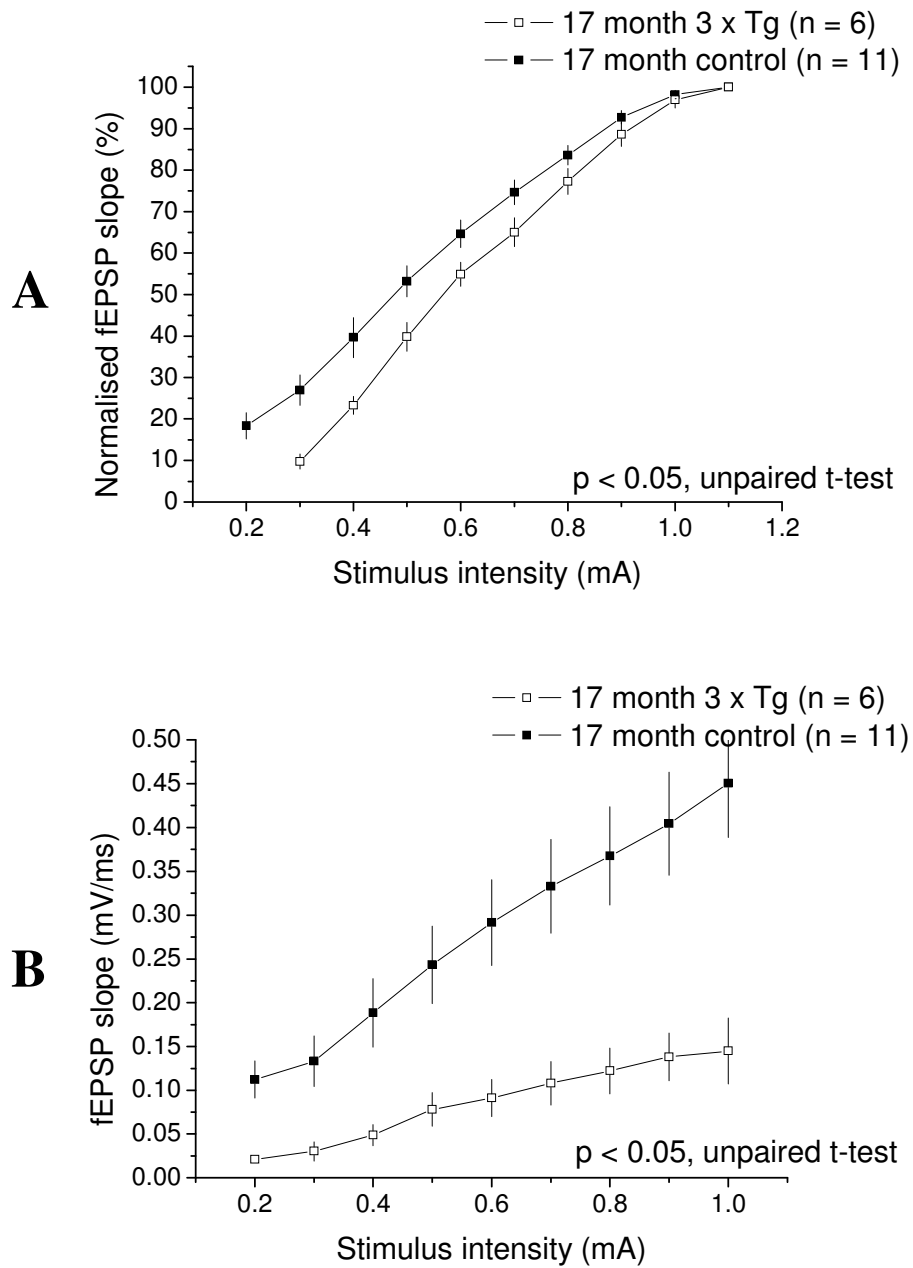


**Figure 3.22: Normalised and non-normalised input-output curves obtained from 17 month old 3xTg and control mice.** The fEPSP slope was measured at a range of stimulus intensities and then normalised in control (n = 11/6) and 3xTg mice (n = 6/3) (**A**). The non-normalised fEPSP slope measurement in control (n = 14/7) and 3xTg mice (n = 11/6) is shown in (**B**).  $p < 0.05$ , unpaired t-test.

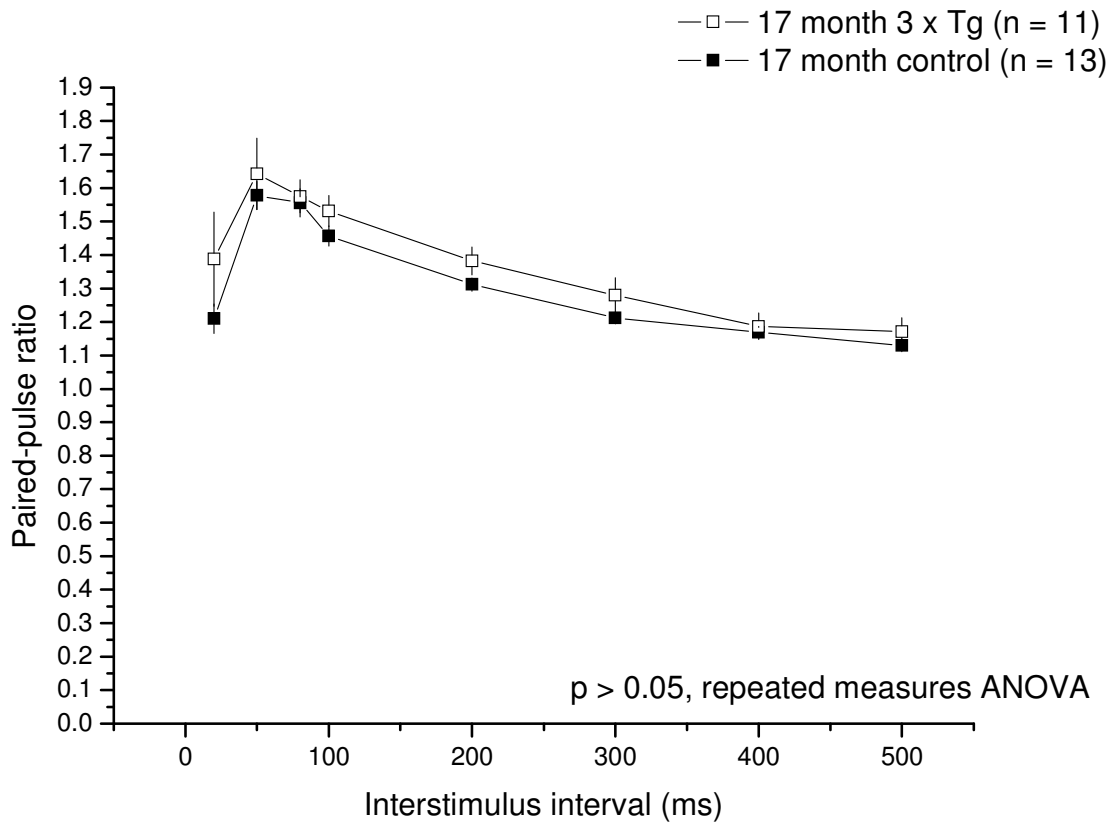


**Figure 3.23: Paired-pulse facilitation determined for 17 month old 3xTg and control mice.** The paired-pulse ratio was calculated at a range of interstimulus intervals in 3xTg mice (n = 11/6) and in control mice (n = 13/6).  $p > 0.05$ , repeated measures ANOVA.

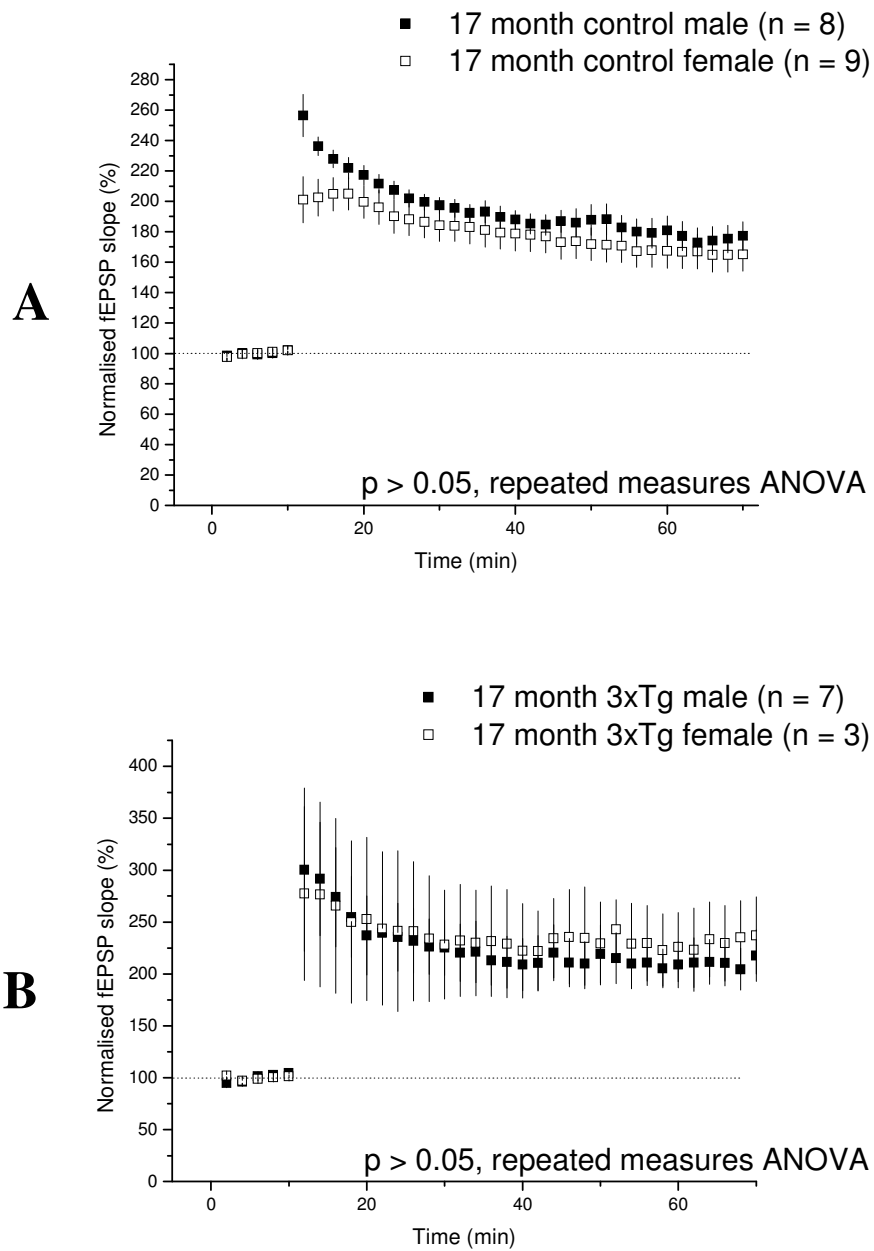


**Figure 3.24: The influence of gender on long-term potentiation obtained in 17 month old 3xTg mice and control mice.** The potentiation of the fEPSP slope obtained following four-pulse theta burst was measured in **(A)** control male (n = 8/3) and female mice (n = 9/3) and **(B)** 3xTg male (n = 7/3) and female mice (n = 3/3). All data are normalised to the average slope of the fEPSP for each genotype prior to delivery of the theta burst stimulus.  $p > 0.05$ , repeated measures ANOVA.

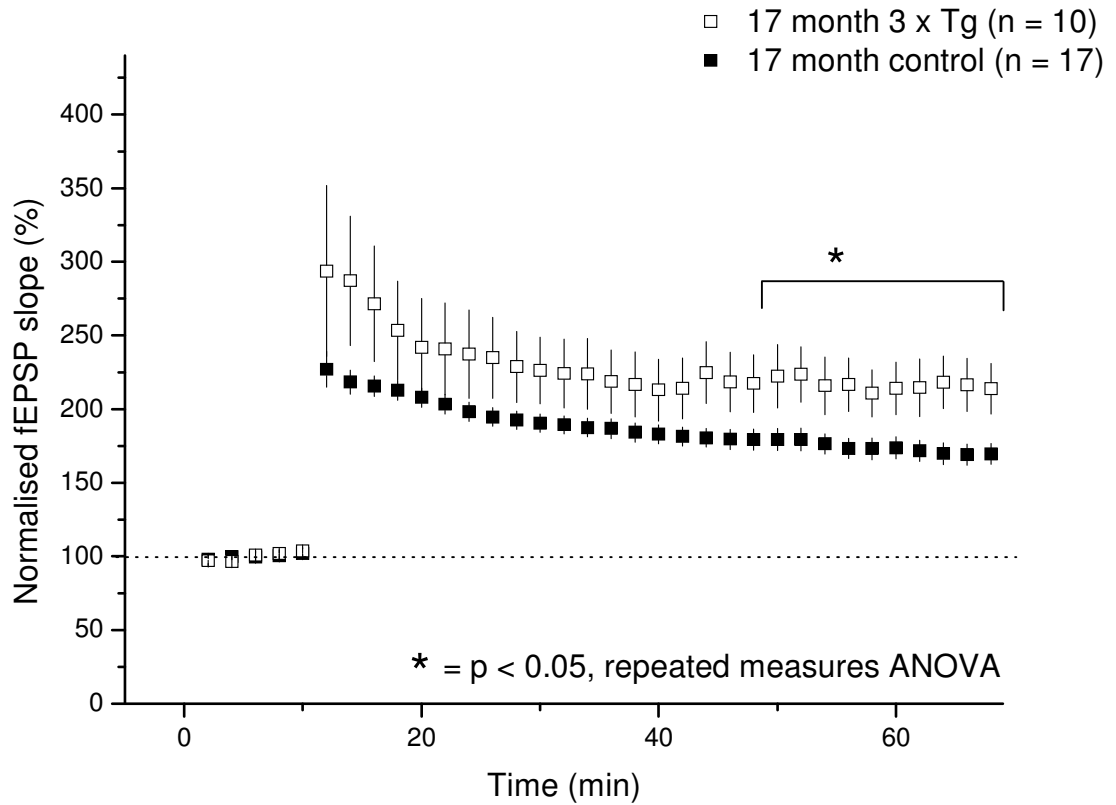


**Figure 3.25: Long-term potentiation in 17 month old 3xTg and control mice.** The potentiation of the fEPSP slope following four pulse theta burst was measured in control mice (n = 17/6) and 3xTg mice (n = 10/6). All data are normalised to the average slope of the fEPSP for each genotype prior to delivery of the theta burst stimulus. \* = p < 0.05, repeated measures ANOVA.

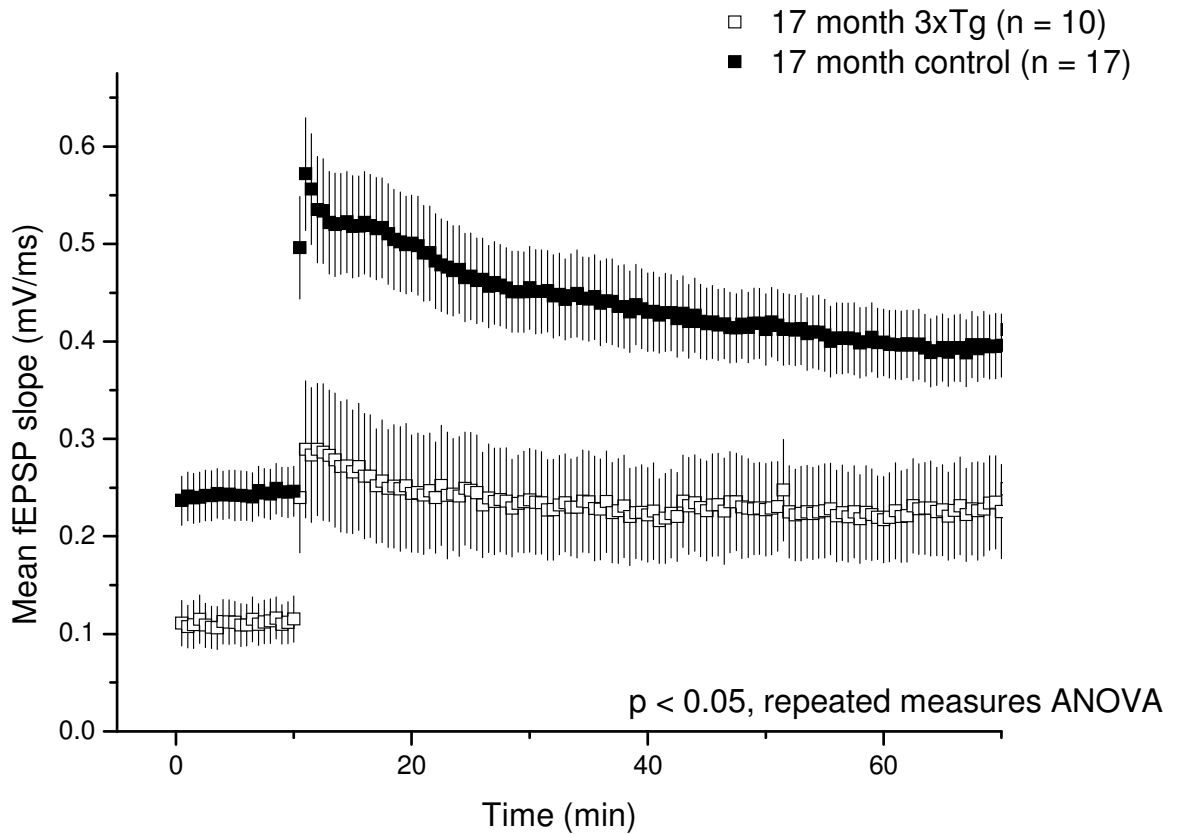


**Figure 3.26: A comparison of long-term potentiation in 17 month old 3xTg and control mice (non-normalised).** The potentiation of the fEPSP slope following four pulse theta burst was measured in control mice (n = 17/6) and 3xTg mice (n = 10/6) and is presented here as the actual values obtained.  $p < 0.05$ , repeated measures ANOVA.

### 3.2.6: Comparison of results obtained in 3xTg and control mice by age

The following graphs present a summary of some of the results obtained over the full age range studied (2 – 17 months old) for 3xTg and control mice. This allows comparison to be carried out not only within but between different age groups.

#### 3.2.6.1: Input-output function

Input-output curves were generated at the ages of 2, 6, 12 and 17 months in 3xTg and control mice. The non-normalised input-output curve, which uses the actual fEPSP slope values, was compared between all ages of 3xTg mice and all ages of control mice studied.

In the control mice, the 2 month group has an fEPSP slope at 1 mA of  $0.46 \pm 0.11$  mV/ms ( $n = 12/7$ ), the 6 month group ( $n = 15/7$ ) of  $0.60 \pm 0.05$  mV/ms, the 12 month group ( $n = 14/7$ ) of  $0.40 \pm 0.04$  mV/ms and the 17 month group ( $n = 11/6$ ) of  $0.45 \pm 0.06$  mV/ms (Fig. 3.27A).

There is a statistically significant effect of age on the fEPSP slope ( $p < 0.05$ , repeated measures ANOVA) but this is not a progressive age-dependent deficit as observed in 3xTg mice.

In the 3xTg mice, the 2 month group ( $n = 13/8$ ) has an fEPSP slope at 1 mA of  $0.71 \pm 0.14$  mV/ms, the 6 month group ( $n = 15/7$ ) of  $0.41 \pm 0.05$  mV/ms, the 12 month group ( $n = 11/7$ ) of  $0.17 \pm 0.02$  mV/ms, and the 17 month group ( $n = 6/3$ ) of  $0.15 \pm 0.04$  mV/ms (Fig. 3.27B).

There is a progressive reduction in the fEPSP slope from the ages of 2 months to 12 months, which then stabilises between 12 and 17 months. There is a statistically significant effect of age between the 2 month group and the other groups ( $p < 0.05$ , repeated measures ANOVA, Newman-Keuls post hoc).

### **3.2.6.2: Maximum fEPSP slope and amplitude**

The maximum fEPSP slope in 3xTg and control was calculated in a number of slices ( $n = 6-14$  slices per age group) using a stimulus intensity of 1.5mA, at the plateau region at the top of the input-output curve. There is a reduction in the fEPSP slope with age in 3xTg mice which is not apparent in control mice. By the age of 12 months in the 3xTg mice the fEPSP slope is significantly lower than that observed in the control and remains so at 17 months ( $p < 0.05$ , unpaired t-test) (Fig. **3.28**).

### **3.2.6.3: Paired-pulse facilitation**

Paired-pulse facilitation was measured and the paired-pulse ratio was recorded from 2, 6, 12 and 17 month 3xTg and control mice and compared.

In the control mice, at 2 months ( $n = 11/6$ ) the paired-pulse ratio at 50ms is  $1.90 \pm 0.07$ , at 6 months ( $n = 13/7$ ) it is  $1.49 \pm 0.03$ , at 12 months ( $n = 14/6$ ) it is  $1.67 \pm 0.05$ , and at 17 months ( $n = 13/6$ ) it is  $1.58 \pm 0.04$  (Fig. **3.29A**).

There is a significant difference in the paired-pulse ratio in 2 month old mice compared with 12 and 17 month mice ( $p < 0.05$ , repeated measures ANOVA, Newman-Keuls post-hoc).

In the 3xTg mice, at 2 months ( $n = 13/8$ ) the paired-pulse ratio at 50ms is  $1.52 \pm 0.05$ , at 6 months ( $n = 13/7$ ) the paired-pulse ratio at 50ms is  $1.56 \pm 0.07$ , at 12 months ( $n = 13/6$ ) the paired-pulse ratio at 50ms is  $1.68 \pm 0.07$ , and at 17 months ( $n = 11/6$ ) the paired-pulse ratio at 50ms is  $1.64 \pm 0.11$  (Fig. **3.29B**).

There is no significant difference in the paired-pulse ratio overall with age in the 3xTg mice ( $p > 0.05$ , repeated measures ANOVA).

#### **3.2.6.4: Long-term potentiation**

In control mice when LTP was normalised the following values were obtained.

In 2 month control mice ( $n = 15/8$ ), the mean enhancement of the fEPSP during the plateau phase from 50-60 minutes following theta burst is  $152 \pm 9\%$ , in 6 month control mice ( $n = 14/8$ ) it is  $170 \pm 6\%$ , in 12 month control mice ( $n = 17/7$ ) it is  $177 \pm 8\%$  and in 17 month control mice ( $n = 17/6$ ) it is  $176 \pm 7\%$  (Fig. **3.30A**).

LTP is significantly lower at 2 months than at the older age ranges ( $p < 0.05$ , repeated measures ANOVA, Newman-Keuls post hoc).

In 3xTg mice when LTP was normalised the following values were obtained. In 2 month 3xTg mice ( $n = 17/8$ ), the mean enhancement of the fEPSP during the plateau phase from 50-60 minutes following theta burst is  $163 \pm 11\%$ , in 6 month

3xTg mice (n = 20/8) it is  $164 \pm 14\%$ , in 12 month 3xTg mice (n = 11/6) it is  $210 \pm 13\%$  and in 17 month 3xTg mice (n = 10/6) it is  $217 \pm 18\%$  (Fig. **3.31A**).

There is an increase in the magnitude of LTP with age which is statistically significant in the 17 month group when compared with the 2 and 6 month groups ( $p < 0.05$ , repeated measures ANOVA, Newman-Keuls post hoc).

### **3.2.6.5: Non-normalised long-term potentiation**

When the slope of the fEPSP is not normalised to control and the actual values (mV/ms) are utilised, in 2 month control mice, the mean enhancement of the fEPSP from 50-60 minutes following theta burst is  $0.32 \pm 0.05$  mV/ms, in 6 month control mice, the mean enhancement is  $0.41 \pm 0.07$  mV/ms, in 12 month control mice, the mean enhancement is  $0.55 \pm 0.07$  mV/ms and in 17 month control mice (n = 17/6), the mean enhancement from 50-60 minutes is  $0.39 \pm 0.03$  mV/ms (Fig. **3.30B**).

In the control mice, there is a significant effect of age on the magnitude of LTP with it appearing lowest at 2 months and highest at 12 months.

When the slope of the fEPSP is not normalised to control and the actual values (mV/ms) are utilised, in 2 month 3xTg mice the mean enhancement of the fEPSP from 50-60 minutes is  $0.57 \pm 0.09$  mV/ms, in 6 month 3xTg mice the mean enhancement is  $0.38 \pm 0.05$  mV/ms, in 12 month 3xTg mice the mean enhancement is  $0.24 \pm 0.04$  mV/ms, and in 17 month 3xTg mice (n = 10/6), the mean enhancement from 50-60 minutes is  $0.23 \pm 0.05$  mV/ms (Fig. **3.31B**).

In the 3xTg mice, there is a decrease in the magnitude of non-normalised LTP with age which appears to stabilise between 12 and 17 months of age. There is a statistically significant difference between 17 months and the other groups, and between 2 and 12 months ( $p < 0.05$ , repeated measures ANOVA, Newman-Keuls post hoc).

#### **3.2.6.6: Summary**

There are several alterations in synaptic transmission which can be observed in the 3xTg mice at different ages. PPF is the only measurement that remains stable with age from 2-17 months. There is a progressive reduction in the fEPSP slope along with a decreased magnitude of non-normalised LTP between 2-12 months. Despite the decrease in the fEPSP slope, there is actually an increased magnitude of LTP with age when the data are normalised. All measurements remain stable between 12 and 17 months. These data show that in the 3xTg mice there are progressive and age-dependent differences in a number of the parameters that measure synaptic function.

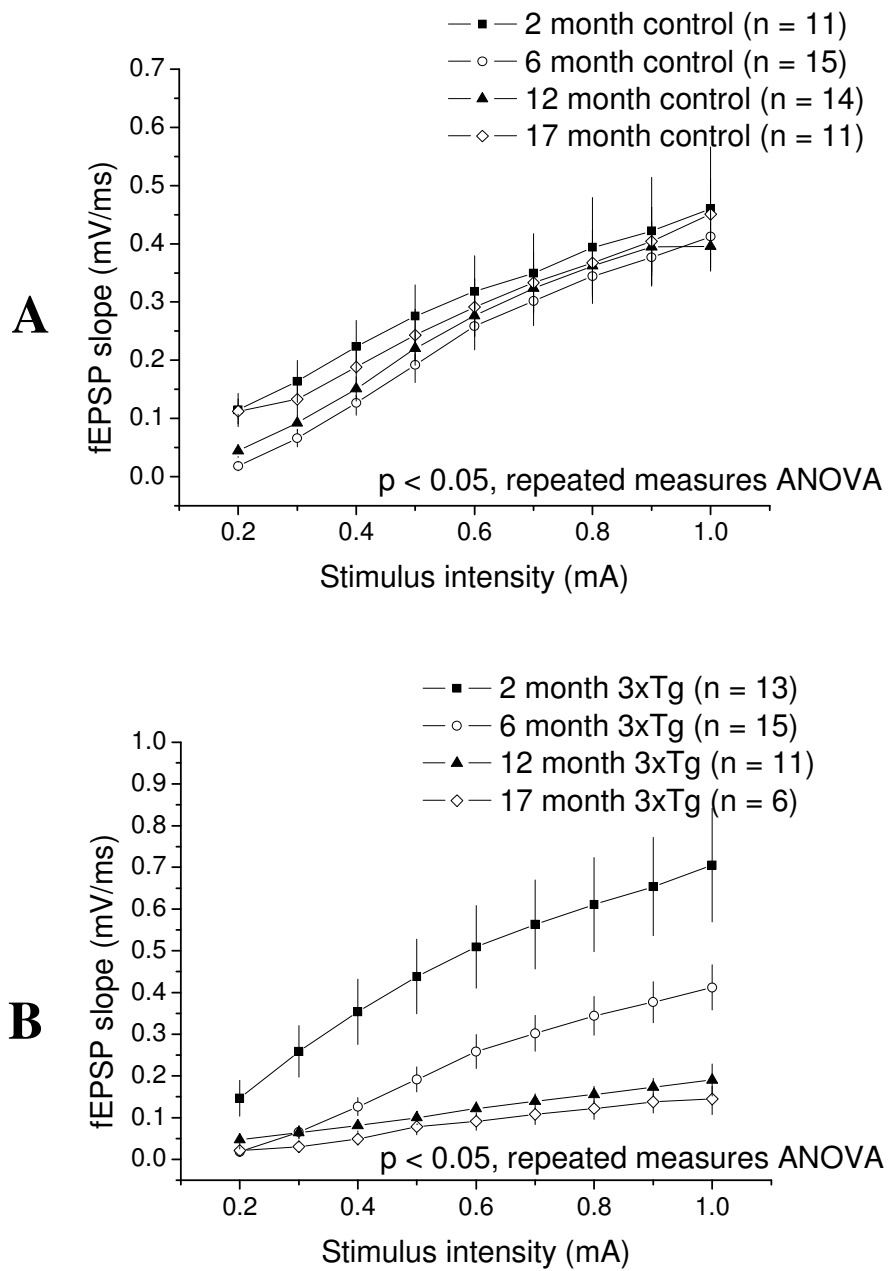


**Figure 3.27: Non-normalised input-output curve for slope obtained at all ages in 3xTg and control mice.** The fEPSP slope data generated at the ages of 2, 6, 12 and 17 months is displayed together for (A) control and (B) 3xTg mice.  $p < 0.05$ , repeated measures ANOVA.

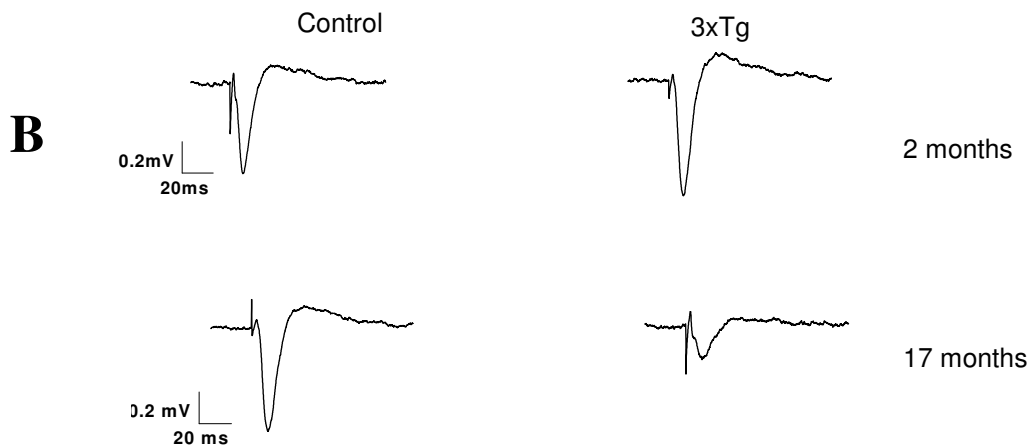
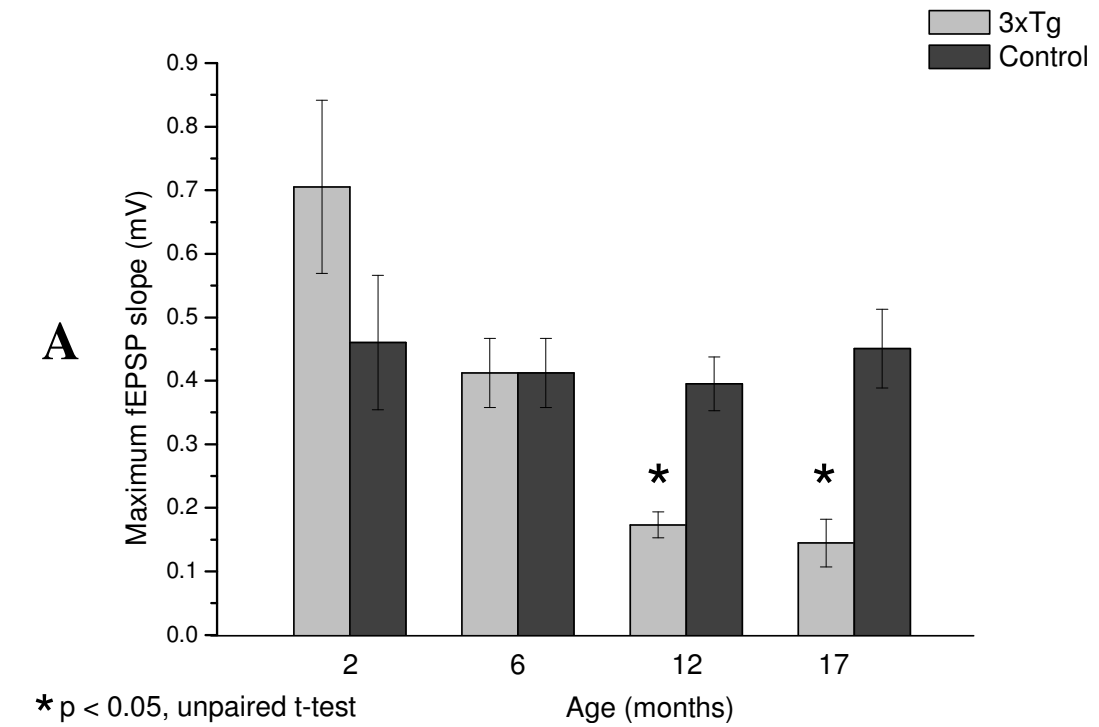


**Figure 3.28: Average maximum fEPSP slope in 3xTg and control at different ages.** The maximum fEPSP slope obtained in a number of slices ( $n \geq 6$  slices per group) is shown for 3xTg and control mice of 2, 6, 12 and 17 months (A).  
 \* =  $p < 0.05$ , unpaired t-test. Sample fEPSP traces for 2 and 17 months are shown below the graph (B).

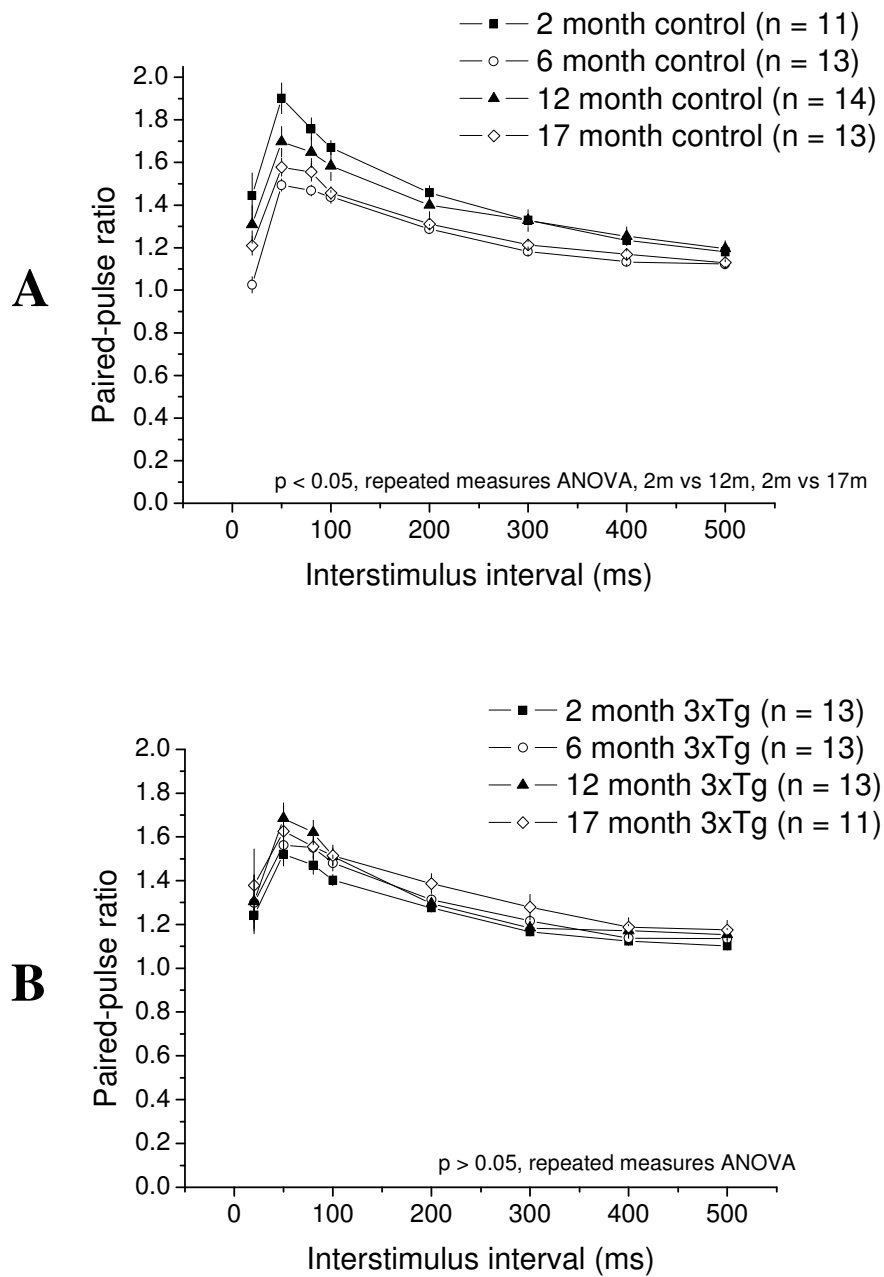


**Figure 3.29: Paired-pulse facilitation determined at all ages in 3xTg and control mice.** The paired-pulse facilitation data generated at the ages of 2, 6, 12 and 17 months is displayed together for (A) control and (B) 3xTg mice. For A,  $p < 0.05$ , repeated measures ANOVA between 2 and 12, and 2 and 17 month groups.  $p > 0.05$  for all other comparisons. For B,  $p > 0.05$ , repeated measures ANOVA.

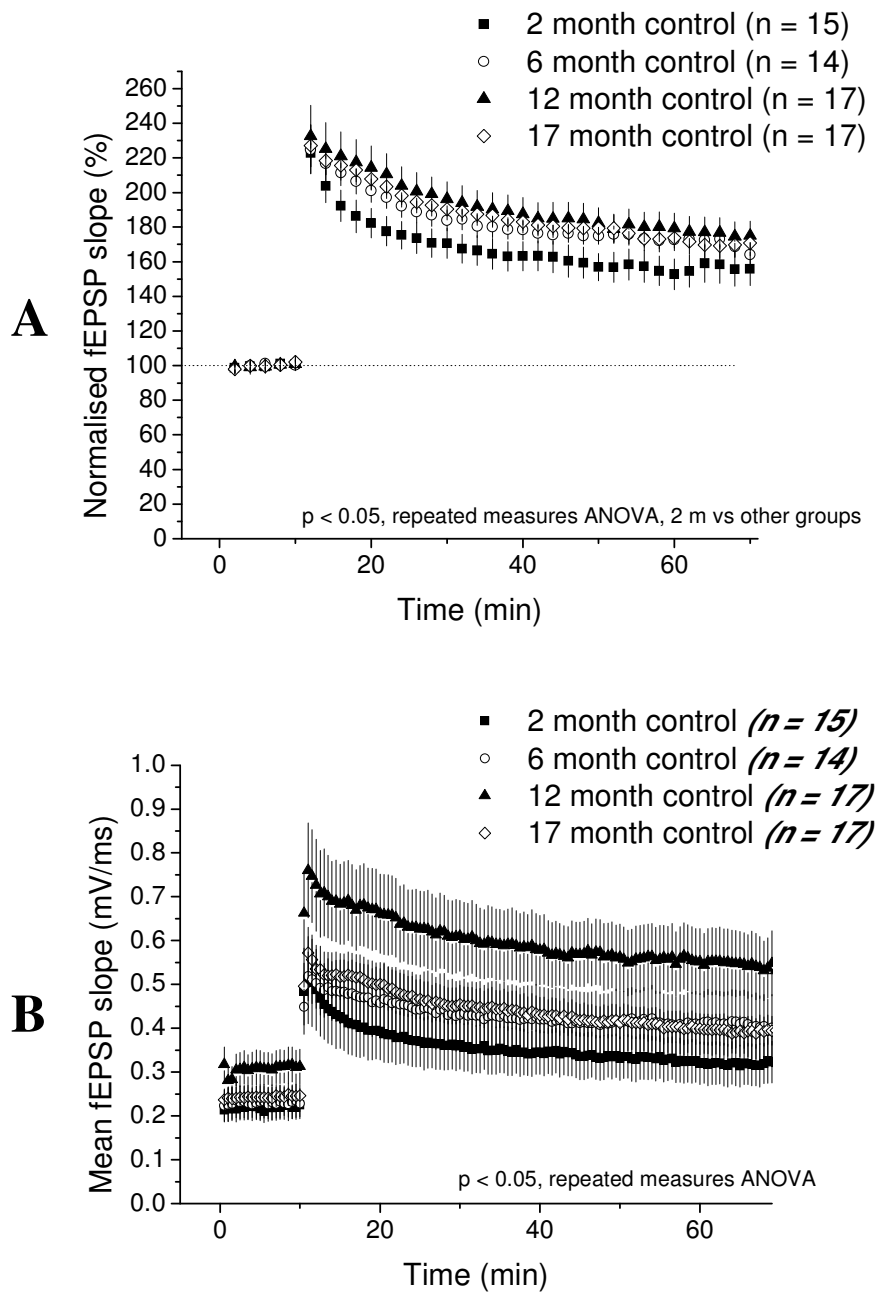


**Figure 3.30: A comparison of normalised and non-normalised LTP in control mice from 2-17 months.** The enhancement of the fEPSP slope obtained following four-pulse theta burst was measured in 2, 6, 12 and 17 month control mice and normalised to the average slope of the fEPSP prior to delivery of the theta burst stimulus (**A**). The potentiation of the fEPSP slope is also presented here as the actual values obtained (**B**). For **A**,  $p < 0.05$ , repeated measures ANOVA between 2 month and other groups.  $p > 0.05$  for all other comparisons. For **B**,  $p < 0.05$ , repeated measures ANOVA.

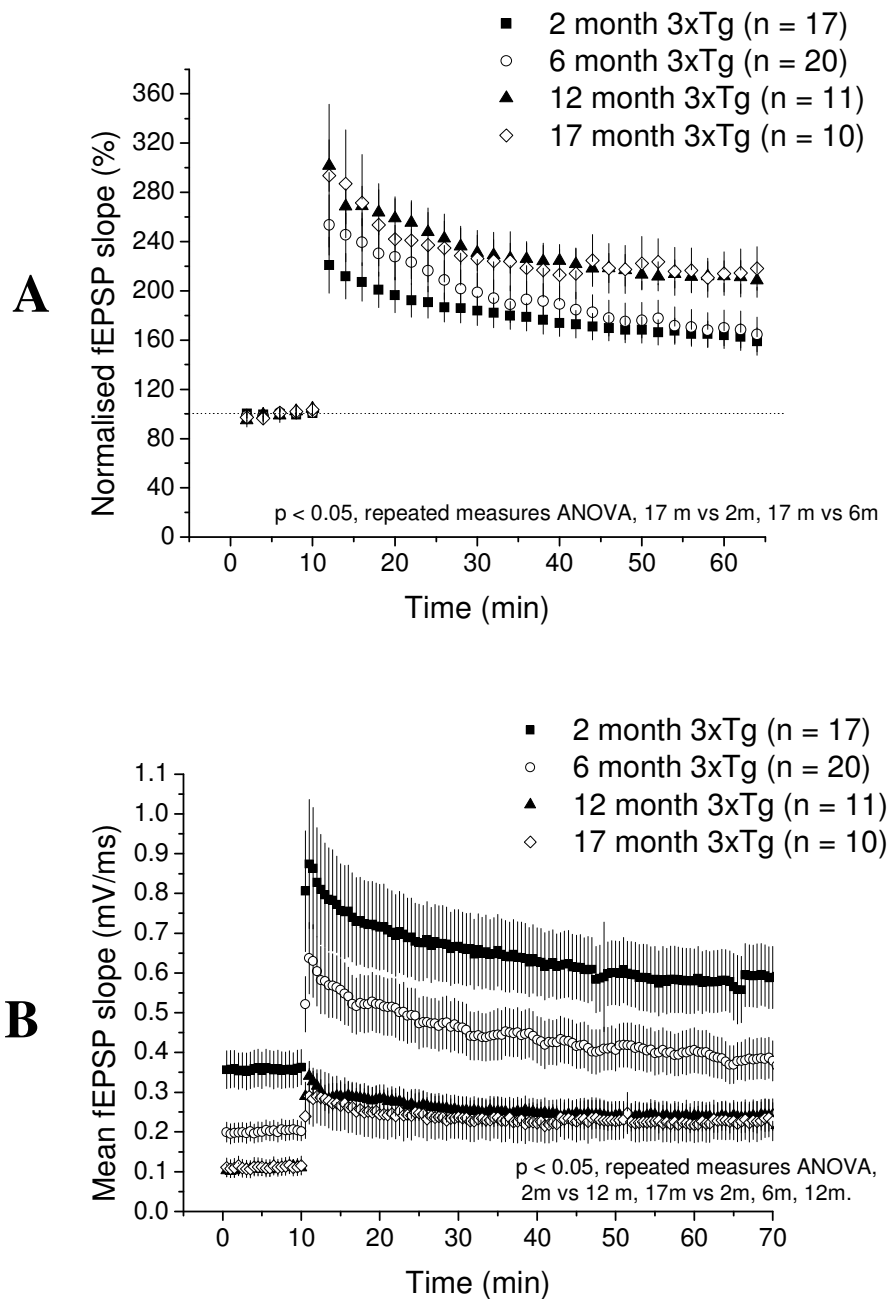


**Figure 3.31: A comparison of normalised and non-normalised LTP in 3xTg mice from 2-17 months.** The enhancement of the fEPSP slope obtained following four-pulse theta burst was measured in 2, 6, 12 and 17 month 3xTg mice and normalised to the average slope of the fEPSP prior to delivery of the theta burst stimulus (**A**). The potentiation of the fEPSP slope is also presented here as the actual values obtained (**B**). For **A**,  $p < 0.05$ , repeated measures ANOVA between 2 and 17 month, and 6 and 17 month groups.  $p > 0.05$  for all other comparisons. For **B**,  $p < 0.05$ , repeated measures ANOVA between 2 and 12 months, 2 and 17 months, 6 and 17 months and 12 and 17 months.  $p > 0.05$  for all other comparisons.

### **3.2.7: Electrophysiological characterisation of 2 month old TASTPM mice**

The TASTPM mouse, which carries both mutant APP and PS1 transgenes, shows A $\beta$  deposition from the age of 3 months, and cognitive deficits from the age of 6 months (Howlett *et al.*, 2004). For this reason, it was decided to use mice of 2 and 6 months of age for electrophysiological studies. 2 month old mice should be free from pathology and should therefore possess normal synaptic function, while 6 month old mice may show electrophysiological deficits, as at this age the A $\beta$  deposition is well established. The control mice for the 3xTg transgenic line were used as a comparison, and due to availability a mixture of male and female TASTPM mice were used for this study.

#### **3.2.7.1: Input-output function**

Input-output curves were generated and compared for 2 month old TASTPM and 2 month old control mice. A normalised input-output curve, where the maximum field slope is set to 100%, was generated, along with a non-normalised input-output curve using the real values.

There is no significant difference ( $p > 0.05$ , unpaired t-test) in the normalised input-output curve in 2 month control ( $n = 12/7$ ) and TASTPM mice ( $n = 9/6$ ) (Fig. 3.32A).

For the non-normalised input-output curve, the control mice exhibit an fEPSP slope at 1 mA of  $0.46 \pm 0.11$  mV/ms while the TASTPM mice exhibit an fEPSP

slope at 1 mA of  $0.45 \pm 0.08$  mV/ms. There is no significant difference ( $p > 0.05$ , unpaired t-test) between the TASTPM and control mice (Fig. **3.32B**).

### **3.2.7.2: Paired-pulse facilitation**

Paired-pulse facilitation was compared between 2 month old TASTPM and control mice. In all experiments, the maximum facilitation was observed at an interstimulus interval of 50ms.

In control mice ( $n = 11/6$ ), the paired-pulse ratio at 50ms is  $1.90 \pm 0.07$  while in TASTPM mice ( $n = 11/7$ ) the paired-pulse ratio at 50ms is  $1.64 \pm 0.09$ .

There is a significant decrease in the paired-pulse ratio of 2 month TASTPM when compared to control mice ( $p < 0.05$ , repeated measures ANOVA followed by unpaired t-test) at an interstimulus interval of 50ms, but not at other interstimulus intervals (Fig. **3.33**).

### **3.2.7.3: Long-term potentiation**

LTP was measured in the CA1 region for 2 month TASTPM and control mice.

In all experiments a baseline fEPSP was recorded at 30 second intervals until the slope of the fEPSP was stabilised and constant over a 10 min period before delivery of the theta burst stimulus. In the following section the slope of the fEPSP is normalised to baseline (i.e. 100%) for each recording.

In 2 month control mice ( $n = 15/8$ ), the peak enhancement of the slope of the fEPSP is  $223 \pm 12\%$ , with a mean from 50-60 minutes following the 4 pulse theta

burst stimulus of  $152 \pm 9\%$ . In 2 month TASTPM mice ( $n = 10/6$ ), the peak enhancement is  $198 \pm 17\%$ , with a mean from 50-60 minutes of  $148 \pm 9\%$ .

There is no significant difference ( $p > 0.05$ , repeated measures ANOVA) between the magnitude of LTP in 2 month TASTPM and control mice (Fig. **3.34**).

#### **3.2.7.4: Summary**

There are no differences in electrophysiology measurements at 2 months in input-output function or LTP, with the sole change a minor reduction in PPF at this age. This suggests that there are few functional changes in the TASTPM mice at 2 months, an age reported to be prior to the development of any overt pathological features.

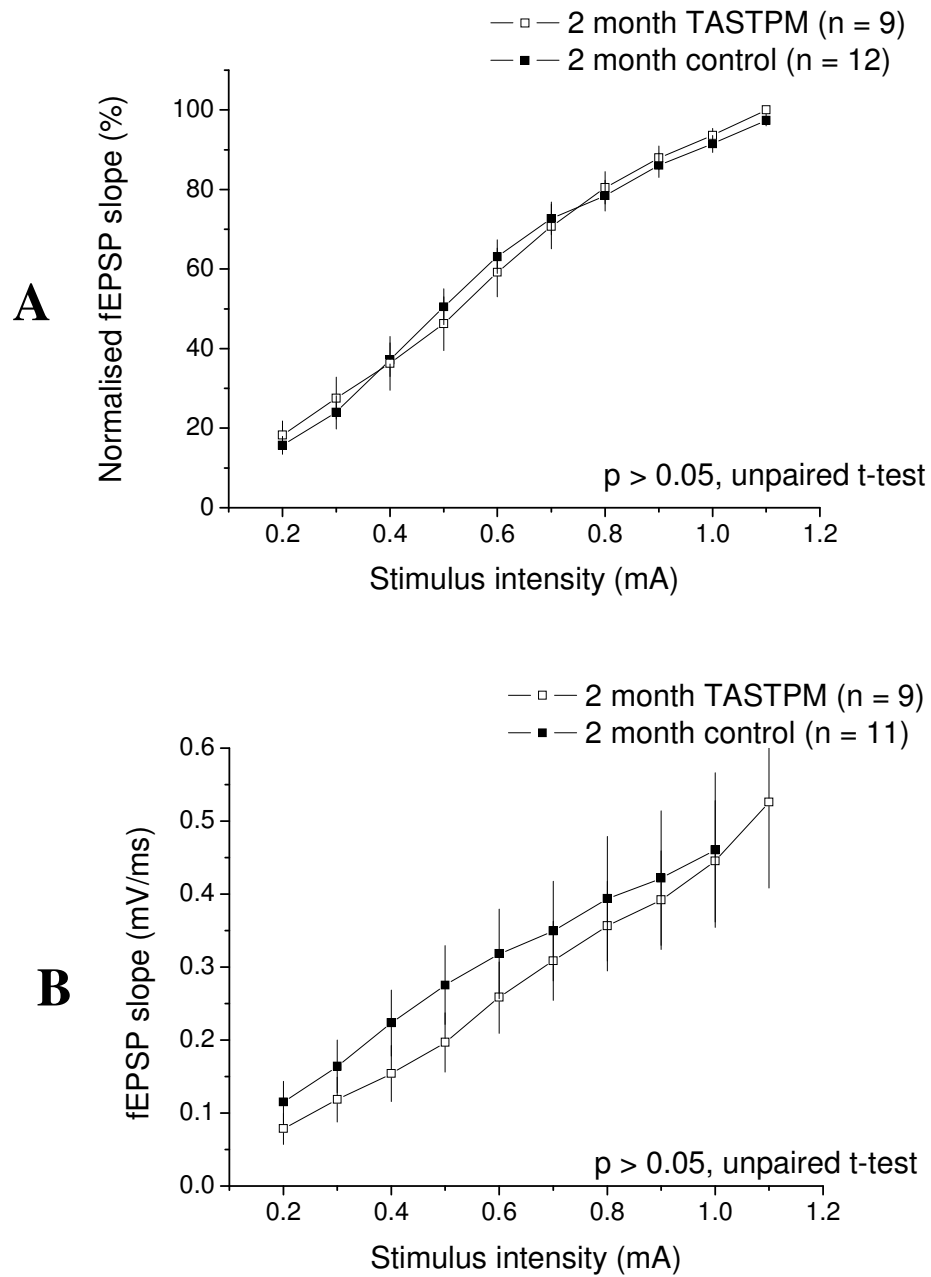


**Figure 3.32: Normalised and non-normalised input-output curves obtained from 2 month old TASTPM and control mice.** The fEPSP slope was measured at a range of stimulus intensities and then normalised in control (n = 12/7) and TASTPM mice (n = 9/6) (A). The non-normalised fEPSP slope measurement in control mice (n = 12/7) and TASTPM mice (n = 9/6) is shown in (B).  $p > 0.05$ , unpaired t-test.

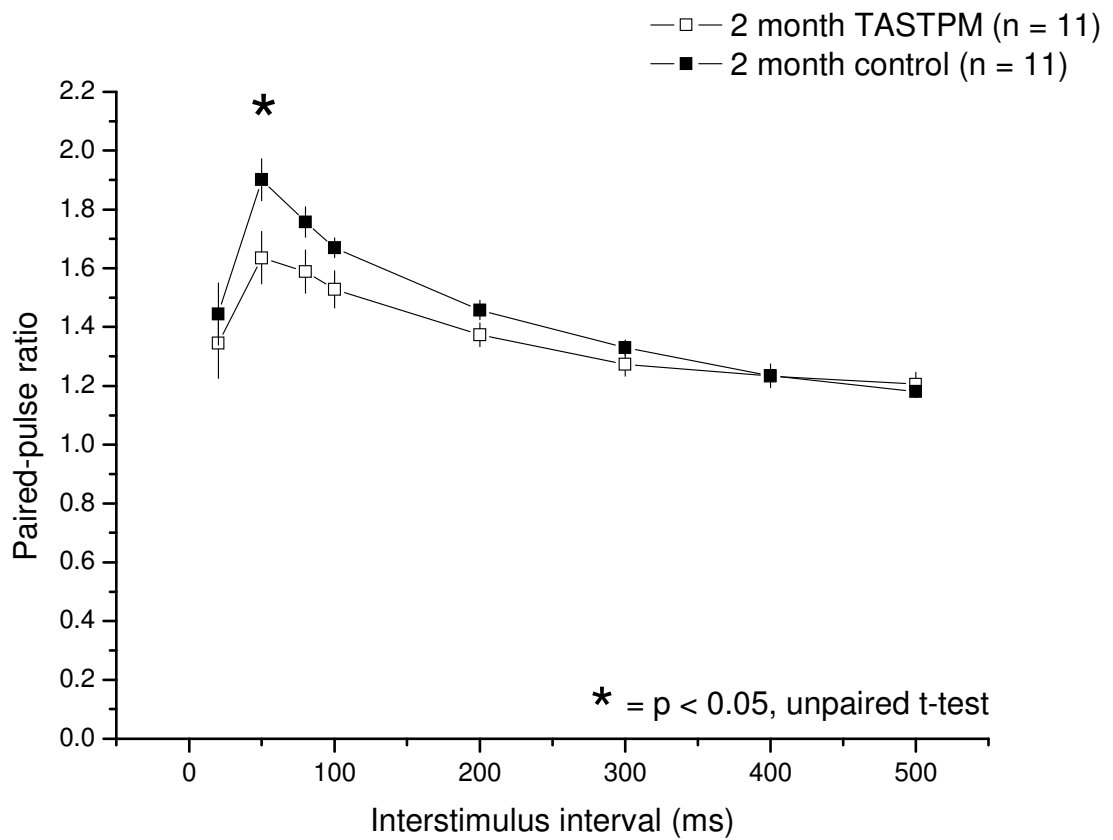


**Figure 3.33: Paired-pulse facilitation determined in 2 month old TASTPM and control mice.** The paired-pulse ratio was calculated at a range of interstimulus intervals in control mice ( $n = 11/6$ ) and TASTPM mice ( $n = 11/7$ ). \* =  $p < 0.05$ , repeated measures ANOVA followed by unpaired t-test.  $p > 0.05$  for all other interstimulus intervals.

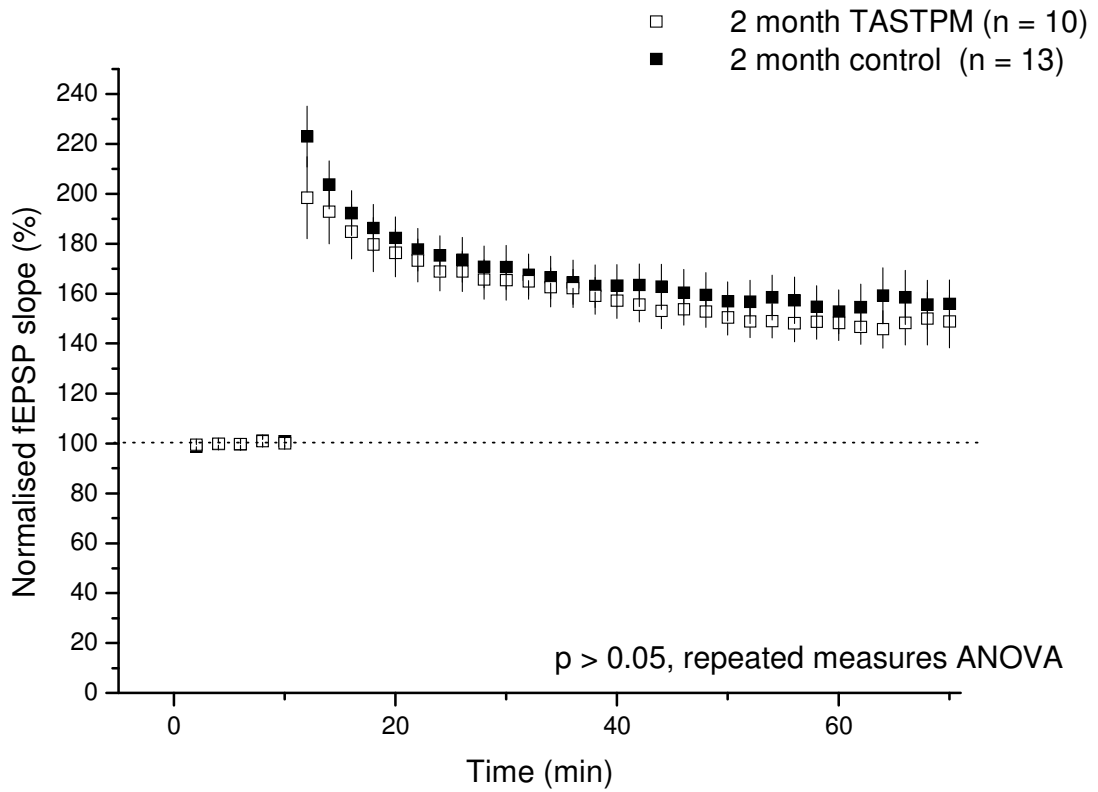


**Figure 3.34: Long-term potentiation in 2 month TASTPM and control mice.**

The potentiation of the fEPSP slope following four pulse theta burst was measured in control mice (n = 15/8) and TASTPM mice (n = 10/6). All data are normalised to the average slope of the fEPSP for each genotype prior to delivery of the theta burst stimulus.  $p > 0.05$ , repeated measures ANOVA.

### 3.2.8: Electrophysiological characterisation of 6 month old TASTPM mice

In the 6 month old TASTPM mice it was much more difficult to obtain an fEPSP of reasonable size to allow further experiments to take place. A large number of slices had to be discarded as an fEPSP could not be obtained or was too small to use. Of the 30 slices tested, only 8 were useable (a total of 27%) and LTP was only induced in 3 of these slices. It is normal for an fEPSP to be obtained in around 80-90% of healthy slices with LTP being induced in the majority of these.

LTP was measured in the CA1 region for 6 month TASTPM and control mice. In all experiments a baseline fEPSP was recorded at 30 second intervals until the slope of the fEPSP was stabilised and constant over a 10 min period before delivery of the theta burst stimulus. In the following section the slope of the fEPSP is normalised to baseline (i.e. 100%) for each recording.

In 6 month TASTPM mice ( $n = 3/2$ ) the peak enhancement of the slope of the fEPSP is  $361 \pm 39\%$ , with a mean from 50-60 minutes following the theta burst stimulus of  $231 \pm 40\%$  (Fig. 3.35).

There is a significant increase ( $p < 0.05$ , repeated measures ANOVA) in the magnitude of LTP obtained in the TASTPM slices. However it should be noted that, as stated above, these slices in which LTP were induced were a very small proportion of those tested and so may not be representative of the functional changes overall in the TASTPM mice. There are also large error bars due to the low number of slices used in the experiment.

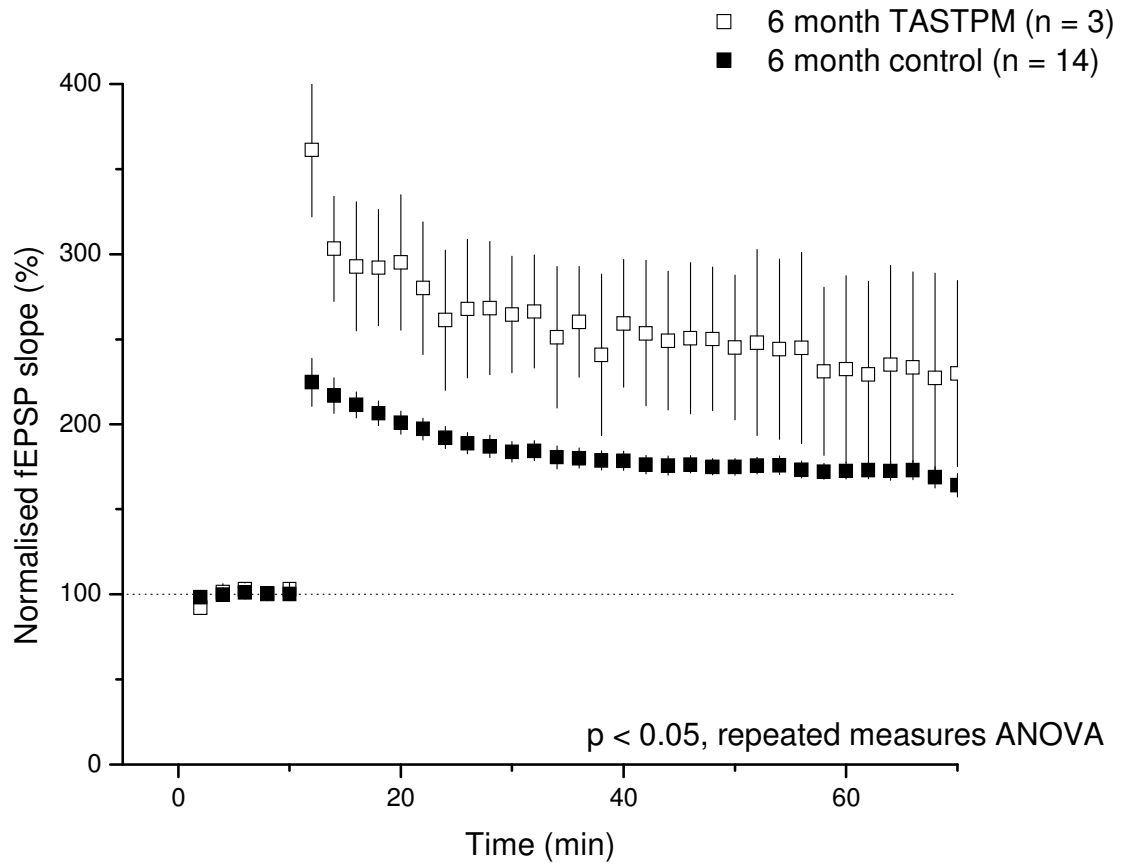


**Figure 3.35: Long-term potentiation in 6 month TASTPM and control mice.**

The potentiation of the fEPSP slope following four pulse theta burst was measured in control mice (n = 14/8) and TASTPM mice (n = 3/2). All data are normalised to the average slope of the fEPSP for each genotype prior to delivery of the theta burst stimulus.  $p < 0.05$ , repeated measures ANOVA.

### **3.2.9: Treatment of 6 month TASTPM slices with kynurenic acid**

#### **3.2.9.1: Introduction**

As a result of the difficulties in obtaining an fEPSP in 6 month TASTPM mice, measures were attempted to improve neuronal viability in the hippocampal slices.

Neuronal injury is an inevitable consequence of the slicing process and is due to a transient period of hypoxia combined with the mechanical severance of dendritic processes. This results in an initial phase of cytotoxic oedema where the opening of membrane cation channels causes  $\text{Na}^+$  influx and a concomitant increase in intracellular  $\text{Cl}^-$  and water, leading to neuronal swelling and possible rupture (Siklos *et al.*, 1997). The following, more slowly-evolving phase, delayed  $\text{Ca}^{2+}$ -induced neuronal degeneration, results in downstream mitochondrial dysfunction, caspase and calcineurin activation and eventual neuronal death (Dong *et al.*, 2009). Excitotoxic mechanisms in brain slices may be different to those observed *in vivo* due to the changes in brain metabolic processes and lack of cerebral blood flow in the isolated preparation.

The initial trigger for these degenerative processes appears to be the simultaneous fusion and exocytosis of multiple synaptic vesicles resulting in a marked increase in extracellular glutamate concentrations (Fiala *et al.*, 2003) which causes the simultaneous activation of glutamate receptors, in particular the NMDA receptor. There are several methods that can be used to reduce the effects of glutamate toxicity during slicing, including modification of the ionic composition of the aCSF or the addition of the compound kynurenic acid. The ability of kynurenic acid to guard against excitotoxicity is due to its actions as a NMDA receptor

antagonist at the glycine site; although it appears to have little effect on protecting against the initial neuronal swelling it is effective at preventing  $\text{Ca}^{2+}$  - induced neuronal degeneration (Richerson and Messer, 1995).

Fitzjohn *et al.*, (2001) reported the ability of kynurenic acid to reverse electrophysiological deficits obtained in the APP<sub>Swe</sub> mouse when added during the slicing process. They suggested that an increased susceptibility to excitotoxicity might underlie some of the observed deficits in these mice, and that the neurons might be more sensitive to insults including hypoxia. The 3xTg and TASTPM mice have also been generated to carry the APP<sub>Swe</sub> mutation. For this reason, experiments were carried out with kynurenic acid added to the aCSF during tissue slicing from the 3xTg and TASTPM mice to observe if this improved slice viability.

### **3.2.9.2: Methods**

To improve the chances of obtaining successful fEPSPs in the 6 month old TASTPM mouse, 1mM of kynurenic acid was added to the aCSF during slicing and for one hour subsequent to this. Slices were then transferred to an incubation pot containing normal aCSF to ensure that the kynurenic acid was washed off prior to transfer to the recording bath. This process was repeated in control mice.

### 3.2.9.3: fEPSP measurements

The fEPSP amplitude at an input stimulation of 1.5mA, at the top of the input output curve, was recorded for a number of slices. The amplitude rather than the slope was chosen as it is easier to record the amplitude in smaller fEPSPs where the shape of the field may be altered. In control mice, the maximum amplitude of the fEPSP is  $1.2 \pm 0.15$  mV under normal conditions. However, in 6 month TASTPM mice the fEPSP amplitude is very small, with an average of  $0.4 \pm 0.10$  mV/ms. When treated with 1mM kynurenic acid, the amplitude increases significantly ( $p < 0.05$ , unpaired t-test) to  $1.72 \pm 0.27$  mV (Fig. **3.36A**).

The percentage of slices which showed useable fEPSPs in the 6 month TASTPM slices was only 27%. However, when kynurenic acid was added during slicing the percentage of slices in which fEPSPs could be obtained increased to 100%, showing that the compound increases slice viability (Fig. **3.36B**).

### 3.2.9.4: Long-term potentiation

LTP was measured in the CA1 region in slices treated with 1mM kynurenic acid. In all experiments a baseline fEPSP was recorded at 30 second intervals until the slope of the fEPSP was stabilised and constant over a 10 min period before delivery of the theta burst stimulus. In the following section the slope of the fEPSP is normalised to baseline (i.e. 100%) for each recording.

The magnitude of LTP obtained in slices treated with 1mM kynurenic acid was also recorded. In untreated TASTPM slices ( $n = 3/2$ ) the peak enhancement of

the slope of the fEPSP is  $361 \pm 39\%$ , with a mean following 4 pulse theta burst stimulus from 50-60 minutes of  $231 \pm 40\%$ . In slices treated with kynurenic acid, ( $n = 10/4$ ), the peak enhancement is  $263 \pm 14\%$ , with a mean from 50-60 minutes of  $166 \pm 7\%$ . This is similar to the results obtained in control mice ( $n = 14/8$ ), where the peak enhancement is  $225\% \pm 14\%$ , with a mean from 50-60 minutes of  $170 \pm 6\%$  (Fig. **3.37A**).

Incubation with 1mM kynurenic acid significantly reduces the magnitude of LTP in 6 month TASTPM slices ( $p < 0.05$ , repeated measures ANOVA). There is no difference between LTP obtained in kynurenic acid treated TASTPM slices compared with control ( $p > 0.05$ , repeated measures ANOVA) (Fig. **3.37B**).

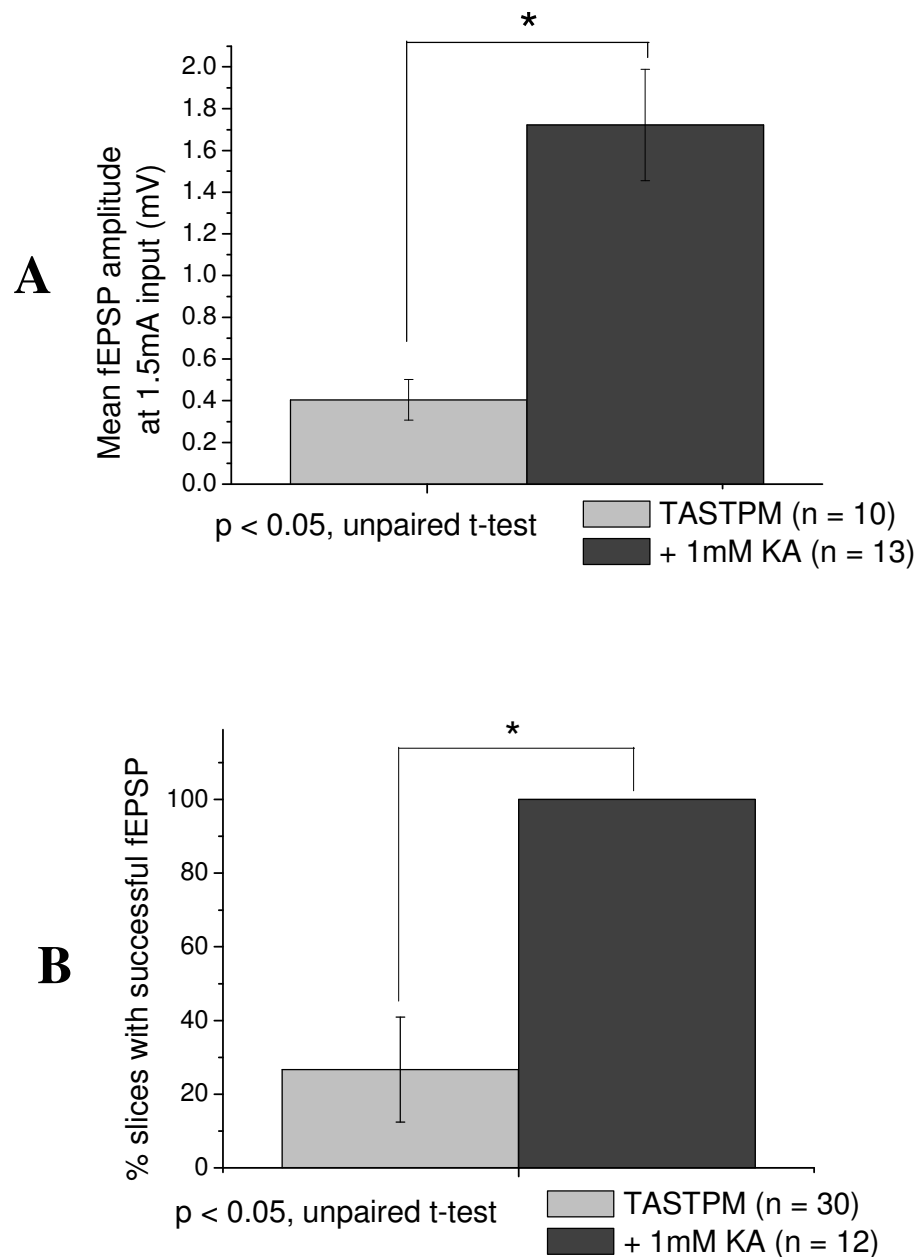


**Figure 3.36: Maximum fEPSP amplitude and percentage of successful fEPSPs obtained from slices in 6 month old TASTPM mice treated with 1mM kynurenic acid.** The fEPSP amplitude at 1.5mA input (which produces the maximum fEPSP) was recorded in slices incubated in normal aCSF ( $n = 10$ ) and aCSF containing 1mM kynurenic acid ( $n = 13$ ) (**A**). The percentage of slices in which an fEPSP could be successfully obtained is shown in (**B**).  $p < 0.05$ , unpaired t-test.

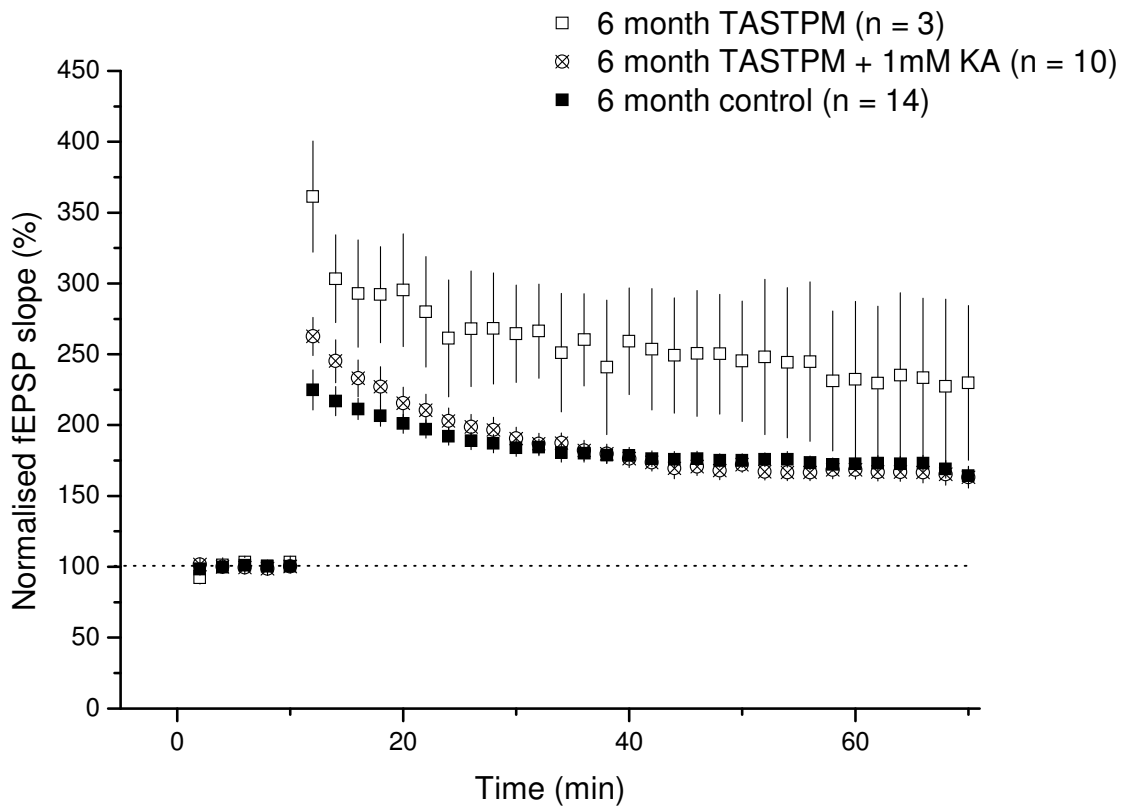


**Figure 3.37: Long term potentiation in 6 month TASTPM mice, with and without treatment with 1mM kynurenic acid, and control mice.** The potentiation of the fEPSP slope obtained following four-pulse theta burst was measured in 6 month control mice (n = 14/8), TASTPM slices incubated in normal aCSF (n = 3/2) and aCSF containing 1mM kynurenic acid (n = 10/4). All data are normalised to the average slope of the fEPSP for each genotype prior to delivery of the theta burst stimulus.  $p < 0.05$ , TASTPM and control.  $p > 0.05$ , TASTPM + 1mM KA and control.

### **3.2.10: Treatment of 12 month 3xTg slices with kynurenic acid**

Following the results obtained in the TASTPM mice, studies were conducted on 12 month 3xTg mice to see if the fEPSP amplitude was increased following treatment with 1mM kynurenic acid. A more detailed analysis including input-output function and PPF could be carried out as fEPSPs are readily obtained in both 12 month control and 3xTg slices.

#### **3.2.10.1: fEPSP measurements**

The fEPSP amplitude at an input stimulation of 1.5mA, at the top of the input output curve, was recorded for a number of slices. In control slices, the maximum fEPSP amplitude is  $1.28 \pm 0.1$  mV. In 3xTg slices incubated in normal aCSF, the fEPSP amplitude is  $0.61 \pm 0.2$  mV. Under normal conditions, there is a significant difference between 3xTg and control ( $p < 0.05$ , unpaired t-test).

Following incubation with 1mM kynurenic acid, there is a slight, but not significant increase in the maximum fEPSP amplitude ( $p > 0.05$ , unpaired t-test) in the control mice, to  $1.5 \pm 0.2$  mV/ms. However, there is a significant increase ( $p < 0.05$ , unpaired t-test) in the maximum fEPSP amplitude in 3xTg mice, to  $1.54 \pm 0.2$  mV/ms (Fig. **3.38**). This shows that incubation with kynurenic acid recovers the fEPSP amplitude in 3xTg mice to a level similar to control, where there is no significant difference between the two groups ( $p > 0.05$ , unpaired t-test).

### 3.2.10.2: Input-output function

Input-output function was also measured in 12 month 3xTg and control mice treated with 1mM kynurenic acid. A normalised input-output curve, where the maximum field slope is set to 100%, was generated, along with a non-normalised input-output curve using the actual values obtained.

In the 12 month control mice, there is no significant difference in the input-output curve between treated and untreated slices ( $p > 0.05$ , unpaired t-test) (Fig. **3.39A**). However in 3xTg mice there is a significant increase in the normalised input-output curve following incubation with kynurenic acid ( $p < 0.05$ , unpaired t-test) (Fig **3.39B**).

For the non-normalised input-output curve, the untreated control mice have an fEPSP slope at 1 mA of  $0.40 \pm 0.04$  mV/ms, and in slices incubated with 1mM kynurenic acid, the control mice have an fEPSP slope at 1 mA of  $0.67 \pm 0.14$  mV/ms (Fig. **3.40A**)

For the non-normalised input-output curve, the untreated 3xTg mice have an fEPSP slope at 1 mA of  $0.17 \pm 0.02$  mV/ms, and in slices incubated with 1mM kynurenic acid, the 3xTg mice have an fEPSP slope at 1 mA of  $0.82 \pm 0.13$  mV/ms (Fig. **3.40B**).

There is a significant increase ( $p < 0.05$ , unpaired t-test) in the fEPSP slope at 0.2 and 0.3mA only in control mice, while there is a significant increase ( $p < 0.05$ , unpaired t-test) at all stimulus intensities from 0.2mA – 1mA in 3xTg mice after kynurenic acid treatment.

### 3.2.10.3: Paired-pulse facilitation

Paired-pulse facilitation was measured in slices from 3xTg and control mice incubated in kynurenic acid. In all experiments, the maximum facilitation was observed at an interstimulus interval of 50ms.

In control mice (n = 14/6) the paired-pulse ratio at 50ms is  $1.67 \pm 0.05$ . In slices treated with 1mM kynurenic acid (n = 14/5), the paired-pulse ratio at 50ms is  $1.45 \pm 0.04$  (Fig. **3.41A**).

In 3xTg mice (n = 13/6), the paired-pulse ratio at 50ms is  $1.68 \pm 0.07$ . In slices treated with 1mM kynurenic acid (n = 11/5), the paired-pulse ratio at 50ms is  $1.34 \pm 0.03$  (Fig. **3.41B**).

There is a significant decrease in PPF in control mice only at interstimulus intervals up to 100ms ( $p < 0.05$ , repeated measures ANOVA followed by unpaired t-test). There is a significant decrease in PPF at all intervals when 3xTg mice are treated with 1mM kynurenic acid ( $p < 0.05$ , repeated measures ANOVA).

### 3.2.10.4: Long-term potentiation

LTP was measured in the CA1 region in slices treated with 1mM kynurenic acid. In all experiments a baseline fEPSP was recorded at 30 second intervals until the slope of the fEPSP was stabilised and constant over a 10 min period before delivery of the theta burst stimulus. In the following section the slope of the fEPSP is normalised to baseline (i.e. 100%) for each recording.

In untreated slices, in 12 month control mice ( $n = 17/7$ ), the peak enhancement of the slope of the fEPSP is  $233 \pm 18\%$ , with a mean from 50-60 minutes following the theta burst stimulus of  $177 \pm 8\%$ . In slices incubated with 1mM kynurenic acid, in 12 month control mice ( $n = 11/4$ ), the peak enhancement is  $176 \pm 14\%$ , with a mean from 50-60 minutes of  $155 \pm 8\%$  (Fig. **3.42A**).

In untreated slices, in 12 month 3xTg mice ( $n = 11/6$ ), the peak enhancement of the fEPSP slope is  $302 \pm 21\%$ , with a mean from 50-60 minutes of  $210 \pm 13\%$ . In slices incubated with 1mM kynurenic acid, in 12 month 3xTg mice ( $n = 8/4$ ), the peak enhancement is  $183 \pm 18\%$ , with a mean from 50-60 minutes of  $140 \pm 5\%$  (Fig **3.42B**).

There is no difference in the magnitude of LTP in control mice with ( $n = 10/4$ ) and without ( $n = 17/7$ ) kynurenic acid. There is a significant decrease in the magnitude of LTP in 3xTg mice ( $n = 11/6$ ) with the addition of 1mM kynurenic acid during slicing ( $n = 8/4$ ).

### **3.2.10.5: Summary**

Incubation of slices with 1mM kynurenic acid improves slice viability in both 3xTg and TASTPM mice. This is shown by the increase in fEPSP amplitude and markedly higher percentage of successful fEPSPs in slices treated with kynurenic acid. In 3xTg mice when other electrophysiological parameters are studied there is found to be a decrease in PPF at all stimulus intensities, and a significant decrease in the magnitude of LTP with kynurenic acid treatment which is not observed in control mice.

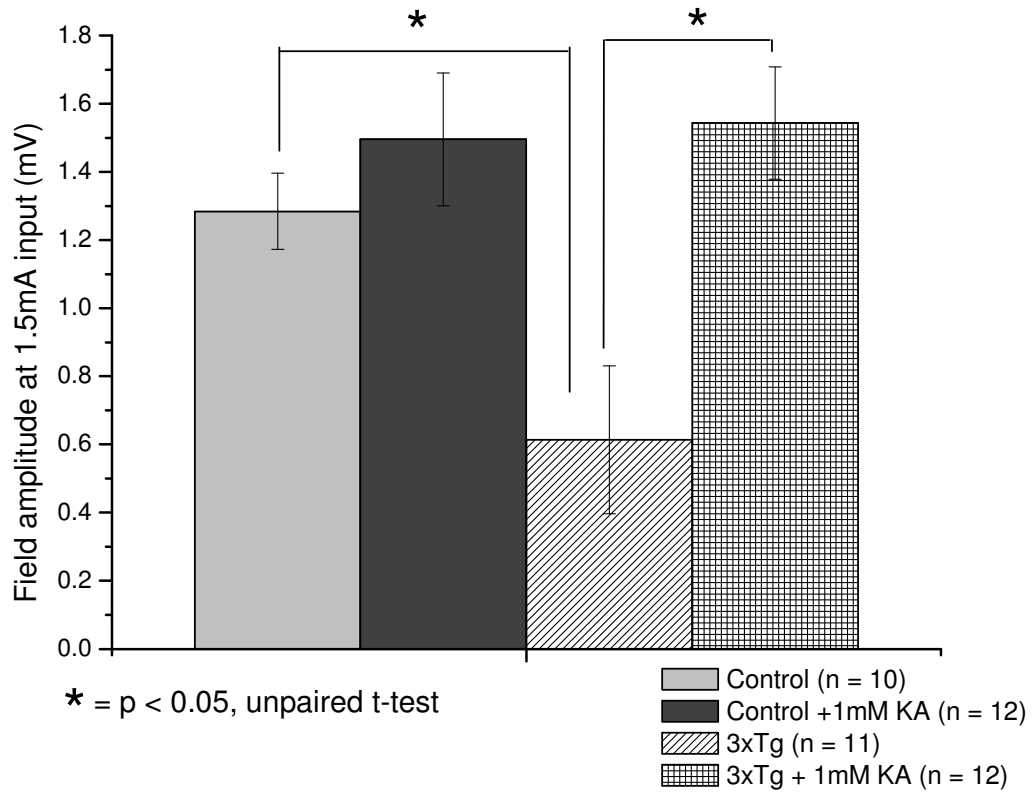


**Figure 3.38: A comparison of fEPSP amplitude in 12 month 3xTg and control mice with and without treatment with 1mM kynurenic acid.** The fEPSP amplitude at 1.5mA input (which produces the maximum fEPSP) was recorded in control slices (n = 10/5) and 3xTg slices (n = 11/6) incubated in normal aCSF, and compared with control slices (n = 12/4) and 3xTg (n = 12/4) incubated in aCSF containing 1mM kynurenic acid. \* =  $p < 0.05$ , unpaired t-test.

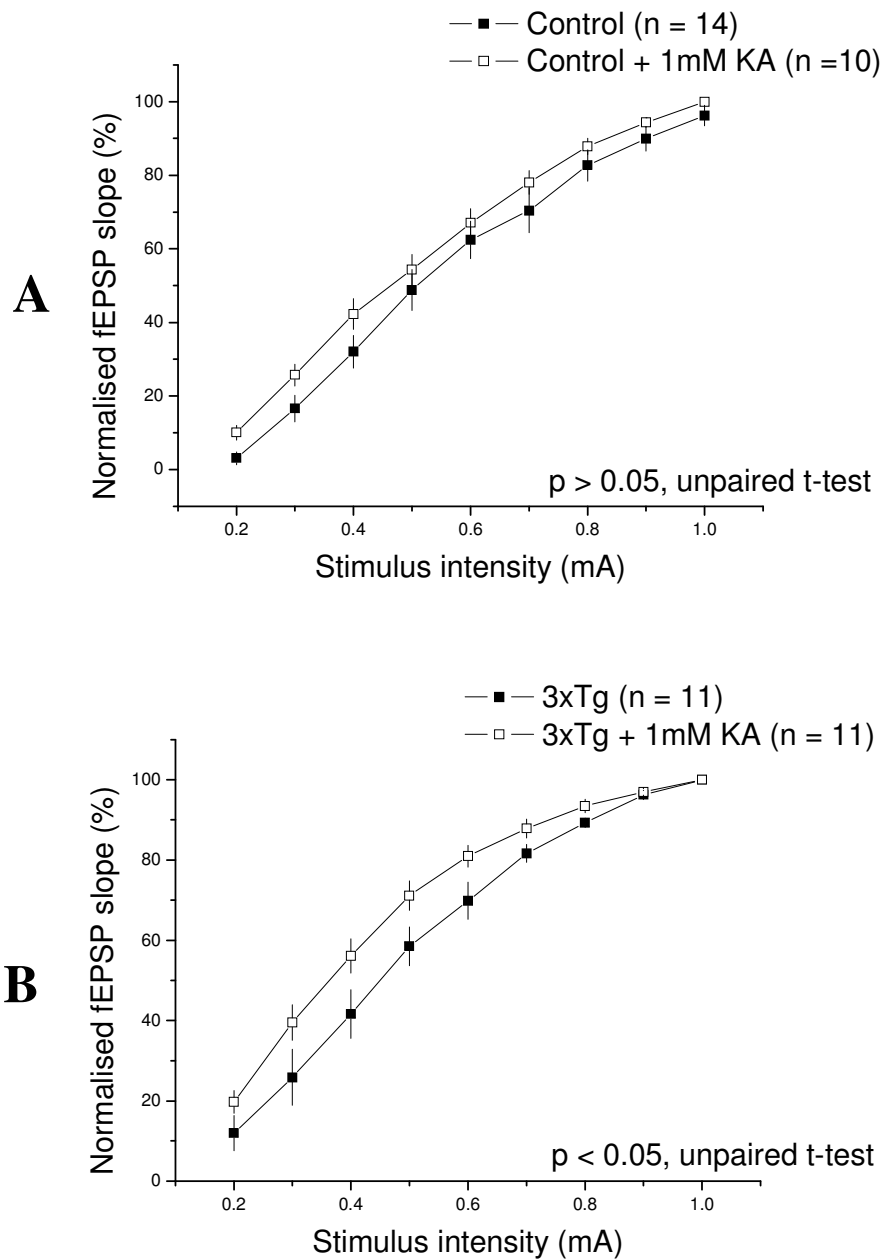


**Figure 3.39: Normalised input-output curves obtained from 12 month old male and female 3xTg and control mice treated with 1mM kynurenic acid.** The fEPSP slope was measured at a range of stimulus intensities and then normalised in slices from control (n = 14/7) and control (n = 10/4) incubated in 1mM kynurenic acid (A).  $p > 0.05$ , unpaired t-test. This was repeated in slices from 3xTg mice (n = 11/6) and 3xTg mice (n = 11/5) incubated in 1mM kynurenic acid (B).  $p < 0.05$ , unpaired t-test.

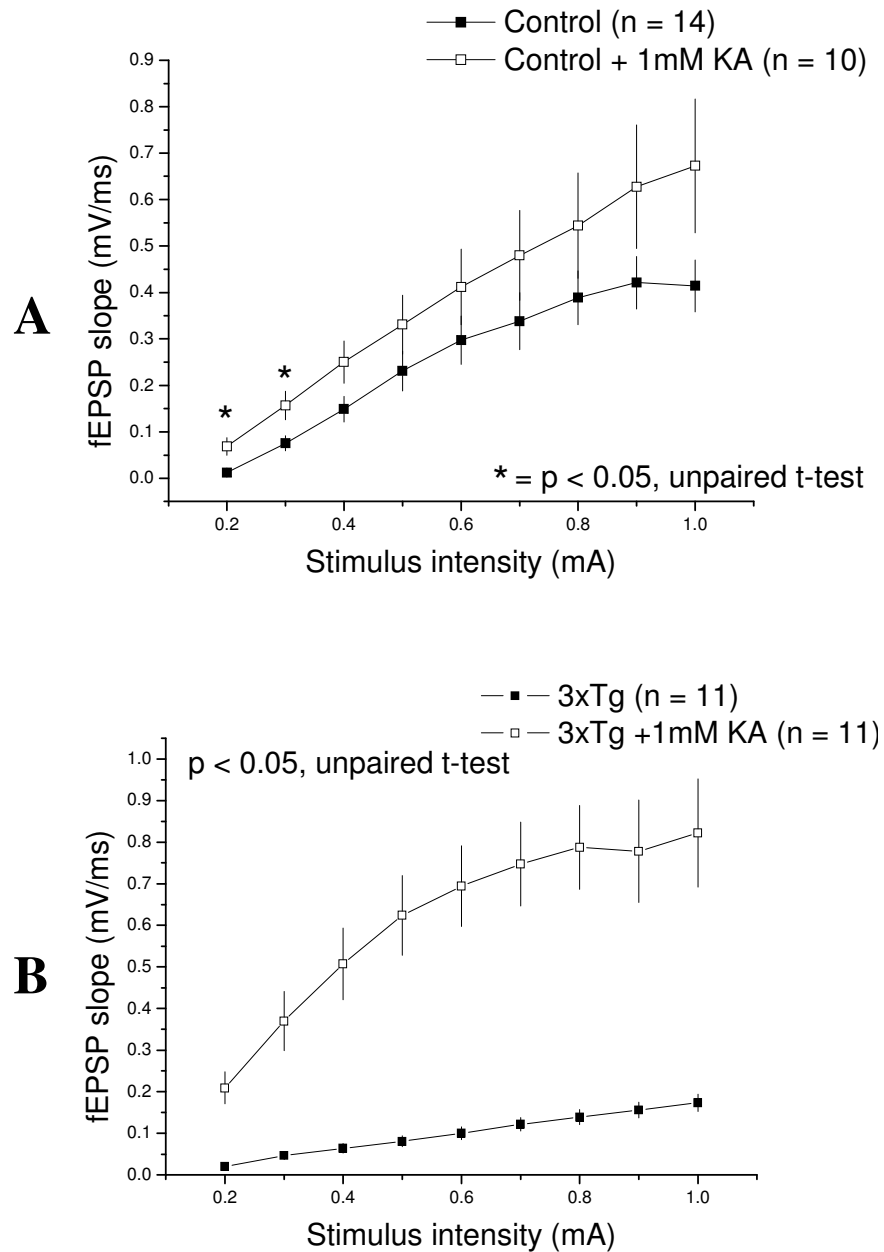


**Figure 3.40: Non-normalised input-output curves obtained from 12 month old male and female 3xTg and control mice treated with 1mM kynurenic acid.**

The fEPSP slope was measured at a range of stimulus intensities in slices from control (n = 14/7) and control incubated in 1mM kynurenic acid (n = 10/4) (A).  $p < 0.05$ , unpaired t-test, at stimulus intensities of 0.2 and 0.3 mA only. The fEPSP slope was measured at a range of stimulus intensities in slices from 3xTg mice (n = 11/6) and 3xTg mice incubated in 1mM kynurenic acid (n = 11/5) (B).  $p < 0.05$ , unpaired t-test.

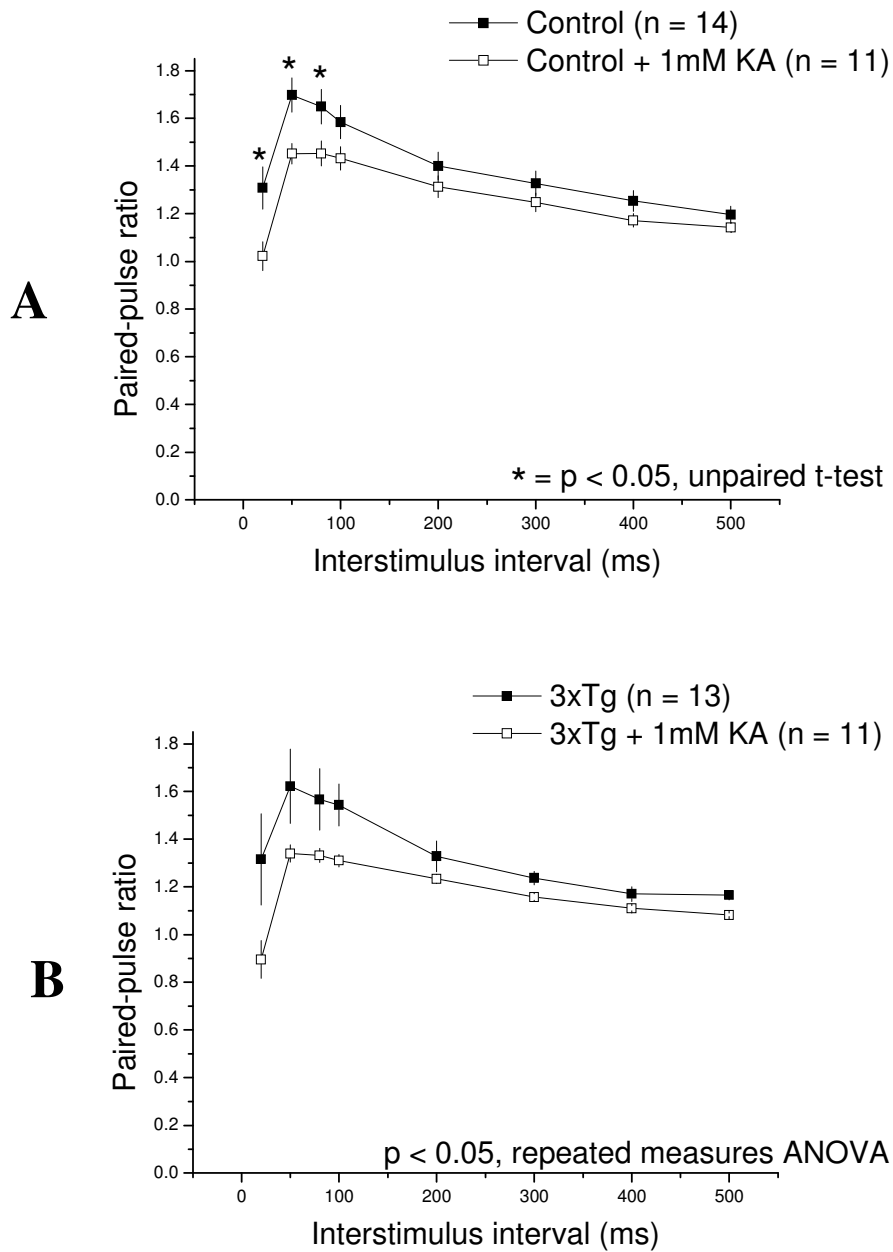


**Figure 3.41: Paired-pulse facilitation determined in 12 month 3xTg and control treated with 1mM kynurenic acid.** The paired-pulse ratio was calculated at a range of interstimulus intervals in control mice in untreated slices (n = 14/7) and slices incubated in 1mM kynurenic acid (n = 11/4) (A).  $p < 0.05$ , repeated measures ANOVA followed by unpaired t-test, at interstimulus intervals up to 100ms only. The paired-pulse ratio was calculated at a range of interstimulus intervals in 3xTg mice in untreated slices (n = 13/6) and slices incubated in 1mM kynurenic acid (n = 11/4) (B).  $p < 0.05$ , repeated measures ANOVA

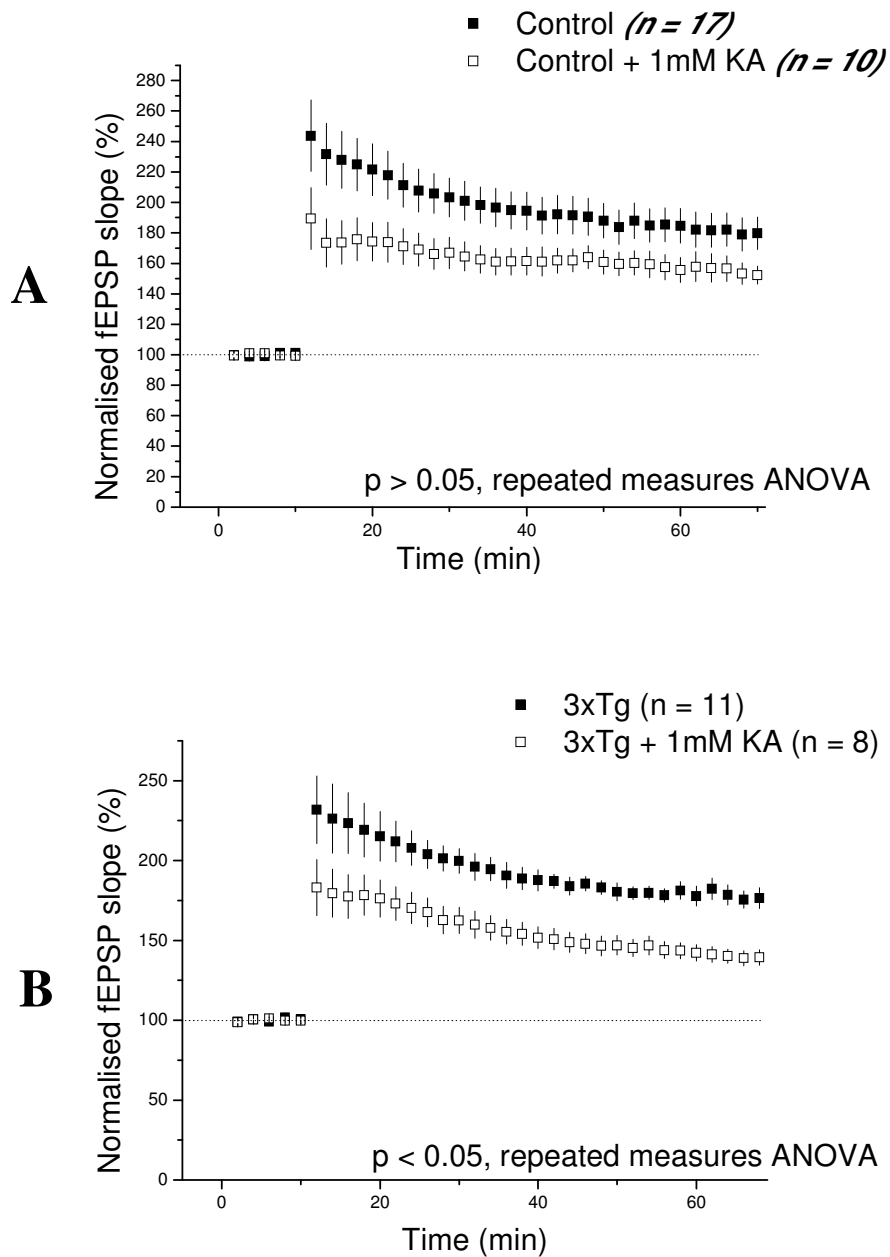


**Figure 3.42: Long term potentiation in 12 month 3xTg and control with and without 1mM kynurenic acid.** The potentiation of the fEPSP slope obtained following four-pulse theta burst was measured in slices from control mice ( $n = 17/7$ ) and control slices incubated in 1mM kynurenic acid ( $n = 10/4$ ) (A).  $p > 0.05$ , repeated measures ANOVA. The potentiation of the fEPSP slope was measured in 3xTg mice ( $n = 11/6$ ) and 3xTg mice incubated in 1mM kynurenic acid ( $n = 8/4$ ). All data are normalised to the average slope of the fEPSP for each genotype prior to delivery of the theta burst stimulus (B).  $p < 0.05$ , repeated measures ANOVA.

### **3.3: Discussion**

Alterations in synaptic transmission and plasticity have been observed in mouse models of AD including the 3xTg and TASTPM models, however results from different research groups have proved inconsistent. Electrophysiological recordings were made from 3xTg and TASTPM mice to observe if there were any differences in synaptic function in these models and if these findings were consistent with previously reported results.

#### **3.3.1: Technical aspects**

There are a number of technical variables which can affect slice viability and LTP measurements, such as the mechanisms of slice preparation, temperature and recording used (summarised in Table **3.1**). For this reason, it is difficult to compare studies of hippocampal electrophysiology between individual research groups if these variables are not standardised. Critically, the stimulation protocol used may result in the activation of distinct signalling pathways; for example the ability of acutely applied A $\beta$  oligomers to impair LTP depends upon the paradigm used (HFS vs. TBS) (Smith *et al.*, 2009).

Other technical issues associated with electrophysiological recordings are the biochemical changes which inevitably occur during the preparation of the hippocampal slice. This may involve alterations in phosphorylation of cellular proteins, such as the AMPA receptor, CaMKII and Src family kinases (Ho *et al.*,

2004) and in gene regulation and transcription (Taubenfeld *et al.*, 2002). Specific to transgenic models of AD, it has been suggested that extracellular soluble A $\beta$  may in fact diffuse out of slices, resulting in a reduction of the concentration of A $\beta$  within the tissue (Waters 2010).

The acute slice preparation is a useful experimental tool to study hippocampal synaptic function, but these examples highlight the limitations present with the technique. There may be biochemical and functional differences in the transgenic mice which might only become apparent using studies in the intact animal e.g. *in vivo* electrophysiology.

**Table 3.1: Technical variables in hippocampal slice recordings**

<b>Variable</b>	<b>Effect</b>	<b>Reference</b>
Hippocampal subdivision (CA1, DG)	Regional anatomical and functional differences	Swanson-Park <i>et al.</i> 1999
Ionic composition of aCSF (Mg <sup>2+</sup> , Ca <sup>2+</sup> , glucose)	Altered neuronal viability and synaptic transmission, likelihood of epileptiform activity	Richerson <i>et al.</i> 1995
Slice preparation (ice cold aCSF, glutamate receptor antagonists)	Degree of excitotoxicity and neuronal viability	Fitzjohn <i>et al.</i> 2001
Slice recovery temperature (cold, room temp., 37°C)	Metabolic alterations, susceptibility to epileptiform activity	Watson <i>et al.</i> 1997
Stimulation protocol (HFS, TBS)	Activation of alternative signalling pathways	Hernandez <i>et al.</i> 2005
Interface or submerged recording	Activation of alternative signalling pathways	Capron <i>et al.</i> 2006
Bath temperature (30°C - 37°C)	Reduction of fEPSP amplitude at higher temperatures	Masino <i>et al.</i> 2000

### **3.3.2: Characterisation of the 3xTg mouse**

In the 3xTg mouse model, multiple parameters were recorded including input-output function, PPF and LTP. The results obtained are discussed below in the following sections.

#### **3.3.2.1: Paired-pulse facilitation in the 3xTg model**

PPF was measured from 2 to 17 months in 3xTg and control mice. In control mice, PPF remained stable with a ratio of 1.5 – 1.7 at 50ms from 6 to 17 months, but there was a significant increase in PPF at 2 months compared with the other ages studied (a ratio of 1.9 at 50ms), a difference that was most marked in male mice. In 3xTg mice, the magnitude of PPF remained stable with age (1.5 – 1.7), with a similar ratio to that of control mice. Consequently, this results in a significant difference between the magnitude of PPF in 3xTg and control mice at 2 months only. However, it is not clear whether this is due to an enhancement of PPF in the younger control mice or a reduction in PPF in the 3xTg mice. The magnitude of PPF recorded in the mouse hippocampus shows variation between research groups; values are generally within the range of 1.3 – 2.0, so PPF in control mice is of the expected range in our colony. Age-dependent differences have not previously been observed in control mice (Ris *et al.*, 2005, Fitzjohn *et al.*, 2010) but a comprehensive analysis of the effects of PPF with ageing has not been carried out so developmental changes, strain or gender-dependent differences can not be ruled out.

PPF is dependent on the intracellular  $\text{Ca}^{2+}$  concentration within the presynaptic terminal, with the residual rise in  $\text{Ca}^{2+}$  following the first stimulus allowing enhanced vesicular neurotransmitter release on the second stimulus (Nathan *et al.*, 1990). The difference in the paired-pulse ratio between 2 month old 3xTg and control mice suggests an alteration in presynaptic function between the two groups. Of the three transgenes present in the 3xTg mouse, PS1 is widely known to be involved in neuronal  $\text{Ca}^{2+}$  regulation, with the PS1<sub>M146V</sub> mutation markedly increasing  $\text{Ca}^{2+}$  release and signalling in cortical neurons (Stutzmann *et al.*, 2004). Oddo *et al* (2003) reported that the PS1<sub>M146V</sub> mutation increased PPF at 6 months in transgenic mice, and this was also observed in double transgenic mice with the additional tau<sub>P301L</sub> transgene. The presence of the single APP<sub>Swe</sub> mutation alone has no effect on the magnitude of PPF (Fitzjohn *et al.*, 2001). Surprisingly, the combination of the three transgenes together in the 3xTg mouse results in a masking of the effects of the PS1<sub>M146V</sub> mutation as PPF has been reported to be normal at 1 and 6 months (Oddo *et al.*, 2003). This result has been replicated in our colony of 3xTg mice at older ages showing that the progression of pathology in these mice does not result in an age-dependent effect on presynaptic function.

### **3.3.2.2: Basal synaptic transmission in the 3xTg model**

The normalised input-output curve reveals the electrical stimulation required to elicit an fEPSP of increasing magnitude. There is a significant rightward shift in 12 and 17 month 3xTg mice. This shows that a higher input current is required to obtain an fEPSP of similar magnitude to control and shows that deficits in basal synaptic transmission are present in these mice at older ages.

The non-normalised output curve provides the actual numerical fEPSP slope values obtained at each stimulus intensity. Control mice show no age-dependent changes in input-output function, but in contrast, 3xTg mice demonstrate a progressive reduction in the fEPSP slope from the ages of 2 to 12 months. In our colony of 3xTg mice at 6 months, there is no difference in input-output function or baseline fEPSP recordings compared to control, while at 12 and 17 months both the input-output curve and the baseline fEPSP recordings are markedly reduced. These findings may reflect the recruitment of a smaller population of neurons at each input intensity, which could be due to neuronal damage through excitotoxicity (discussed in more detail in Section **3.3.1.7**.) However, at 2 months there is a significant enhancement in the baseline fEPSP. These results show that basal synaptic transmission is enhanced in young 3xTg mice. The mechanism of this perturbation is not known and may vary depending on the stimulus intensity, as experimental stimulus strength can differentially affect presynaptic and postsynaptic function (Chakroborty *et al.*, 2009). However, it may involve an increase in neuronal excitability as 3xTg mice show a hyperactivity of glutamatergic synapses in the hippocampus observed as an increased rate of spontaneous firing in patch clamp studies (Arsenault *et al.*, 2011). This increased excitatory drive may result in a degree of network dysfunction; this has been suggested as a factor contributing to cognitive dysfunction in other transgenic models of AD and is discussed further below in Section **3.3.2.6**.

The fEPSP slope value obtained in the 3xTg mice at 2 months of 0.4mV/ms at 1mA is similar to that obtained by Chakroborty *et al.* (2009), showing that the magnitude is within the normal range, but the values are markedly less than the

1mV/ms at 1mA obtained by Oddo *et al.* (2003), which may reflect differences in experimental protocol for extracellular recording. Oddo *et al.* (2003) reported a normal input-output function in the 3xTg mouse at 1 month of age, but a reduction in the fEPSP slope at 6 months; this occurred in control but was more marked in 3xTg mice. At this age, the fEPSP slope in 3xTg mice was ~ half that of control, a ratio which is not observed in our colony of mice until 12 months of age. This suggests that the development of pathological features has occurred more rapidly in the colony of mice studied by Oddo *et al.* This group also observed identical changes in the single-transgenic PS1<sub>M146V</sub> and double-transgenic PS1<sub>M146V</sub>, tau<sub>P301L</sub> models, implicating the PS1 transgene in alterations of basal synaptic transmission. However, these results were not replicated by another group who noted no difference in synaptic function in PS1<sub>M146V</sub> mice (Wang *et al.*, 2004). In 3xTg mice, Chakroborty *et al.* (2009) reported no differences in input-output function at 6-8 weeks of age, but noted the presence of alterations in evoked postsynaptic Ca<sup>2+</sup> release (see Section 3.3.2.5). It is possible that there are age-independent changes in basal synaptic transmission due to the presence of the transgenes during development, as observed in our colony of mice at 2 months where despite the lack of observed biochemical changes (see Chapter 4) there are electrophysiological differences at this age. These alterations in basal synaptic transmission are followed by age-dependent deficits linked to the development of pathological features in 3xTg mice.

### **3.3.2.3: Long-term potentiation in the 3xTg model**

LTP was measured in our colony of 3xTg mice at ages from 2 to 17 months to observe if there were any alterations in this form of synaptic plasticity. To

summarise, in our colony at 2 and 6 months there are no differences in the enhancement of the fEPSP slope observed relative to the baseline following the theta burst stimulus compared to control mice. However, at 12 and 17 months there is a significant increase in the enhancement following theta burst which occurs during the initial peak phase at 12 months and the plateau phase (characteristic of LTP) at 17 months. However, it should be remembered that the overall magnitude of LTP still remains reduced when compared to control due to the smaller baseline fEPSP amplitude (see Section 3.3.2.2). However, these results show that despite the reduction in basal synaptic transmission, LTP can still be induced in the 3xTg mice and appears to show an age-dependent enhancement. There are several possible reasons for this finding which will be discussed in more detail below.

A distinction should be made between enhancement of the peak phase following the theta burst protocol, observed in 12 month 3xTg, and enhancement of the later plateau phase observed in 17 month 3xTg. The peak phase incorporates a short-term process of synaptic facilitation known as post-tetanic potentiation (PTP). While LTP is considered to involve both pre- and post-synaptic mechanisms (see Chapter 1.5.3), PTP is regarded as a purely presynaptic phenomenon. Similar to PPF, it is dependent on intracellular  $\text{Ca}^{2+}$  and involves enhanced neurotransmitter release, a consequence of an increase in the  $\text{Ca}^{2+}$  sensitivity of vesicular fusion (Korogod *et al.*, 2007). In these experiments there is an overlapping contribution of PTP and LTP and it is likely that in the 3xTg mice there are alterations in both processes.

As the increase in LTP occurs at older ages in the 3xTg mice it is conceivable that this change in synaptic plasticity is linked to the development of pathology and A $\beta$  deposition. The enhanced susceptibility to excitotoxicity observed in these mice at older ages will result in many neurons showing dysfunction or even death. As a result, LTP may be induced only in a subset of neurons which remain healthy; it is possible that compensatory mechanisms are present which may influence plasticity in these remaining neurons. Even though a smaller fEPSP is generated the enhancement in the 3xTg mice following theta burst is greater than in control, but this may not be representative of the full neuronal population. The reported perturbations in Ca<sup>2+</sup> homeostasis could also affect the magnitude of LTP, which is critically dependent on the intracellular Ca<sup>2+</sup> concentration for its induction. Finally, the presence of the PS1 and APP transgenes can alter the magnitude of LTP obtained (see Section **3.3.2.4** below).

Several groups have studied synaptic plasticity in the 3xTg mouse model. Oddo *et al.* (2003) reported a decrease in the magnitude of LTP at 6 months in the 3xTg mouse when compared to control, but there are several differences in this study which should be taken into consideration. This group observed a marked increase in LTP in control mice between the ages of 1 month and 6 months, from around 140% to 190%, which served to enhance the reported deficit in the 3xTg mice. Although an age-dependent increase was observed in our colony of mice from 2 to 6 months this was not as marked; the magnitude of potentiation was 157% at 2 months and 170% at 6 months. An important observation is the use by Oddo *et al.* of four bursts of high-frequency stimulation (HFS) repeated at 20 second intervals for the induction of LTP. This is characterised as a very strong stimulation protocol in comparison to TBS, and it is known that the choice of

induction protocol recruits different biochemical pathways (Hernandez *et al.*, 2005). Another technical difference that can influence the interpretation of results is the use of an interface chamber by Oddo *et al.* rather than a submersion recording chamber as used in my experiments. In other studies of 3xTg mice, Chakroborty *et al.* (2009) showed no changes in the magnitude of LTP induced in young 3xTg mice at 6-8 weeks. This finding would be expected if the perturbation of LTP is linked to the age-dependent development of pathological features. Another group to have studied synaptic plasticity in the 3xTg mouse reported that at 10 months the magnitude of LTP induced by TBS was similar to that obtained in control mice, which is in contrast to the original findings (Zhang *et al.*, 2010b). From these studies it is evident that the measurement of LTP in the 3xTg mouse has given inconsistent results and must be interpreted with care due to variations in technical protocol between individual groups.

#### **3.3.2.4: Effects of the individual transgenes on synaptic plasticity**

A number of studies have been carried out to investigate the effects of APP, PS1 and tau transgene expression on synaptic plasticity. In the original paper which characterised the 3xTg model, Oddo *et al.* reported that LTP could be induced normally in both the single transgenic PS1<sub>M146V</sub> and the double transgenic PS1<sub>M146V</sub>, tau<sub>p301L</sub> mice at 2 and 6 months of age. Immediately following induction there was actually a significant increase in the magnitude of potentiation in the PS1<sub>M146V</sub> mice at 6 months of age when compared to control. Similar effects of the PS1<sub>M146V</sub> mutation were observed in another study, but interestingly this change was accompanied by a decrease in the magnitude of the sustained phase of LTP, L-LTP, and both E-LTP and L-LTP reduced with

advancing age in older mice (Auffret *et al.*, 2010). These findings suggest that there may be a dissociation between the effects of PS1<sub>M146V</sub> on E-LTP and L-LTP. As my studies of the 3xTg mice only examined E-LTP, it would be of interest to investigate whether there were differences in L-LTP in these mice. Studies using other PS1 transgenic mice suggest that familial AD mutations may have an overall effect of enhancing the magnitude of LTP. Both PS1 $\Delta$ E9 (exon 9 deleted) and PS1<sub>A246E</sub> mice exhibit increased potentiation compared to control following LTP induction, an effect which has been attributed to an enhancement in postsynaptic intracellular Ca<sup>2+</sup> following NMDA receptor activation (Parent *et al.*, 1999, Zaman *et al.*, 2000). A similar mechanism could be present in the 3xTg mice, which might result in the observed increase in LTP. If alterations in Ca<sup>2+</sup> signalling become more pronounced with age this could result in the increased potentiation observed in older mice relative to the baseline fEPSP.

In contrast, there is evidence that familial APP mutations may reduce the magnitude of LTP, although there have been conflicting results between research groups, with some reporting no effect of APP mutation on synaptic plasticity (Fitzjohn *et al.*, 2001). This inconsistency may be due to differences in experimental protocol (see Section 3.3.1) which can have a marked effect on the results obtained. In the commonly used Tg2576 model, which expresses the single APP<sub>Swe</sub> transgene, several groups have reported reduced hippocampal LTP. For example, in the CA1 region, LTP is normal until 8 months, but there is a decrease in the magnitude of LTP at 15 months with no reduction in basal fEPSP amplitude (Chapman *et al.*, 1999b). Similarly, reduced LTP has been reported in another region of the hippocampus, the DG, from the age of 4 months (Jacobsen *et al.*, 2006). This suggests that the APP<sub>Swe</sub> transgene causes an age-dependent

reduction of synaptic plasticity in the hippocampus. However, the mechanism underlying this is not fully understood.

Several studies have used the application of A $\beta$  oligomer preparations to study the effects of acute exposure to A $\beta$  on synaptic plasticity in hippocampal slices. This may mimic some of the effects of excessive A $\beta$  generation associated with APP transgene expression. The treatment of isolated hippocampal slices with A $\beta$  oligomers reduces the magnitude of LTP which can be obtained (Walsh *et al.*, 2002, Shankar *et al.*, 2008) although this may also be dependent on the stimulation protocol used (Smith *et al.*, 2009). This perturbation is thought to occur through an NMDA receptor-mediated pathway, with A $\beta$  causing AMPA receptor endocytosis and leading to loss of dendritic spines (Hsieh *et al.*, 2006). Another possibility is that A $\beta$  oligomers increase susceptibility to excitotoxicity, and this is discussed in Section **3.3.2.7**.

The 3xTg mouse also carries the tau<sub>P301L</sub> transgene, but relatively little work has been carried out on the effects of tau mutations on synaptic plasticity. One study found that LTP was enhanced in 2 month tau<sub>P301L</sub> mice prior to the development of tau hyperphosphorylation (Boekhoorn *et al.*, 2006). Another investigation reported a requirement for the tau protein in acute A $\beta$ -induced impairment of LTP, although the mechanism underlying this interaction is not known (Shipton *et al.*, 2011). This finding reveals that the presence of the tau<sub>P301L</sub> transgene may also affect synaptic plasticity. However, the similar results obtained in this thesis for the 3xTg and for the TASTPM mice that do not carry the tau transgene, suggest that tau may have little effect on synaptic function in these models.

In conclusion, there may be differential effects of the APP and PS1 transgenes on LTP. This complexity highlights the difficulties of using models such as the 3xTg that contain multiple transgenes, which may have conflicting effects on synaptic function. Further work is required using standardised procedures between laboratories to help explain the discrepancies in the 3xTg model and other mouse models of AD. It is likely that alterations in synaptic plasticity occur through a number of different age-dependent and age-independent processes and further work would be required to separate the mechanisms involved. It would be interesting to use immunohistochemical approaches and neuronal imaging to study glutamate receptor localisation and other molecular alterations which occur in LTP and link this more closely to the development of pathological changes.

### **Alterations in synaptic function in the 3xTg model: multiple hypotheses**

There are several factors which have been mentioned above that could result in alterations in synaptic function, and it is likely a combination of these which cause the electrophysiological changes in the 3xTg mice. These include alterations in Ca<sup>2+</sup> regulation and homeostasis, neuronal network dysfunction and the progressive development of pathological features causing an increased susceptibility to excitotoxicity. The overall effects of these on synaptic function will be discussed in more detail below.

#### **3.3.2.5: Calcium regulation in the 3xTg model**

The regulation of neuronal Ca<sup>2+</sup> regulation is critical for all forms of plasticity from PPF to LTP, and the dynamics of Ca<sup>2+</sup> release influences the magnitude and

direction of synaptic plasticity (Cormier *et al.*, 2001). Disruptions in  $\text{Ca}^{2+}$  homeostasis have been suggested as a cause of alterations in synaptic function in the 3xTg model. From an early age, neurons from 3xTg mice show enhanced  $\text{Ca}^{2+}$ -induced  $\text{Ca}^{2+}$  release (CICR), a process whereby the influx of  $\text{Ca}^{2+}$  into the neuron, primarily through the NMDA receptor, results in activation of the ryanodine receptor (RyR) and the consequent release of further  $\text{Ca}^{2+}$  from the endoplasmic reticulum (ER) stores (Sandler and Barbara, 1999). Cortical neurons from 3xTg mice at ages from 6 weeks to 18 months display enhanced CICR in response to RyR activation (Stutzmann *et al.*, 2006), as do hippocampal CA1 neurons at 6-8 weeks, which is accompanied by an increase in expression of the RyR in the ER membrane (Chakroborty *et al.*, 2009). Interestingly, these alterations in  $\text{Ca}^{2+}$  release appear to be solely due to the presence of the PS1<sub>M146V</sub> mutation, as similar changes are observed in single transgenic PS1<sub>M146V</sub> mice, but not in the double transgenic APP<sub>Swe</sub>, tau<sub>P301L</sub> mice (Stutzmann *et al.*, 2006). Presenilins may function as leak channels to control steady state  $\text{Ca}^{2+}$  levels in the ER, with impairment due to mutation resulting in a higher concentration of  $\text{Ca}^{2+}$  in the ER and increased RyR expression (Zhang *et al.*, 2010a). In addition,  $\text{Ca}^{2+}$  responses in neuronal dendrites and spines are enhanced in response to NMDA receptor activation in the 3xTg mice and the TASTPM mice, both of which carry the PS1<sub>M146V</sub> mutation (Goussakov *et al.*, 2010).

These results suggest that there may be age-independent, lifelong disruptions in  $\text{Ca}^{2+}$  functioning in the 3xTg mice which affect aspects of synaptic plasticity. It has been reported that PPF and input-output function are similar to control in the 3xTg mice under normal conditions, but are altered by the presence of the RyR antagonist dantrolene in 3xTg mice only (Chakroborty *et al.*, 2009). These results

suggest that there may be compensatory mechanisms present in these mice to maintain neuronal homeostasis. However, it is possible that under conditions of neuronal stress both pre- and post-synaptic alterations in synaptic function could manifest themselves; these changes could contribute to the differences in input-output function and LTP observed in the 3xTg mice. Further work would be required to investigate whether alterations in  $\text{Ca}^{2+}$  function are a feature of our colony of 3xTg mice. Such studies could deploy techniques such as whole-cell voltage clamp or  $\text{Ca}^{2+}$  imaging with fluorescent dyes to observe  $\text{Ca}^{2+}$  transients in individual neurons.

### **3.3.2.6: The network dysfunction hypothesis**

There is growing interest in the way that individual molecular and neuronal alterations may affect functioning at the network level. It has been suggested that an imbalance between excitatory and inhibitory transmission in the hippocampus results in alterations in synaptic function in mouse models of AD. A general increase in neuronal excitability, which manifests as an increased amplitude of evoked excitatory postsynaptic currents (EPSCs) and a decreased amplitude of evoked inhibitory postsynaptic currents (IPSCs), occurs in the CA1 region of the CRND8 mouse, which expresses both the  $\text{APP}_{\text{Swe}}$  and  $\text{APP}_{\text{Ind}}$  (V717F) mutations (Jolas *et al.*, 2002). This mouse shows a decrease in the maximum fEPSP amplitude and an increase in the magnitude of LTP, similar to my findings in the 3xTg mouse. In the J20 mouse, which expresses the same mutations on a different background strain, GABAergic fibre sprouting in the dentate gyrus (DG) is observed and suggested to be a compensatory remodelling of the hippocampal circuits to protect against aberrant excitatory network activity (Palop *et al.*,

2007). These models suggest that widespread changes in inhibitory and excitatory activity may result in alterations of neuronal circuitry.

In the 3xTg mouse model, studies in the entorhinal cortex (EC) have shown a higher frequency of spontaneous EPSCs in 6-8 week old mice, suggesting an increased activity of glutamatergic synapses. This perturbation does not appear to alter total synapse number as levels of the presynaptic protein synaptophysin remain unchanged (Arsenault *et al.*, 2011). The EC, DG and CA1 regions are linked through a primarily unidirectional neuronal pathway, and A $\beta$  pathology in the EC has been shown to affect functioning of CA1 neurons (Harris *et al.*, 2010). In my study of 3xTg mice, alterations in the fEPSP amplitude in the CA1 region occurred from the age of 12 months, but no increased frequency of epileptiform bursting was observed. This suggests that there are no major abnormalities in GABAergic functioning, although confirmation of this would require a more detailed study. It would be interesting to observe the frequency of spontaneous EPSCs and amplitude of evoked EPSCs/ IPSCs in the 3xTg mice with the use of whole-cell voltage clamp techniques. Interestingly, it has been suggested that the relative contribution of glutamatergic and GABAergic neurons may depend on the LTP induction protocol used; differences may occur between HFS and TBS (Jolas *et al.*, 2002) and this should be taken into account when comparing experimental results from different laboratories. Overall, it is possible that alterations in the balance between excitatory and inhibitory transmission within the hippocampal network could be a mechanism involved in changes in synaptic plasticity in 3xTg mice.

### 3.3.2.7: Excitotoxicity and its mechanisms

In both the 3xTg and the TASTPM mouse models (discussed in Section 3.3.3), there is a marked reduction in the magnitude of the fEPSP in the CA1 region with increasing age. However, incubation with 1mM kynurenic acid during slicing enhanced neuronal viability as shown by an increase in the fEPSP amplitude combined with a higher percentage of slices in which an fEPSP could be obtained. This suggests that a susceptibility to excitotoxicity may underlie some of the observed results in these mice, in particular the age-dependent reduction of fEPSP amplitude. This feature appears to be due to the presence of the APP or PS1 transgenes, as it is common to both strains of transgenic mice.

Neuronal death and dysfunction due to glutamate excitotoxicity is a mechanism considered to be important in AD. This form of neurotoxicity involves the influx of  $\text{Ca}^{2+}$  through the NMDA receptor and subsequent release of  $\text{Ca}^{2+}$  from internal stores, resulting in the activation of downstream signalling pathways (Dong *et al.*, 2009). Consequently, the NMDA receptor channel blocker memantine is now used therapeutically as a treatment for AD. The increased susceptibility to excitotoxicity in transgenic mice could be associated with a number of different biochemical and functional changes, which could be studied using several different techniques.

It is most likely that this feature is due to dysfunction of the glutamatergic neurotransmitter system, although alterations in other neurotransmitters such as GABA could alter the inhibitory-excitatory balance within the hippocampus. The role of the NMDA receptor in this process could be confirmed by the use of selective antagonists, for example the use-dependent channel blocker MK-801.

Alterations could occur at any stage during glutamatergic synaptic transmission, for example in transmitter release, glutamate uptake and transport, or the intracellular  $\text{Ca}^+$  response to NMDA receptor activation.

The release of glutamate in response to neuronal damage could be measured using electrochemical techniques, as it is possible that increased presynaptic vesicular release in response to hypoxic or mechanical insult could contribute to enhanced excitotoxic damage. Alternatively, glutamate uptake could be indirectly measured using techniques such as the measurement of synaptically activated glutamate transporter currents; astrocytes within the CA1 region are thought to take up the majority of glutamate released through a high level of expression of glutamate transporters (Diamond 2005). These cells rapidly decarboxylate and inactivate glutamate to form glutamine, which diffuses across the extracellular space and can enter presynaptic terminals. It is possible that in transgenic mice there is an alteration in glutamate uptake by astrocytic cells and this could be measured using antagonists for the most abundant transporter proteins, excitatory amino-acid transporters 1 and 3 (EAAT1, EAAT3), such as the commonly used TBOA (Danbolt 2001). Evidence suggests that in conditions of cellular stress such as ischemia, alterations in ionic balance such as an increase in extracellular  $\text{K}^+$  caused by disrupted metabolic function may result in the reversal of transporter uptake. This occurs because the movement of glutamate across the transporter is dependent on the electrochemical gradient of cations such as  $\text{K}^+$  and  $\text{Na}^+$  and could contribute to an increase in the synaptic glutamate concentration, which promotes excitotoxicity (Roettger and Lipton, 1996).

There is evidence that both APP and PS1 can influence neuronal sensitivity to cellular stressors and may have their effects through alterations of neuronal  $\text{Ca}^{2+}$  homeostasis.  $\text{A}\beta$  oligomers interact with the NMDA receptor in a binding complex and increase intraneuronal  $\text{Ca}^{2+}$ , an effect blocked by the clinically used antagonist memantine (De Felice *et al.*, 2007). In human cortical neurons, application of  $\beta$ -amyloid peptides enhances neurotoxicity mediated by the NMDA receptor and increases the  $\text{Ca}^{2+}$  response to excitotoxic insult (Mattson *et al.*, 1992). It is therefore possible that neuronal tissue containing elevated levels of  $\text{A}\beta$  peptide, as in the 3xTg and TASTPM mice, may be 'primed' to show an enhanced response to an external excitotoxic event. In addition, single transgenic  $\text{PS1}_{\text{M146V}}$  knock-in mice show enhanced kainic acid-induced neurodegeneration *in vivo*, with dissociated neurons showing a greater intracellular  $\text{Ca}^{2+}$  response to exogenous glutamate exposure, an enhancement of glutamate-induced oxidative stress, and mitochondrial dysfunction (Guo *et al.*, 1999). It is possible that in 3xTg and TASTPM mice the combination of the  $\text{APP}_{\text{Swe}}$  and  $\text{PS1}_{\text{M146V}}$  mutations may result in an enhanced  $\text{Ca}^{2+}$  response to glutamate release during excitotoxic insults such as brain slicing, which increases the level of neuronal degeneration observed in these mice.

The increased susceptibility to excitotoxicity is age-dependent as there is a progressive reduction in the magnitude of the fEPSP with increasing age. It is known that  $\text{Ca}^{2+}$  regulation in hippocampal neurons alters with age as a result of a reduction in NMDA receptor expression combined with an increase in  $\text{Ca}^{2+}$  channel expression (Kumar *et al.*, 2009). It is possible that this feature of the ageing brain is exacerbated in the 3xTg and TASTPM mice due to the presence of pathological features such as  $\text{A}\beta$  deposition. Fitzjohn *et al.* (2001) have

reported that in aged APP<sub>Swe</sub> mice kynurenic acid is only partially successful in restoring the fEPSP to normal magnitude, suggesting that a point is reached when pathological features in these mice are sufficiently advanced to affect basal synaptic transmission through a different mechanism.

Pre-treatment of 3xTg hippocampal slices with kynurenic acid increased the fEPSP slope, measured by the input-output curve, showing that the same current evokes a larger synaptic response and therefore that the viability of the slice has improved. This occurs in 3xTg mice at all stimulus intensities and in control mice at lower stimulation intensities, showing that kynurenic acid has an effect, although more modest, in normal brain slices. These observations suggest that some neuronal damage through excitotoxicity is an inevitable part of the slice preparation process. In addition in 3xTg mice there is a decrease in PPF and a reduced magnitude of LTP with kynurenic acid treatment. These findings suggest that the prevention of excitotoxicity may result in alterations in pre- and postsynaptic function which may alter electrophysiological measurements.

Previously published work has shown similar conclusions in two other mouse models of AD. Age-related deficits are apparent in basal synaptic transmission in 12 month old single-transgenic APP<sub>Swe</sub> transgenic mice and in 14 month old APP<sub>Swe</sub> x PS1<sub>A246E</sub> mice (Fitzjohn *et al.*, 2001, Fitzjohn *et al.*, 2010). However, these deficits can be abolished by incubation of the hippocampal slices in aCSF containing 1mM of kynurenic acid during preparation, suggesting that these mice also have an increased susceptibility to excitotoxic neuronal damage. The authors suggest this may be a result of the background strain, but the presence of similar findings in our colony of TASTPM mice argue against this as the C57BL/6

background is relatively resistant to excitotoxicity (Schauwecker and Steward, 1997).

Several methods are used by research groups to improve slice viability and reduce glutamate release. Most commonly used are slicing in ice-cold aCSF, the use of a glutamate receptor antagonist such as kynurenic acid, or slicing in aCSF with a different ionic composition from the recording solution. The use of each of these processes may have a different effect on slice recordings. In hippocampal extracellular recordings the use of the fEPSP as a measure of slice 'health' may result in recordings being made from viable but damaged neurons, or from a subset of CA1 neurons which are for some reason less susceptible to injury. This makes comparison between groups challenging when different slice preparation methods are used. For example, Oddo *et al.* (2003) used ice-cold aCSF in their 3xTg hippocampal preparation which acts to limit glutamate release but has been also shown to cause metabolic alterations within the slice (Watson *et al.*, 1997). In my studies, none of these measures were routinely used due to the ease at which an fEPSP could be obtained in non-transgenic mice. However, based on the findings in this thesis I would take measures to reduce excitotoxicity during slice preparation in any future experiments carried out.

In conclusion, these results have shown that an altered susceptibility to excitotoxicity following neuronal stressors may be a feature of mouse models of AD possessing the APP<sub>Swe</sub> or PS1 transgenes. It is likely that this involves alterations in glutamatergic transmission, such as neurotransmitter release, receptor or transporter function, but the mechanisms underlying this would require further study. It is not known whether this phenomenon is observed in

other APP transgenic mice and it is likely that this will be affected by the background strain of the mouse and the variables inherent in each model. It also highlights that differences in experimental procedures between research groups which influence excitotoxic mechanisms could explain some of the disparate findings in measurements of synaptic function in mouse models of AD.

### **3.3.2.8: Summary of electrophysiological findings in 3xTg mice**

In summary, the 3xTg mice show several electrophysiological changes including an age-dependent decrease in the fEPSP amplitude and an increase in the magnitude of LTP when normalised from 12 months onwards. This suggests that the development of pathological changes is linked to alterations in synaptic function in these mice. In particular, these mice may show a particular susceptibility to excitotoxicity under conditions of enhanced cellular stress. There may also be a contribution of other age-dependent and -independent mechanisms, which have been previously explored by other groups, such as alterations in  $\text{Ca}^{2+}$  functioning, although further experiments would be required to ascertain if this was a significant factor in our colony of 3xTg mice.

The deficits originally reported by other groups initially occurring at 6 months of age were not observed in our 3xTg mice. Firstly, differences in experimental protocol may also affect measurements of synaptic function and this should be taken into consideration when comparing results. However, the lack of observed changes at this age, when  $\text{A}\beta$  deposition should be established, shows that the development of pathological features occurs later in this colony than previously reported, and this is supported by the biochemical data presented in Chapter 4.

The presence of such differences between individual colonies of 3xTg mice should be taken into account for future studies of this model.

### **3.3.3: TASTPM mouse**

Studies of synaptic function and plasticity were carried out in TASTPM mice at 2 months and 6 months of age. The aim was to compare results obtained in the 3xTg mice with the TASTPM mice to attempt to elucidate the effects of the individual transgenes, in particular the tau transgene, and to see if similar changes in synaptic function were observed in the two models.

#### **3.3.3.1: Synaptic function in 2 month TASTPM mice**

PPF, input-output function and LTP were measured in 2 month old TASTPM mice. In these mice, cerebral A $\beta$  accumulation occurs from the age of 3 months (Howlett *et al.*, 2004). As A $\beta$  pathology initiates in the cortex and then progresses to the hippocampus, it is unlikely that there is any A $\beta$  accumulation in the hippocampus by 2 months and as a result the presence of electrophysiological changes was not expected.

In the TASTPM mice at 2 months old an fEPSP is readily obtainable and this is of similar magnitude to the control mice, resulting in a normal input-output curve. This finding shows that at 2 months there are no differences in basal synaptic transmission. There is a reduction in the magnitude of PPF, which is only significant at an interstimulus interval of 50ms. The value obtained at this interval is similar to that obtained in the 3xTg mice, and due to the lack of other

alterations in TASTPM mice it is likely that the effect is due to an increase in the magnitude of PPF in control mice, the mechanism of which is unknown. Importantly, the control mice used are of mixed C57BL/6 x 129/Sv background, similar to the 3xTg mice, while the TASTPM mice are on a pure C57BL/6 background. Strain-dependent differences have been observed in measures of synaptic function (Nguyen 2006) and so this could account for the minor difference observed in PPF between the control and TASTPM. Preliminary experiments (data not shown) using C57/BL6 mice have shown a similar level of PPF to that observed in TASTPM mice, suggesting the difference may be due to background strain.

There is no difference in the magnitude of LTP obtained in 2 month TASTPM mice and control mice, showing that LTP can be induced and maintained normally in TASTPM mice of this age. Overall, these results show that prior to the development of A $\beta$  deposition there are no functional changes observed due to the presence of the transgenes.

### **3.3.3.2: Synaptic function in 6 month TASTPM mice**

By 6 months, the TASTPM mice show plaque deposition in the cortex and marked APP expression in the hippocampus, in particular in the CA1 and CA3 regions (Howlett *et al.*, 2004). At this age, marked abnormalities in synaptic function were observed in hippocampal slices. It proved difficult in the majority of slices to obtain an fEPSP of sufficient magnitude for meaningful experiments to be performed. This suggests the presence of significant neuronal dysfunction or toxicity in hippocampal neurons in the TASTPM mice at the age of 6 months.

A similar reduction in basal synaptic transmission has been observed previously in TASTPM mice at 8 months (Spencer *et al.*, 2004).

As the TASTPM mouse carries the APP<sub>Swe</sub> and PS1<sub>M146V</sub> transgenes similar to the 3xTg mouse, it is likely that similar mechanisms account for the alterations in synaptic function observed. In particular, treatment with 1mM kynurenic acid markedly increased the magnitude of the fEPSP to the levels obtained in control mice. This observation suggests that an increased susceptibility to excitotoxicity is also a feature of the TASTPM mouse model (see Section 3.3.2.7). This shows that the susceptibility is due to the presence of the APP<sub>Swe</sub> or the PS1<sub>M146V</sub> mutations, with the major contribution likely to be the APP<sub>Swe</sub> mutation as this feature also occurs in single APP transgenic mice (Fitzjohn *et al.*, 2001). Considering the data obtained from the TASTPM and the 3xTg mice together, it is likely that the presence of the tau<sub>P301L</sub> transgene has little effect on the changes to the fEPSP and LTP. It also shows that, as the TASTPM mouse is generated on a different background strain than the 3xTg mouse, the susceptibility appears to be independent of the strain used to generate the model.

Synaptic plasticity was studied in slices from 6 month old TASTPM mice either in normal aCSF or aCSF additionally containing kynurenic acid. In normal aCSF, LTP was only induced in a small subset of the experiments due to the marked reduction of fEPSP amplitude in the slices. Therefore, it is probable that the increased magnitude of LTP observed in the TASTPM mice is due to the low sample size used, reflecting a neuronal population which for some reason was less susceptible to the effects of excitotoxicity. When LTP was induced in slices incubated with kynurenic acid, the magnitude was similar to that obtained in

control slices. This finding shows that despite the presence of the APP transgene, LTP can be expressed at normal levels in TASTPM mice. As this model was only studied up to the age of 6 months, it is not known whether age-dependent alteration in synaptic plasticity would become evident, particularly due to the presence of plaque deposition at older ages.

In conclusion, the TASTPM mice exhibit electrophysiological changes which are similar to those observed in the 3xTg mice, suggesting that a susceptibility to excitotoxicity may be a feature of multiple mouse models of AD. However, direct comparisons between the two models are made difficult due to the marked differences in the time course of the development of pathology in the 3xTg and TASTPM mice. In the TASTPM mice this occurs much earlier in the lifespan, possibly due to the more rapid onset of A $\beta$  deposition in this mouse model. Due to this feature, this model may be a useful tool for electrophysiology studies.

### **3.3.3: Summary**

Changes in synaptic function are a feature of a number of mouse models of AD including the 3xTg and TASTPM mice. In particular, an age-dependent reduction in the amplitude of the fEPSP is observed in both models. This is accompanied by a relative increase in the magnitude of LTP in aged 3xTg mice. However, the mechanism of these changes are not fully understood and are complicated by the difficulties in the use of the hippocampal slice model, where alterations in experimental protocol can cause marked differences in the results obtained. In addition, the slow development of pathological features in our colony of 3xTg mice, as shown by the biochemical measurements in Chapter 4, made studies difficult and complicates comparisons with the work of other groups. These

findings show that it is important to characterise the development of biochemical changes in individual colonies of the 3xTg mice in order to link this with other findings, such as studies of synaptic function. Further work, which could include more detailed electrophysiological studies (eg single cell voltage-clamping), immunohistochemistry, imaging, and *in vivo* studies, is required to elucidate the mechanisms which underlie changes in synaptic functioning in mouse models of AD. In particular, studies of our colonies of 3xTg and TASTPM mice have shown that an increased susceptibility to excitotoxicity may be a characteristic of multiple mouse models. This observation could be used to further study the mechanisms which underlie the excitotoxic neuronal death which is present in AD and its relationship to cellular stressors. However, the use of multiple models, combined with a standardised experimental approach, is required to give a full picture of synaptic function in AD.

## **Chapter 4**

# **Biochemistry**

## 4.1: Introduction

One of the aims of this thesis is to observe at which stage of phenotype development in the 3xTg and TASTPM models the molecular changes occur relative to the electrophysiological deficits. It is hypothesised that events such as kinase activation and hyperphosphorylation of cellular proteins may occur in parallel to functional alterations in synaptic activity and plasticity; any biochemical changes which are present at this time point may therefore be a contributory factor to synaptic dysfunction. The links between these different aspects are summarised in Fig. 4.1.

In this chapter, the levels and phosphorylation of a number of proteins are measured by Western blotting in both the 3xTg and TASTPM models at several ages and in different regions of the brain. A homogenised lysate of frozen brain tissue (cortical samples for all experiments except those described in section 4.2.3 and 4.2.7) was used; sample preparation is discussed in section 2.2.2.

To establish that transgene expression was present, overexpression of APP was confirmed using the antibody 6E10, raised against the first 16 residues of the amyloid  $\beta$  protein. 6E10 only recognises human protein, which contains three amino acid differences within the 6E10 recognition region, compared to the mouse orthologue (DeStrooper *et al.*, 1995). Although 6E10 is directed against A $\beta$  it also recognises this sequence within full length APP, and so can be used to measure the expression of human APP which has a high molecular weight on a Western blot.

The 3xTg mouse also has a mutated tau transgene, so the use of the total tau antibody Tau5, was used to verify this. Measurement of total tau protein expression also allowed analysis of the stoichiometry of phosphorylation of specific residues on the protein to be carried out. The antibody AT8, which recognises phosphorylated serine 202 and threonine 205, and antibodies for serine 396 and 404 were chosen as these are sites which are known to be hyperphosphorylated in Alzheimer's disease and associated with the kinase GSK3 (Mandelkow *et al.*, 1992).

CRMP2 is a protein which regulates microtubule assembly and has been previously studied in our lab. Importantly, hyperphosphorylation of CRMP2 has been shown to be an early marker of AD progression in both human and transgenic mouse tissue (Cole *et al.*, 2007b). An antibody to total CRMP2 was used, along with two different phospho-specific antibodies, for CRMP2 at the 509/514 and 522 sites. These sites are key residues for phosphorylation of the protein, with the 509/514 sites phosphorylated by the enzyme GSK3. Prior to GSK3 phosphorylation of the 509/514 sites, the 522 site must be phosphorylated by the priming kinase Cdk5.

Cdk5 is regulated by an activator protein known as p35, and cleavage of p35 by calpain results in the generation of a fragment known as p25. p25 binding results in altered cellular localisation and activation of Cdk5. Increased p25 levels or altered Cdk5 activity have been reported in some studies of AD brain and may contribute to disease progression (Patrick *et al.*, 1999). A p35 antibody, which also detects p25, was used to examine any possible changes in these proteins.

Finally, an antibody to the synaptic vesicle protein synaptophysin was also used as synaptic loss is reported to be present in mouse models of AD. As synaptic dysfunction was observed in the 3xTg and TASTPM models (see Chapter 3) I wanted to observe if there were global changes in the expression of synaptic proteins.

In summary, in this chapter I have used Western blotting to examine a range of proteins which are associated with AD in the 3xTg and TASTPM mouse models.

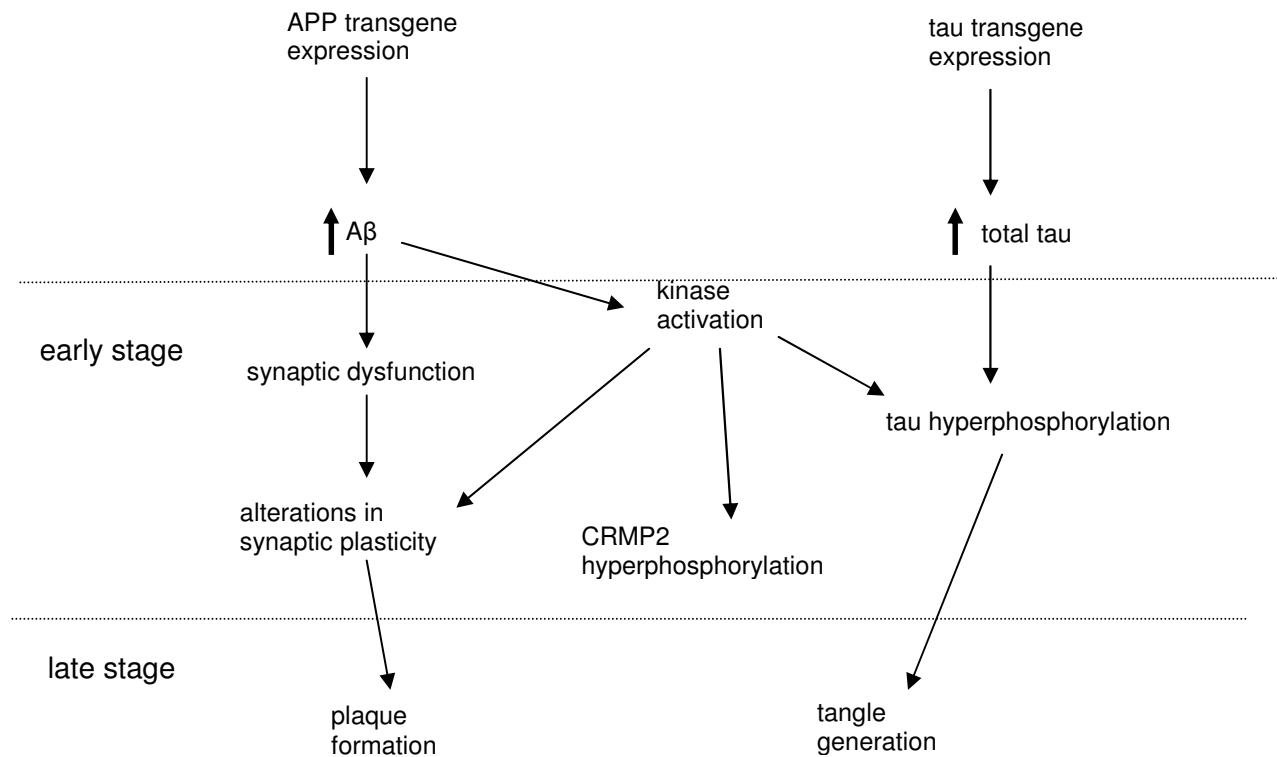


**Figure 4.1: Synaptic and biochemical alterations in mouse models of AD.** In mouse models expressing the APP transgene the excessive generation of A $\beta$  results in direct effects on synaptic function and alterations in synaptic plasticity. Additionally, hyperphosphorylation of cellular proteins such as CRMP2 and tau occur through the activity of cellular protein kinases; kinases such as GSK3 may themselves have an influence on synaptic function and plasticity. These processes occur at an early stage of pathological development but the exact time course of progression is not known. It is hypothesised that if molecular changes such as protein phosphorylation occur prior to or concurrently with observed alterations in synaptic transmission that they may have a role in the development of synaptic dysfunction.

## 4.2: Results

### 4.2.1: Age dependent effects on cortical expression of AD-related proteins in 3xTg mice

Western blotting was carried out on cortical lysates from mice of different ages to chart any differences in pathological features which might be linked to the electrophysiological findings. 3xTg mice of 2 months of age, before the appearance of any deficits, were compared to 12 month old mice, an age when the changes in synaptic function were first noted. At 2 months of age there is no evidence reported of A $\beta$  or tau deposition or any cognitive deficits in this model (Billings *et al.*, 2005). In addition, only very minor differences are observed in specific aspects of electrophysiology at this age, including changes in PPF and non-normalised LTP, suggesting the mice may show some molecular abnormalities despite undetectable pathology at 2 months. At 12 months old the electrophysiological deficits are more pronounced with a reduction in fEPSP amplitude and alterations in LTP; these coincide with detection of amyloid plaques and hyperphosphorylated tau (Oddo *et al.*, 2003). It was therefore hypothesised that biochemical changes responsible for the major electrophysiological deficits would become apparent between the ages of 2 and 12 months. In these experiments, male and female mice were analysed separately to see if there were gender-specific differences in the expression or modification of AD related proteins during ageing.

#### **4.2.1.1: APP**

The presence of the APP<sub>Swe</sub> transgene in the 3xTg mice was confirmed by genotyping (carried out by Linda Gallacher). As expected, there is a significant difference ( $p < 0.05$ , two-way ANOVA) in the levels of human APP between the 3xTg and control mice at both 2 and 12 month of age in both male (Fig. **4.2A**) and female (Fig. **4.3A**) mice with expression of this protein absent in control mice. There is a trend for increased hAPP expression as the mice age, in both male and female 3xTg mice (Fig. **4.2A** - males, **4.3A** - females). This confirms that the transgene is present and functional (Fig. **4.2A** - males, **4.3A** - females).

#### **4.2.1.2: CRMP2 (total and phosphorylated)**

There is no difference in the expression of total CRMP2 between 3xTg and control ( $p > 0.05$ , two-way ANOVA) at 2 or 12 months (Fig. **4.2B** - males, Fig. **4.3B** - females), and in contrast to previous findings in this model (Cole *et al.*, 2007b) the CRMP2 protein from 3xTg cortex did not exhibit increased phosphorylation at either the 509/514 (Fig. **4.2C** - GSK3 sites) or 522 (Fig. **4.2D** - Cdk5 sites) residues in males at both ages examined ( $p > 0.05$ , two-way ANOVA). Identical findings were obtained from cortex of the female 3xTg mice (Fig. **4.3C** and **D**).

#### **4.2.1.3: Tau (total and phosphorylated)**

The presence of the tau<sub>p301L</sub> transgene in the 3xTg mice was confirmed by genotyping (carried out by Linda Gallacher). There is a significant increase ( $p <$

0.05, two-way ANOVA) in the levels of total tau in the male 3xTg mice compared to the control, although in contrast to APP there is no significant difference in expression of the transgenic tau between 2 month and 12 month 3xTg ( $p > 0.05$ , two-way ANOVA). However this may be related to the small sample set as the average expression was greater in 12 month old 3xTg than 2 month old 3xTg, yet endogenous tau expression in the control male mice showed a trend for a decrease with age (Fig. **4.4A**). There is also a strong trend for increased total tau in the female 3xTg compared to control at both ages, although this does not reach significance ( $p = 0.067$ ) (Fig. **4.5A**). In contrast to the male mice there is no difference in tau expression ( $p > 0.05$ , two-way ANOVA) between 2 or 12 month old animals in either genotype (Fig. **4.5A**).

There is no increase in phosphorylation of tau ( $p > 0.05$ , two-way ANOVA) at the AD related AT8 or 404 epitopes in the male 3xTg compared to controls at either age (Fig. **4.4B** and **C**). In fact, there seems to be a decreased level of tau 396 phosphorylation in the 12 month male 3xTg compared to the control although this does not reach significance (Fig. **4.4D**). Perhaps surprisingly phosphorylation at the AT8 epitope in female 12 month old 3xTg mice is reduced ( $p < 0.05$ , two-way ANOVA) compared to controls (Fig. **4.5B**), and this seems to be related to an increase in AT8 phosphorylation in the older control mice that is not recapitulated in the older 3xTg female mice (Fig. **4.5B**). As in the male mice, there are no differences observed in 404 phosphorylation ( $p > 0.05$ , two-way ANOVA) across all 4 groups (Fig. **4.5C**); there is a slightly reduced level of tau 396 phosphorylation in the female 3xTg compared to control in both 2 and 12 month old mice (Fig. **4.5D**), which just fails to reach significance in the 12 month mice ( $p = 0.054$ ). This suggests that although the levels of total tau are

increased this is not matched by an increase in phosphorylation at the sites investigated.

#### **4.2.1.4: Other proteins**

There are no clear differences ( $p > 0.05$ , two-way ANOVA) in the levels of synaptophysin or the Cdk5 co-factors p35 or p25 in male (Fig. 4.6) or female (Fig. 4.7) 3xTg compared to control mice at the ages measured, and the expression of these proteins does not alter with age or gender in either genotype.

#### **4.2.1.5: Summary**

Although the expression of the APP and tau transgenes is confirmed these results suggest that some of the processes associated with the development of pathology, such as the hyperphosphorylation of tau originally observed by Oddo *et al.* and the hyperphosphorylation of CRMP2 which was observed previously in our lab from tissue from a different colony (Cole *et al.*, 2007b) are developing more slowly in our colony of 3xTg mice. There appears to be higher tau expression in female 3xTg mice at 12 months than in control animals or in male 3xTg mice. However the level of phosphorylation of some key residues on tau in the female 3xTg actually appears to decrease compared with control animals. No changes in expression or modification of APP, tau, CRMP2, synaptophysin, or p35 in 3xTg cortex were observed that could explain the reported electrophysiological or behavioural abnormalities in these animals.

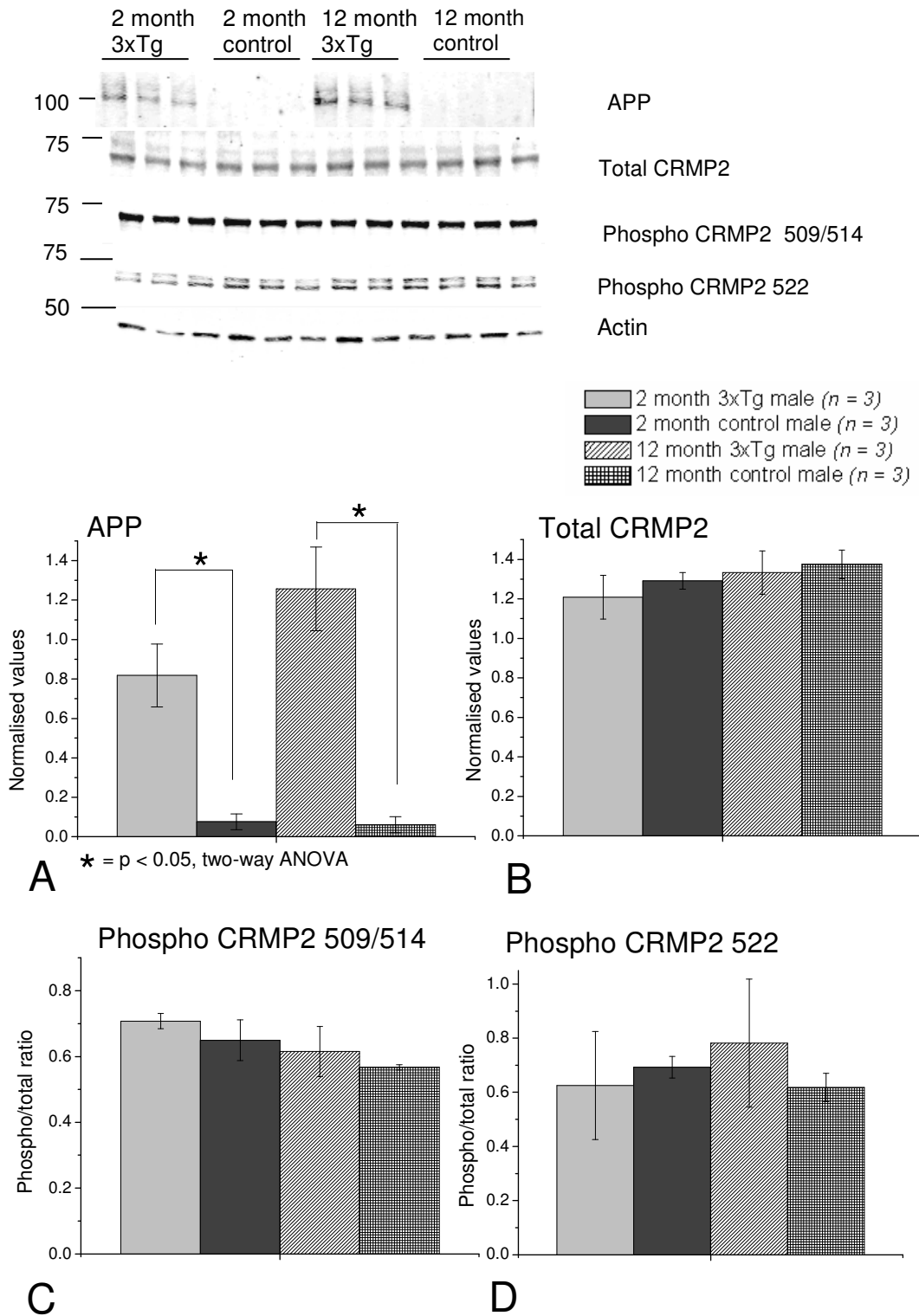


**Figure 4.2: APP, total and phosphorylated CRMP2 in 2 and 12 month male 3xTg and control mice.** 10 $\mu$ g of cortical lysate ( $n = 3$  in each group) was used in SDS-PAGE, transferred to a nitrocellulose membrane and probed with the following antibodies: 6E10 (A), Total CRMP2 (B), CRMP2 phospho 509/514 (C), CRMP2 phospho 522 (D). Representative blots are displayed along with the graphs showing densitometry calculations. APP and total CRMP2 are normalised to actin while phosphorylated CRMP2 is normalised to total CRMP2 protein.  $\star = p < 0.05$ , two-way ANOVA.

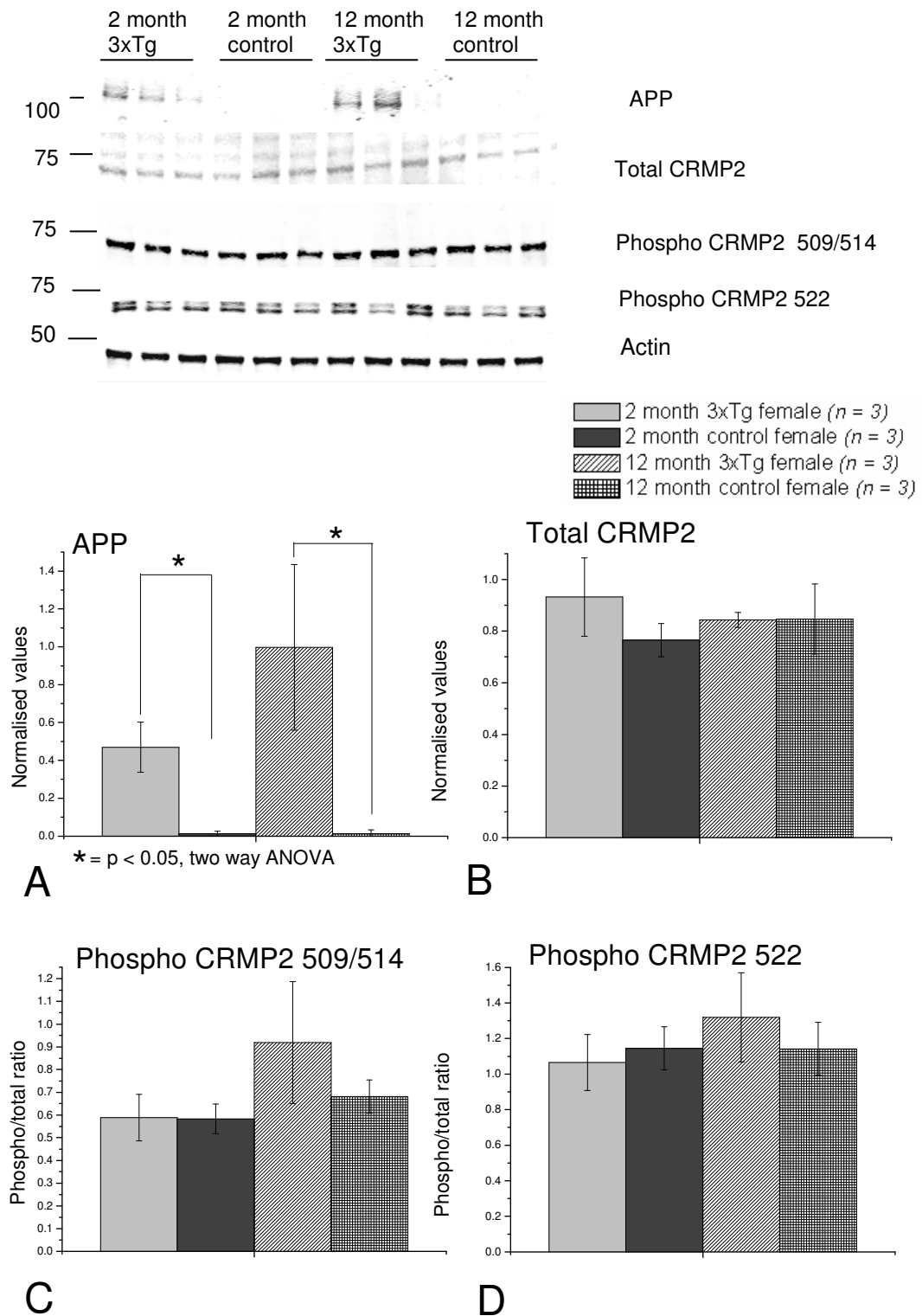


**Figure 4.3: APP, total and phosphorylated CRMP2 in 2 and 12 month female 3xTg and control mice.** 10 $\mu$ g of cortical lysate (n = 3 in each group) was used in SDS-PAGE, transferred to a nitrocellulose membrane and probed with the following antibodies: 6E10 (A), Total CRMP2 (B), CRMP2 phospho 509/514 (C), CRMP2 phospho 522 (D). Representative blots are displayed along with the graphs showing densitometry calculations. APP and total CRMP2 are normalised to actin while phosphorylated CRMP2 is normalised to total CRMP2 protein.  $\star = p < 0.05$ , two-way ANOVA.

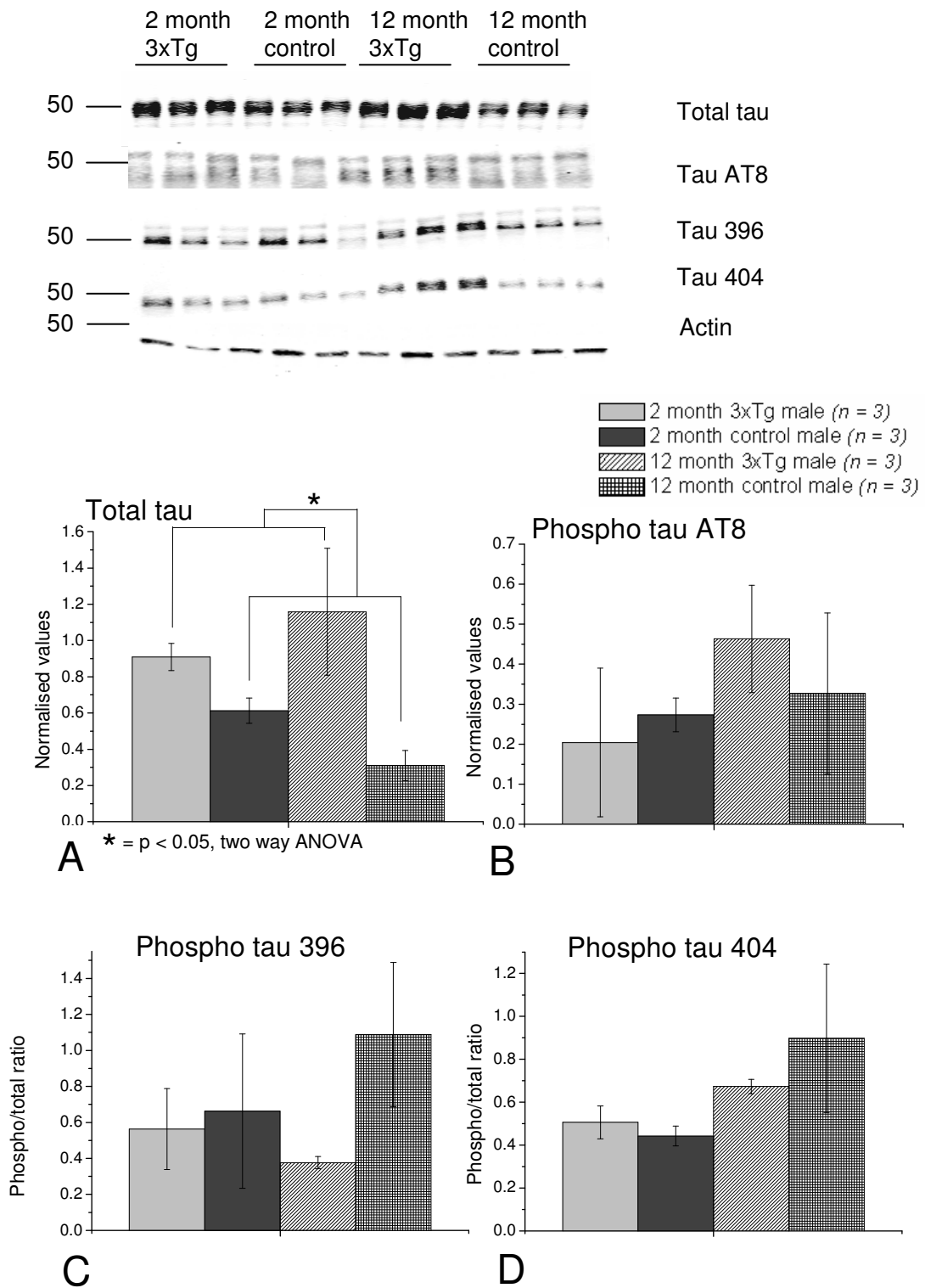


**Figure 4.4: Total and phosphorylated tau in 2 and 12 month male 3xTg and control mice.** 10 $\mu$ g of cortical lysate ( $n = 3$  in each group) was used in SDS-PAGE, transferred to a nitrocellulose membrane and probed with the following antibodies: Tau5 (A), Tau AT8 (B), Tau phospho 396 (C), Tau phospho 404 (D). Representative blots are displayed along with the graphs showing densitometry calculations. Total tau is normalised to actin while phosphorylated tau is normalised to total tau. \* =  $p < 0.05$ , two-way ANOVA.

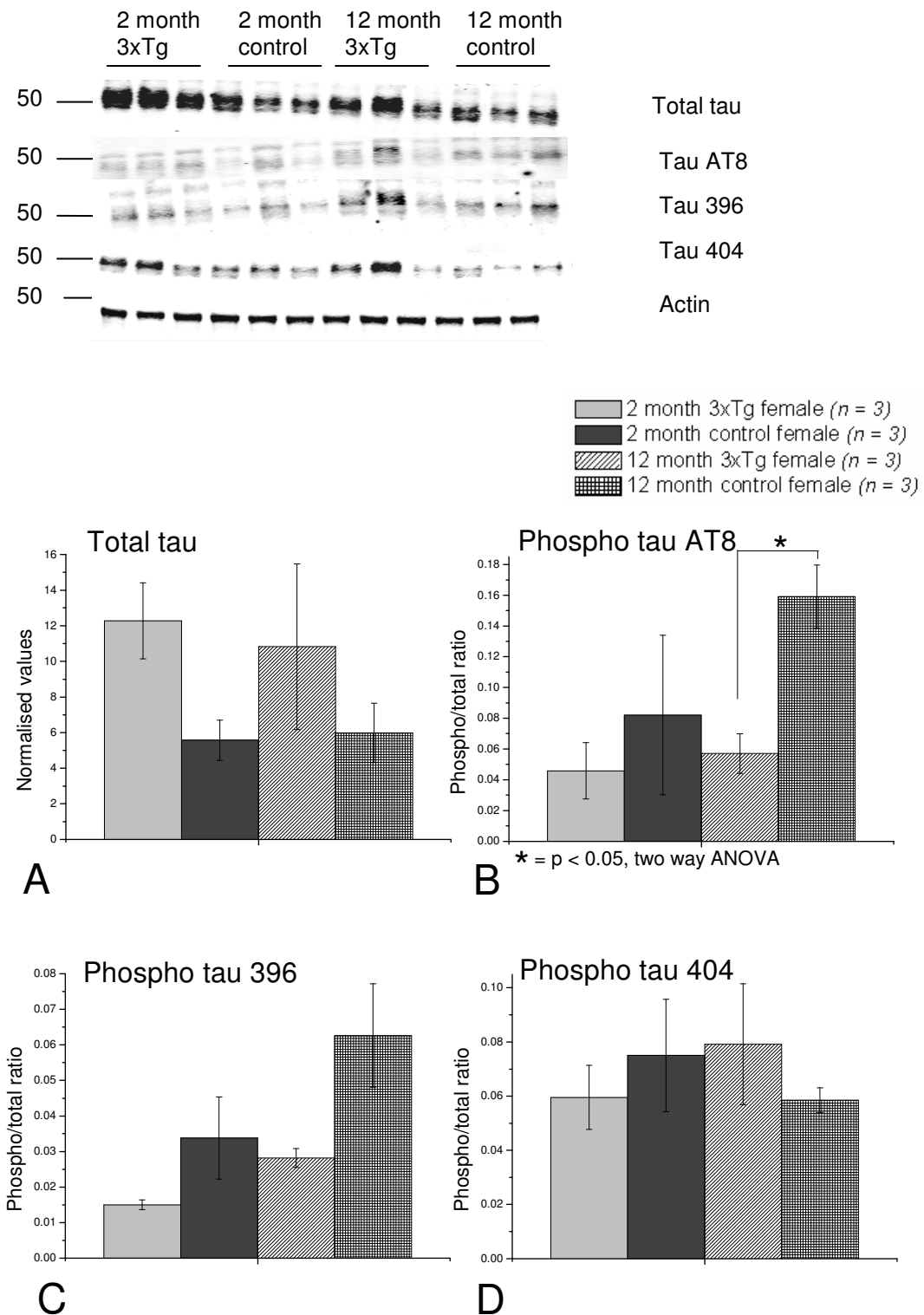


**Figure 4.5: Total and phosphorylated tau in 2 and 12 month female 3xTg and control mice.** 10 $\mu$ g of cortical lysate ( $n = 3$  in each group) was used in SDS-PAGE, transferred to a nitrocellulose membrane and probed with the following antibodies: Tau5 (A), Tau AT8 (B), Tau phospho 396 (C), Tau phospho 404 (D). Representative blots are displayed along with the graphs showing densitometry calculations. Total tau is normalised to actin while phosphorylated tau is normalised to total tau. \* =  $p < 0.05$ , two-way ANOVA.

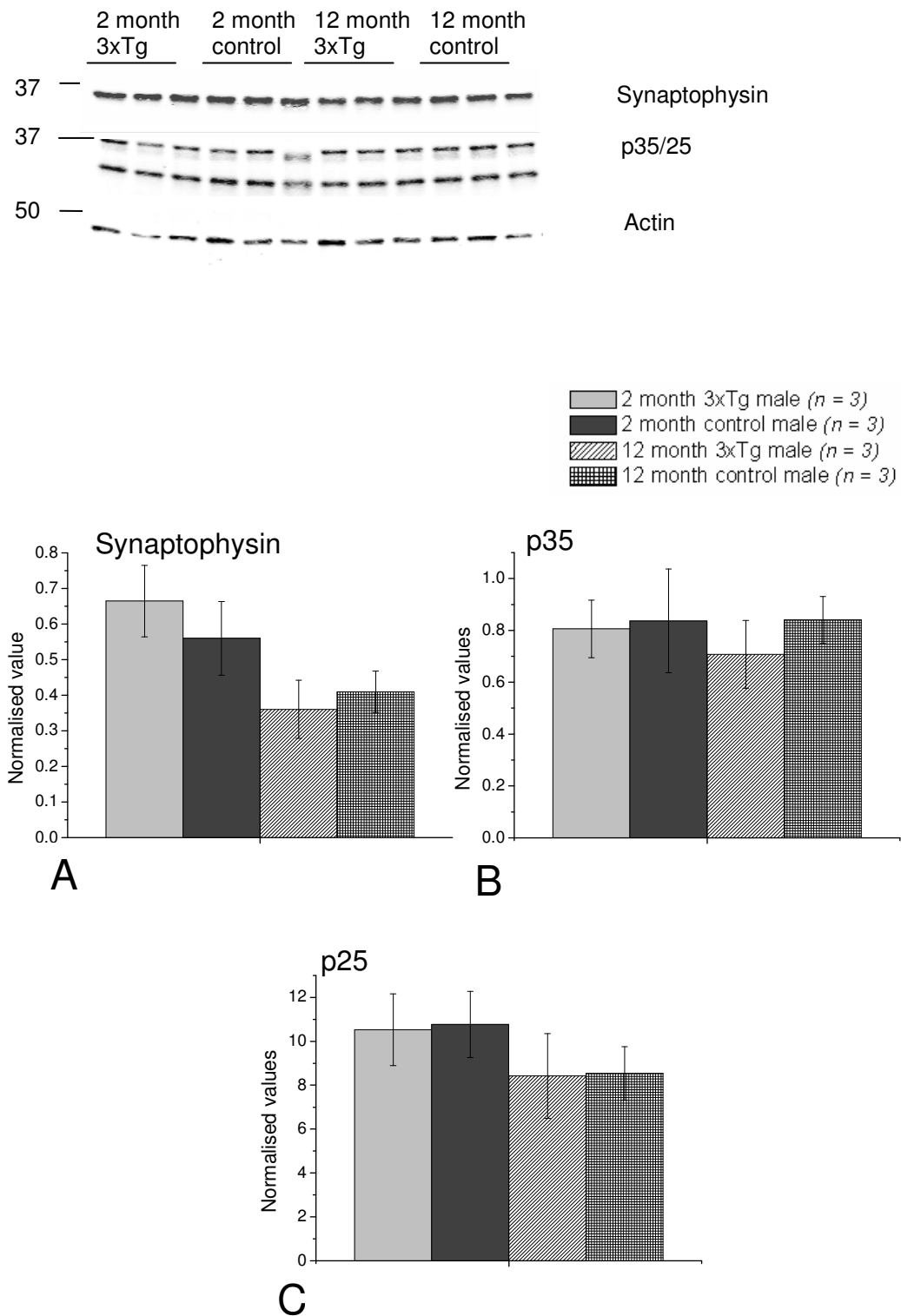


**Figure 4.6: Synaptophysin, p35 and p25 in 2 and 12 month male 3xTg and control mice.** 10 $\mu$ g of cortical lysate ( $n = 3$  in each group) was used in SDS-PAGE, transferred to a nitrocellulose membrane and probed with the following antibodies: Synaptophysin (A), p35 (B) which also shows p25 (C), and actin. Representative blots are displayed along with the graphs showing densitometry calculations. Synaptophysin, p35 and p25 are normalised to actin.

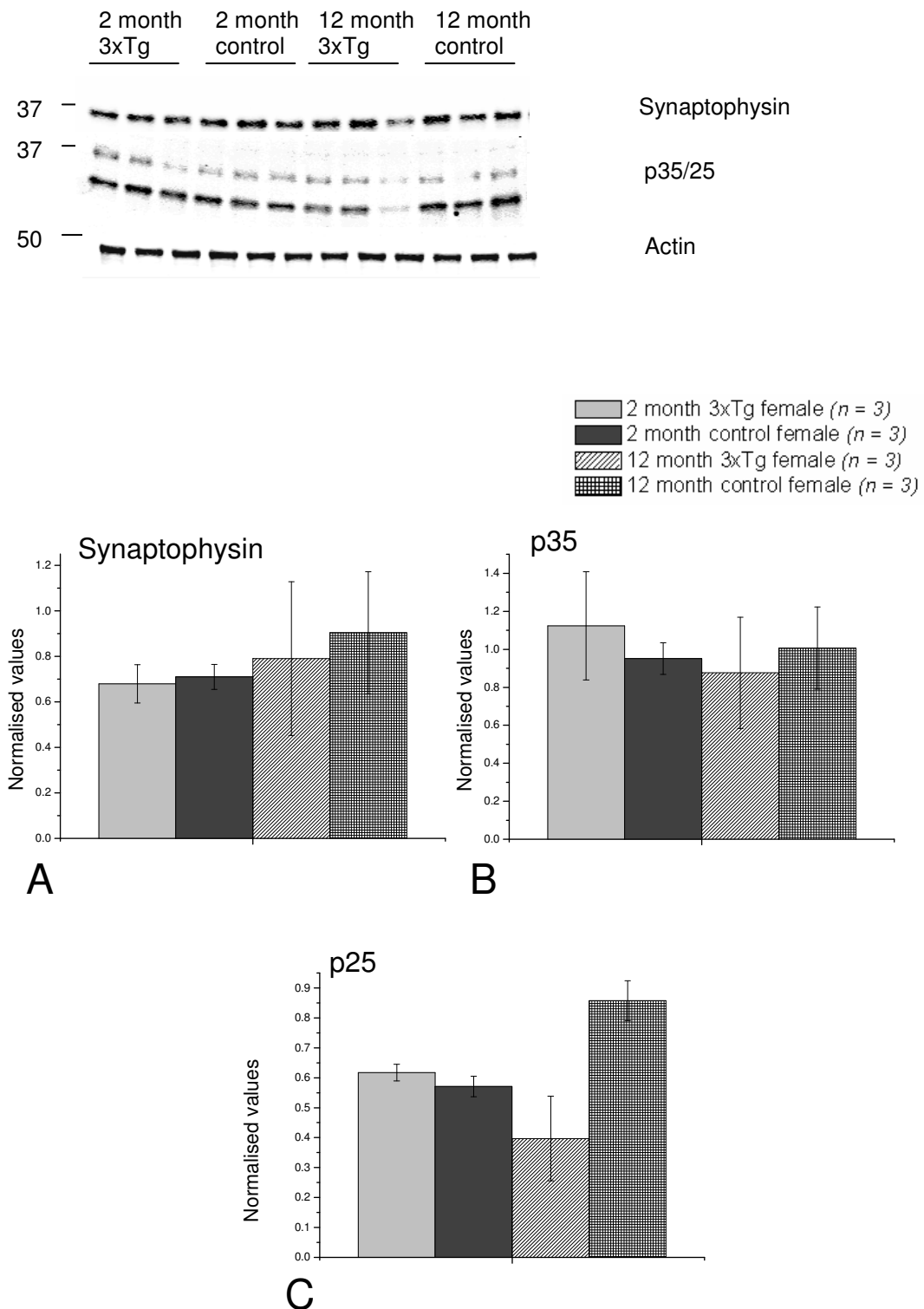


**Figure 4.7: Synaptophysin, p35 and p25 in 2 and 12 month female 3xTg and control mice.** 10 $\mu$ g of cortical lysate ( $n = 3$  in each group) was used in SDS-PAGE, transferred to a nitrocellulose membrane and probed with the following antibodies: Synaptophysin (A), p35 (B) which also shows p25 (C), and actin. Representative blots are displayed along with the graphs showing densitometry calculations. Synaptophysin, p35 and p25 are normalised to actin.

#### **4.2.2: Analysis of cortical expression of AD-related proteins in aged 3xTg mice**

Western blotting was carried out on mice of 17 months of age, when the pathology was expected to be well developed with amyloid plaques and neurofibrillary tangles apparent. It was hoped to find biochemical differences that might correlate with the electrophysiological alterations that occur at this age, which include a marked reduction in fEPSP amplitude and changes in LTP expression. Due to the late occurrence of electrophysiological deficits in our colony of 3xTg mice, it seemed important to characterise the development of biochemical changes as the mice aged to see if this too differed from that previously reported. In contrast to the original report of this model studies by Mastrangelo *et al.* (2008) and Hirata-Fukae *et al.* (2008) suggested that plaque pathology may not be apparent until 14 or 15 months of age, and it is known that tangle pathology occurs late in the lifespan at around 12-18 months.

The experiments at 17 months were carried out in male mice only due to availability and the potential for gender-dependent differences.

#### 4.2.2.1: APP

As expected there is a significant difference in APP expression in 17 month old 3xTg mice compared to control ( $p < 0.05$ , unpaired t-test), with no expression detected in control mice (Fig. **4.8A**) which confirms that the transgene is present in these mice.

#### 4.2.2.2: CRMP2 (total and phosphorylated)

There is no difference ( $p > 0.05$ , unpaired t-test) in the levels of total CRMP2 between 17 month old 3xTg and control mice (Fig. **4.8B**). However, there is a significant increase in phosphorylation ( $p < 0.05$ , unpaired t-test) at the 509/514 residues (Fig. **4.8C** – GSK3 sites). This was previously observed in our lab in 6 month old 3xTg mice Cole *et al* (2007), so this biochemical change is occurring at a much later stage of development in the 3xTg colony than that observed previously. There is no difference ( $p > 0.05$ , unpaired t-test) in phosphorylation at the 522 residues between the 3xTg and controls (Fig. **4.8D** – Cdk5 sites), in contrast to previous work in the model.

#### 4.2.2.3: Tau (total and phosphorylated)

There is a significant increase ( $p < 0.05$ , unpaired t-test) in the expression of tau in 3xTg mice at 17 months compared to control (Fig. **4.9A**). There is no increase ( $p > 0.05$ , unpaired t-test) in phosphorylation at the AT8 (Fig. **4.9B**) or 396 (Fig. **4.9C**) epitopes, although this may be due to the small sample set as there is a

trend for increased phosphorylation, particularly at the 396 and 404 epitopes (similar to data from 12 month old mice, see section **4.2.1.3**). This very nearly reaches significance at the 404 epitope ( $p = 0.054$ , independent t-test) (Fig. **4.9D**).

#### **4.2.2.4: Other proteins**

There is no difference ( $p > 0.05$ , unpaired t-test) in the levels of synaptophysin or p35/p25 Cdk5 co-factors in 3xTg mice compared to control mice at 17 months (Fig. **4.10**).

#### **4.2.2.5: Summary**

Although APP and tau are overexpressed, the only other molecular changes detected are an increase in phosphorylated CRMP2 at the 509/514 epitope, and a slight increase in tau phosphorylation. This suggests that the marked hyperphosphorylation of cellular proteins expected is not occurring at this age in our colony of 3xTg mice. As tau hyperphosphorylation occurs prior to tangle formation this suggests this feature has not developed in these mice, although confirmation of this would require further studies such as immunohistochemical analysis.

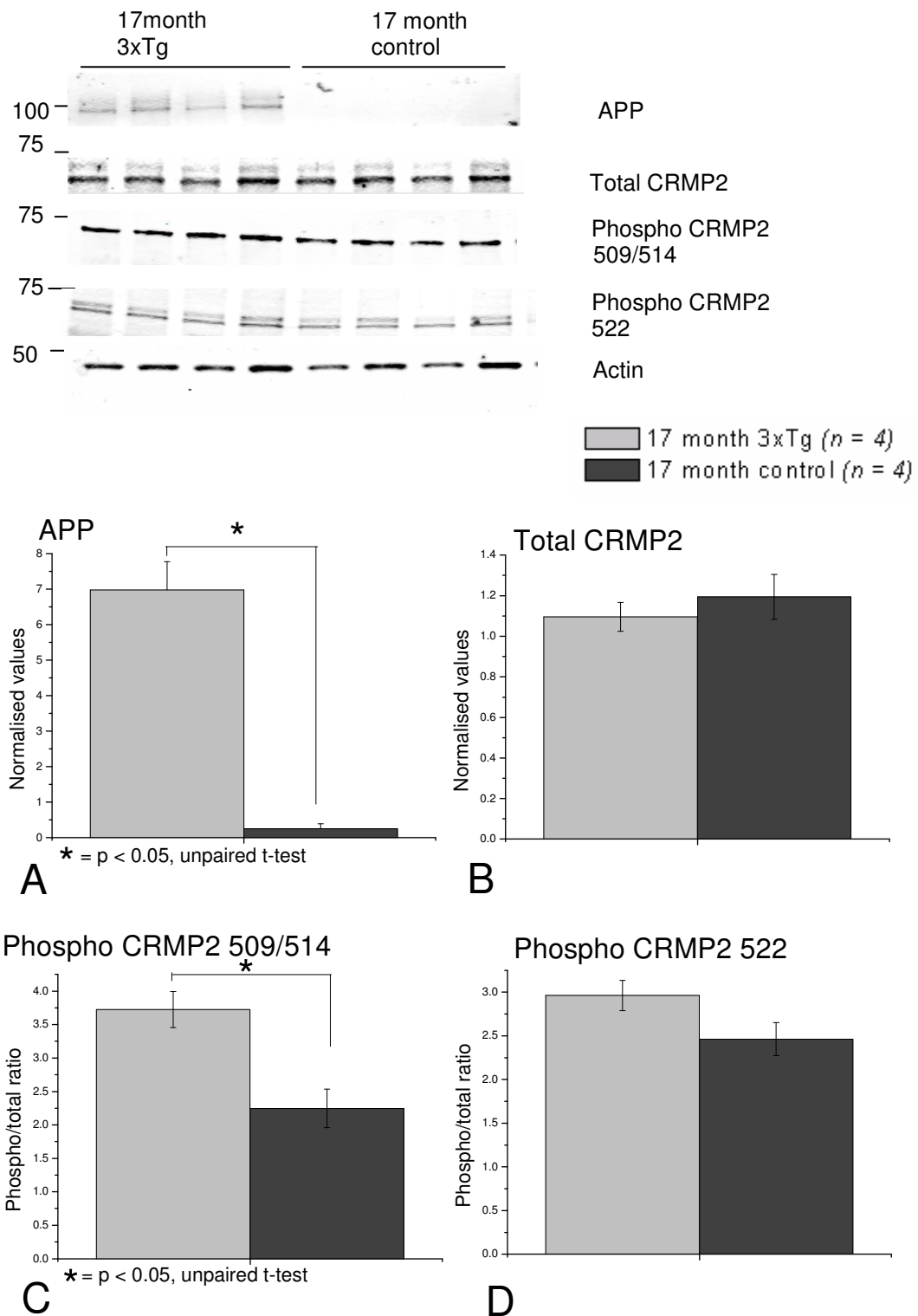


**Figure 4.8: APP, total and phosphorylated CRMP2 in 17 month 3xTg and control mice.** 10 $\mu$ g of cortical lysate (n = 4 in each group) was used in SDS-PAGE, transferred to a nitrocellulose membrane and probed with the following antibodies: 6E10 (A), Total CRMP2 (B), CRMP2 phospho 509/514 (C), CRMP2 phospho 522 (D). Representative blots are displayed along with the graphs showing densitometry calculations. APP and total CRMP2 are normalised to actin while phosphorylated CRMP2 is normalised to total CRMP2 protein. \* =  $p < 0.05$ , unpaired t-test.

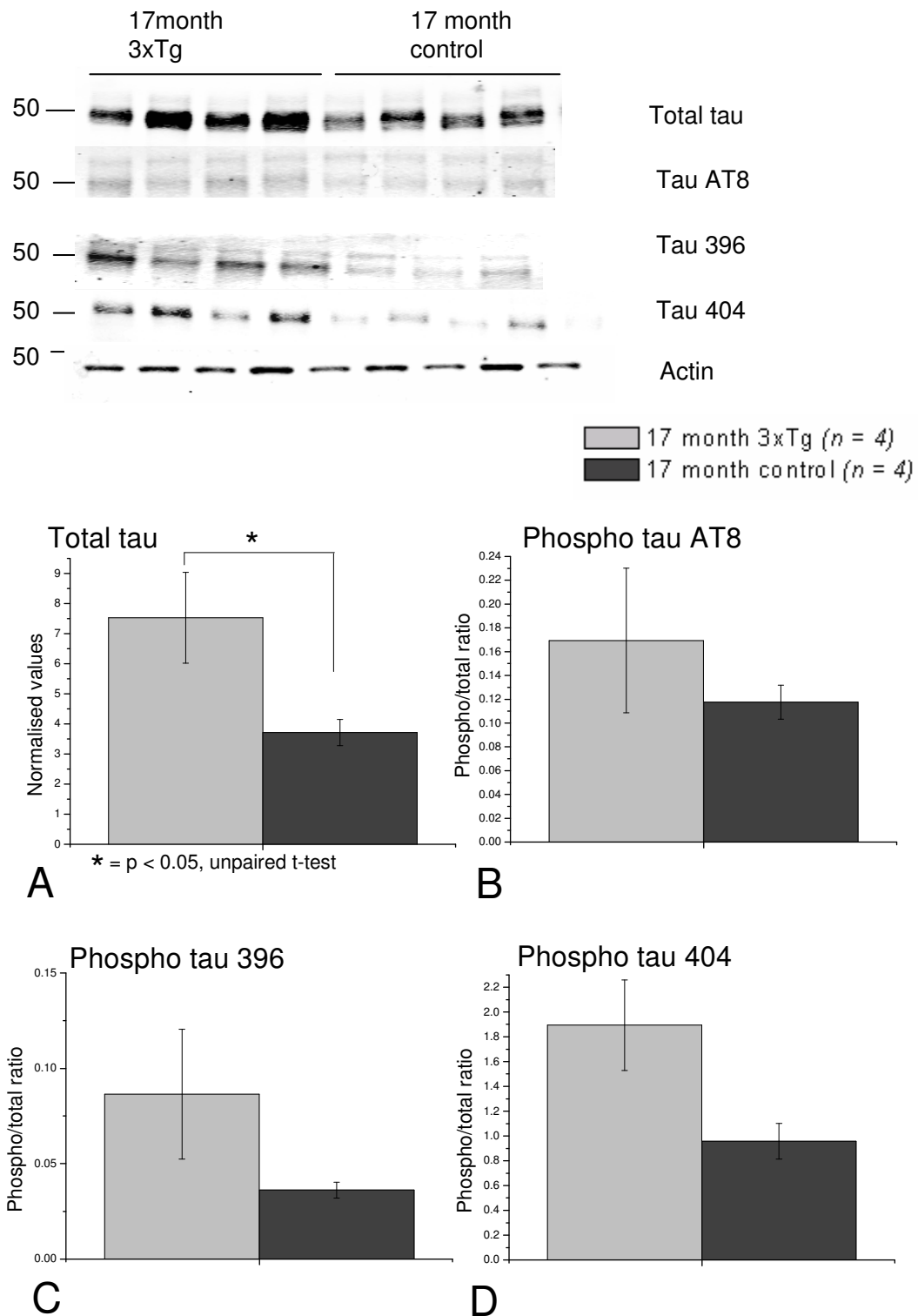


**Figure 4.9: Total and phosphorylated tau in 17 month 3xTg and control mice.** 10 $\mu$ g of cortical lysate (n = 4 in each group) was used in SDS-PAGE, transferred to a nitrocellulose membrane and probed with the following antibodies: Tau5 (A), Tau AT8 (B), Tau phospho 396 (C), Tau phospho 404 (D). Representative blots are displayed along with the graphs showing densitometry calculations. Total tau is normalised to actin while phosphorylated tau is normalised to total tau. \* =  $p < 0.05$ , unpaired t-test.

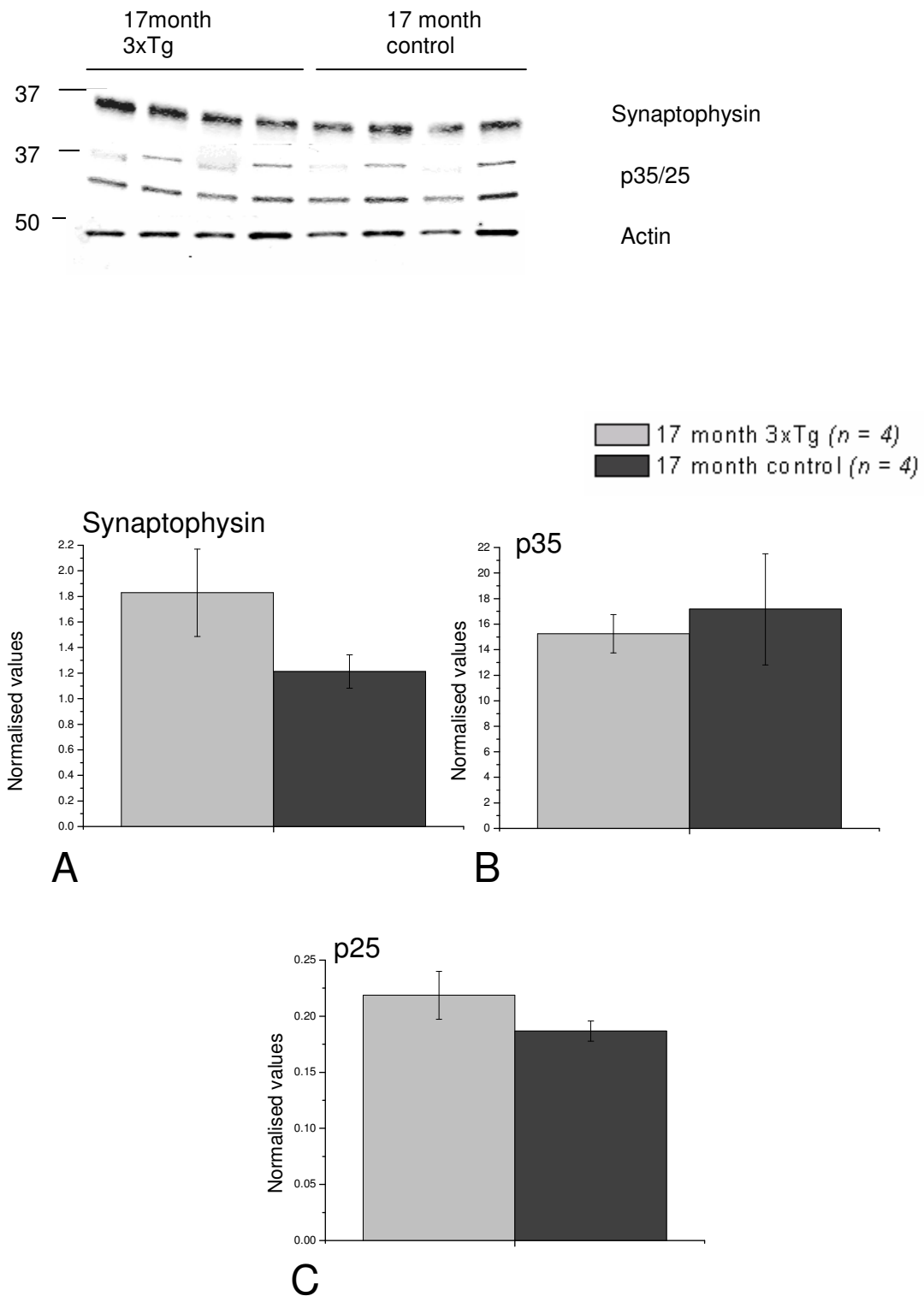


**Figure 4.10: Synaptophysin, p35 and p25 in 17 month 3xTg and control mice.** 10 $\mu$ g of cortical lysate (n = 4 in each group) was used in SDS-PAGE, transferred to a nitrocellulose membrane and probed with the following antibodies: Synaptophysin (A), p35 (B) which also shows p25 (C), and actin. Representative blots are displayed along with the graphs showing densitometry calculations. Synaptophysin, p35 and p25 are normalised to actin.

### **4.2.3: AD related protein expression and phosphorylation in different brain regions in 17 month mice**

It is known that different areas of the brain are more susceptible to the development of pathology in AD than others. The entorhinal cortex and hippocampus seem particularly vulnerable to tau pathology, as it is there that neurofibrillary tangle formation initiates. Later affected are areas of the cortex such as the frontal and temporal regions. However, some areas of the brain such as the somatosensory cortex and the cerebellum are relatively spared from the pathological features. Little is known about the mechanisms that control the susceptibility of particular subsets of neurons.

A similar progression from one brain region to another occurs in the 3xTg mouse model. Tau pathology is first apparent in the hippocampus, in particular the neurons of the CA1 region, and spreads to involve the cortex (Oddo *et al.*, 2003, Oddo *et al.*, 2007). The A $\beta$  pathology initiates in the cortex, in particular the frontal regions, before spreading several months later to the hippocampus in a progression that appears to be a reversal of the pattern of tau deposition.

For this reason it was decided to study three brain regions in the 3xTg mouse: the hippocampus, the region used for electrophysiological experiments, the cortex, which was used for the majority of biochemical analysis, and the cerebellum, which should be relatively free of pathological features. This was carried out in 17 month old male mice using the same cortical samples as in the previous experiments (section 4.2.2). The samples consisted of cortex from one hemisphere which was mainly the frontal/temporal regions, the hippocampal formation from the same hemisphere, and the whole cerebellum. If a difference

between brain regions was observed then the experiment was repeated in control mice to determine if this was a region-specific effect observed in the normal mouse brain.

#### **4.2.3.1: APP**

There is a significant difference in APP expression between the cortex and the cerebellum, and the hippocampus and cerebellum, with APP levels being lowest in the cerebellum ( $p < 0.05$ , one-way ANOVA) (Fig. **4.11A**), suggesting that the transcription of the APP<sub>Swe</sub> transgene is likely reduced in this region or the stability of APP is reduced in the cerebellum. There is no difference ( $p > 0.05$ , one-way ANOVA) between APP expression in the hippocampus and cortex (Fig. **4.11A**).

#### **4.2.3.2: CRMP2 (total and phosphorylated)**

There is no difference ( $p > 0.05$ , one-way ANOVA) in the level of total CRMP2 between the cortex, hippocampus and cerebellum (Fig. **4.11B**). There is a significant difference ( $p < 0.05$ , one-way ANOVA) in the level of phosphorylated CRMP2 at the 509/514 residues between the hippocampus and the cerebellum but no difference ( $p > 0.05$ , one-way ANOVA) between hippocampus and cortex. The cortical phosphorylation of CRMP2 falls between that of cerebellum and hippocampus but the sample number was too small to provide statistical difference between measures in the cortex and other tissues (Fig. **4.11C** – GSK3 sites). There is also no difference ( $p > 0.05$ , one-way ANOVA) in the level of phosphorylated CRMP2 at the 522 residue (Fig. **4.11D**

– Cdk5 sites). However phosphorylation of CRMP2 at both residues shows the same pattern of distribution in the brain regions measured, with levels lowest in the hippocampus and highest in cerebellum (Fig. **4.11B - D**).

#### **4.2.3.3: Tau (total and phosphorylated) in 3xTg mice**

There is no difference ( $p > 0.05$ , one-way ANOVA) in the levels of total tau between the hippocampus, cortex and cerebellum (Fig. **4.12A**). However, there is significantly higher phosphorylation of tau at the AT8 epitope (Fig. **4.12B**) and at the 396 epitope (Fig. **4.12C**) in the cerebellum compared to the other brain regions (hippocampus and cortex) ( $p < 0.05$ , one-way ANOVA). In contrast there is significantly reduced phosphorylation of tau at 404 in the cerebellum compared to hippocampus ( $p < 0.05$ , one-way ANOVA) but no difference between hippocampus and cortex, or cerebellum and cortex (Fig. **4.12D**).

As the region-specific phosphorylation of tau appeared markedly different in the cerebellum, control mouse samples were probed with the Tau5, AT8, 396 and 404 antibodies to determine if this was a hallmark of the disease process or normal regulation of tau in mice.

#### **4.2.3.4: Tau (total and phosphorylated) in control mice**

There is no difference ( $p > 0.05$ , one-way ANOVA) in levels of total tau between 17 month old control hippocampus, cortex and cerebellum (Fig. **4.13A**). However, there is a significant increase ( $p < 0.05$ , one-way ANOVA) in the levels of tau phosphorylation at the AT8 epitope (Fig. **4.13B**) and the 396 epitope (Fig. **4.13C**) between the cerebellum and the other brain regions. There is also a

significant reduction ( $p < 0.05$ , one-way ANOVA) in tau 404 phosphorylation in the cerebellum compared to cortex (Fig. **4.13D**) but no difference ( $p > 0.05$ , one-way ANOVA) between hippocampus and cortex, or hippocampus and cerebellum. This is very similar to the observations in the 3xTg mice and suggests that there are region-specific differences in the phosphorylation of tau in normal mice, a pattern which is not altered in this AD model.

#### **4.2.3.5: Other proteins**

There is a trend for higher levels of synaptophysin in the cortex which nearly reaches significance ( $p = 0.054$ , compared with cerebellum,  $p = 0.059$ , compared with hippocampus, one-way ANOVA) (Fig. **4.14A**).

There is a significant difference ( $p < 0.05$ , one-way ANOVA) between the levels of p35 in the hippocampus and the other brain regions (cortex and cerebellum), with p35 lower in the hippocampus (Fig. **4.14B**). There is also a significant difference ( $p < 0.05$ , one-way ANOVA) between the levels of p25 in the cortex compared with the other brain regions (Fig. **4.14C**), with levels higher in the cortex and at a similar level in hippocampus and cerebellum.

#### **4.2.3.6: Summary**

These results show that the most marked differences in protein levels occur in the cerebellum, with many of the proteins in the cortex and hippocampus expressed and regulated at similar levels. Therefore the biochemical analysis carried out in the cortex should be a reasonable surrogate for the biochemical status of the hippocampal slices from these mice used in the electrophysiology studies.

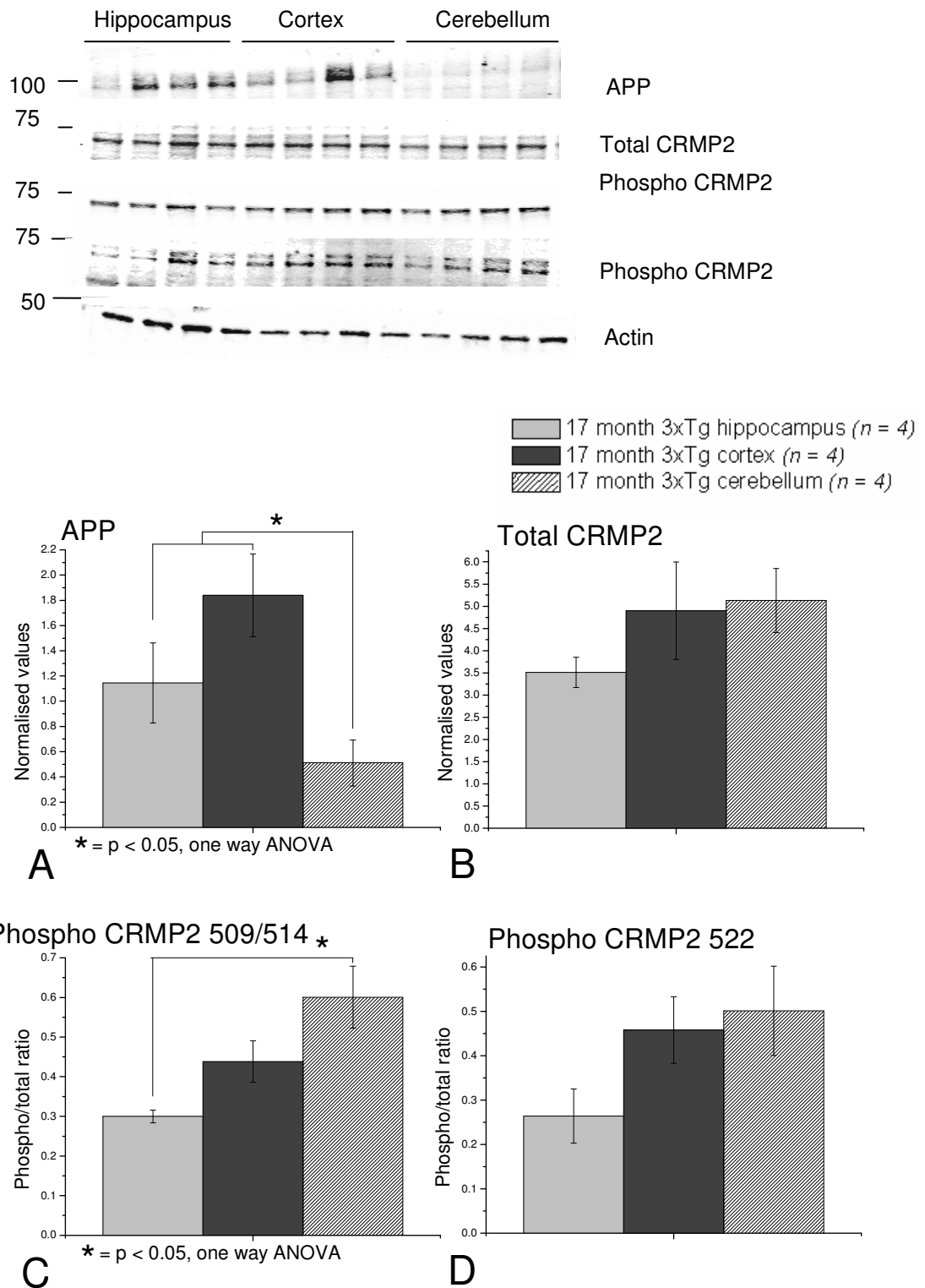


**Figure 4.11: APP, total and phosphorylated CRMP2 in 17 month 3xTg hippocampus, cortex and cerebellum.** 10 $\mu$ g of hippocampal, cortical and cerebellar lysate from 17 month old 3xTg male mice ( $n = 4$  of each region) was used in SDS-PAGE, transferred to a nitrocellulose membrane and probed with the following antibodies: 6E10 (A), Total CRMP2 (B), CRMP2 phospho 509/514 (C), CRMP2 phospho 522 (D). Representative blots are displayed along with the graphs showing densitometry calculations. APP and total CRMP2 are normalised to actin while phosphorylated CRMP2 is normalised to total CRMP2 protein. \* =  $p < 0.05$ , one way ANOVA.

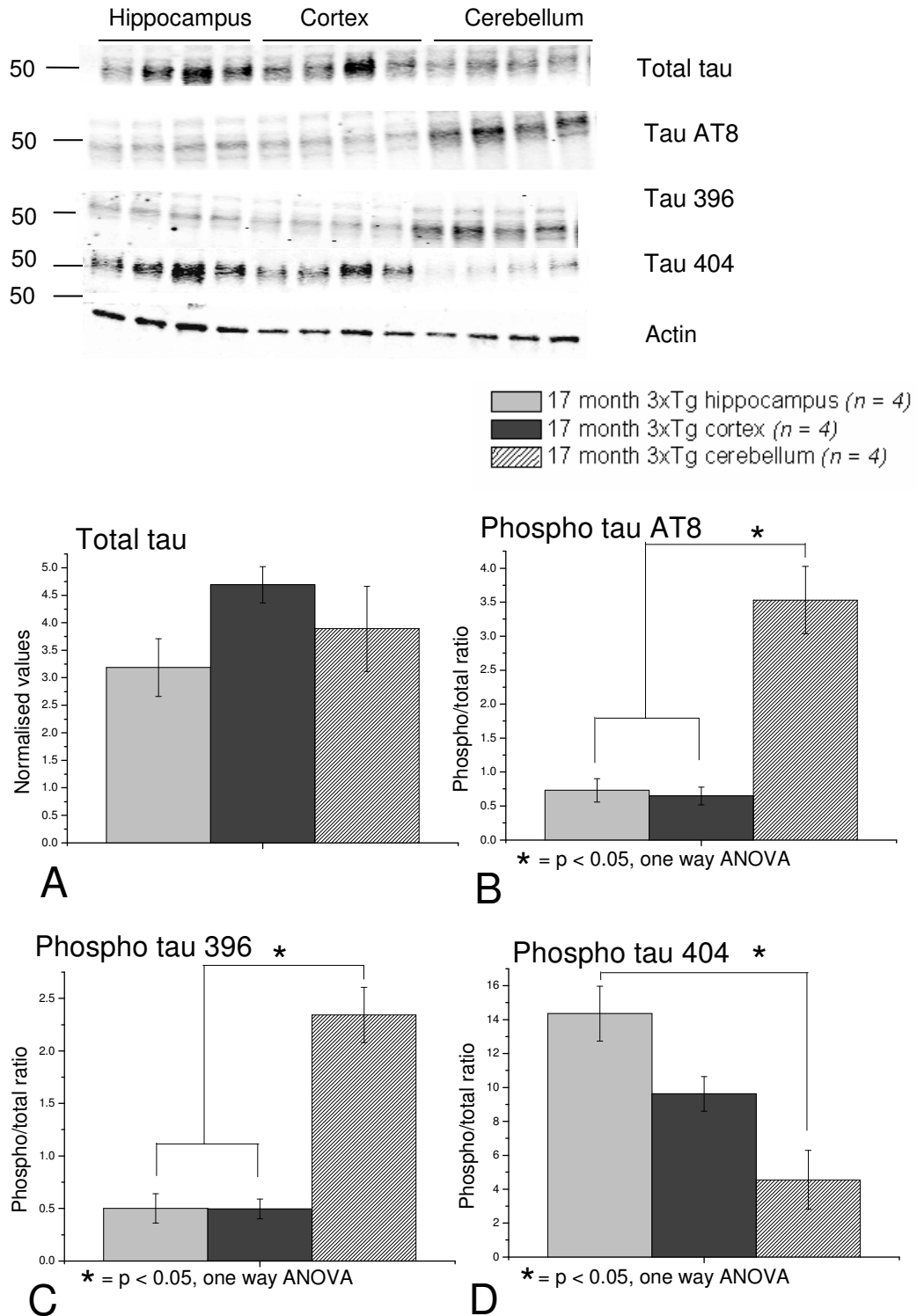


**Figure 4.12: Total and phosphorylated tau in 17 month 3xTg hippocampus, cortex and cerebellum.** 10 $\mu$ g of hippocampal, cortical and cerebellar lysate from 17 month old 3xTg male mice ( $n = 4$  of each region) was used in SDS-PAGE, transferred to a nitrocellulose membrane and probed with the following antibodies: Tau5 (A), Tau AT8 (B), Tau phospho 396 (C), Tau phospho 404 (D). Representative blots are displayed along with the graphs showing densitometry calculations. Total tau is normalised to actin while phosphorylated tau is normalised to total tau. \* =  $p < 0.05$ , one way ANOVA.

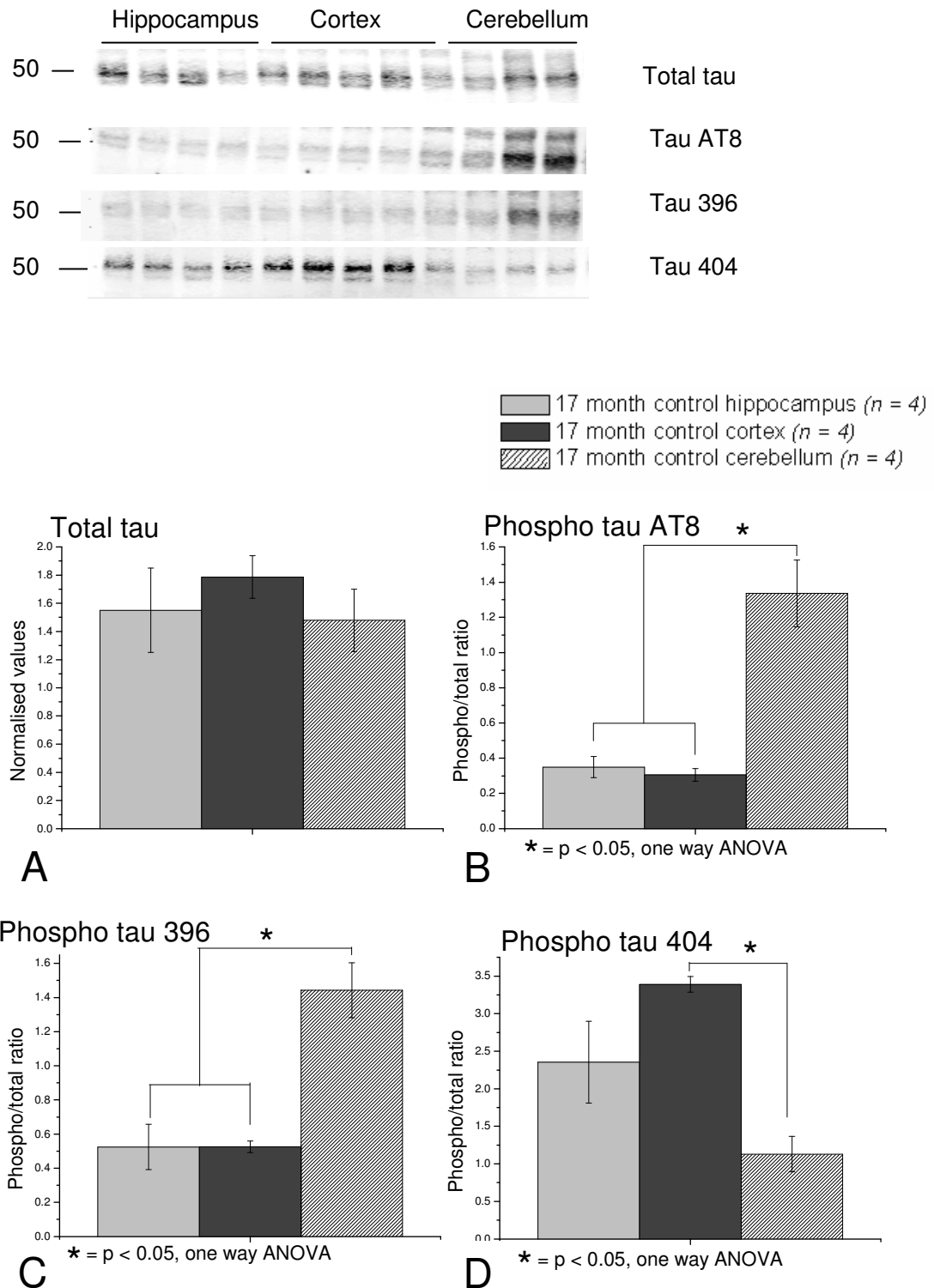


**Figure 4.13: Total and phosphorylated tau in 17 month control hippocampus, cortex and cerebellum.** 10 $\mu$ g of hippocampal, cortical and cerebellar lysate from 17 month old control male mice ( $n = 4$  of each region) was used in SDS-PAGE, transferred to a nitrocellulose membrane and probed with the following antibodies: Tau5 (A), Tau AT8 (B), Tau phospho 396 (C), Tau phospho 404 (D). Representative blots are displayed along with the graphs showing densitometry calculations. Total tau is normalised to actin while phosphorylated tau is normalised to total tau. \* =  $p < 0.05$ , one way ANOVA.

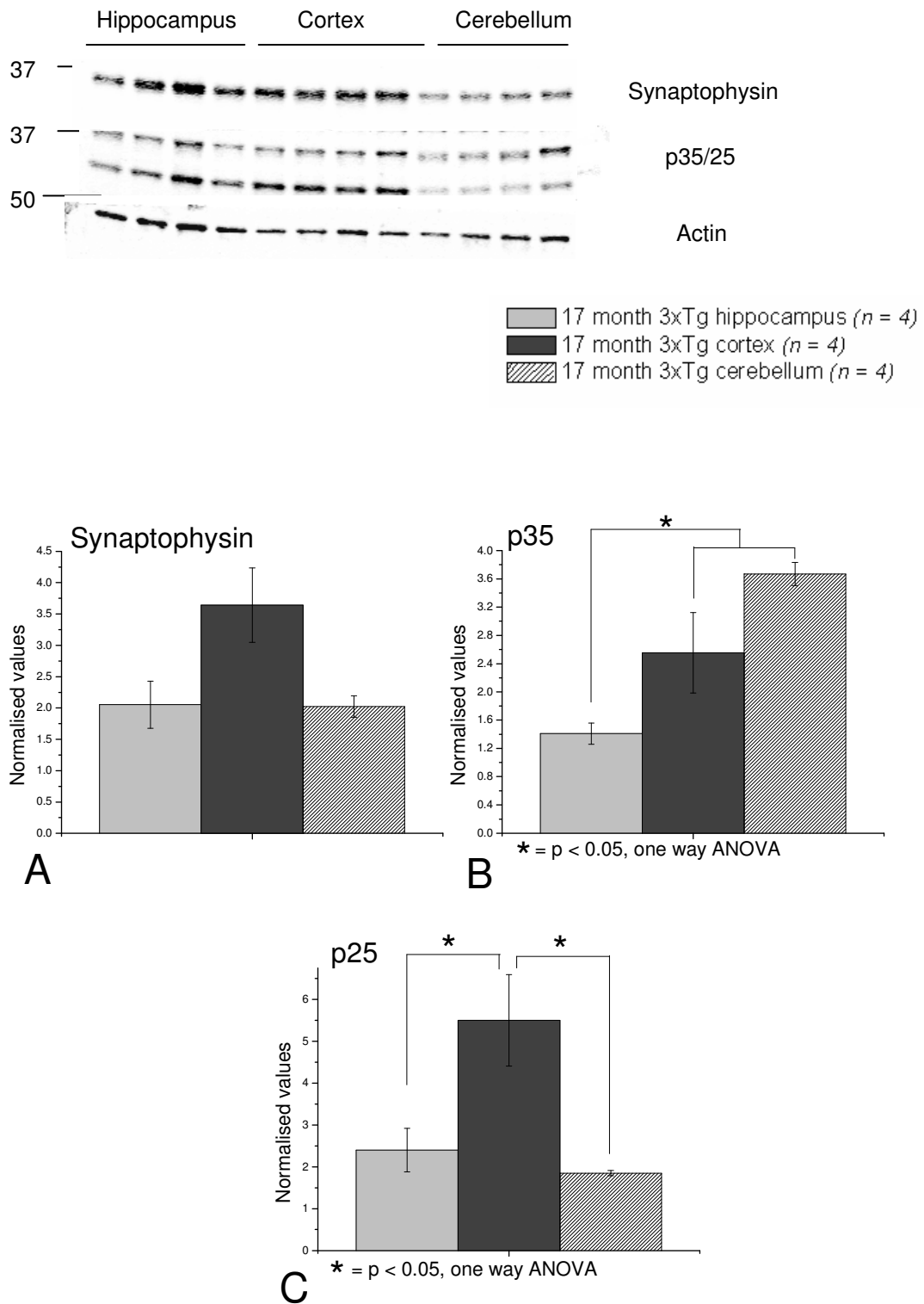


**Figure 4.14: Synaptophysin, p35 and p25 in 17 month 3xTg hippocampus, cortex and cerebellum.** 10 $\mu$ g of hippocampal, cortical and cerebellar lysate from 17 month old 3xTg male mice ( $n = 4$  of each region) was used in SDS-PAGE, transferred to a nitrocellulose membrane and probed with the following antibodies: Synaptophysin (A), p35 (B) which also shows p25 (C), and actin. Representative blots are displayed along with the graphs showing densitometry calculations. Synaptophysin, p35 and p25 are normalised to actin. \* =  $p < 0.05$ , one way ANOVA.

#### **4.2.4: Correlations between APP, tau and electrophysiology in 3xTg mice**

Cortical tissue was stored from some mice which had also been used for hippocampal extracellular recording, so data from Western blotting and electrophysiology was available from the same animals. I attempted to detect correlations between the levels of proteins such as APP and tau and measurements such as the maximum fEPSP amplitude and LTP values in the same mice. Experimental data were available from 6 of the 3xTg mice at 12 months and 4 at 17 months. Densitometry values were used for 6E10 (used to measure total APP) and Tau5 (used to measure total tau) blots as a measure of the levels of these proteins, and the average maximum fEPSP amplitude and average magnitude of LTP in the plateau phase were used as electrophysiological measurements. Each mouse was ranked by transgene expression level (a surrogate measure of pathology development) and by electrophysiological measures from the highest to lowest values, and I looked for an inverse correlation between the levels of APP and/or tau and the fEPSP/LTP measurements.

The data collected (Fig. **4.15**) shows there is no simple correlation between the levels of APP and tau and the electrophysiological measurements, suggesting that larger numbers of experimental animals and a more complex statistical investigation will be required for such an analysis. As expected a mouse expressing higher levels of APP usually also expresses a higher level of tau (due to co-integration of the transgene) and the mice with the highest APP/tau expression (mouse B at 6 months and mouse J at 12 months) had the smallest (or second smallest) fEPSP amplitude and magnitude of LTP of the group.

Mouse	APP	Rank	Tau	Rank	fEPSP	Rank	LTP	Rank
<b>A</b>	1.00	2	1	5	0.94	3	205.1	2
<b>B</b>	1.01	1	3.33	=2	0.28	5	142.1	6
<b>C</b>	0.54	5	3.33	=2	0.67	4	188.9	3
<b>D</b>	0.67	4	2.71	4	Not measured	N/A	181.9	4
<b>E</b>	0.27	6	0.73	6	1.15	1	226.5	1
<b>F</b>	0.85	3	6.81	1	1.13	2	161.5	5
<b>G</b>	1.00	4	1	3	1.19	1	242.3	3
<b>H</b>	1.07	3	0.65	4	0.36	3	294.7	1
<b>I</b>	3.01	2	1.38	2	0.36	2	249.3	2
<b>J</b>	3.37	1	3.29	1	0.34	4	167.4	4

**Figure 4.15: Biochemical and electrophysiological measurements in individual 3xTg mice.** Mice **A – F** are 6 months of age while mice **G – J** are 12 months of age. Densitometry values from APP and tau blots are shown in the table along with measurements of the average maximum fEPSP amplitude and average magnitude of LTP after 60 minutes. Each mouse is given a ranking based on the highest values for the group. Cells shaded in grey represent the subgroup with highest protein expression and lowest electrophysiological measurements.

Conversely mouse E had lowest APP/tau expression and the largest fEPSP and LTP of the 6 month old animals. However, other than these extreme measures little is gained from the analysis.

#### **4.2.5: Biochemical profiles in 2 month old TASTPM mice**

##### **4.2.5.1: Overview**

Hippocampal slices were prepared from the TASTPM mouse at 2 months and 6 months of age for electrophysiological analysis, with 2 month old mice showing normal synaptic plasticity and 6 month old mice showing marked deficits, with a reduction in fEPSP amplitude (Chapter 3.2.6, 3.2.7). Previous reports indicated that TASTPM mice show A $\beta$  deposition in the cortex and hippocampus; cortical A $\beta$  deposition initiates at 3-4 months and is well established by 6 months, and this is also the age when cognitive deficits present (Howlett *et al.*, 2004). The pathology develops more rapidly in these mice than in single transgenic APP mice due to the additional expression of mutant human PS1. Therefore I examined protein expression in 2 and 6 month old brain lysates to directly compare with the electrophysiological studies and as likely representations of pre- and post-plaque deposition.

Male and female mice were analysed separately as it is known that the pathology initiates earlier in female TASTPM mice (Howlett *et al.*, 2004).

#### **4.2.5.2: APP**

As expected there is a significant increase in the level of APP (measured using the 6E10 antibody) in TASTPM compared with control mice ( $p < 0.05$ , two-way ANOVA), with 6E10 staining of APP effectively absent in control mice (Fig. **4.16A**). There is no effect of gender ( $p > 0.05$ , two-way ANOVA) on APP expression in TASTPM mice.

#### **4.2.5.3: CRMP2 (total and phosphorylated)**

Total CRMP2 levels (Fig. **4.16B**) and phosphorylated CRMP2, at either the 509/514 (Fig. **4.16C** – GSK3 sites) or 522 sites (Fig. **4.16D** – Cdk5 sites) are not significantly different ( $p > 0.05$ , two-way ANOVA) between the 2 month old TASTPM mice and age-matched controls. There is also no effect of gender ( $p > 0.05$ , two-way ANOVA) on total CRMP2 or CRMP2 phosphorylated at the 509/514 residues.

#### **4.2.5.4: Tau (total and phosphorylated)**

There is no difference ( $p > 0.05$ , two-way ANOVA) in total tau levels in the TASTPM mice compared with control mice which is expected as these mice do not possess a tau transgene (Fig. **4.17A**). There is a decrease ( $p < 0.05$ , two-way ANOVA) in the phosphorylation of tau at the AT8 epitope (Fig. **4.17B**), but no changes ( $p > 0.05$ , two-way ANOVA) at the 396 (Fig. **4.17C**) or 404 (Fig. **4.17D**) phosphorylation sites in TASTPM compared to control. There is no effect

of gender ( $p > 0.05$ , two-way ANOVA) on total tau or phosphorylation at the 396 or 404 epitopes with either genotype. However, there is a significant difference ( $p < 0.05$ , two-way ANOVA) between the levels of 404 phosphorylation in male and female TASTPM mice with a higher level of phosphorylation in female mice.

#### **4.2.5.5: Other proteins**

There is no difference ( $p > 0.05$ , two-way ANOVA) in synaptophysin levels in the TASTPM mice compared to control (Fig. **4.18A**). In addition, there is no effect of genotype or gender ( $p > 0.05$ , two-way ANOVA) on the levels of p35 (Fig. **4.18B**) or p25 (Fig. **4.18C**).

#### **4.2.5.6: Summary**

The only biochemical changes detected in 2 month TASTPM mice are the expected high levels of APP expression and a reduction in the phosphorylation of the tau 404 epitope compared to control mice. However as there are no detectable deficits in electrophysiology at this age it must be assumed that these biochemical alterations do not themselves directly affect LTP in 2 month old hippocampal slices.

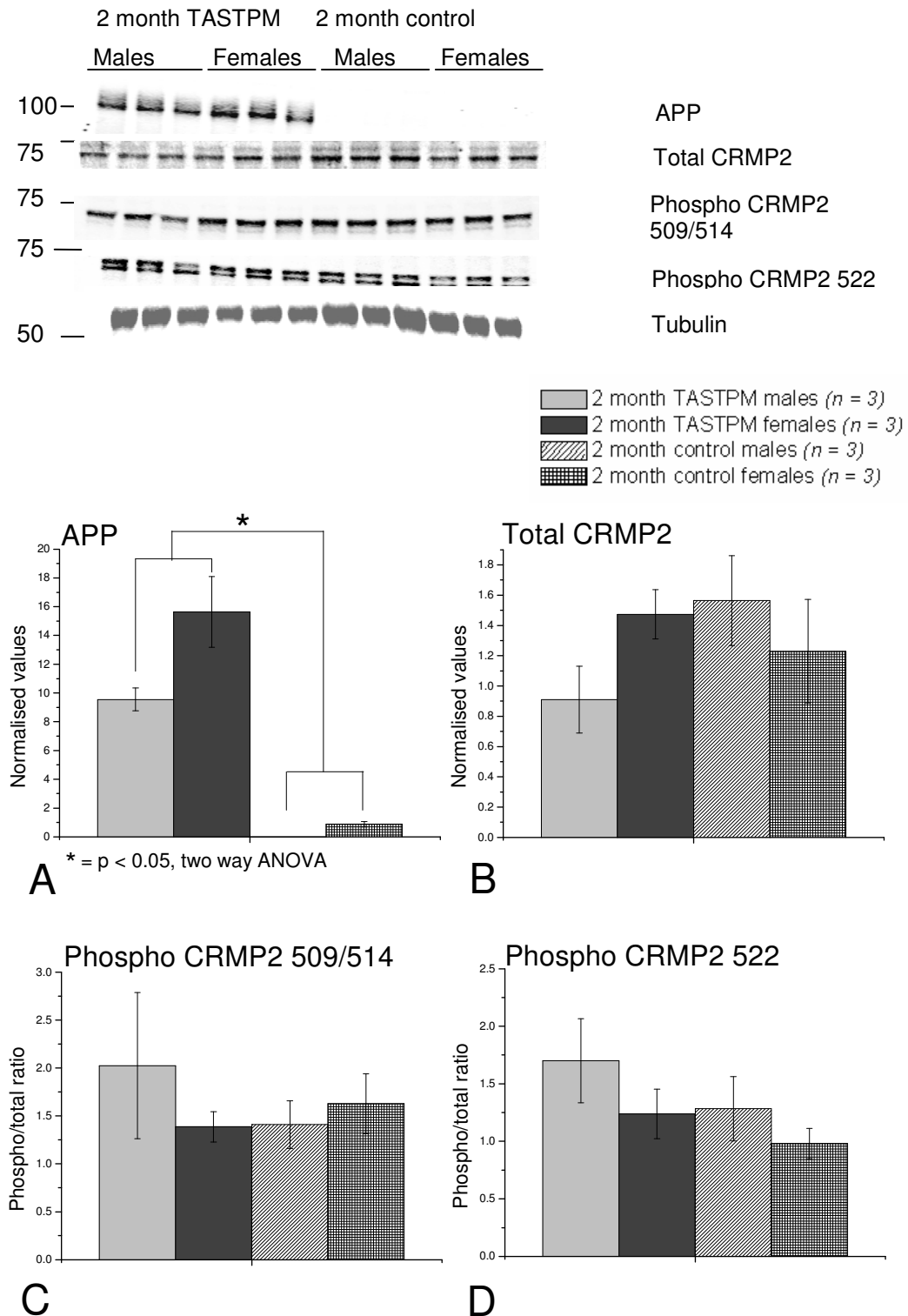


**Figure 4.16: APP, total and phosphorylated CRMP2 in 2 month TASTPM male and female mice.** 10 $\mu$ g of cortical lysate from 2 month old TASTPM and control male ( $n = 3$  in each group) and female ( $n = 3$  in each group) mice was used in SDS-PAGE, transferred to a nitrocellulose membrane and probed with the following antibodies: 6E10 (A), Total CRMP2 (B), CRMP2 phospho 509/514 (C), CRMP2 phospho 522 (D). Representative blots are displayed along with the graphs showing densitometry calculations. APP and total CRMP2 are normalised to tubulin while phosphorylated CRMP2 is normalised to total CRMP2 protein. \* =  $p < 0.05$ , two way ANOVA.

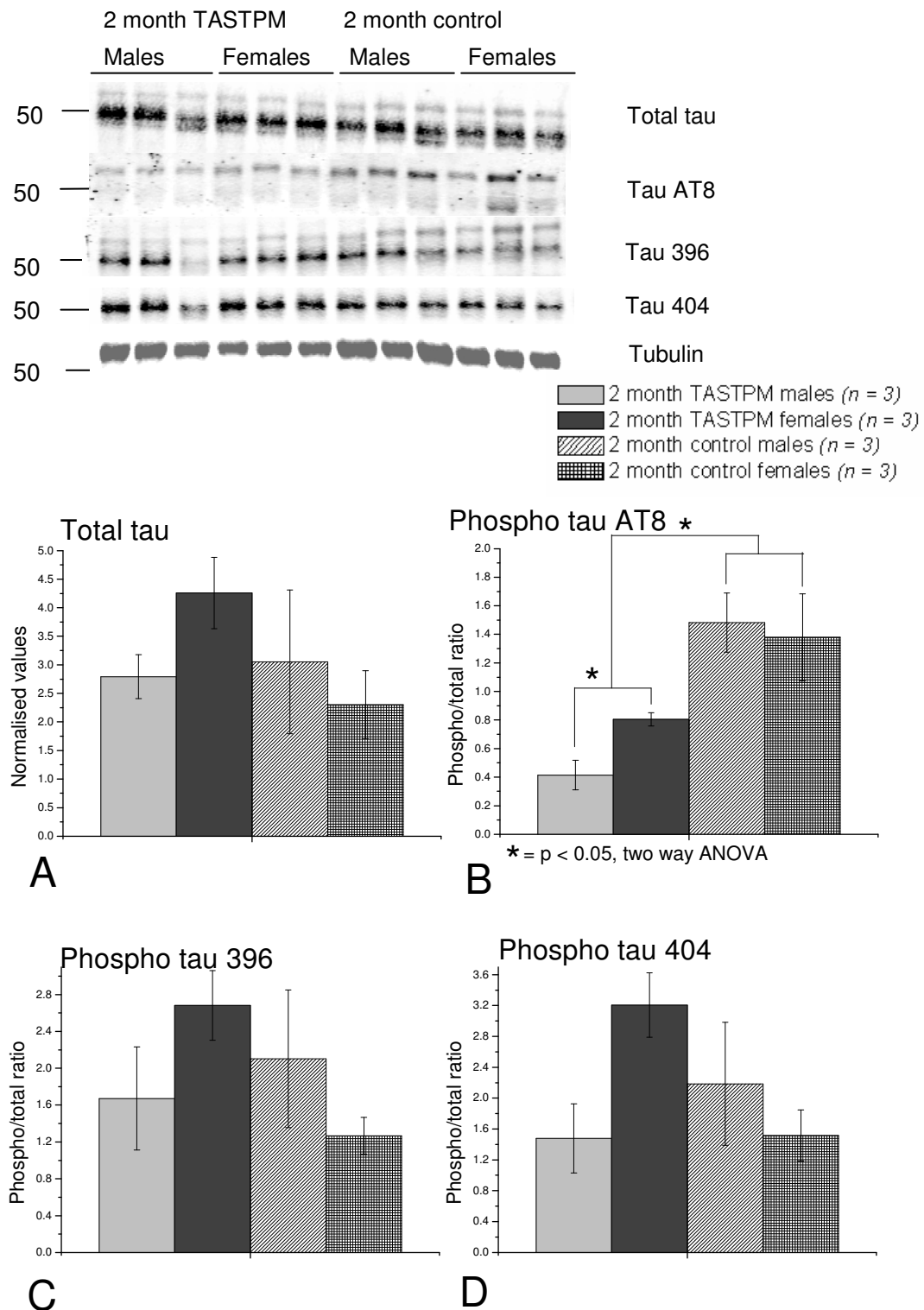


**Figure 4.17: Total and phosphorylated tau in 2 month TASTPM male and female mice.** 10 $\mu$ g of cortical lysate from 2 month old TASTPM and control male ( $n = 3$  in each group) and female ( $n = 3$  in each group) mice was used in SDS-PAGE, transferred to a nitrocellulose membrane and probed with the following antibodies: Tau5 (A), Tau AT8 (B), Tau phospho 396 (C), Tau phospho 404 (D). Representative blots are displayed along with the graphs showing densitometry calculations. Total tau is normalised to tubulin while phosphorylated tau is normalised to total tau. \* =  $p < 0.05$ , two way ANOVA.

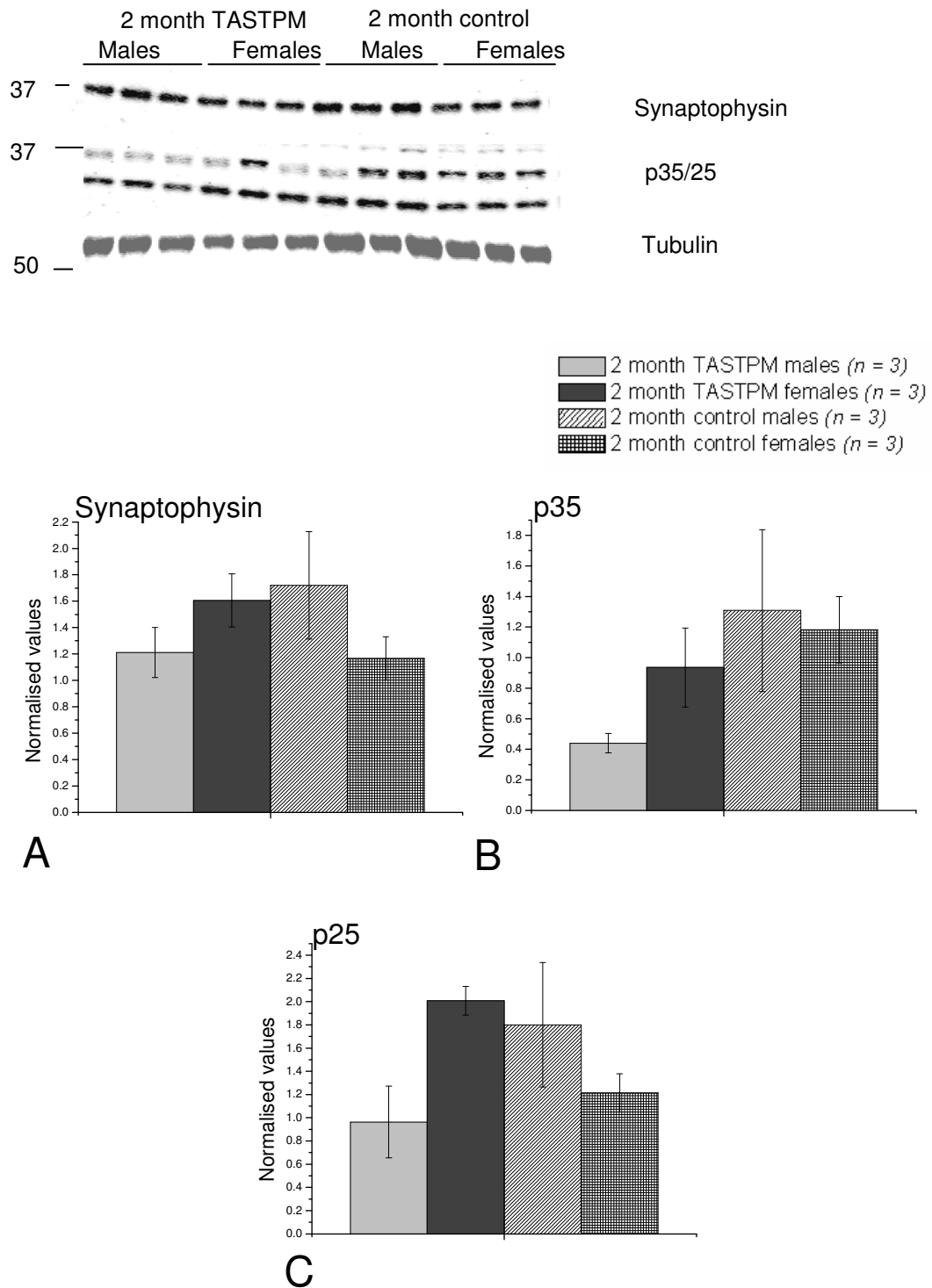


**Figure 4.18: Synaptophysin, p35 and p25 in 2 month TASTPM male and female mice.** 10 $\mu$ g of cortical lysate from 2 month old TASTPM and control male ( $n = 3$  in each group) and female ( $n = 3$  in each group) mice was used in SDS-PAGE, transferred to a nitrocellulose membrane and probed with the following antibodies: Synaptophysin (A), p35 (B) which also shows p25 (C), and actin. Representative blots are displayed along with the graphs showing densitometry calculations. Synaptophysin, p35 and p25 are normalised to tubulin.

#### **4.2.6: Biochemical profiles in 6 month old TASTPM mice**

At 6 months of age the TASTPM mice show marked electrophysiological deficits including a reduction in fEPSP amplitude (Chapter 3.2.7), while plaque pathology is reported to be well established (Howlett *et al.*, 2004). Western blotting was carried out on brain lysates from mice of this age to investigate whether any biochemical changes might be responsible for the electrophysiological deficits.

##### **4.2.6.1: APP**

As expected the 6E10 antibody shows the presence of the human APP transgene in all of the TASTPM mice, while this human protein is not present in control mice ( $p < 0.05$ , two-way ANOVA). There is no difference ( $p > 0.05$ , two-way ANOVA) in the levels of APP at this age between male and female TASTPM mice (Fig. 4.19A).

##### **4.2.6.2: CRMP2 (total and phosphorylated)**

There is no difference ( $p > 0.05$ , two-way ANOVA) in levels of total CRMP2 in six month old TASTPM mice (Fig. 4.19A). However, there is a significantly higher level ( $p < 0.05$ , two-way ANOVA) of phosphorylated CRMP2 at the 509/514 residues (Fig. 4.19C - GSK3 sites) compared to age-matched controls. This hyperphosphorylation of CRMP2 is in agreement with work previously carried out in the lab (Cole *et al.*, 2007b). The data suggests that the presence of both the APP and PS1 transgenes promotes increased phosphorylation of

CRMP2 at this residue. However, there is no difference ( $p > 0.05$ , two-way ANOVA) in the levels of phosphorylation at the 522 residue (Fig. 4.19D – Cdk5 sites). There is no effect of gender ( $p > 0.05$ , two-way ANOVA) on total CRMP2 or phosphorylated CRMP2 (Fig. 4.19A - D) in either TASTPM or control mice.

#### 4.2.6.3: Tau (total and phosphorylated)

There is no difference ( $p > 0.05$ , two-way ANOVA) in levels of total tau (Fig. 4.20A) in the 6 month old TASTPM mice compared with age matched controls, or in the levels of tau phosphorylation at the AT8 (Fig. 4.20B), 396 (Fig. 4.20C) or 404 (Fig. 4.20D) epitopes. There is also no effect of gender ( $p > 0.05$ , two-way ANOVA) on tau phosphorylation.

#### 4.2.6.4: Other proteins

There is no difference ( $p > 0.05$ , two-way ANOVA) in synaptophysin levels in the TASTPM mice compared to control (Fig. 4.21A). In addition, there is no effect of genotype or gender ( $p > 0.05$ , two-way ANOVA) on the levels of p35 (Fig. 4.21B) or p25 (Fig. 4.21C).

#### 4.2.6.5: Summary

As expected, the 6 month TASTPM mice express a high level of APP although, unlike the findings at 2 months, there is no difference in APP levels between male and female mice. The hyperphosphorylation of CRMP2 at the 509/514 residue observed at 6 months of age (but not at 2 months of age) suggest that pathological alterations subsequent to APP processing by PS1 are beginning to

develop between 2 and 6 months and could be linked to the reported cognitive decline and the deficits I observed in the electrophysiological measurements. However, whether the abnormal changes in CRMP2 are linked to any of these deficits requires further study.

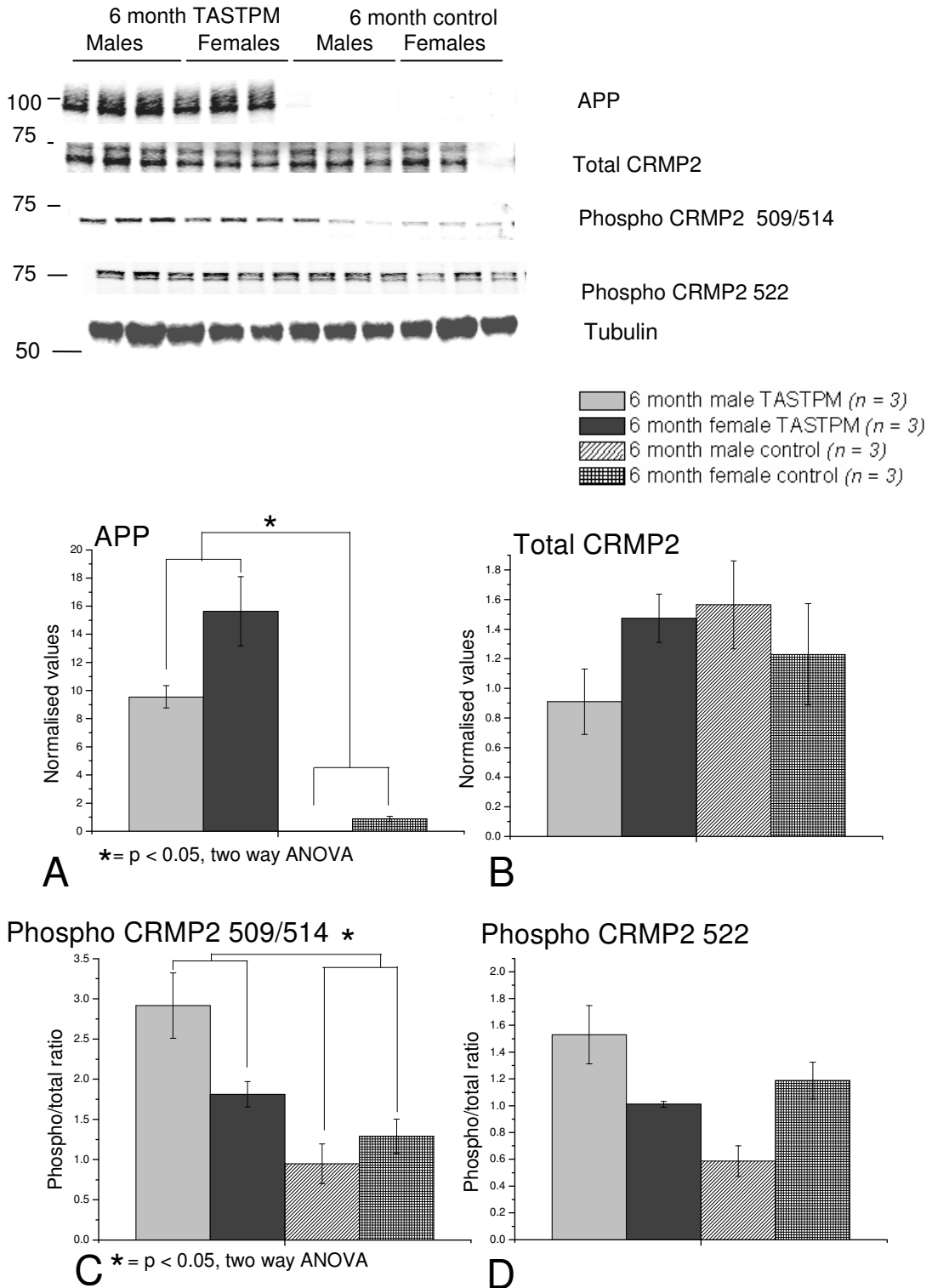


**Figure 4.19: APP, total and phosphorylated CRMP2 in 6 month TASTPM male and female mice.** 10 $\mu$ g of cortical lysate from 6 month old TASTPM and control male ( $n = 3$  in each group) and female ( $n = 3$  in each group) mice was used in SDS-PAGE, transferred to a nitrocellulose membrane and probed with the following antibodies: 6E10 (A), Total CRMP2 (B), CRMP2 phospho 509/514 (C), CRMP2 phospho 522 (D). Representative blots are displayed along with the graphs showing densitometry calculations. APP and total CRMP2 are normalised to tubulin while phosphorylated CRMP2 is normalised to total CRMP2 protein. \* =  $p < 0.05$ , two way ANOVA.

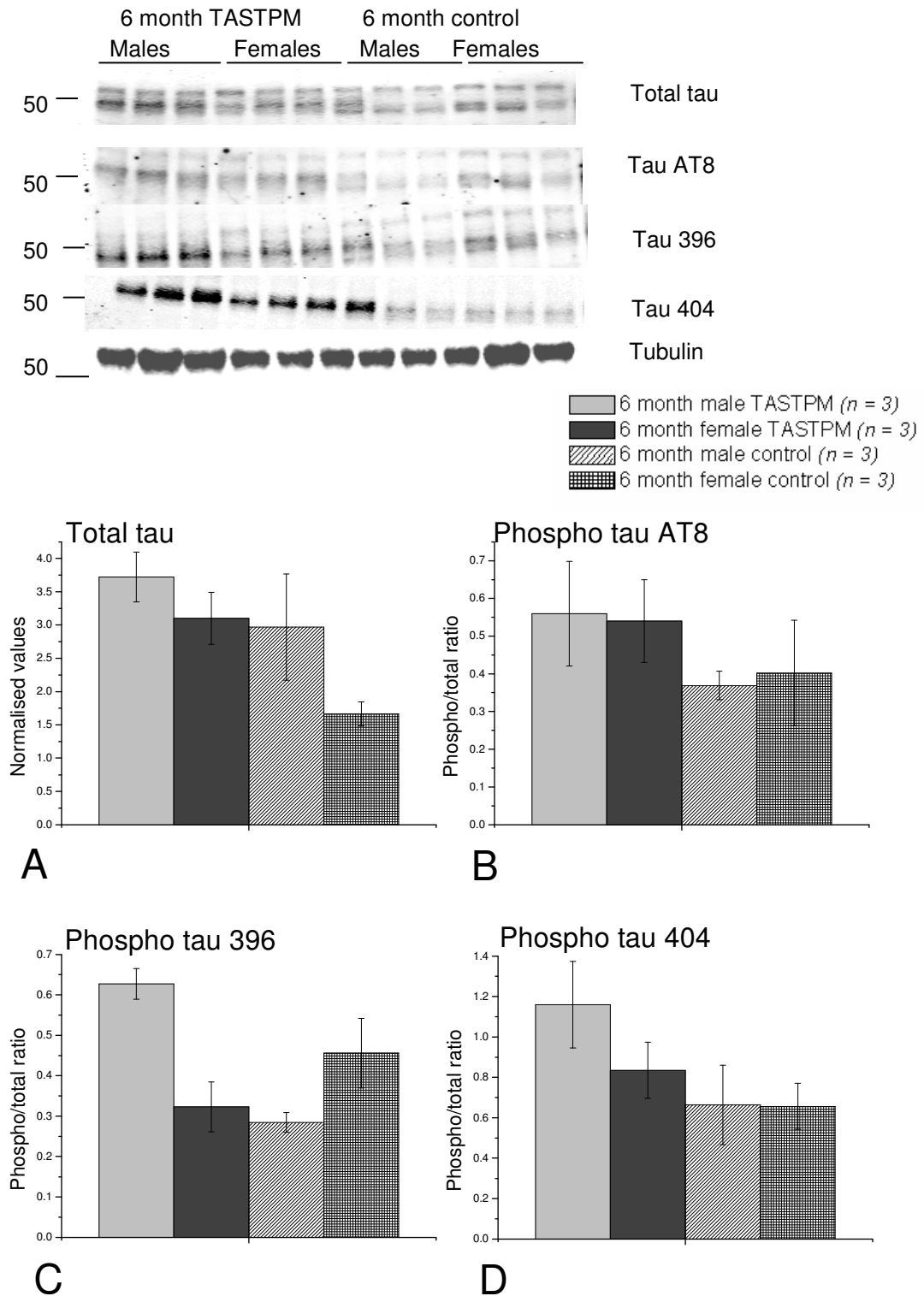


**Figure 4.20: Total and phosphorylated tau in 6 month TASTPM male and female mice.** 10 $\mu$ g of cortical lysate from 6 month old TASTPM and control male ( $n = 3$  in each group) and female ( $n = 3$  in each group) mice was used in SDS-PAGE, transferred to a nitrocellulose membrane and probed with the following antibodies: Tau5 (A), Tau AT8 (B), Tau phospho 396 (C), Tau phospho 404 (D). Representative blots are displayed along with the graphs showing densitometry calculations. Total tau is normalised to tubulin while phosphorylated tau is normalised to total tau.

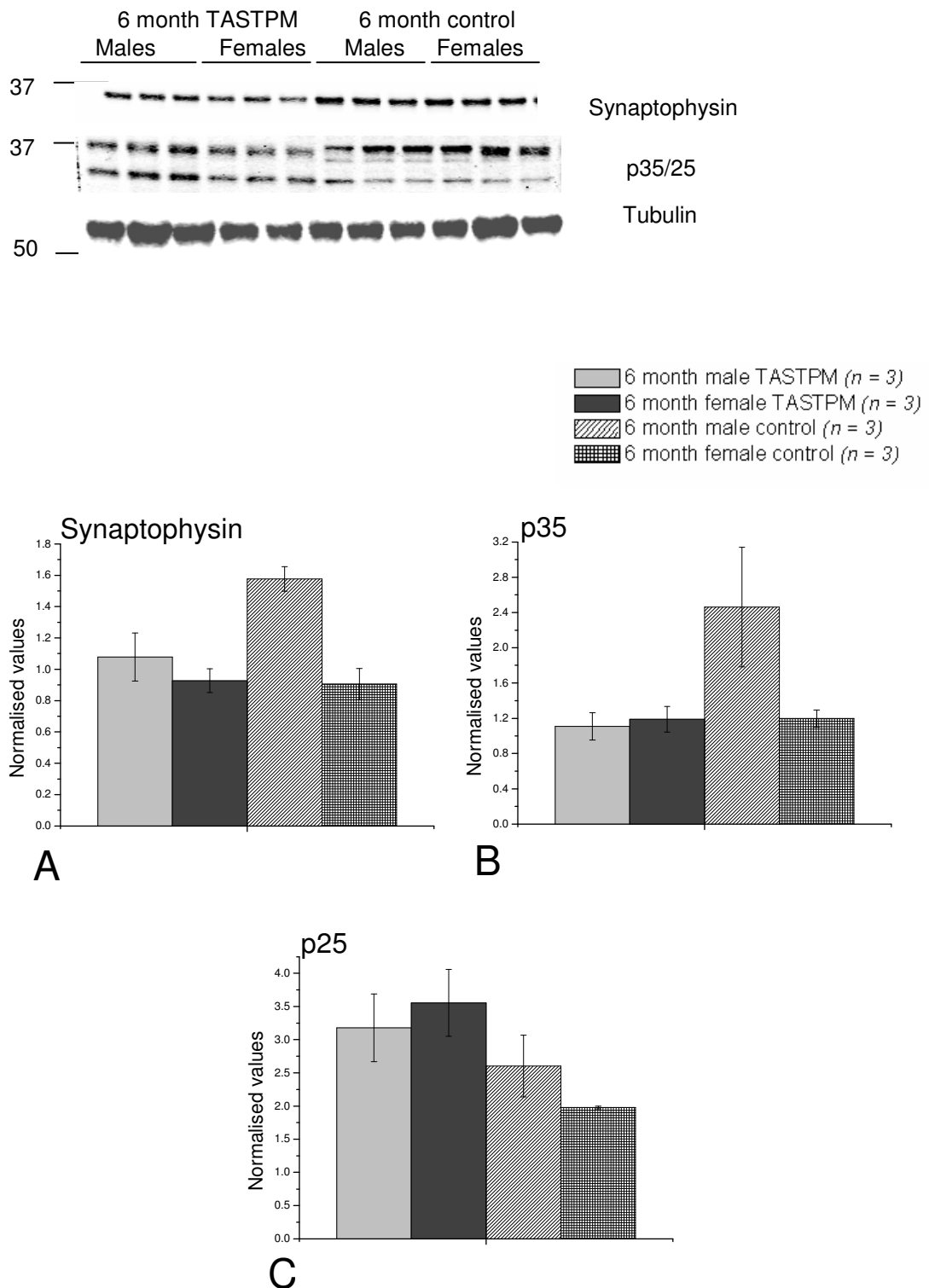


**Figure 4.21: Synaptophysin, p35 and p25 in 6 month TASTPM male and female mice.** 10 $\mu$ g of cortical lysate from 6 month old TASTPM and control male (n = 3 in each group) and female (n = 3 in each group) was used in SDS-PAGE, transferred to a nitrocellulose membrane and probed with the following antibodies: Synaptophysin (A), p35 (B) which also shows p25 (C), and actin. Representative blots are displayed along with the graphs showing densitometry calculations. Synaptophysin, p35 and p25 are normalised to tubulin.

#### **4.2.7: AD related protein expression and phosphorylation in different brain regions of TASTPM mice**

Much less is known about the spatial progression of A $\beta$  pathology in the TASTPM mice, however it is hypothesised to follow the same pattern as other models, with initiation in the cortex which then spreads to the hippocampus, with the cerebellum relatively spared. Samples from 6 month old TASTPM hippocampus, cortex, and cerebellum were used to compare the levels of protein expression in these regions. Male mice only were used for this experiment.

##### **4.2.7.1: APP**

There is a significant difference ( $p < 0.05$ , one-way ANOVA) in APP expression between the cortex, hippocampus and cerebellum, with levels highest in the cortex and lowest in the cerebellum (Fig. 4.22A). Similar to the 3xTg mice, the APP transgene is expressed under the Thy-1 promoter which results in a lower level of expression in the cerebellum.

##### **4.2.7.2: CRMP2 (total and phosphorylated)**

There is a significant difference ( $p < 0.05$ , one-way ANOVA) in levels of total CRMP2 between cortex, hippocampus and cerebellum (Fig. 4.22B), with levels lowest in the hippocampus and highest in the cerebellum. There is a significant difference ( $p < 0.05$ , one-way ANOVA) in CRMP2 phosphorylation at the 509/514 residues between the cortex and cerebellum, with levels lowest in the cerebellum. There is no difference ( $p > 0.05$ , one-way ANOVA) between hippocampus and cortex, or hippocampus and cerebellum (Figure 4.22C – GSK3

sites). Despite the higher expression of CRMP2 in the cerebellum the levels of CRMP2 phosphorylated at the 522 residue are significantly higher ( $p < 0.05$ , one-way ANOVA) in the cortex and hippocampus compared with the cerebellum (Fig. 4.22D – Cdk5 sites).

#### 4.2.7.3: Tau (total and phosphorylated)

Total tau levels are significantly higher ( $p < 0.05$ , one-way ANOVA) in the cerebellum, with no difference ( $p > 0.05$ , one-way ANOVA) between hippocampus and cortex (Fig. 4.23A). The cerebellum also shows significantly lower ( $p < 0.05$ , one-way ANOVA) levels of tau phosphorylated at the 396 (Fig. 4.23B) and 404 (Fig. 4.23C) epitopes compared to the other regions. However between the cortex and hippocampus there is little difference, apart from tau 404 phosphorylation which shows a trend for a reduction in the cortex ( $p = 0.06$ ). These results show that, overall, the pattern of tau phosphorylation in the cerebellum of the TASTPM mice (as seen with control and 3xTg mice at an older age) is different from other brain regions.

#### 4.2.7.4: Other proteins

There is no difference ( $p > 0.05$ , one-way ANOVA) in synaptophysin levels between the cortex, hippocampus and cerebellum (Fig. 4.24A). Levels of p35 are significantly lower ( $p < 0.05$ , one-way ANOVA) in the hippocampus compared with the cortex and cerebellum, but there is no difference between the two latter regions (Fig. 4.24B) Levels of p25 are significantly higher ( $p < 0.05$ , one-way

ANOVA) in the cortex than in the hippocampus and cerebellum; there is no difference between these regions (Fig. 4.24C).

#### **4.2.7.5: Summary**

Similar to the 3xTg and control mice there are marked differences in CRMP2 and tau regulation in the cerebellum relative to the cortex and hippocampus in the TASTPM model. There does not appear to be any major spatial alterations specific to this model or to the transgenes expressed. Therefore, the biochemical assessment of the cortex should be a reasonable surrogate for what is happening in the hippocampus and allow comparisons with deficits in hippocampal electrophysiology.

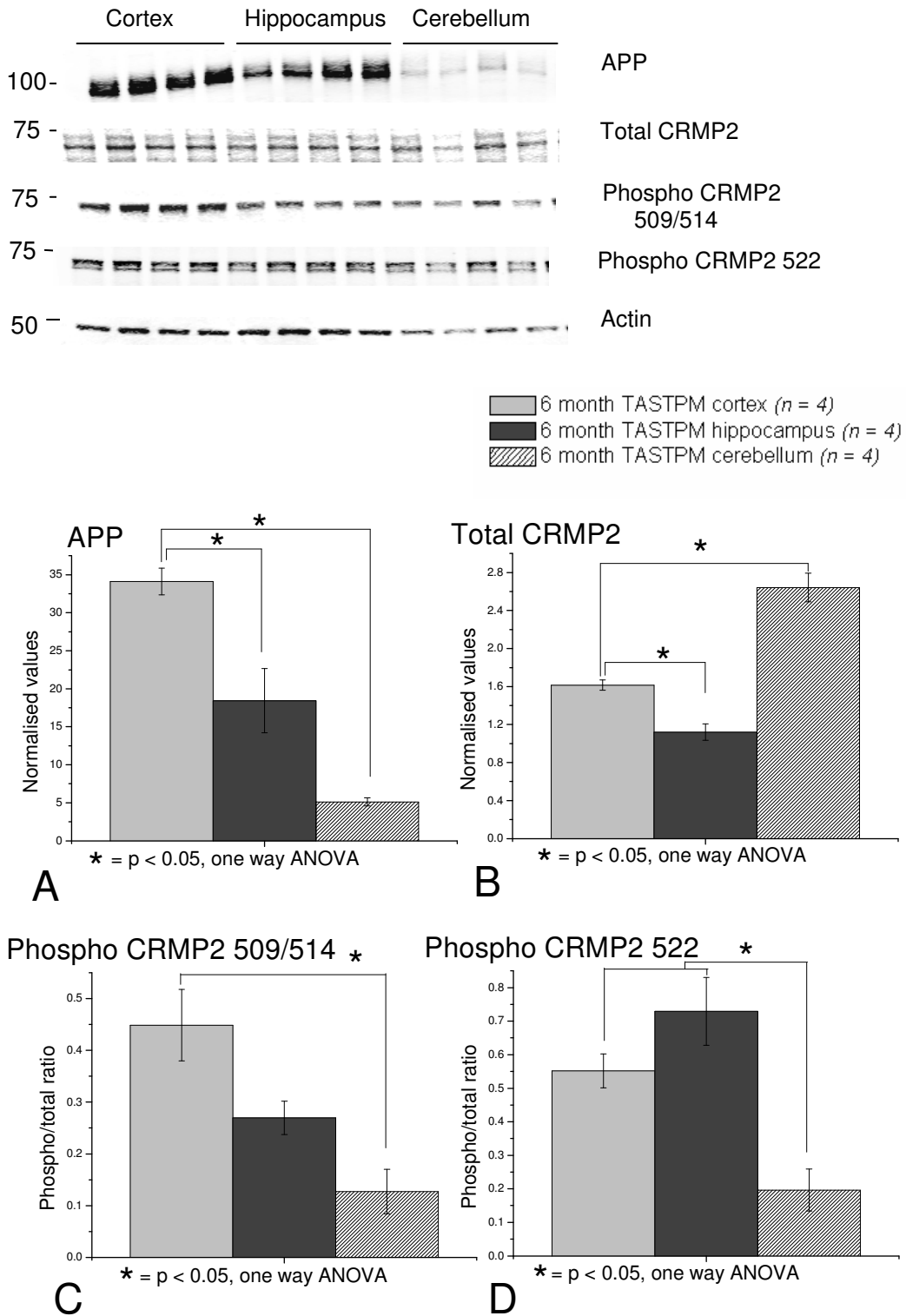


**Figure 4.22: APP, total and phosphorylated CRMP2 in 6 month TASTPM hippocampus, cortex and cerebellum.** 10 $\mu$ g of hippocampal, cortical and cerebellar lysate from 6 month old TASTPM male mice (n = 4 of each region) was used in SDS-PAGE, transferred to a nitrocellulose membrane and probed with the following antibodies: 6E10 (A), Total CRMP2 (B), CRMP2 phospho 509/514 (C), CRMP2 phospho 522 (D). Representative blots are displayed along with the graphs showing densitometry calculations. APP and total CRMP2 are normalised to actin while phosphorylated CRMP2 is normalised to total CRMP2 protein. \* =  $p < 0.05$ , one way ANOVA.

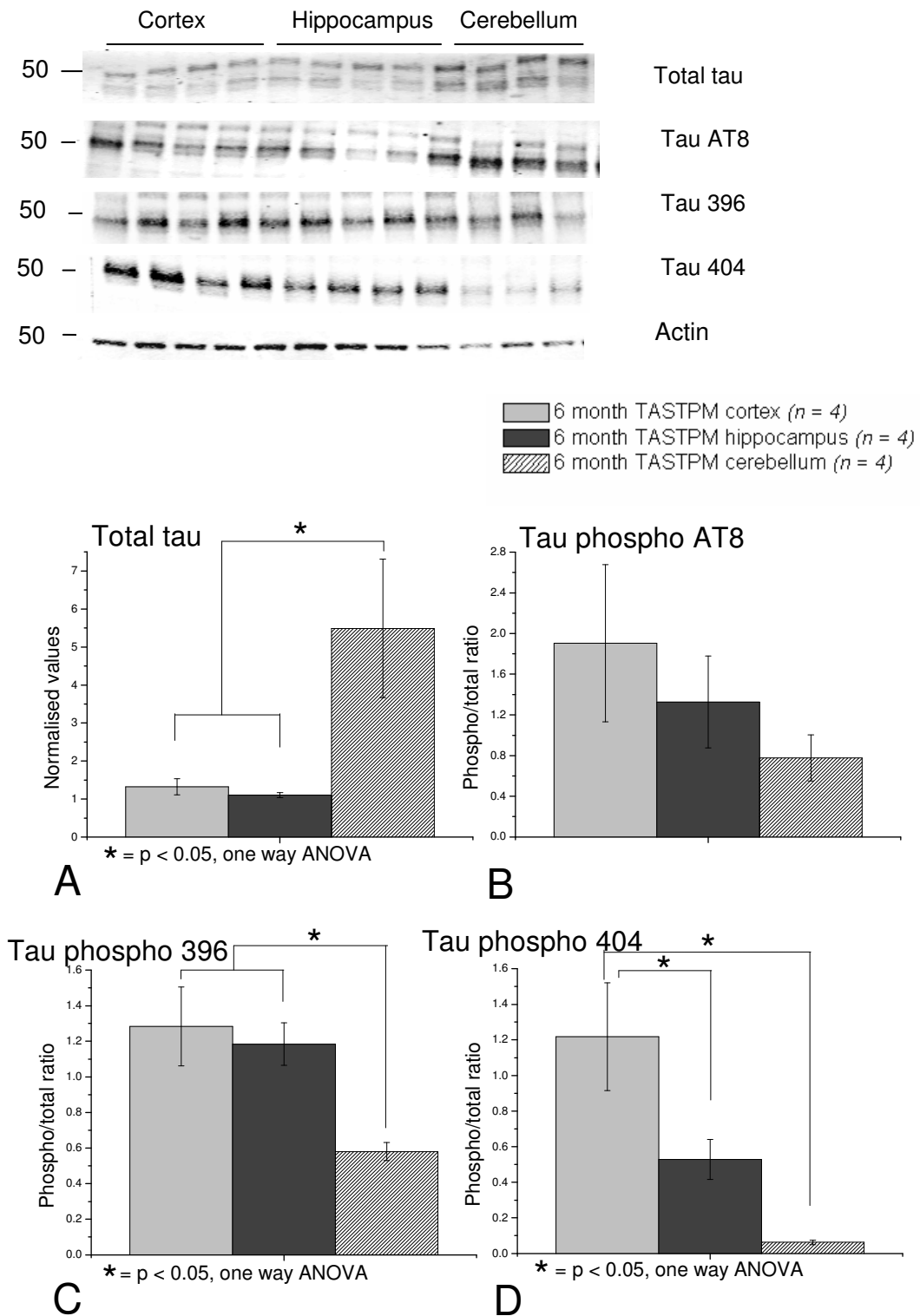


**Figure 4.23: Total and phosphorylated tau in 6 month TASTPM hippocampus, cortex and cerebellum.** 10 $\mu$ g of hippocampal, cortical and cerebellar lysate from 6 month old TASTPM male mice ( $n = 4$  of each region) was used in SDS-PAGE, transferred to a nitrocellulose membrane and probed with the following antibodies: Tau5 (A), Tau AT8 (B), Tau phospho 396 (C), Tau phospho 404 (D). Representative blots are displayed along with the graphs showing densitometry calculations. Total tau is normalised to actin while phosphorylated tau is normalised to total tau.  $\star = p < 0.05$ , two way ANOVA.

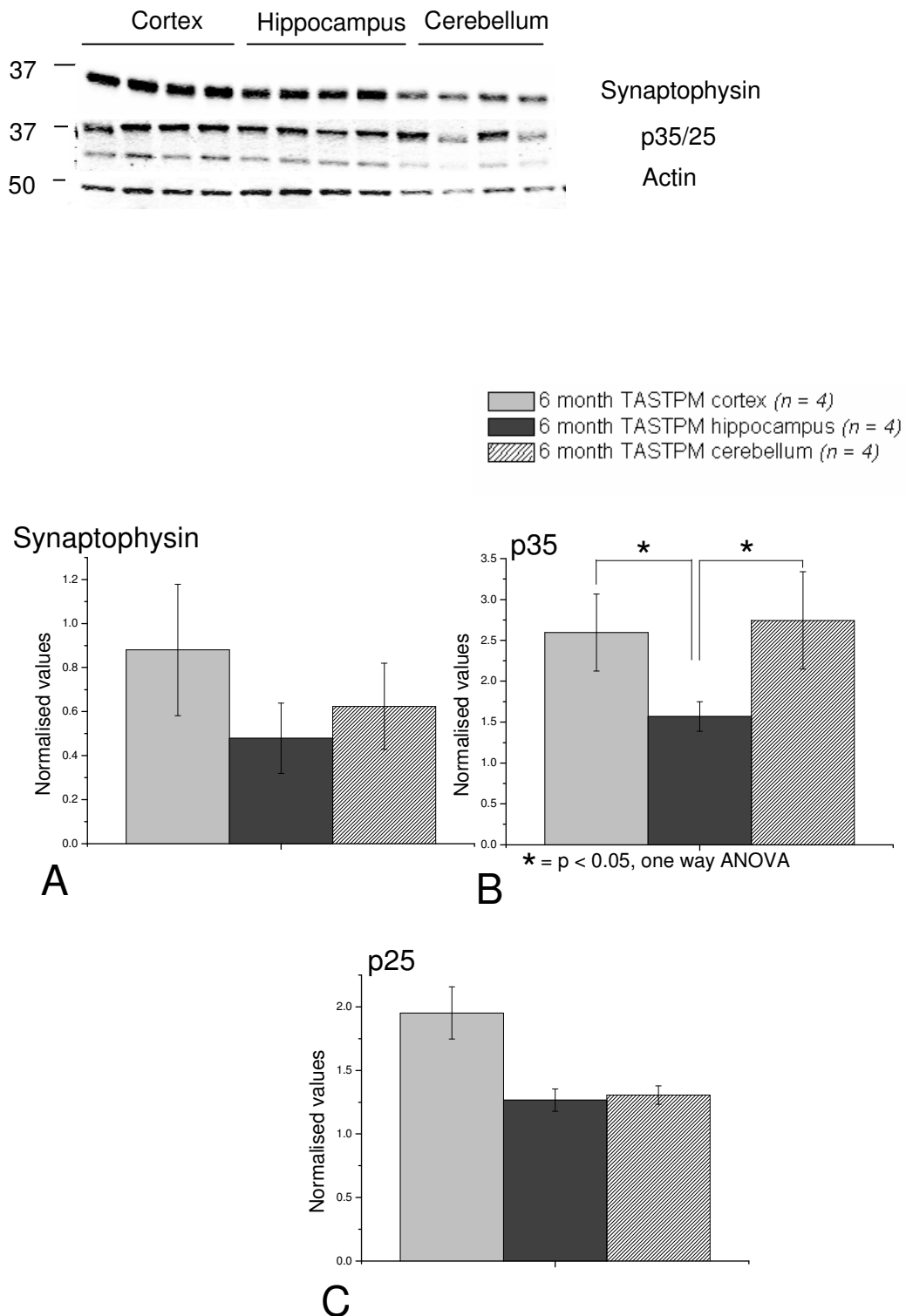


**Figure 4.24: Synaptophysin, p35 and p25 in 6 month TASTPM hippocampus, cortex and cerebellum.** 10 $\mu$ g of hippocampal, cortical and cerebellar lysate from 6 month old TASTPM male mice (n = 4 of each region) was used in SDS-PAGE, transferred to a nitrocellulose membrane and probed with the following antibodies: Synaptophysin (A), p35 (B) which also shows p25 (C), and actin. Representative blots are displayed along with the graphs showing densitometry calculations. Synaptophysin, p35 and p25 are normalised to actin. \* =  $p < 0.05$ , two way ANOVA.

#### **4.2.8: Kynurenic acid treatment**

The presence of kynurenic acid during hippocampal slice preparation was able to rescue the deficits in fEPSP amplitude in 12 month old 3xTg and 6 month old TASTPM mice (Chapter 3.2.8, 3.2.9). Therefore, I examined expression and regulation of the proteins found to be altered in these models in slices treated with or without kynurenic acid to further correlate slice biochemistry with electrophysiological measurements.

Brain slices from the hippocampus and cortex of 12 month old control and 3xTg mice were prepared as for electrophysiology (Chapter 2.2.1) and then incubated for one hour at room temperature in aCSF or aCSF containing 1mM kynurenic acid. The slices were then snap frozen, stored at -80°C and subsequently processed for Western blotting (Chapter 2.2.2). Blotting was performed to detect the following: total CRMP2, phosphorylated CRMP2 509/514, total GSK3 $\beta$ , Phospho GSK3 $\alpha/\beta$  Ser 21/9, total tau, phosphorylated tau AT8 epitope, phosphorylated tau 404 epitope, total MAPK, phosphorylated MAPK Thr209/Tyr 204, total PKB, phosphorylated PKB at serine 473, and actin as a loading control. Slices from 3 mice were used in each group.

No differences were observed in the levels or regulation of any of these proteins (Fig. 4.25). This argues against alterations in their expression or regulation underlying the kynurenic acid-sensitive electrophysiological deficits in these models.

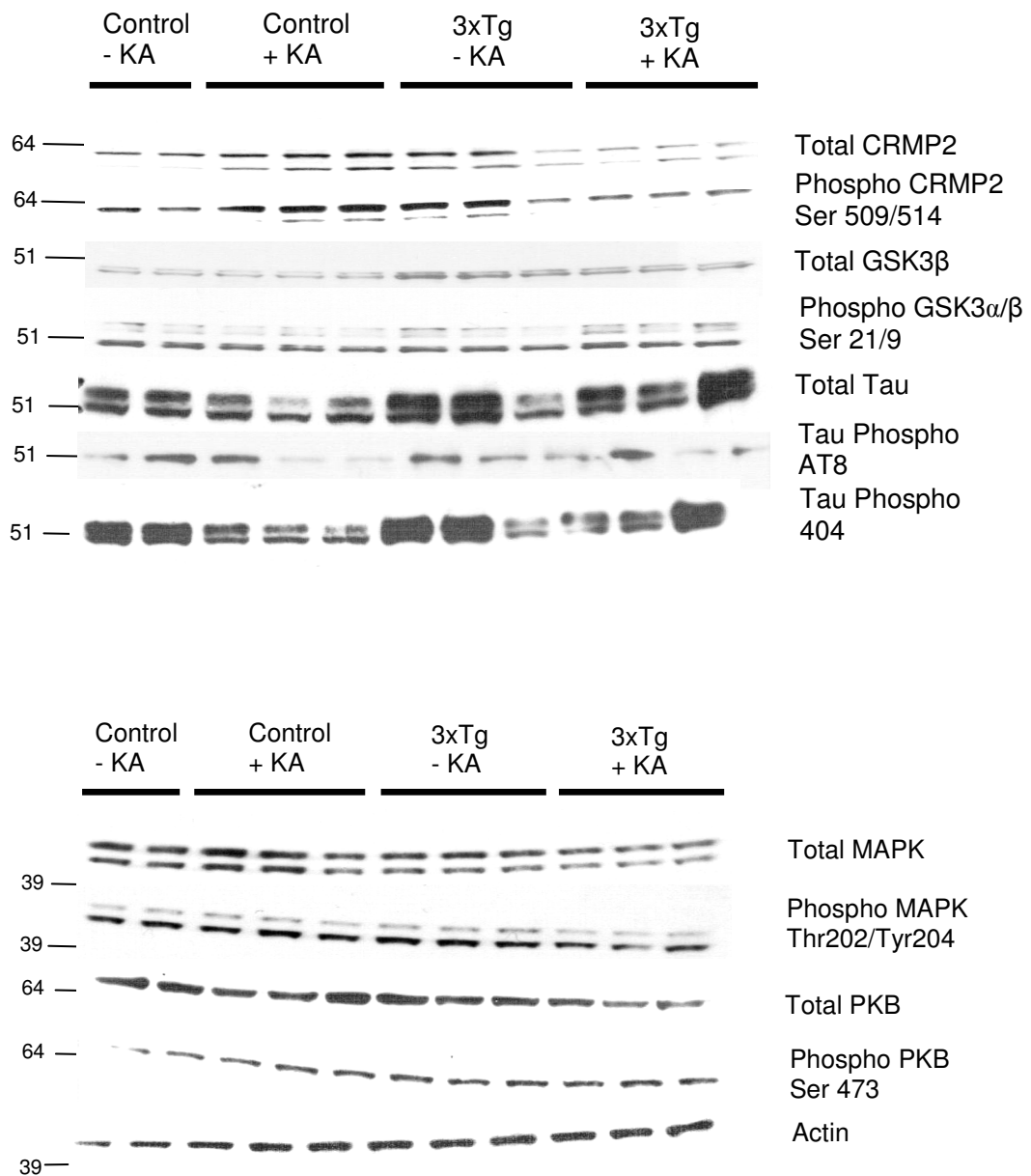


**Figure 4.25: Kynurenic acid treatment of slices from 12 month old 3xTg and control mice.** 10 $\mu$ g of hippocampal/cortical slice lysate from 12 month old 3xTg and control mice, incubated in normal aCSF or 1mM kynurenic acid, was used in SDS-PAGE, transferred to a nitrocellulose membrane and probed with the following antibodies: total CRMP2, phosphorylated CRMP2 509/514, total GSK3 $\beta$ , Phospho GSK3 $\alpha/\beta$  Ser 21/9, total tau, tau AT8, tau 404, total MAPK, phosphorylated MAPK Thr209/Tyr 204, total PKB, phosphorylated PKB Ser 473, and actin. Representative blots are shown above.

## **4.3: Discussion**

### **4.3.1: Technical aspects**

There are a number of technical limitations which must be considered when interpreting the data obtained in the Western blot experiments. Firstly, an average of three mice of each gender and genotype were used for each experiment and, due to the marked variability in protein expression between individual animals, it would be advisable to increase the sample size to improve the robustness of the data. Western blotting is a semi-quantitative technique, which measures relative protein expression, although I have attempted to limit the inherent variability of the technique by focusing on comparisons within gels and normalising to actin. In many cases I carried out multiple experiments using the same samples which provided similar results, suggesting that the Western blotting protocol used is a highly reproducible method of measuring protein levels. However, a greater sample size and use of additional loading controls, such as GAPDH or tubulin, and internal standards (where available) would improve the robustness of the results obtained.

The use of Western blotting has provided an indirect measure of some of the biochemical changes which may be associated with the development of the pathological features in the transgenic mice. However, no direct conclusions about the progression of amyloid and tau pathology can be drawn from this data; this would require the use of other techniques such as immunohistochemical staining of brain slices to examine A $\beta$  deposition and tangle formation. Unfortunately, these additional experiments were not possible during the time

course of my PhD studies but would be necessary to give a full analysis of the development of pathological features in the 3xTg and TASTPM mice.

### **4.3.2: Analysis of cortical expression of AD-related proteins in 3xTg mice**

The expression of a number of proteins was analysed at 2, 12 and 17 months in 3xTg cortex to provide a biochemical assessment at the same developmental stage as the electrophysiological measurements. The 3xTg mouse is a widely used model of AD, and as such biochemical or electrophysiological changes linked to disease progression would hopefully mirror at least some aspect of the development of the human pathology. One key aim of my thesis was to identify any biochemical changes associated with the genetic modification of the 3xTg mice that could be used as early-stage biomarkers of cellular damage, or developed as possible drug targets for the treatment of AD.

#### **4.3.2.1: APP expression in 3xTg mice**

Expression of the APP<sub>Swe</sub> transgene was studied in order to confirm the excess APP generation during the lifespan of this model. I observed that there was a significantly higher level of APP present at all ages studied.

In AD, the deposition of A $\beta$  is a progressive process, which involves not only a gradual increase in plaque load but also a regional dependence with pathology initiating in the cortex then later spreading to the hippocampus (Braak and Braak, 1991). Ideally a mouse model would replicate these characteristics of the condition. In this respect the 3xTg mouse has been reported to show an age-

dependent increase in A $\beta$  levels and plaque formation, with a brain region-specific progression similar to human AD. 6E10 staining occurs exclusively in the CNS and most strongly in the cortex, hippocampus and thalamus showing that the expression of the APP<sub>Swe</sub> transgene is region specific (Oddo *et al.*, 2003).

The presence of region-specific A $\beta$  accumulation suggest that the 3xTg mouse is a good model for studying this feature of AD, although marked differences in the time course of this process are now being reported, with plaque development in the cortex ranging from 6 months to over 18 months (Oddo *et al.*, 2003, Mastrangelo and Bowers, 2008). The original report observed the early deposition of intraneuronal A $\beta$  between 3 and 4 months in the cortex, and by 6 months in the hippocampus (Oddo *et al.*, 2003). In our colony of 3xTg mice, APP expression shows a trend for an increase with age between 2 and 12 months although this does not reach statistical significance. This suggests that APP accumulation may not be maximal at 2 months, or even at 12 months of age. In a previous study, cortical 6E10 staining was found to be present from 2 months at low levels and increased progressively to the age of 26 months; this age-dependent increase occurred gradually and was purely intraneuronal until the development of plaques at 18 months (Mastrangelo and Bowers, 2008). In our colony of 3xTg mice it is likely that plaque development occurs late in the lifespan, although further immunohistochemical studies would be required to confirm this.

To further explore this area, and to confirm the presence of elevated A $\beta$  levels in our colony of 3xTg mice, would require the use of more specific A $\beta$  antibodies which is technically more difficult due to the small molecular weight of the

protein and its lower abundance. Immunohistochemical techniques could also be used to give a measure of amyloid plaque deposition in the 3xTg mice. Both methods have been successfully used by other research groups to give a more detailed analysis of the development of pathology in these mice (see Chapter 1.4.5).

Although not studied in detail, gender did not affect APP expression at 2 or 12 months in our colony of 3xTg mice. It has been suggested by others that female 3xTg mice exhibit more extensive amyloid pathology, which manifests as an increase in A $\beta$  load and plaque numbers, and also develop plaques earlier in the lifespan (Hirata-Fukae *et al.*, 2008, Carroll *et al.*, 2010). These effects become markedly more pronounced with ageing, so it is possible that a difference might be observed in our colony at older ages such as in the 17 month group; these experiments were not carried out due to low numbers of mice available at this age.

#### **4.3.2.2: Tau expression in 3xTg mice**

The method of derivation of the model means that in the founder line the APP and tau transgenes are co-integrated at a single locus, hence both human genes (APP and tau) are expressed at a similar level (Oddo *et al.*, 2003).

I found a higher level of tau expression relative to controls in all ages of 3xTg mice. The 3xTg mouse carries both human tau and the endogenous mouse tau genes, and both are recognised by the tau5 antibody, so the two to threefold higher levels of tau in these mice suggest that the human protein has been

expressed. However, Oddo *et al.* (2003) reported up to an eightfold increase in total tau levels; this is much higher than observed in our colony and could contribute to the slower development of disease-related symptoms.

I observed no age-dependent increase in total tau expression in our colony of 3xTg mice. The development of tau pathology is known to occur subsequent to that of A $\beta$ , and studies using antibodies specific for human tau have suggested this is relatively late in the lifespan of the model. Immunohistochemical studies have observed human-specific tau immunoreactivity to a limited extent in animals from 2 months onwards, but this only becomes pronounced from around 6 months of age (Oddo *et al.*, 2003, Mastrangelo and Bowers, 2008); The tau<sub>P301L</sub> mutation in the 3xTg mice is known to accelerate the process of filament formation which eventually leads to tangle generation (vonBergem *et al.*, 2001), however the original report suggests that this does not occur until approximately 12 months and tangles are initially observed in hippocampus only (Oddo *et al.*, 2007). It is therefore likely that in our colony of 3xTg mice the deposition of tau was not sufficient even in older mice to allow any age-dependent differences to be observed.

One limitation of using only the Tau5 antibody is that it detects both human and mouse tau and so the individual levels of these cannot be calculated. To complicate matters further, human and mouse tau can co-aggregate in tangles (Sydow and Mandelkow, 2010). A combination of total tau and human or mouse specific antibodies, combined with immunohistochemical studies, would be required to study further the expression of tau in the 3xTg mice and its relationship to the tangle pathology observed in AD. There is also a distinction

between soluble tau and insoluble, tangle-associated tau, with the two pools separable by fractionation. Insoluble tau increases with ageing and may show a distinct pattern of phosphorylation compared to soluble tau (Hirata-Fukae *et al.*, 2009). In our colony of 3xTg it is likely that only soluble forms of tau were present even at 17 months of age.

The levels of tau expression at 2 and 12 months in our male and female 3xTg mice were similar. In comparison to the A $\beta$  pathology, little has been reported on gender-dependent differences in tau pathology. No gender difference was found in hippocampal total tau levels at ages up to 9 months (Clinton *et al.*, 2007) or in the phosphorylation of tau at several epitopes in aged 3xTg mice (Hirata-Fukae *et al.*, 2008). Overall this suggests that tau expression is not affected by gender in this mouse model.

#### **4.3.2.3: Tau phosphorylation in 3xTg mice**

Hyperphosphorylation of tau occurs prior to tangle formation in AD and has been reported previously to occur in the 3xTg mouse. For example, increased phosphorylation occurs at sites recognised by the AT100 and 12E8 antibodies (Thr 212/Ser 214 and Ser262) in 6 month old 3xTg mice, but not at the AT8 (Ser 202, Thr 205) and AT180 (Thr 231) sites until around 12-15 months (Oddo *et al.*, 2007). In our colony of 3xTg mice there was no difference in levels of phosphorylation at any site investigated (including AT8) compared to control mice. The possible exception was in males at 17 months where there was a trend for an increase at the 396 and 404 epitopes.

In human AD, in contrast to A $\beta$  pathology, tau pathology initiates in the hippocampus and spreads to the cortex (Braak and Braak, 1991), so the hyperphosphorylation of tau in the 3xTg mice may be expected to occur later in this region of the brain. There are, however, marked differences between experimental reports with regard to the time course of these phosphorylation events. In the original paper by Oddo *et al.* (2003), increased phosphorylation at the AT8 epitope was apparent at 12 months of age in the hippocampus and previous work in our lab, using tissue from a different colony of 6 month old 3xTg mice, found increased phosphorylation at the AT8 epitope in the cortex (Cole *et al.*, 2007b). However, one study reports that PHF-1 phosphorylation (which recognises phosphorylated residues including both 396 and 404 sites) is not apparent until 15 or 16 months in the 3xTg and may not be detectable in the cortex until 26 months of age (Mastrangelo and Bowers, 2008), while another reports a low level of cortical staining at this site from 9 months (Oh *et al.*, 2010). Such discrepancies between groups serve to highlight the inconsistencies of the 3xTg model and the differences between individual colonies of these mice. In our colony of 3xTg mice it is likely that the lack of a significant difference in AT8, 396 or 404 phosphorylation reflects a very slow progression of tau pathology compared to previous studies.

It should not be forgotten that there are a large number of potentially phosphorylatable sites on human tau and over 35 sites are phosphorylated in tangles from AD brain (Hanger *et al.*, 2007). Many of the AD-related phosphorylation sites have not been studied in the 3xTg model, mainly as it is technically challenging to quantify phosphorylation of so many tau residues from a single sample. However this will be essential to establish whether each

becomes hyperphosphorylated in the model and if they follow separate time courses which may permit correlation to symptoms of the disease.

#### **4.3.2.4: CRMP2 phosphorylation in 3xTg mice**

Previous work in our lab, using samples from a different colony of 3xTg mice, showed an increase in CRMP2 phosphorylation at both the 509/514 GSK3 sites and the Cdk5 site at serine 522 in the cortex at 2 months of age (Cole *et al.*, 2007b). However, in our 3xTg colony an increase in CRMP2 phosphorylation is only apparent at the 509/514 sites and occurs in older animals, again suggesting that the pathological features are developing more slowly in these mice. A marked decline in the inactive serine 9-phosphorylated form of GSK3 $\beta$  (an indication of increased GSK3 $\beta$  activity) has previously been reported between 12 and 15 months of age in 3xTg mice (Oddo *et al.*, 2007) and this could be associated with the increase in CRMP2 509/514 phosphorylation observed. It is unclear why there is no concomitant increase in CRMP2 522 phosphorylation, as this is the Cdk5 priming site for GSK3 phosphorylation of the 509/514 residues, and thus is a limiting step in the phosphorylation of 509/514. The data is consistent with my analysis of the regulatory subunits of Cdk5 (see sections **4.2.1.4 / 4.2.2.4**) which are not altered in my 3xTg mice compared to control. An alternative explanation is that the change in 509/514 phosphorylation is due to a change in phosphatase activity rather than an increase in GSK3 activity. Phosphorylation at the GSK3 and Cdk5 sites is regulated by separate protein phosphatases (Cole *et al.*, 2008).

The phosphorylation of CRMP2 is increased in human AD cortical tissue (Cole *et al.*, 2007b) so the higher level of phosphorylation observed in the 3xTg mouse

may suggest a mechanistic link between APP or tau pathology and the regulation of CRMP2, and hence may be a useful characteristic of this model; indeed the late development of this feature in our colony of mice is consistent with CRMP2 phosphorylation changes occurring subsequent to abnormal APP processing.

#### **4.3.2.5: p35/p25 in 3xTg mice**

The generation of p25 from p35 and subsequent activation of Cdk5 has been suggested to contribute to neurodegeneration in AD but this has been disputed (Patrick *et al.*, 1999, Tandon *et al.*, 2003). I did not find any difference in the levels of the Cdk5 co-factor p35 or its cleavage product p25 at any age in the 3xTg mice compared to controls. This is in agreement with previous work in our lab which found no differences in p35 or p25 levels, or Cdk5 expression or activity, in the cortex of 6 month old 3xTg mice compared to age matched controls (Cole *et al.*, 2007b). In contrast, an age-dependent increase in Cdk5 activity has been reported in another study by Oddo *et al.* (2007) which studied mice of 6, 12 and 17 months. An increase in p25 levels, the co-factor which causes prolonged activation of Cdk5, could account for the increased Cdk5 activity in these mice. In contrast, there were no changes in p35 levels (Oddo *et al.*, 2007). It was suggested that these changes could partially mediate the increase in tau phosphorylation observed with advancing age in their study, when accompanied by a higher level of GSK3 $\beta$  activity. The discrepancies between these reports suggest that further studies of p35/p25 and Cdk5 activity are required in the 3xTg mice. However, the lack of any differences in our colony of 3xTg mice could be explained by the relatively slow development of pathology

resulting in a delay in alterations of Cdk5 or p35/p25 activity which may also partly explain the slow development of tau hyperphosphorylation in these mice.

#### **4.3.2.6: Synaptophysin in 3xTg mice**

In AD, the majority of studies have shown a decrease in synaptophysin levels in both cortex and hippocampus and this is due to an initial loss of synapses followed by neuronal death (Masliah *et al.*, 1991). I found no difference in synaptophysin levels in 3xTg mice compared to control at any age. As synaptophysin is a synaptic vesicle protein, this suggests that even at 17 months of age the synapses within the cortex remain relatively well preserved. However, there is the possibility that synaptophysin is still present in neurons, and thus detectable by Western blotting, despite the retraction of dendritic spines and so this would have to be confirmed by immunohistochemical or imaging studies. However, the results in our colony of 3xTg are in agreement with several groups who have reported no change in synaptophysin levels in 3xTg mice (Hirata-Fukae *et al.*, 2009, Julien *et al.*, 2010, Arsenault *et al.*, 2011), and levels of other presynaptic proteins such as dynamin and synaptotagmin are also unchanged (Yao *et al.*, 2005b). It would be interesting to look at postsynaptic proteins such as PSD-95 as alterations in these have previously been reported (Arsenault *et al.*, 2011).

The lack of alterations in synaptic proteins or neuronal loss in the 3xTg mice highlights the limitations of this model in that it only replicates some of the pathological features of AD.

It is likely that in 3xTg mice the synapses remain intact, but this does not rule out the possibility of structural changes within the synapse. Hirata-Fukae *et al.* (2009) report no changes in synaptophysin at ages up to 23 months but a trend for reduced NMDA receptor 2A and AMPA GluR2 subunit expression with ageing. I attempted to characterise NMDA receptor levels in our 3xTg mice but this was unsuccessful due to a lack of antibody specificity. It would be interesting to study glutamate receptor expression in these mice which would require the use of imaging and immunohistochemical techniques and could further correlate biochemical and electrophysiological data.

#### **4.3.2.7: Summary**

The increased levels of APP and tau protein shows that the 3xTg mice are expressing the transgenes as expected. An age-dependent increase in the expression of APP mirrors that observed in AD, although no such gradual increase is observed with transgenic tau. Other features such as hyperphosphorylation of CRMP2 are observed, albeit relatively late in the life of our colony of 3xTg mice, and this late onset significantly limits the use of the model. Unfortunately, the lack of biochemical changes in the 3xTg mice means that it is difficult to carry out one of the early aims of the project which was to provide links between synaptic function and alterations in protein phosphorylation.

An ideal model of AD would develop pathological features earlier than 12 to 18 months aiding more rapid assessment of the contribution of pathology to behavioural or electrophysiological changes. Unfortunately, the delayed onset of the phenotype and lack of biochemical differences observed at earlier ages have

made studies in our colony of 3xTg mice difficult in the timeframe of PhD studies. However, variability within this model has been reported by other groups (Hirata-Fukae *et al.*, 2008), and it is this variability from colony to colony and research group to research group which is the most frustrating aspect of the model. It becomes almost impossible to design studies using the model, as the timeframe for development of features is difficult to predict. In addition, crossing onto other lines with different aspects of AD would have to be very carefully controlled with littermates from the original cross. These technical problems will limit the usefulness of the 3xTg in the study of AD.

#### **4.3.3: AD related protein expression and phosphorylation in different brain regions of 3xTg**

Protein expression was measured in the hippocampus, cortex and cerebellum of 17 month 3xTg mice. This was primarily to ensure that there were no obvious biochemical differences between the cortex (main biochemical studies) and hippocampus (electrophysiological studies). Cerebellar tissue was used as a control as levels of the transgenic human APP are much reduced in this region.

As expected, APP levels in our colony of 3xTg mice were significantly higher in the cortex and hippocampus than in the cerebellum. It is likely that this is due to protein stability, as the transgene is driven by the Thy-1 promoter which is expressed at its highest levels in this region (Andra *et al.*, 1996). This mirrors human AD, where the cerebellum is relatively resistant to developing the pathological features of the disease, possibly due to a lower level of APP protein expression (Causevic *et al.*, 2010).

The levels of total tau in 3xTg mice remain stable across the cortex, hippocampus and cerebellum. This is likely due to the high abundance of endogenous mouse tau which is detected by the antibody. In humans total tau levels are similar in the cortex and hippocampus and again reduced in the cerebellum (Causevic *et al.*, 2010), but the phosphorylation status of tau has not been studied. In 3xTg mice there is a marked increase in tau phosphorylation at the AT8 and 396 epitopes, with a reduction at the 404 epitope in the cerebellum compared to the other brain regions. However the level of tau phosphorylation is similar between cortex and hippocampus. This is also observed in control mice, suggesting that regulation of tau phosphorylation is region-specific in the mouse brain, and the regional variation is not related to the genetic modification.

In the 3xTg mouse the levels of p25 and p35 also vary across different brain regions, with p35 levels highest in the cerebellum and p25 highest in the cortex. However, this may be related to the normal distribution of these proteins in mouse brain, as region-specific differences have previously been observed in rodents (Wu *et al.*, 2000).

In conclusion, I have observed region-specific differences in tau protein levels and phosphorylation in both 3xTg and control mice but it is not known if similar changes are apparent in human brain. As abnormal phosphorylation of tau is associated with tangle formation and thus AD development it is important to understand the normal physiological regulation of tau by phosphorylation. If there are brain region specific differences this implies differential activity of pathways that control tau phosphorylation in healthy brain, and has to be kept in mind when developing interventions targeting tau phosphorylation.



#### **4.3.4: Correlations between biochemical changes and electrophysiology in 3xTg mice**

For some of the 3xTg mice the hippocampus was used for electrophysiological recordings while the cortex from the same animal was homogenised to generate protein lysates. In these samples, I tried to correlate levels of APP and tau to deficits in the maximum fEPSP amplitude and LTP values but the number of animals available was too small to reach solid conclusions.

I could not demonstrate a direct linear association between the fEPSP amplitude (the strength of basal synaptic transmission) and the magnitude of LTP obtained suggesting that even in the mice with some neuronal dysfunction the ability of the neurons to undergo synaptic plasticity is not affected. However, it should be noted that due to the nature of the technique there is significant variation between individual slices even in the same mouse and that the values reported are an average of several results pooled together. It is interesting that the two 12 month old mice with the highest levels of tau had the smallest fEPSP, while the mouse with the lowest APP and tau expression had the highest fEPSP amplitude and magnitude of LTP. At 17 months, the mouse with the highest levels of APP and tau also had the lowest fEPSP amplitude and magnitude of LTP. This suggests that there is some link between the expression of the transgenic proteins and the electrophysiological changes. However, this clearly needs a more robust investigation with larger numbers of animals. Indeed ideally an inducible system, where the transgenes could be activated to specific levels, would be needed to truly show a cause and effect relationship between protein expression and electrophysiological deficit. Another group has reported that in double transgenic

APP<sub>Swe</sub> x PS1<sub>M146L</sub> mice there was no correlation between brain A $\beta$  levels and basal synaptic transmission or LTP, although there was a weak correlation between LTP and cognitive deficits in a Morris water maze task (Trinchese *et al.*, 2004).

The biochemical analysis was done in the cortex and the electrophysiology in the hippocampus, and although the levels of APP and tau are similar in both there may still be some variation between the brain regions. To improve this experiment, it would be necessary to carry out the Western blotting in the hippocampus; the cortex was generally used for experiments as a larger volume of tissue could be obtained. In our colony of 3xTg mice, no correlation was attempted between behavioural performance and electrophysiological or biochemical changes; A $\beta$  load has been linked to cognitive deficits in a number of transgenic mouse models and has been suggested to correlate with synaptic loss (Gordon *et al.*, 2001).

#### **4.3.5: Analysis of cortical expression of AD-related proteins in TASTPM mice**

I analysed the same set of proteins in the cortex of the TASTPM mouse to extend the search for abnormal expression or regulation of proteins that could be linked to the electrophysiological deficits in these models. I also wanted to compare the development of pathology between the double-transgenic TASTPM and the 3xTg model. One consideration in interpreting this data is that the TASTPM mice are derived from a C57BL/6 background, while the control mice used are mixed C57BL/6 x 129/Sv, due to limitations in the animals available for these

experiments. Anatomical and metabolic differences have been observed in the brains of different inbred mouse strains (Penet *et al.*, 2006), and so it would be desirable to confirm the results obtained and compare any differences observed in the TASTPM mice with the pure C57BL/6 strain.

#### **4.3.5.1: APP expression in TASTPM mice**

I confirmed APP<sub>swe</sub> expression in the TASTPM mice, with none detectable in age-matched control mice. Amyloid deposition initiates at 3 months and shows an age-dependent progression in the cortex of this model (Howlett *et al.*, 2004). Limited biochemical and immunohistochemical studies of A $\beta$  pathology have previously been carried out in the TASTPM mouse. However, one study found both extensive APP and punctuate A $\beta$  staining by the age of 6 months in the cortex and hippocampus (Maheswaran *et al.*, 2009). The progression of plaque pathology has been better characterised in the TAS10 mouse from which the TASTPM mouse is derived. The TAS10 mouse shows significant age-dependent increases in A $\beta$  in the hippocampus and cortex, with plaque deposition most marked in the cortex (Richardson *et al.*, 2003). In theory the development of pathology should occur more rapidly in the TASTPM mouse compared to the TAS10 line due to the presence of the PS1<sub>M146V</sub> transgene.

#### **4.3.5.2: Tau expression and phosphorylation in TASTPM mice**

I observed no difference in levels of total tau in TASTPM mice at either 2 and 6 months, which is expected as these mice express only endogenous mouse tau protein. I also checked whether the presence of the APP<sub>Swe</sub> and PS1<sub>M146V</sub>

transgenes are capable of causing biochemical alterations in tau. At 2 months of age tau phosphorylation is similar to control levels at the 396 and 404 epitopes, the only exception being a reduction in the phosphorylation of tau at the AT8 epitope in the TASTPM which is not present at 6 months. Indeed at 6 months of age there are no significant differences in tau phosphorylation between TASTPM and controls.

It has previously been reported that an increase in tau phosphorylation at the AT8 epitope is associated with dystrophic neurites in the cortex of 8 month old TASTPM mice. These neurites are closely associated with amyloid plaque deposition (Howlett *et al.*, 2008b). The location of the hyperphosphorylated tau suggests that it may be regulated by the functional alterations that occur in neuronal processes disrupted by amyloid deposition. This feature has also been reported in other mouse models. For example, a similar pattern of hyperphosphorylated tau has been observed adjacent to amyloid plaques in the APP23 model, which expresses the APP<sub>Swe</sub> mutation (Sturchler-Pierrat *et al.*, 1997). This implies that the presence of the APP mutation alone is sufficient to alter the pattern of phosphorylation at multiple tau residues and this may be associated with early tau pathology.

However, the progression to neurofibrillary tangles has not been observed in mice in which a tau transgene is not present. This suggests that although there is an interaction between A $\beta$  deposition and tau phosphorylation other mechanisms (or distinct phosphorylation sites) are involved in the initiation of tangle pathology.

#### **4.3.5.3: CRMP2 phosphorylation in TASTPM mice**

I observed no difference in CRMP2 levels or phosphorylation at either the 509/514 or 522 sites in 2 month old TASTPM mice compared with controls. However, by 6 months of age there is an increase in CRMP2 phosphorylation observed in the TASTPM mice at the 509/514 sites. Previous work in our lab on a different cohort described an increase in phosphorylation at these sites from 2 months of age (Cole *et al.*, 2007), again indicating some variability in the rate of progression of the disease between individual colonies. Cole *et al.* also showed that CRMP2 hyperphosphorylation is only observed in models which express a PS1 mutation which accelerates the deposition of A $\beta$  and was not found in single transgenic mice such as the Tg2576 (APP<sub>Swe</sub>) model. This suggests that double or triple transgenic models such as the 3xTg or TASTPM may be better models of this aspect of human AD, with the more rapid development of this feature in the TASTPM mice making it a particularly useful model. Interestingly abnormally high CRMP2 phosphorylation appears very specific to AD, not being detectable in other forms of human dementia including tauopathy (Cole, AR, personal communication). Therefore the pathways responsible for the change in phosphorylation may represent AD specific cellular defects and CRMP2 phosphorylation may provide an additional biochemical means to distinguish AD from non-AD dementia.

#### **4.3.5.4: p35/p25 in TASTPM mice**

In our colony of TASTPM mice there is no significant difference in p35 or p25 levels compared to controls at 2 months or 6 months. This suggests that the

levels of this co-factor and subsequent alterations in Cdk5 activity do not make a major contribution to the biochemical changes observed in TASTPM mice.

#### **4.3.5.5: Synaptophysin in TASTPM mice**

In both 2 and 6 month TASTPM mice there is no difference in the levels of synaptophysin, which implies that there is no synaptic loss associated with the progression of A $\beta$  deposition in TASTPM mice. This is in agreement with previously published work where no difference in synaptophysin levels was found in these mice (Hirata-Fukae *et al.*, 2009), suggesting that the cognitive decline described in these mice is not associated with synaptic loss. This synaptic stability may explain reflect the lesser magnitude of cognitive changes in the TASTPM mice compared with the memory loss observed in AD (Howlett *et al.*, 2008b). It is not known whether synaptic loss would occur with further ageing of these mice, as the pathological features become more advanced and cognitive deficits become more severe. However, the lack of changes in synaptophysin at 6 months suggest that, similar to the 3xTg mouse, the TASTPM mouse fails to model the synaptic loss observed in AD. As with the 3xTg mouse, it would be interesting to investigate more thoroughly if there were functional alterations occurring within the synapse, for example in the molecular composition or receptor numbers and distribution. This would be particularly relevant in the hippocampus where I observed that neuronal plasticity is impaired and this could potentially be linked to synaptic alterations.

#### 4.3.5.6: Summary

Although 2 month and 6 month old mice were not directly compared, the changes present in 6 month mice such as hyperphosphorylation of CRMP2 and suggest that there is an age-dependent increase in the severity of the biochemical phenotype observed. This correlates temporally with the reported cognitive deficits in these mice and the electrophysiological changes observed. However, one caveat is that the control mice were of a mixed background; to improve these experiments they would need to be repeated with pure C57BL/6 mice as a control and with a larger number of mice. However, the biochemical and electrophysiological differences in the TASTPM mice at 6 months show that the development of disease features occurs much earlier in this mouse model compared to the 3xTg mice. There are several possible reasons for this: differences in background strain, the method of transgene integration and generation of the model, and genetic drift in the 3xTg colony. Alternatively tau expression may have a protective effect when combined with APP and PS1 mutations, although there is little other evidence for this. Therefore, the TASTPM mice appear a more practical model for the study of certain aspects of AD. However, they are not useful for the study of mechanisms related to tangle pathology. The TASTPM mouse does develop minor changes in the phosphorylation of tau, but it is not clear whether the pattern of phosphorylation is that similar to that observed in human AD. It is likely that there are multiple biochemical changes present in each transgenic model and further work is required to understand which of these is most important in the progression of AD.

#### **4.3.6: AD related protein expression and phosphorylation in different brain regions of TASTPM mice**

Similar to the 3xTg mouse, the TASTPM mouse expresses the transgenes under the Thy-1 promoter, so as was expected the cerebellum expressed relatively low levels of APP even in 6 month old male mice. The expression pattern was similar to that observed in the 3xTg mice, with levels lowest in the cerebellum and highest in the cortex. In the TASTPM mouse, amyloid deposition initiates in the cortex (Howlett *et al.*, 2004) so it is not surprising that this region shows the highest levels of APP. In contrast to 3xTg and control mice, there is a significantly elevated level of total tau in the cerebellum compared with the other brain regions; there is also a different pattern of phosphorylation in these mice, with the highest phosphorylation at the 396 epitope in the cortex and hippocampus, and the 404 epitope in the cortex. This shows that there is altered phosphorylation at these epitopes which may suggest that the levels of APP or APP processing is higher in these brain regions in the TASTPM compared to 3xTg, but this was not assessed. Similarly, there is a higher level of phosphorylation of CRMP2 at the 509/514 and 522 sites in the hippocampus and cortex compared to cerebellum, despite higher total CRMP2 in the cerebellum.

#### **4.3.7: Effects of kynurenic acid**

In Chapter 3 I demonstrated that hippocampal slice viability was markedly improved by incubation with 1mM kynurenic acid, as observed by an increased probability of obtaining an fEPSP and an increase in the maximum fEPSP amplitude in both aged 3xTg and TASTPM mice. Identifying molecular

processes associated with the electrophysiological deficits that are prevented by kynurenic acid would give clues to the underlying cause of the deficit.

A number of signalling pathways have been implicated in glutamate-induced excitotoxicity, for example the mitogen-activated protein kinase cascade (MAPK cascade) which is one of the most important signalling pathways within the cell. In neurons,  $\text{Ca}^{2+}$  influx through the NMDA receptor or voltage-dependent  $\text{Ca}^{2+}$  channels leads to the sequential activation of the proteins Ras, Raf, MAPK/ERK kinase (MEK), and finally MAPK. This is followed by the activation of multiple cytoplasmic and nuclear targets including other kinases and transcription factors (Thomas and Huganir, 2004). Pharmacological inhibitor studies have shown that MAPK is involved in the induction of LTP in the hippocampus (English and Sweatt, 1997). In addition, there is a transient increase in the phosphorylation of MAPK at the activation sites (Thr 202/Tyr 204) in slices maintained *in vitro* in the first hour following slicing (Ho *et al.*, 2004). However, no differences are observed in our colony of control or 3xTg mice in either total MAPK or Thr 202/Tyr 204 phosphorylation between slices incubated in normal aCSF and 1mM kynurenic acid.

The PI3K (phosphoinositide 3-kinase)/PKB (protein kinase B) cascade is also an important signalling pathway which regulates neuronal survival and aspects of cellular metabolism. The generation of phosphoinositides such as PIP3 by the enzyme PI3K results in the localisation of PKB to the membrane, where it is phosphorylated and activated by another kinase, PDK-1. This results in the activation of downstream signalling pathways, including the regulation of apoptotic proteins (Brunet *et al.*, 2001). Although this pathway is usually

activated by trophic factors, stimulation of the NMDA receptor leads to a  $\text{Ca}^{2+}$ -dependent phosphorylation and activation of PKB (Perkinton *et al.*, 2002). However, there is no difference in either total levels of PKB or activated PKB (phosphorylated at the Ser 473 site) in slices treated with 1mM kynurenic acid.

GSK3 $\beta$  is activated downstream of the PI3K/PKB pathway and has a number of diverse actions. It has been linked to neuronal survival following glutamate-induced excitotoxicity, with activation resulting in neuronal death (Liang and Chuang, 2007). However, the expression of GSK3 $\beta$  and its phosphorylation at the activation site Ser 9 was not affected by kynurenic acid treatment of the slices, and not different between control and 3xTg tissue.

As well as phosphorylation by GSK3, CRMP2 can be cleaved by neuronal calpains, and this modification is one of the main features observed in neurons surviving NMDA toxicity (Bretin *et al.*, 2006). However, I found no differences in the phosphorylation or cleavage of CRMP2 following treatment with kynurenic acid in 3xTg mice or control.

#### **4.3.7.1: Technical aspects**

Although the data obtained in this study was negative there are a number of procedures that could be optimised or altered that may improve the chances of finding the molecules responsible for the electrophysiological deficits observed. Firstly there is a high degree of variation between individual slices when probing for expression and modification of these proteins (especially tau). I would therefore recommend much larger sample sizes for each group when attempting this type of experiment. Unfortunately due to time and cohort numbers I was not

able to generate these sample sizes to give greater confidence in the data. In addition it should be noted that slices were incubated for one hour at room temperature before being snap frozen for analysis. Alterations in protein phosphorylation have been reported up to six hours after slicing (Taubenfeld *et al.*, 2002) and so it may be worthwhile to obtain slices from several time points to investigate any delayed biochemical changes. However, my electrophysiological measurements were obtained in hippocampal slices maintained from one hour up to eight hours *in vitro*, therefore the changes responsible for the electrophysiological differences should be apparent in the timeframe studied. Thirdly, the slices which were used for biochemical analysis were maintained at room temperature while slices used for electrophysiological recordings were subsequently placed in a heated bath at approximately 32°C; previous work in our lab has shown that the phosphorylation of some proteins such as tau can be temperature-dependent (Ritchie Williamson, personal communication). Another limitation is that the recordings of neuronal function were made solely from the hippocampus while the whole slice was used for biochemical analysis, which included the full hippocampus and an area of cortex. This means that any region-specific differences might not be apparent in a whole slice lysate. The CA1 pyramidal neurons of the hippocampus are particularly susceptible to the effects of cellular stressors such as ischemia (Taubenfeld *et al.*, 2002) and so it is possible that a degree of neuronal dysfunction occurred in this population which was not observed in other cellular types. An alternative approach would be to employ microscopy to observe the morphology of the neurons within the hippocampus and assess single cell biochemical parameters

including neuronal death. However this also comes with limitations, in particular the semi quantitative nature and quality of antibodies.

Finally, I have focused on specific candidate proteins based on current knowledge of signalling pathways and disease pathology. The key proteins in these neuronal changes in response to APP and tau overexpression may be unrelated to the biochemical pathways I studied. Other enzymes such as calmodulin-dependent kinase II (CaMKII) and Src family kinases, which can modulate NMDA receptor function, are transiently activated in hippocampal slices (Ho *et al.*, 2004) along with the induction of multiple transcription factors which could mediate cellular survival (Taubenfeld *et al.*, 2002). It would be interesting to know the levels of glutamate receptor subunits in case there are any alterations in receptor expression; this was attempted but was not successful due to the poor quality of Western blots with the specific antibodies available. Similarly, there might be alterations in other proteins associated with glutamate signalling such as amino-acid transporters. Therefore, further work is needed to elucidate the mechanisms by which kynurenic acid treatment protects neurons against the cellular stresses associated with the slicing process specifically in the AD model tissue.

## **Chapter 5**

# **Behaviour**

## 5.1: Introduction

3xTg mice show behavioural alterations such as alterations in circadian rhythm, locomotor activity and exploratory behaviour prior to 6 months of age, before the development of significant plaque pathology (see Chapter 1.4.5). In addition, cognitive deficits have been reported in the 3xTg mouse model from the age of 4 months, when impairment is seen in long-term spatial learning in the MWM, and deficits in short-term memory are observed at 6 months (Billings *et al.*, 2005).

This chapter aims to characterise aspects of the behavioural and cognitive phenotype in 3xTg mice. These experiments used male mice only to avoid the complications of the oestrous cycle on mouse behaviour. Initially, 4 month old 3xTg mice were placed in an activity box for 15 minutes on four consecutive days to observe locomotor and exploratory activity. When the mice reached 6 months old, an age at which cognitive deficits are reported to be apparent, they were subsequently tested in a rewarded alternation T-maze task. This is a spatial learning task which measures aspects of hippocampal function and has not previously been reported in 3xTg mice. Initially, mice were tested without a delay between the phases of each trial, with a time delay added later to increase the difficulty of the task.

In summary, the first section of this chapter describes the use of the activity box to characterise locomotor activity, while the second section reports the results of the rewarded alternation T-maze task used as a test of cognitive function in the 3xTg mice.

## 5.2: Results

### 5.2.1: Activity box in 4 month 3xTg males

4 month 3xTg and control male mice were tested in an activity box, which consisted of a Perspex box attached to an activity monitor which used infrared beams to measure the movements of each mouse (see Chapter 2.2.3). Measures recorded were slow and fast mobile counts, which are a measure of horizontal exploratory activity, slow and fast rearing counts, which are a measure of vertical activity, and total mobile time.

#### 5.2.1.1: Mobile counts

Mobile counts were recorded from the number of horizontal beam breaks and divided into fast mobile counts (Fig. 5.1A) and slow mobile counts (Fig. 5.1B). Main effects analysis of the slow mobile counts shows a significant effect of strain ( $F_{(1,20)} = 5.3$ ,  $p < 0.05$ , repeated measures ANOVA), day ( $F_{(3,60)} = 3.2$ ,  $p < 0.05$ , repeated measures ANOVA), and time ( $F_{(2,40)} = 3.2$ ,  $p < 0.05$ , repeated measures ANOVA), with the interaction between these factors also significant (strain x day x subtrial  $F_{(6,120)} = 3.8$ ,  $p < 0.05$ , repeated measures ANOVA). Main effects analysis of the fast mobile counts shows a significant effect of strain ( $F_{(1,20)} = 7.8$ ,  $p < 0.05$ , repeated measures ANOVA), day ( $F_{(3,60)} = 4.2$ ,  $p < 0.05$ , repeated measures ANOVA), and time ( $F_{(2,40)} = 117.3$ ,  $p < 0.05$ , repeated measures ANOVA), with the interaction between these factors also significant

(strain x day x subtrial  $F_{(6,120)} = 6.3$ ,  $p < 0.05$ , repeated measures ANOVA). This shows that there is a difference in activity between the control and 3xTg mice in this task.

The significant effect of time suggests that habituation occurs to the novel environment in both strains of mice within each individual trial. However, control mice appear to show inter-trial habituation which is absent in the 3xTg mice; this is particularly noticeable in the first five minutes of each trial. This can be confirmed statistically, as for the slow mobile counts there is a significant interaction between the first time bin and the trial day in control mice (day x subtrial  $F_{(3,30)} = 7.1$ ,  $p < 0.05$ , repeated measures ANOVA) while in the 3xTg mice there is no significant difference (day x subtrial  $F_{(3,30)} = 8.5$ ,  $p > 0.05$ , repeated measures ANOVA). Similarly, in the fast mobile counts there is a significant interaction between the first time bin and the trial day in control mice (day x subtrial  $F_{(3,30)} = 6.3$ ,  $p < 0.05$ , repeated measures ANOVA) while in the 3xTg mice there is no significant difference (day x subtrial  $F_{(3,30)} = 1.2$ ,  $p > 0.05$ , repeated measures ANOVA).

#### **5.2.1.2: Total mobile time**

When total mobile time is calculated (Fig. **5.2**), main effects analysis of the slow mobile counts shows a significant effect of strain ( $F_{(1,20)} = 6.3$ ,  $p < 0.05$ , repeated measures ANOVA), and time ( $F_{(2,40)} = 124.2$ ,  $p < 0.05$ , repeated measures ANOVA), with the effects of day just failing to reach significance ( $F_{(3,60)} = 2.7$ ,  $p = 0.052$ , repeated measures ANOVA). The interaction between all three factors is significant (strain x day x subtrial  $F_{(6,120)} = 4.1$ ,  $p < 0.05$ , repeated measures

ANOVA) showing that there is a difference between 3xTg and control, with 3xTg mice less active overall in the activity box.

As with the fast and slow mobile counts, the control mice appear to show inter-trial habituation which is absent in the 3xTg mice. In control mice there is a significant interaction between the first time bin and the trial day (day x subtrial  $F_{(3,30)} = 6.5$ ,  $p < 0.05$ , repeated measures ANOVA) while in the 3xTg mice there is no significant difference (day x subtrial  $F_{(3,30)} = 0.5$ ,  $p > 0.05$ , repeated measures ANOVA).

#### **5.2.1.3: Other measures**

The slow and fast rearing counts were used as a measure of vertical exploratory behaviour, and there is no difference observed at any time point between 3xTg and control mice in this measure ( $p > 0.05$ , repeated measures ANOVA).

#### **5.2.1.4: Summary**

When performance of 4 month 3xTg male mice is measured in the activity box, the 3xTg mice show a decrease in the mobile counts and total mobile time calculated. This shows that there is a reduction in exploratory activity in 3xTg mice compared to control and this is particularly apparent during the first five minutes of each trial.

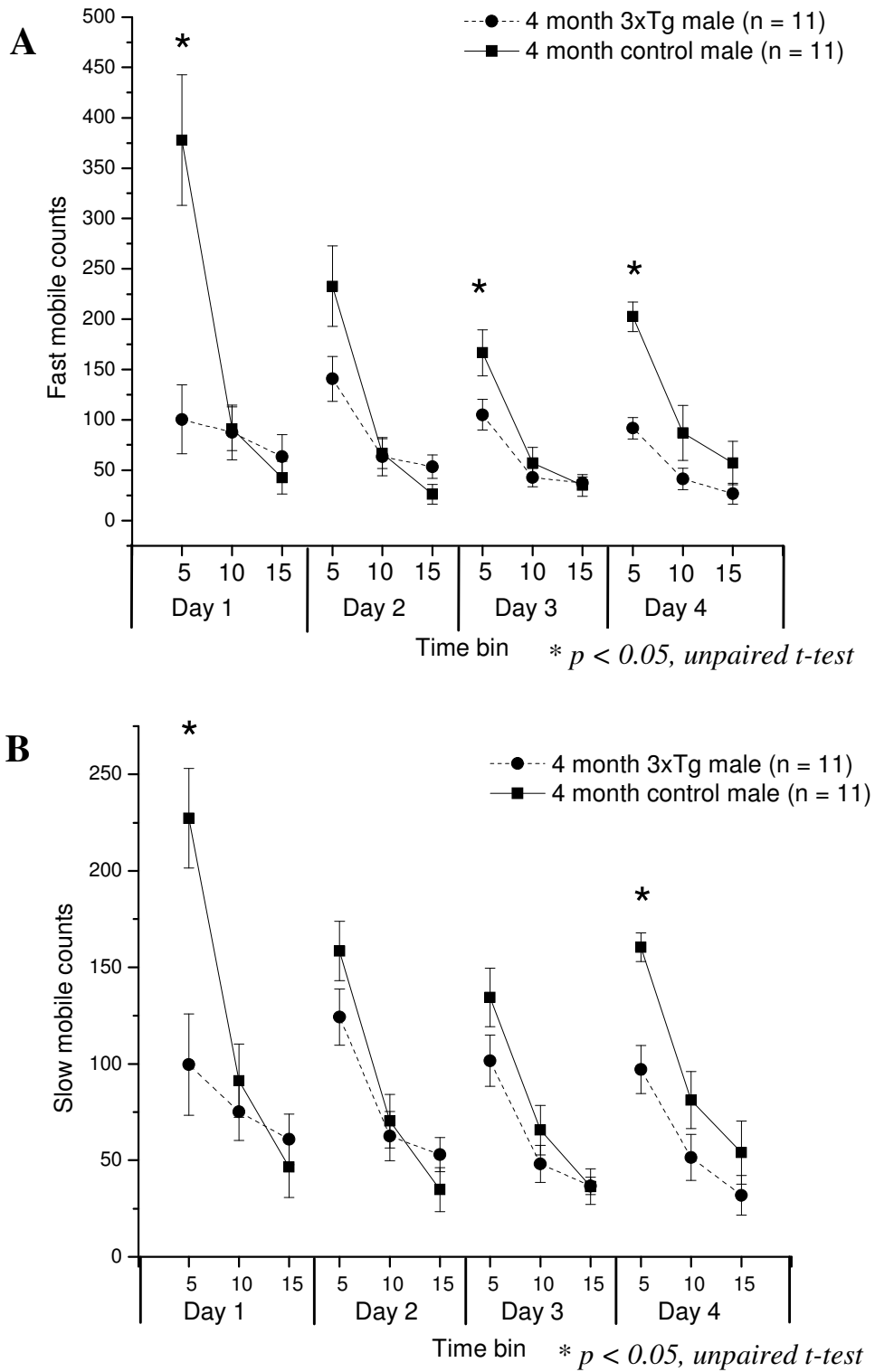


**Figure 5.1: Fast and slow mobile counts measured in the activity box.** Mean counts for each 5 minute time bin over four consecutive days are shown for fast mobile (A) and slow mobile (B) counts in 4 month 3xTg and control mice.

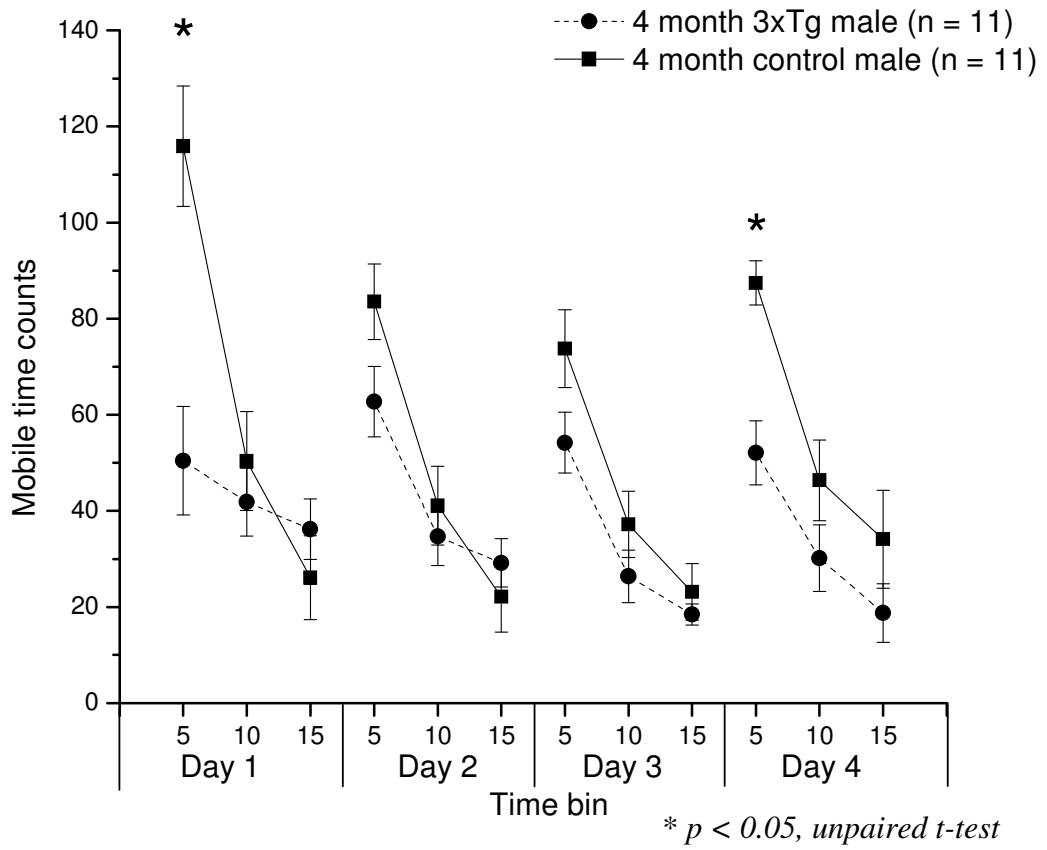


**Figure 5.2: Total mobile counts measured in the activity box.** Mean counts for each 5 minute time bin over four consecutive days are shown for the total mobile counts in 4 month 3xTg and control mice.

## 5.2.2: T-maze performance in 6 month 3xTg male mice

6 month 3xTg and control mice were trained in a rewarded alternation T-maze task (see Chapter 2.2.3) and the mean percentage of correct entries was calculated for each group for each day of the trial. In 3xTg mice, the percentage of correct entries remains relatively stable over all days; this is similar to the control mice although the percentage correct in the control group is on average slightly higher (Fig. 5.3A). As there was no significant difference between the individual days ( $p > 0.05$ , repeated measures ANOVA), the data from all nine trials was pooled together. Overall, the mean percentage correct in the 3xTg mice is  $74.2 \pm 1.2\%$  while in the control it is  $80.6 \pm 2.2\%$  (Fig. 5.4) There is a small but statistically significant reduction in performance ( $p < 0.05$ , unpaired t-test) in the 3xTg mice compared with the control.

### 5.2.2.1: T-maze results (delay)

Following the initial experiments, further trials were carried out with a delay of either thirty or sixty seconds introduced between the forced stage and the choice stage. This makes the task more difficult and was intended to make any cognitive deficits in the 3xTg mice more apparent. A longer 120 second delay was also attempted, but the mice were unable to perform above chance levels on this task so further trials were not carried out with this time delay. Due to similar performance of the control and 3xTg mice on the delayed T-maze task only six trials were carried out.

There is no difference between the performance of 3xTg and control at either delay time on any of the six trials (Fig. 5.3B). When the overall performance is

measured, with a thirty second delay the percentage correct for 3xTg mice is  $79.8 \pm 4.2\%$  while for the control mice it is  $78.2 \pm 3.3\%$ . With a sixty second delay, the percentage correct for 3xTg mice is  $75.5 \pm 4.4\%$  while for the control mice it is  $67.8 \pm 4.8\%$  (Fig 5.4). The sixty second delay increases the difficulty of the task and the performance of the control mice is significantly lower ( $p < 0.05$ , paired t-test) while that of the 3xTg mice remains stable. There is however no difference in performance between the 3xTg and control mice at either a thirty or sixty second delay.

#### **5.2.2.2: Summary**

There is a minor reduction in performance in the no-delay T-maze task by the 3xTg mice at 6 months but overall the marked cognitive deficits expected at this age are not observed. This is in agreement with the lack of electrophysiological and biochemical phenotype at this age.

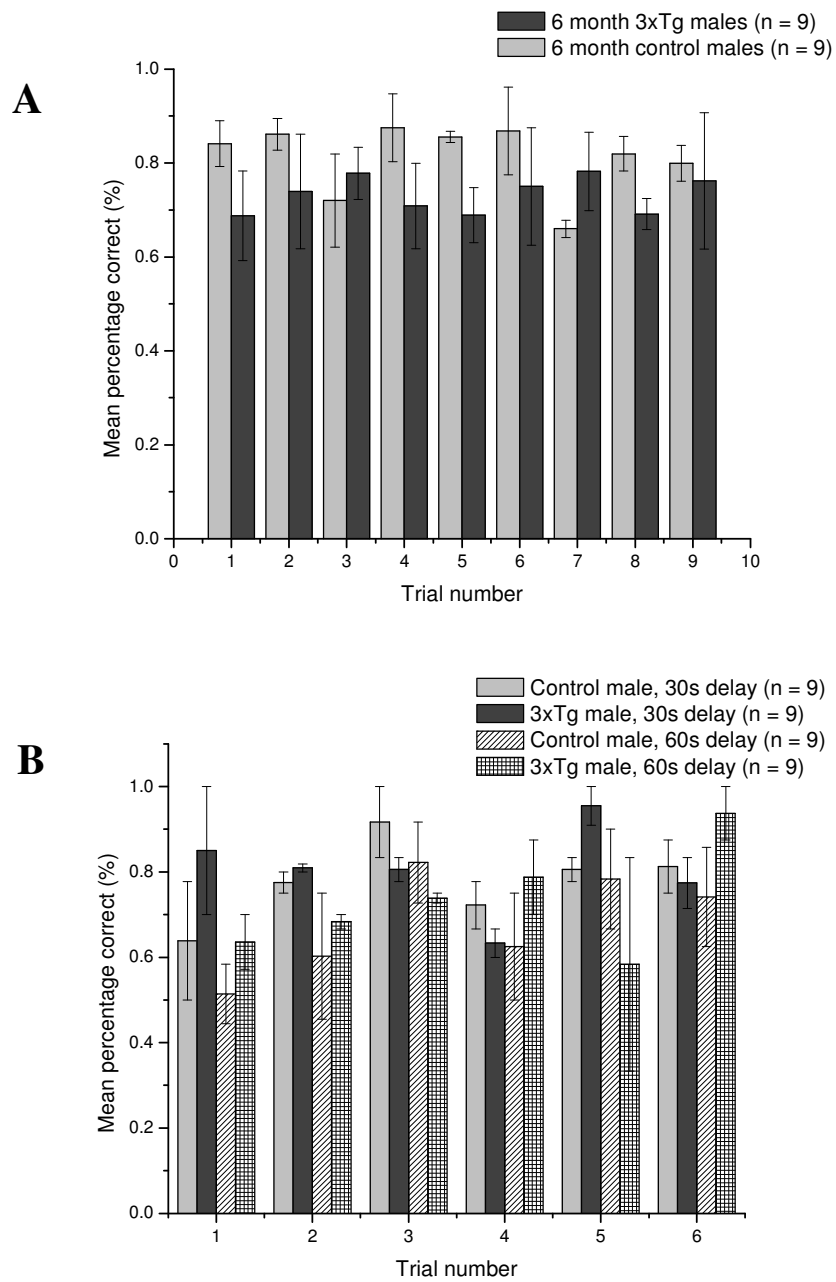


**Figure 5.3: Percentage of correct entries in 3xTg and control.** The mean percentage correct for each group over nine consecutive days is shown in **A**. The mean percentage correct when a delay of thirty seconds or sixty seconds is added for six consecutive days is shown in **B**.

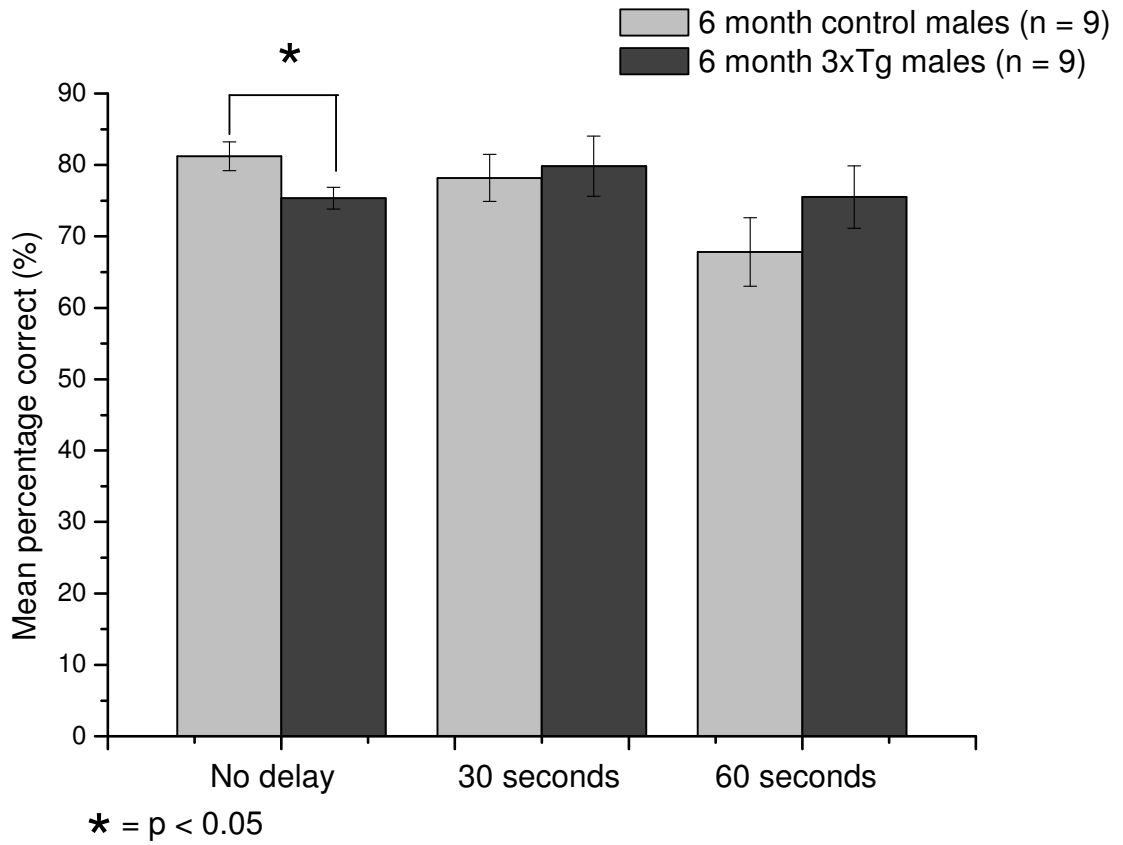


**Figure 5.4: Mean percentage of correct entries for all trials.** The graph shows the percentage correct when all the days of the trial are pooled together for 3xTg and control, with no delay, a thirty second delay or a sixty second delay.

## 5.3: Discussion

In male 3xTg mice, the activity box was used to measure exploratory and locomotor activity, while the T-maze test was used to test cognitive function. Mice were tested in the activity box at 4 months and trained in the T-maze task at 6 months, as this was an age when intraneuronal A $\beta$  was expected to be present based on previous reports (Oddo *et al.*, 2003). Previous studies have also shown an impairment in hippocampal-dependent cognitive performance from the age of 4 months, which is thought to be linked to A $\beta$  accumulation (Billings *et al.*, 2005).

### 5.3.1: Activity box

The activity box was used as a measure of spontaneous locomotor activity in 4 month old 3xTg and control male mice. Mobile counts were used as a measure of horizontal exploratory activity and horizontal counts as a measure of vertical activity. It was found that the 3xTg mice were markedly less mobile in the initial five minutes after they are placed in the box, and this was most pronounced on the first of the four trials, showing that the 3xTg mice remain stationary for prolonged periods of time when first placed in the box. The 3xTg mice also show lower inter-trial habituation than the control mice, which showed a marked reduction in the number of mobile counts over the first three days. However, there was no difference in the number of rearing counts between the two groups, showing that vertical exploratory activity is similar.

Several other groups have carried out behavioural tests on the 3xTg mice at various ages using the activity box and larger open field, with similar findings. In young (2.5 month old) male 3xTg mice, there was no difference in activity in the two tests, showing that there are no locomotor changes present prior to the development of pathology. However, reduced activity was reported in 6 month male and 12 month female 3xTg mice, with the presence of 'strong initial freezing behaviour' in the open field test in the male mice (Gimenez-Llort *et al.*, 2007). Similarly, the behaviour of 8 month 3xTg mice in the open field was characterised by limited exploratory behaviour and freezing (Sterniczuk *et al.*, 2010a). Finally, in a ten minute activity box study, 3xTg mice showed both reduced horizontal and vertical activity with frequent short episodes of low activity lasting from 5-30 seconds (Arsenault *et al.*, 2011). Importantly, these mice do not show any locomotor or co-ordination difficulties which could affect their behaviour (Sterniczuk *et al.*, 2010a). This was also observed in our colony of 3xTg mice which could successfully complete a rotarod task (data not shown) and showed no noticeable differences in locomotion. These data are not included in the thesis as both groups of mice showed a high level of passive rotations (clinging onto and rotating with the rod) which prevented analysis of the results.

It is clear that the phenotype of the 3xTg involves a reduction in exploratory behaviour and increased freezing which is linked to the development of pathological features in these mice. However, the motivating factor behind this behaviour is unclear. One study suggests it represents a higher level of anxiety and reduced fear threshold, another increased emotionality, and the other suggests the behaviour is 'seizure-like', although no evidence for the presence of seizures has been noted in the 3xTg mice (Gimenez-Llort *et al.*, 2007, Sterniczuk

*et al.*, 2010a, Arsenault *et al.*, 2011). It has been shown that freezing responses of 3xTg mice in a brightly lit chamber is significantly higher than control and can be reduced by the administration of the anxiolytic benzodiazepine diazepam (Espana *et al.*, 2010). This suggests that the freezing response may partially be an anxiety-linked behaviour. The presence of increased urination and defecation, an index of emotional behaviour, was also reported by Gimenez-Llort *et al.* in their study; this was also observed in our colony of 3xTg mice. However, in the elevated plus maze test, which is classically used as a measure of anxiety, no difference was observed between 3xTg and control by two separate groups (Gimenez-Llort *et al.*, 2007, Sterniczuk *et al.*, 2010a). In addition, it has been reported that there is no increase in plasma corticosterone levels, which can be used as a biochemical marker of the response to stressful tasks, in male 3xTg mice following testing in the MWM (Clinton *et al.*, 2007). This suggests that the reduction in exploratory behaviour in the 3xTg mouse is a complex response to a novel environment which is not yet fully understood. In addition, a comprehensive study of both male and female mice at similar ages has not been carried out and would be required to fully characterise this type of behaviour. In our colony of 3xTg mice, only male mice were used and this was at 4 months of age, early in the time course of A $\beta$  deposition. As the evidence suggests that the development of pathology is occurring more slowly in our colony of 3xTg mice, the behavioural changes are likely due to age-independent effects of transgene overexpression or very early biochemical alterations. Emotional behaviour in the 3xTg mouse has been linked to the amygdala, where intraneuronal A $\beta$  has been shown to accumulate at 6 months, earlier than in the cortex or the hippocampus (Espana *et al.*, 2010). As biochemical changes in the amygdala were not studied

in our colony of 3xTg mice, the possibility of a link between A $\beta$  accumulation in this region of the brain and the observed behaviour in the activity box cannot be ruled out. Further work would be required using a range of tests to examine emotional behaviour in 3xTg mice and how this may relate to behavioural disturbances which are observed in AD.

### **5.3.2: T-maze performance**

At 6 months, both 3xTg and control mice were tested in a T-maze task to observe any hippocampal-dependent cognitive deficits that might be apparent at this age. Initially, mice were habituated to the apparatus by being placed inside with their littermates. It was observed at this stage and in the initial stages of testing that many of the 3xTg mice showed reduced activity and a reluctance to explore, which could be linked to the low levels of activity observed in the activity box. For this reason, food restriction was required to encourage the mice to carry out the task. Our colony of 3xTg mice showed a significantly higher body weight than control mice, which is thought to be due to increased appetite and food intake (Knight *et al.*, 2010). In this respect, motivation to obtain a food reward might be different between the 3xTg mice and control. For this reason, food restriction was carried out proportionally to body weight to negate any differences in food-motivated behaviour.

In the no-delay T-maze task, which was carried out for nine consecutive days, the mice show the ability to complete the task from the first trial, reaching rates of 70-80% correct choices. No improvement or decline was observed throughout subsequent trials. On nearly all days, there was a trend for the performance of the

3xTg mice being slightly lower than the control mice, suggesting that there may be a degree of cognitive decline in these mice. This results in a small but significant reduction of the percentage correct from 81% in the control mice to 74% in the 3xTg mice. However, there was marked variation between individual mice in both the control and 3xTg groups, with some making consistently correct choices and others multiple errors. This shows the importance of using a large sample size of mice; an increased number of mice could not be used in this study due to the time constraints of the task, but would be a way to improve experiments by reducing the effects of individual variability. In addition, it would be interesting to measure biochemical changes in individual mice to see if there was any correlation between performance in the task and the levels of AD-associated proteins.

Following this task, a delay of 30 or 60 seconds was introduced in an attempt to make the trials more difficult, and this was carried out for six consecutive days. However, in this task there was no significant difference between the performance of control and 3xTg mice at either delay time on any of the trials. Overall, the percentage correct for the 30 second delay is slightly greater than the 60 second delay, reflecting the additional difficulty produced by increasing the time between trials. Unfortunately, due to the way the study was carried out there is no coexisting data for these trials for responses without a delay. It would be interesting to observe if there was still a difference in this task between the two groups or if the 3xTg mice had shown an improvement. As the two sets of experiments were carried out back-to-back on the same cohort of mice, it is possible that the average performance of the 3xTg mice would have increased. Overall, the results on the harder 30 and 60 second delay trials show that the

3xTg mice are able to carry out this task without difficulty. This contrasts with previous work in which these mice show marked cognitive deficits at the same age (Billings *et al.*, 2005).

Surprisingly, relatively few cognitive tests have been carried out in 3xTg mice. Deficits have been observed in the MWM at 6 months (Billings *et al.*, 2005) but enhanced performance in a contextual fear conditioning task, which depends upon both amygdala and hippocampus, is observed at the same age (España *et al.*, 2010). One study using an object recognition task did not report deficits in performance in the 3xTg mice until the age of 9 months (Clinton *et al.*, 2007); such a task requires hippocampal functioning but may also involve some cortical processing (Broadbent *et al.*, 2004). It is therefore likely that the onset of cognitive deficits may vary depending on the specific task used.

The rewarded alternation T-maze is also thought to be a task which is primarily hippocampal-dependent. Deficits in T-maze performance have previously been correlated to impairments in LTP in the CA1 and DG regions in APP<sub>Swe</sub> mice (Chapman *et al.*, 1999b). However, at this age there are no electrophysiological changes apparent in our colony of 3xTg mice (see Chapter 3). The pathological features present in 3xTg mice have also been linked to the onset of behavioural deficits, with A $\beta$  oligomers linked to cognitive performance in the Morris water maze (Billings *et al.*, 2007) and intraneuronal A $\beta$  accumulation in the amygdala thought to contribute to alterations in inhibitory avoidance learning (España *et al.*, 2010). A role has been suggested for both A $\beta$  and tau, as reduction of the levels of both proteins is required to improve cognitive performance in aged 3xTg mice (Oddo *et al.*, 2006b). In our colony of 3xTg mice, there is a lack of marked

biochemical changes in APP or tau at 6 months (see Chapter 4), suggesting that the pathological features are not yet well developed at this age. Overall, the lack of an electrophysiological or biochemical phenotype in these 3xTg mice at 6 months therefore correlates with the behavioural findings which show that hippocampal functioning remains relatively unaffected at this age.

## **Chapter 6**

# **Conclusions and Perspectives**

**Table 6.1: Summary of main findings in 3xTg mice**

Age	Electrophysiology					Biochemistry						Behaviour
	I/O	PPF	Normalised LTP	Non-norm. LTP	Deficits prevented by KA	APP	Tau	P-Tau AT8	P-Tau 396	P-Tau 404	P-CRMP2	
<b>2 months</b>	NC	↓	NC	↑	-	↑	↑	NC	NC	NC	NC	↓ locomotor activity (4 months)
<b>6 months</b>	NC	NC	NC	NC	-	-	-	-	-	-	-	NC in T-maze alternation task (6 months)
<b>12 months</b>	↓	NC	↑ initial	↓	YES	↑	↑	NC	NC	NC	NC	-
<b>17 months</b>	↓	NC	↑ plateau	↓	-	↑	↑	NC	NC	NC	↑ 509/514	-

All data are in comparison with control mice. NC = no change, ↑ = increase, ↓ = decrease, - = not measured.

I/O = input-output, PPF = paired-pulse facilitation, LTP = long-term potentiation, KA = kynurenic acid, P-tau = phosphorylated tau, P-CRMP2 = phosphorylated CRMP2.

**Table 6.2: Summary of main findings in TASTPM mice**

Age	Electrophysiology					Biochemistry					
	I/O	PPF	Normalised LTP	Non-norm. LTP	Deficits prevented by KA	APP	Tau	P-Tau AT8	P-Tau 396	P-Tau 404	P-CRMP2
<b>2 months</b>	NC	↓ 50ms only	NC	NC	-	↑	↑	↓	NC	NC	NC
<b>6 months</b>	Not measured due to marked reduction in fEPSP amplitude				YES	↑	↑	NC	NC	NC	↑

All data are in comparison with control mice. NC = no change, ↑ = increase, ↓ = decrease, - = not measured.

I/O = input-output, PPF = paired-pulse facilitation, LTP = long-term potentiation, KA = kynurenic acid, P-tau = phosphorylated tau, P-CRMP2 = phosphorylated CRMP2.

## Conclusions and perspectives

The work presented here has further characterised the phenotype of the 3xTg and TASTPM mouse models of AD through biochemical, behavioural and electrophysiological studies. This section summarises the key findings of this thesis and the contribution of these to AD research, limitations of these studies and suggestions for alternative approaches or further work.

The major biochemical, behavioural and electrophysiological findings reported for 3xTg mice are summarised in Table **6.1**, and for TASTPM mice in Table **6.2**.

### 6.1: Electrophysiology

I have carried out experiments to study synaptic function, including basal synaptic transmission and LTP, in the 3xTg and TASTPM models. Previous work has shown that the 3xTg mice show an age-dependent reduction in the magnitude of LTP from the age of 6 months (Oddo *et al.*, 2003) while no previous electrophysiological studies of the TASTPM mouse have been published.

In this thesis, I have shown that in our colony of 3xTg mice early alterations in synaptic function occur at the age of 2 months and manifest as an increase in basal synaptic transmission with no change in the magnitude of LTP. The mechanisms underlying this are not known and would require further, more detailed studies, for example the use of voltage clamp techniques to measure the properties of individual neurons. It is possible that the elevation in basal

transmission may represent an increase in the intrinsic excitability of glutamatergic neurons which has previously been reported in this model (Arsenault *et al.*, 2011) or alterations in postsynaptic  $\text{Ca}^{2+}$  regulation associated with the presence of the transgenes (Chakroborty *et al.*, 2009).

I have also shown that, in contrast to the colony of 3xTg mice studied by Oddo *et al.*, alterations in synaptic function are not present in our colony of 3xTg mice until the age of 12 months. This is observed as a marked reduction in the amplitude of the fEPSP suggesting a deficit in basal synaptic transmission. Despite this, LTP can be induced normally up to the age of 17 months although the absolute magnitude of potentiation is reduced due to the smaller fEPSP amplitude. This shows that there are major differences in the phenotype of our colony of 3xTg mice compared with that originally characterised.

Previous studies in APP transgenic mice have shown a similar reduction in the fEPSP amplitude, but this could be reversed by the presence of the glutamate receptor antagonist kynurenic acid within the solution during hippocampal slice preparation (Fitzjohn *et al.*, 2001). I replicated this in 3xTg mice and have shown that treatment with 1mM kynurenic acid during slicing restores fEPSP amplitude to the levels observed in control mice. Importantly, this shows that glutamate-induced excitotoxicity is a major factor influencing slice viability and may have an effect on the results obtained using the hippocampal slice preparation. This has relevance for the wider study of synaptic plasticity in transgenic mouse models, as it highlights the importance of standardising extracellular recording protocols and taking measures to improve neuronal viability within the hippocampal slice.

I have shown that in the TASTPM mouse model, there are no alterations in basal synaptic transmission or LTP at the age of 2 months showing that synaptic function at this age remains normal. However, at 6 months, there is a marked reduction in the amplitude of the fEPSP and the percentage of successful fEPSPs obtained. Similar to the 3xTg mice, this can be completely prevented by incubation with 1mM kynurenic acid during slicing.

These findings suggest that a common feature of mouse models of AD possessing the APP and PS1 transgenes may be an enhanced vulnerability to the high levels of glutamate release associated with the slice preparation process. This increased susceptibility to excitotoxicity may represent the presence of neurons within the hippocampus which are 'primed' to undergo dysfunction under conditions of enhanced cellular stress. The molecular mechanisms underlying this process are not known, but are likely to involve dysfunction of components of the glutamatergic neurotransmitter pathway, for example alterations in glutamate release or uptake by astrocytes, the influence of A $\beta$  oligomers on NMDA receptor function, or the alterations in intracellular Ca<sup>2+</sup> regulation which can occur with the PS1 mutation. Further study of these mechanisms would require the combined use of several different techniques, for example the use of immunofluorescence to observe NMDA receptor numbers and localisation combined with electrophysiological techniques to measure glutamate uptake and release within the synapse or with neuronal Ca<sup>2+</sup> imaging to measure intracellular Ca<sup>2+</sup> transients.

It is not known if the increased susceptibility to excitotoxicity occurs in hippocampal neurons *in vivo* in the 3xTg or TASTPM mice, and this would

require further studies in the intact animal. It would be interesting to observe if the hippocampal neurons of these mice are more susceptible to a variety of other cellular stressors, for example conditions of metabolic or oxidative stress, and if this is a contributory mechanism to neuronal dysfunction in AD.

## **6.2: Biochemistry**

In this thesis I have quantified the expression of several AD-associated proteins associated with the pathological features of AD in order to observe the presence of any biochemical changes which might be associated with my electrophysiological findings in the 3xTg and TASTPM mice.

I have found that in 3xTg mice, although the presence of elevated levels of APP and tau confirmed the presence of the transgenes, there was little age-dependent increase in the levels of these proteins. I did not observe hyperphosphorylation of tau at the AT8, 396 or 404 epitopes which has been reported to occur from the age of 12 months (Oddo *et al.*, 2007) although there was a trend for increased phosphorylation at the age of 17 months. The lack of biochemical changes in our colony of 3xTg mice suggest that there may be a delayed onset of the pathological features associated with the phenotype, although this would require further imaging or immunohistochemical studies to observe plaque and tangle deposition.

I have also studied other cellular proteins such as CRMP2, which may be phosphorylated in the early stages of AD progression and seems to be a feature relatively specific to AD (Williamson *et al* 2011, in press). At 17 months, enhanced phosphorylation of the 509/514 residues (GSK3 sites) was observed.

Although this is later than previously observed in our lab, it did occur prior to other biochemical changes in the 3xTg mice studied and thus may be an early feature of disease progression. Other proteins such as synaptophysin were not altered in this model, suggesting that synaptic loss does not occur; to provide a more sensitive measure of synaptic number this could be confirmed by imaging in these mice to observe the density of dendritic spines.

The relatively minor biochemical changes in our colony of 3xTg mice supports the conclusion of my electrophysiological studies, which suggest the delayed onset of disease-related deficits in our colony (observed as a normal magnitude of LTP at 17 months). Unfortunately, I was unable to observe any molecular changes which might be associated with the enhanced susceptibility to excitotoxicity observed in these mice. Further work would be required to elucidate the biochemical pathways associated with this feature; candidates for further Western blotting or immunohistochemistry experiments include NMDA receptor subunits,  $\alpha$  and  $\beta$ -secretase enzymes, and the excitatory amino acid transporters.

I also carried out similar biochemical studies in the TASTPM mice. In these mice, I found no major alterations in protein levels at 2 months, supporting the finding that synaptic function is normal in these mice at this age. At 6 months, I observed increased phosphorylation at the CRMP2 509/514 residue, which suggests that the early development of biochemical changes occurs more rapidly in this model than in our 3xTg colony. This may explain the earlier onset of the reduction of fEPSP amplitude observed in slices prepared under normal conditions (6 months in TASTPM mice vs. 12 months in 3xTg mice). Unfortunately, I was unable to

characterise the progression of biochemical changes at older ages in these mice due to breeding difficulties and premature mortality; it would be interesting to follow the progression of pathology in these mice as they age and whether this is linked to the development of alterations in basal synaptic transmission or LTP.

### **6.3: Behaviour**

In this thesis I also carried out behavioural experiments on the 3xTg mice, comprising an activity box study and cognitive testing in the rewarded alternation T-maze task. Performance in the T-maze has not previously been reported in these mice but is thought to be hippocampal-dependent, similar to the MWM. I found that in the activity box the 3xTg mice showed a reduced level of activity when compared to control mice, and this is in support of previously reported findings which have shown increased freezing and anxiety-like behaviour in this model. This is independent of the development of pathological features as it was observed at 4 months and shows that these mice have an early behavioural phenotype due to the presence of the transgenes. In cognitive studies of 6 month 3xTg mice, I did not observe any deficits in performance in the T-maze alternation task. This is in agreement with the lack of biochemical changes present in these mice at this age. Based on this knowledge, it would be interesting to carry out cognitive testing in older 3xTg mice, for example at 12 or 17 months, although it would be necessary to use a more complex task capable of detecting early, more subtle cognitive deficits.

#### **6.4: Final conclusions**

The main aims of this thesis were to observe the progression of synaptic, biochemical and behavioural alterations in the 3xTg and TASTPM models of AD. Unfortunately, I did not observe the electrophysiological and cognitive deficits originally reported with the generation of the 3xTg model, and this is supported by the lack of biochemical changes I observed using Western blotting. This suggests that the development of the pathological features is delayed in our colony of 3xTg mice. The most likely reason for the delay is a degree of genetic drift which has occurred in this model over multiple generations when housed in separate locations. To resolve this, the only solution would be to re-derive the mice from the original colony. These findings show the importance of careful characterisation of the development of pathological features in individual colonies of transgenic mice in order to link this with other experimental findings such as electrophysiology studies.

The delayed onset of the phenotype in the 3xTg mice has made it difficult to carry out one of the initial aims of my thesis, which was to observe any early biochemical alterations associated with disease progression. However, in the TASTPM mice the development of a biochemical phenotype occurred more rapidly and one of the early changes observed was the hyperphosphorylation of CRMP2 (also observed in the 3xTg mice at 17 months). This suggests that this feature is an early molecular change associated with APP transgene expression. As it has been suggested that hyperphosphorylation of CRMP2 is an event specific to AD, this could be an important marker of disease progression and

suggests that the activation of protein kinases such as GSK3 is an important early feature of AD development.

Another initial aim of my thesis was to directly compare electrophysiological and biochemical decline in the 3xTg and TASTPM models in order to gain insight into the role of tau in AD pathology, but the dramatic differences observed between different cohorts of 3xTg mice makes this difficult. However, the presence of an enhanced susceptibility to excitotoxicity in both the 3xTg and TASTPM mice does suggest that this feature is independent of the expression of the tau transgene. As the TASTPM mouse develops both electrophysiological and biochemical changes at a relatively early age, it may be a useful model for studying aspects of AD associated with A $\beta$  pathology. It would be interesting to add a mutant tau transgene into this model to establish whether tau mutation has any effect on these features.

One of the major findings of my thesis is the enhanced susceptibility of hippocampal neurons to excitotoxicity which occurs in both the 3xTg and TASTPM mouse models and so may represent a common feature of transgenic mouse models of AD possessing the APP transgene. The molecular mechanisms which underlie this process require further study, but could result in a degree of neuronal dysfunction which, if present in the intact animal, could render hippocampal neurons more susceptible to the effects of cellular stressors and accelerate the progression of AD pathology.

Although transgenic mice such as the 3xTg or TASTPM mice have their limitations and cannot model all aspects of AD they have been critical in increasing our understanding of the disease. I hope that the work presented in this

thesis and the characterisation of the phenotype of these mice can contribute to our knowledge of the molecular mechanisms underlying human AD and subsequently provide a means to confirm whether potential interventions have physiological or behavioural outcomes prior to human studies.

## References

Ables, J. L., Breunig, JJ, Eisch, AJ, and Rakic, P (2011) Not(ch) just development: Notch signalling in the adult brain. *Nat Rev Neurosci* **12**:269-283.

Alford, S., Frenguelli, BG, Schofield, JG, and Collingridge, GL (1993) Characterization of Ca<sup>2+</sup> signals induced in hippocampal CA1 neurones by the synaptic activation of NMDA receptors. *J Physiol* **469**:693-716.

Allinson, T. M., Parkin, ET, Turner, AJ, and Hooper, NM (2003) ADAMs family members as amyloid precursor protein alpha-secretases. *J Neurosci Res* **74**:342-352.

Alonso, A. D., Di, CJ, Li, B, Corbo, CP, Alaniz, ME, Grundke-Iqbal, I et al. (2010) Phosphorylation of tau at Thr212, Thr231, and Ser262 combined causes neurodegeneration. *J Biol Chem* **285**:30851-30860.

Alonso, A. D., Grundke-Iqbal, I, Barra, HS, and Iqbal, K (1997) Abnormal phosphorylation of tau and the mechanism of Alzheimer neurofibrillary degeneration: sequestration of microtubule-associated proteins 1 and 2 and the disassembly of microtubules by the abnormal tau. *Proc Natl Acad Sci U S A* **94**:298-303.

Alonso, Adel C., Mederlyova, A, Novak, M, Grundke-Iqbal, I, and Iqbal, K (2004) Promotion of hyperphosphorylation by frontotemporal dementia tau mutations. *J Biol Chem* **279**:34873-34881.

Altman, R. and Rutledge, JC (2010) The vascular contribution to Alzheimer's disease. *Clin Sci (Lond)* **119**:407-421.

Andra, K., Abramowski, D, Duke, M, Probst, A, Wiederhold, KH, Burki, K et al. (1996) Expression of APP in transgenic mice: a comparison of neuron-specific promoters. *Neurobiol Aging* **17**:183-190.

Antonell, A., Balasa, M, Oliva, R, Llado, A, Bosch, B, Fabregat, N et al. (2011) A novel PSEN1 gene mutation (L235R) associated with familial early-onset Alzheimer's disease. *Neurosci Lett* **496**:40-42.

Arsenault, D., Julien, C, Tremblay, C, and Calon, F (2011) DHA Improves Cognition and Prevents Dysfunction of Entorhinal Cortex Neurons in 3xTg-AD Mice. *PLoS ONE* **6**:e17397

Auffret, A., Gautheron, V, Mattson, MP, Mariani, J, and Rovira, C (2010) Progressive age-related impairment of the late long-term potentiation in Alzheimer's disease presenilin-1 mutant knock-in mice. *J Alzheimers Dis* **19**:1021-1033.

Basi, G. S., Hemphill, S, Brigham, EF, Liao, A, Aubele, DL, Baker, J et al. (2010) Amyloid precursor protein selective gamma-secretase inhibitors for treatment of Alzheimer's disease. *Alzheimers Res Ther* **2**:36

- Basun, H., Bogdanovic, N, Ingelsson, M, Almkvist, O, Naslund, J, Axelman, K et al. (2008) Clinical and neuropathological features of the arctic APP gene mutation causing early-onset Alzheimer disease. *Arch Neurol* **65**:499-505.
- Berezovska, O., Lleo, A, Herl, LD, Frosch, MP, Stern, EA, Bacskai, BJ et al. (2005) Familial Alzheimer's disease presenilin 1 mutations cause alterations in the conformation of presenilin and interactions with amyloid precursor protein. *J Neurosci* **25**:3009-3017.
- Bertram, L. and Tanzi, RE (2004) The current status of Alzheimer's disease genetics: what do we tell the patients? *Pharmacol Res* **50**:385-396.
- Billings, L. M., Green, KN, McGaugh, JL, and LaFerla, FM (2007) Learning decreases A beta\*56 and tau pathology and ameliorates behavioral decline in 3xTg-AD mice. *J Neurosci* **27**:751-761.
- Billings, L. M., Oddo, S, Green, KN, McGaugh, JL, and LaFerla, FM (2005) Intraneuronal Aβ causes the onset of early Alzheimer's disease-related cognitive deficits in transgenic mice. *Neuron* **45**:675-688.
- Bittner, T., Fuhrmann, M, Burgold, S, Ochs, SM, Hoffmann, N, Mitteregger, G et al. (2010) Multiple events lead to dendritic spine loss in triple transgenic Alzheimer's disease mice. *PLoS ONE* **5**:e15477
- Bliss, T. V. and Lomo, T (1973) Long-lasting potentiation of synaptic transmission in the dentate area of the anaesthetized rabbit following stimulation of the perforant path. *J Physiol* **232**:331-356.
- Boekhoorn, K., Terwel, D, Biemans, B, Borghgraef, P, Wiegert, O, Ramakers, GJ et al. (2006) Improved long-term potentiation and memory in young tau-P301L transgenic mice before onset of hyperphosphorylation and tauopathy. *J Neurosci* **26**:3514-3523.
- Bordji, K., Becerril-Ortega, J, Nicole, O, and Buisson, A (2010) Activation of extrasynaptic, but not synaptic, NMDA receptors modifies amyloid precursor protein expression pattern and increases amyloid-ss production. *J Neurosci* **30**:15927-15942.
- Braak, H. and Braak, E (1991) Neuropathological staging of Alzheimer-related changes. *Acta Neuropathol* **82**:239-259.
- Bradford, M. M. (1976) A rapid and sensitive method for the quantitation of microgram quantities of protein utilizing the principle of protein-dye binding. *Anal Biochem* **72**:248-254.
- Breen, K. C., Bruce, M, and Anderton, BH (1991) Beta amyloid precursor protein mediates neuronal cell-cell and cell-surface adhesion. *J Neurosci Res* **28**:90-100.
- Bretin, S., Rogemond, V, Marin, P, Maus, M, Torrens, Y, Honnorat, J et al. (2006) Calpain product of WT-CRMP2 reduces the amount of surface NR2B NMDA receptor subunit. *J Neurochem* **98**:1252-1265.

- Broadbent, N. J., Squire, LR, and Clark, RE (2004) Spatial memory, recognition memory, and the hippocampus. *Proc Natl Acad Sci U S A* **101**:14515-14520.
- Brooks, S. P., Pask, T, Jones, L, and Dunnett, SB (2005) Behavioural profiles of inbred mouse strains used as transgenic backgrounds. II: cognitive tests. *Genes Brain Behav* **4**:307-317.
- Brown, J. T., Richardson, JC, Collingridge, GL, Randall, AD, and Davies, CH (2005) Synaptic transmission and synchronous activity is disrupted in hippocampal slices taken from aged TAS10 mice. *Hippocampus* **15**:110-117.
- Brunet, A., Datta, SR, and Greenberg, ME (2001) Transcription-dependent and -independent control of neuronal survival by the PI3K-Akt signaling pathway. *Curr Opin Neurobiol* **11**:297-305.
- Burwell, R. D. and Amaral, DG (1998) Cortical afferents of the perirhinal, postrhinal, and entorhinal cortices of the rat. *J Comp Neurol* **398**:179-205.
- Cairns, N. J., Bigio, EH, Mackenzie, IR, Neumann, M, Lee, VM, Hatanpaa, KJ et al. (2007) Neuropathologic diagnostic and nosologic criteria for frontotemporal lobar degeneration: consensus of the Consortium for Frontotemporal Lobar Degeneration. *Acta Neuropathol* **114**:5-22.
- Carroll, J. C., Rosario, ER, Kreimer, S, Villamagna, A, Gentschein, E, Stanczyk, FZ et al. (2010) Sex differences in beta-amyloid accumulation in 3xTg-AD mice: role of neonatal sex steroid hormone exposure. *Brain Res* **1366**:233-245.
- Causevic, M., Farooq, U, Lovestone, S, and Killick, R (2010) beta-Amyloid precursor protein and tau protein levels are differently regulated in human cerebellum compared to brain regions vulnerable to Alzheimer's type neurodegeneration. *Neurosci Lett* **485**:162-166.
- Chakroborty, S., Goussakov, I, Miller, MB, and Stutzmann, GE (2009) Deviant ryanodine receptor-mediated calcium release resets synaptic homeostasis in presymptomatic 3xTg-AD mice. *J Neurosci* **29**:9458-9470.
- Chapman, P. F., White, GL, Jones, MW, Cooper-Blacketer, D, Marshall, VJ, Irizarry, M et al. (1999a) Impaired synaptic plasticity and learning in aged amyloid precursor protein transgenic mice. *Nat Neurosci* **2**:271-276.
- Chapman, P. F., White, GL, Jones, MW, Cooper-Blacketer, D, Marshall, VJ, Irizarry, M et al. (1999b) Impaired synaptic plasticity and learning in aged amyloid precursor protein transgenic mice. *Nat Neurosci* **2**:271-276.
- Chen, G., Chen, KS, Knox, J, Inglis, J, Bernard, A, Martin, SJ et al. (2000) A learning deficit related to age and beta-amyloid plaques in a mouse model of Alzheimer's disease. *Nature* **408**:975-979.
- Chishti, M. A., Yang, DS, Janus, C, Phinney, AL, Horne, P, Pearson, J et al. (2001) Early-onset amyloid deposition and cognitive deficits in transgenic mice expressing a double mutant form of amyloid precursor protein 695. *J Biol Chem* **276**:21562-21570.

Clinton, L. K., Billings, LM, Green, KN, Caccamo, A, Ngo, J, Oddo, S et al. (2007) Age-dependent sexual dimorphism in cognition and stress response in the 3xTg-AD mice. *Neurobiol Dis* **28**:76-82.

Coesmans, M., Weber, JT, De Zeeuw, CI, and Hansel, C (2004) Bidirectional parallel fiber plasticity in the cerebellum under climbing fiber control. *Neuron* **44**:691-700.

Cole, A. R., Astell, A, Green, C, and Sutherland, C (2007a) Molecular connexions between dementia and diabetes. *Neurosci Biobehav Rev* **31**:1046-1063.

Cole, A. R., Noble, W, van Aalten, L, Plattner, F, Meimaridou, R, Hogan, D et al. (2007b) Collapsin response mediator protein-2 hyperphosphorylation is an early event in Alzheimer's disease progression. *J Neurochem* **103**:1132-1144.

Cole, A. R., Soutar, MP, Rembutsu, M, van Aalten, L, Hastie, CJ, Mclauchlan, H et al. (2008) Relative resistance of Cdk5-phosphorylated CRMP2 to dephosphorylation. *J Biol Chem* **283**:18227-18237.

Cole, S. L. and Vassar, R (2007) The Alzheimer's disease beta-secretase enzyme, BACE1. *Mol Neurodegener* **2**:22

Collingridge, G. L., Kehl, SJ, and McLennan, H (1983) Excitatory amino acids in synaptic transmission in the Schaffer collateral-commissural pathway of the rat hippocampus. *J Physiol* **334**:33-46.

Colton, C. A., Wilcock, DM, Wink, DA, Davis, J, Van Nostrand, WE, and Vitek, MP (2008) The effects of NOS2 gene deletion on mice expressing mutated human AbetaPP. *J Alzheimers Dis* **15**:571-587.

Corder, E. H., Saunders, AM, Strittmatter, WJ, Schmechel, DE, Gaskell, PC, Small, GW et al. (1993) Gene dose of apolipoprotein E type 4 allele and the risk of Alzheimer's disease in late onset families. *Science* **261**:921-923.

Corkin, S., Amaral, DG, Gonzalez, RG, Johnson, KA, and Hyman, BT (1997) H. M.'s medial temporal lobe lesion: findings from magnetic resonance imaging. *J Neurosci* **17**:3964-3979.

Cormier, R. J., Greenwood, AC, and Connor, JA (2001) Bidirectional synaptic plasticity correlated with the magnitude of dendritic calcium transients above a threshold. *J Neurophysiol* **85**:399-406.

Cruz, J. C., Tseng, HC, Goldman, JA, Shih, H, and Tsai, LH (2003) Aberrant Cdk5 activation by p25 triggers pathological events leading to neurodegeneration and neurofibrillary tangles. *Neuron* **40**:471-483.

Danbolt, N. C. (2001) Glutamate uptake. *Prog Neurobiol* **65**:1-105.

Davies, C. H. and Collingridge, GL (1996) Regulation of EPSPs by the synaptic activation of GABAB autoreceptors in rat hippocampus. *J Physiol* **496** ( Pt 2):451-470.

Dawson, G. R., Seabrook, GR, Zheng, H, Smith, DW, Graham, S, O'Dowd, G et al. (1999) Age-related cognitive deficits, impaired long-term potentiation and reduction in synaptic marker density in mice lacking the beta-amyloid precursor protein. *Neuroscience* **90**:1-13.

Dawson, H. N., Ferreira, A, Eyster, MV, Ghoshal, N, Binder, LI, and Vitek, MP (2001) Inhibition of neuronal maturation in primary hippocampal neurons from tau deficient mice. *J Cell Sci* **114**:1179-1187.

De Felice, F. G., Velasco, PT, Lambert, MP, Viola, K, Fernandez, SJ, Ferreira, ST et al. (2007) Abeta oligomers induce neuronal oxidative stress through an N-methyl-D-aspartate receptor-dependent mechanism that is blocked by the Alzheimer drug memantine. *J Biol Chem* **282**:11590-11601.

De, Jonghe C., Esselens, C, Kumar-Singh, S, Craessaerts, K, Serneels, S, Checler, F et al. (2001) Pathogenic APP mutations near the gamma-secretase cleavage site differentially affect Abeta secretion and APP C-terminal fragment stability. *Hum Mol Genet* **10**:1665-1671.

De, Strooper B., Annaert, W, Cupers, P, Saftig, P, Craessaerts, K, Mumm, JS et al. (1999) A presenilin-1-dependent gamma-secretase-like protease mediates release of Notch intracellular domain. *Nature* **398**:518-522.

Del Vecchio, R. A., Gold, LH, Novick, SJ, Wong, G, and Hyde, LA (2004) Increased seizure threshold and severity in young transgenic CRND8 mice. *Neurosci Lett* **367**:164-167.

Delaney, K. R. and Tank, DW (1994) A quantitative measurement of the dependence of short-term synaptic enhancement on presynaptic residual calcium. *J Neurosci* **14**:5885-5902.

Deshpande, A., Mina, E, Glabe, C, and Busciglio, J (2006) Different conformations of amyloid beta induce neurotoxicity by distinct mechanisms in human cortical neurons. *J Neurosci* **26**:6011-6018.

DeStrooper, B., Simons, M, Multhaup, G, Van, LF, Beyreuther, K, and Dotti, CG (1995) Production of intracellular amyloid-containing fragments in hippocampal neurons expressing human amyloid precursor protein and protection against amyloidogenesis by subtle amino acid substitutions in the rodent sequence. *EMBO J* **14**:4932-4938.

Diamond, J. S. (2005) Deriving the glutamate clearance time course from transporter currents in CA1 hippocampal astrocytes: transmitter uptake gets faster during development. *J Neurosci* **25**:2906-2916.

Dodart, J. C., Meziane, H, Mathis, C, Bales, KR, Paul, SM, and Ungerer, A (1999) Behavioral disturbances in transgenic mice overexpressing the V717F beta-amyloid precursor protein. *Behav Neurosci* **113**:982-990.

Dong, X. X., Wang, Y, and Qin, ZH (2009) Molecular mechanisms of excitotoxicity and their relevance to pathogenesis of neurodegenerative diseases. *Acta Pharmacol Sin* **30**:379-387.

- Duarte, A. I., Santos, P, Oliveira, CR, Santos, MS, and Rego, AC (2008) Insulin neuroprotection against oxidative stress is mediated by Akt and GSK-3beta signaling pathways and changes in protein expression. *Biochim Biophys Acta* **1783**:994-1002.
- Ekstrom, A. D., Kahana, MJ, Caplan, JB, Fields, TA, Isham, EA, Newman, EL et al. (2003) Cellular networks underlying human spatial navigation. *Nature* **425**:184-188.
- English, J. D. and Sweatt, JD (1997) A requirement for the mitogen-activated protein kinase cascade in hippocampal long term potentiation. *J Biol Chem* **272**:19103-19106.
- Espana, J., Gimenez-Llort, L, Valero, J, Minano, A, Rabano, A, Rodriguez-Alvarez, J et al. (2010) Intraneuronal beta-Amyloid Accumulation in the Amygdala Enhances Fear and Anxiety in Alzheimer's Disease Transgenic Mice. *Biol Psychiatry* **67**:513-521.
- Fiala, J. C., Kirov, SA, Feinberg, MD, Petrak, LJ, George, P, Goddard, CA et al. (2003) Timing of neuronal and glial ultrastructure disruption during brain slice preparation and recovery in vitro. *J Comp Neurol* **465**:90-103.
- Fitzjohn, S. M., Kuenzi, F, Morton, RA, Rosahl, TW, Lewis, H, Smith, D et al. (2010) A study of long-term potentiation in transgenic mice over-expressing mutant forms of both amyloid precursor protein and presenilin-1. *Mol Brain* **3**:21
- Fitzjohn, S. M., Morton, RA, Kuenzi, F, Rosahl, TW, Shearman, M, Lewis, H et al. (2001) Age-related impairment of synaptic transmission but normal long-term potentiation in transgenic mice that overexpress the human APP695SWE mutant form of amyloid precursor protein. *J Neurosci* **21**:4691-4698.
- Foster, N. L., Chase, TN, Mansi, L, Brooks, R, Fedio, P, Patronas, NJ et al. (1984) Cortical abnormalities in Alzheimer's disease. *Ann Neurol* **16**:649-654.
- Francis, R., McGrath, G, Zhang, J, Ruddy, DA, Sym, M, Apfeld, J et al. (2002) *aph-1* and *pen-2* are required for Notch pathway signaling, gamma-secretase cleavage of betaAPP, and presenilin protein accumulation. *Dev Cell* **3**:85-97.
- Frasca, A., Aalbers, M, Frigerio, F, Fiordaliso, F, Salio, M, Gobbi, M et al. (2011) Misplaced NMDA receptors in epileptogenesis contribute to excitotoxicity. *Neurobiol Dis*
- Frey, U., Huang, YY, and Kandel, ER (1993) Effects of cAMP simulate a late stage of LTP in hippocampal CA1 neurons. *Science* **260**:1661-1664.
- Frey, U. and Morris, RG (1997) Synaptic tagging and long-term potentiation. *Nature* **385**:533-536.
- Fukumoto, H., Asami-Odaka, A, Suzuki, N, Shimada, H, Ihara, Y, and Iwatsubo, T (1996) Amyloid beta protein deposition in normal aging has the same characteristics as that in Alzheimer's disease. Predominance of A beta 42(43) and association of A beta 40 with cored plaques. *Am J Pathol* **148**:259-265.

- Games, D., Adams, D, Alessandrini, R, Barbour, R, Berthelette, P, Blackwell, C et al. (1995) Alzheimer-type neuropathology in transgenic mice overexpressing V717F beta-amyloid precursor protein. *Nature* **373**:523-527.
- Gatz, M., Mortimer, JA, Fratiglioni, L, Johansson, B, Berg, S, Andel, R et al. (2007) Accounting for the relationship between low education and dementia: a twin study. *Physiol Behav* **92**:232-237.
- Gendron, T. F. and Petrucelli, L (2009) The role of tau in neurodegeneration. *Mol Neurodegener* **4**:13
- Giannakopoulos, P., Herrmann, FR, Bussiere, T, Bouras, C, Kovari, E, Perl, DP et al. (2003) Tangle and neuron numbers, but not amyloid load, predict cognitive status in Alzheimer's disease. *Neurology* **60**:1495-1500.
- Giese, K. P., Fedorov, NB, Filipkowski, RK, and Silva, AJ (1998) Autophosphorylation at Thr286 of the alpha calcium-calmodulin kinase II in LTP and learning. *Science* **279**:870-873.
- Gimenez-Llort, L., Blazquez, G, Canete, T, Johansson, B, Oddo, S, Tobena, A et al. (2007) Modeling behavioral and neuronal symptoms of Alzheimer's disease in mice: a role for intraneuronal amyloid. *Neurosci Biobehav Rev* **31**:125-147.
- Glabe, C. G. and Kaye, R (2006) Common structure and toxic function of amyloid oligomers implies a common mechanism of pathogenesis. *Neurology* **66**:S74-S78.
- Good, C. D., Johnsrude, IS, Ashburner, J, Henson, RN, Friston, KJ, and Frackowiak, RS (2001) A voxel-based morphometric study of ageing in 465 normal adult human brains. *Neuroimage* **14**:21-36.
- Gordon, M. N., King, DL, Diamond, DM, Jantzen, PT, Boyett, KV, Hope, CE et al. (2001) Correlation between cognitive deficits and Abeta deposits in transgenic APP+PS1 mice. *Neurobiol Aging* **22**:377-385.
- Gotz, J., Chen, F, van Dorpe, J, and Nitsch, RM (2001) Formation of neurofibrillary tangles in P301l tau transgenic mice induced by Abeta 42 fibrils. *Science* **293**:1491-1495.
- Goussakov, I., Miller, MB, and Stutzmann, GE (2010) NMDA-mediated Ca(2+) influx drives aberrant ryanodine receptor activation in dendrites of young Alzheimer's disease mice. *J Neurosci* **30**:12128-12137.
- Grant, S. G., O'Dell, TJ, Karl, KA, Stein, PL, Soriano, P, and Kandel, ER (1992) Impaired long-term potentiation, spatial learning, and hippocampal development in fyn mutant mice. *Science* **258**:1903-1910.
- Gravina, S. A., Ho, L, Eckman, CB, Long, KE, Otvos, L, Jr., Younkin, LH et al. (1995) Amyloid beta protein (A beta) in Alzheimer's disease brain. Biochemical and immunocytochemical analysis with antibodies specific for forms ending at A beta 40 or A beta 42(43). *J Biol Chem* **270**:7013-7016.

- Grundke-Iqbal, I., Iqbal, K, Tung, YC, Quinlan, M, Wisniewski, HM, and Binder, LI (1986) Abnormal phosphorylation of the microtubule-associated protein tau (tau) in Alzheimer cytoskeletal pathology. *Proc Natl Acad Sci U S A* **83**:4913-4917.
- Guo, Q., Fu, W, Sopher, BL, Miller, MW, Ware, CB, Martin, GM et al. (1999) Increased vulnerability of hippocampal neurons to excitotoxic necrosis in presenilin-1 mutant knock-in mice. *Nat Med* **5**:101-106.
- Haass, C., Lemere, CA, Capell, A, Citron, M, Seubert, P, Schenk, D et al. (1995) The Swedish mutation causes early-onset Alzheimer's disease by beta-secretase cleavage within the secretory pathway. *Nat Med* **1**:1291-1296.
- Hamilton, L. K., Aumont, A, Julien, C, Vadnais, A, Calon, F, and Fernandes, KJ (2010) Widespread deficits in adult neurogenesis precede plaque and tangle formation in the 3xTg mouse model of Alzheimer's disease. *Eur J Neurosci* **32**:905-920.
- Hanger, D. P., Anderton, BH, and Noble, W (2009a) Tau phosphorylation: the therapeutic challenge for neurodegenerative disease. *Trends Mol Med* **15**:112-119.
- Hanger, D. P., Anderton, BH, and Noble, W (2009b) Tau phosphorylation: the therapeutic challenge for neurodegenerative disease. *Trends Mol Med* **15**:112-119.
- Hanger, D. P., Byers, HL, Wray, S, Leung, KY, Saxton, MJ, Seereeram, A et al. (2007) Novel phosphorylation sites in tau from Alzheimer brain support a role for casein kinase 1 in disease pathogenesis. *J Biol Chem* **282**:23645-23654.
- Hardy, J. and Allsop, D (1991) Amyloid deposition as the central event in the aetiology of Alzheimer's disease. *Trends Pharmacol Sci* **12**:383-388.
- Harold, D., Abraham, R, Hollingworth, P, Sims, R, Gerrish, A, Hamshere, ML et al. (2009) Genome-wide association study identifies variants at CLU and PICALM associated with Alzheimer's disease. *Nat Genet* **41**:1088-1093.
- Harris, J. A., Devidze, N, Verret, L, Ho, K, Halabisky, B, Thwin, MT et al. (2010) Transsynaptic progression of amyloid-beta-induced neuronal dysfunction within the entorhinal-hippocampal network. *Neuron* **68**:428-441.
- Hartman, R. E., Laurer, H, Longhi, L, Bales, KR, Paul, SM, McIntosh, TK et al. (2002) Apolipoprotein E4 influences amyloid deposition but not cell loss after traumatic brain injury in a mouse model of Alzheimer's disease. *J Neurosci* **22**:10083-10087.
- Heneka, M. T., O'Banion, MK, Terwel, D, and Kummer, MP (2010) Neuroinflammatory processes in Alzheimer's disease. *J Neural Transm* **117**:919-947.

Hernandez, F., Gomez de, BE, Fuster-Matanzo, A, Lucas, JJ, and Avila, J (2010) GSK3: a possible link between beta amyloid peptide and tau protein. *Exp Neurol* **223**:322-325.

Hernandez, R. V., Navarro, MM, Rodriguez, WA, Martinez, JL, Jr., and LeBaron, RG (2005) Differences in the magnitude of long-term potentiation produced by theta burst and high frequency stimulation protocols matched in stimulus number. *Brain Res Brain Res Protoc* **15**:6-13.

Herreman, A., Hartmann, D, Annaert, W, Saftig, P, Craessaerts, K, Serneels, L et al. (1999) Presenilin 2 deficiency causes a mild pulmonary phenotype and no changes in amyloid precursor protein processing but enhances the embryonic lethal phenotype of presenilin 1 deficiency. *Proc Natl Acad Sci U S A* **96**:11872-11877.

Hirata-Fukae, C., Li, HF, Hoe, HS, Gray, AJ, Minami, SS, Hamada, K et al. (2008) Females exhibit more extensive amyloid, but not tau, pathology in an Alzheimer transgenic model. *Brain Res* **1216**:92-103.

Hirata-Fukae, C., Li, HF, Ma, L, Hoe, HS, Rebeck, GW, Aisen, PS et al. (2009) Levels of soluble and insoluble tau reflect overall status of tau phosphorylation in vivo. *Neurosci Lett* **450**:51-55.

Ho, O. H., Delgado, JY, and O'Dell, TJ (2004) Phosphorylation of proteins involved in activity-dependent forms of synaptic plasticity is altered in hippocampal slices maintained in vitro. *J Neurochem* **91**:1344-1357.

Hoe, H. S., Fu, Z, Makarova, A, Lee, JY, Lu, C, Feng, L et al. (2009) The effects of amyloid precursor protein on postsynaptic composition and activity. *J Biol Chem* **284**:8495-8506.

Holcomb, L., Gordon, MN, McGowan, E, Yu, X, Benkovic, S, Jantzen, P et al. (1998) Accelerated Alzheimer-type phenotype in transgenic mice carrying both mutant amyloid precursor protein and presenilin 1 transgenes. *Nat Med* **4**:97-100.

Hooper, C., Killick, R, and Lovestone, S (2008) The GSK3 hypothesis of Alzheimer's disease. *J Neurochem* **104**:1433-1439.

Hooper, C., Markevich, V, Plattner, F, Killick, R, Schofield, E, Engel, T et al. (2007) Glycogen synthase kinase-3 inhibition is integral to long-term potentiation. *Eur J Neurosci* **25**:81-86.

Howlett, D. R., Bowler, K, Soden, PE, Riddell, D, Davis, JB, Richardson, JC et al. (2008a) Abeta deposition and related pathology in an APP x PS1 transgenic mouse model of Alzheimer's disease. *Histol Histopathol* **23**:67-76.

Howlett, D. R., Bowler, K, Soden, PE, Riddell, D, Davis, JB, Richardson, JC et al. (2008b) Abeta deposition and related pathology in an APP x PS1 transgenic mouse model of Alzheimer's disease. *Histol Histopathol* **23**:67-76.

Howlett, D. R., Richardson, JC, Austin, A, Parsons, AA, Bate, ST, Davies, DC et al. (2004) Cognitive correlates of Abeta deposition in male and female mice

bearing amyloid precursor protein and presenilin-1 mutant transgenes. *Brain Res* **1017**:130-136.

Hsia, A. Y., Masliah, E, McConlogue, L, Yu, GQ, Tatsuno, G, Hu, K et al. (1999) Plaque-independent disruption of neural circuits in Alzheimer's disease mouse models. *Proc Natl Acad Sci U S A* **96**:3228-3233.

Hsiao, K., Chapman, P, Nilsen, S, Eckman, C, Harigaya, Y, Younkin, S et al. (1996) Correlative memory deficits, Abeta elevation, and amyloid plaques in transgenic mice. *Science* **274**:99-102.

Hsieh, H., Boehm, J, Sato, C, Iwatsubo, T, Tomita, T, Sisodia, S et al. (2006) AMPAR removal underlies Abeta-induced synaptic depression and dendritic spine loss. *Neuron* **52**:831-843.

Hung, A. Y., Haass, C, Nitsch, RM, Qiu, WQ, Citron, M, Wurtman, RJ et al. (1993) Activation of protein kinase C inhibits cellular production of the amyloid beta-protein. *J Biol Chem* **268**:22959-22962.

Hutton, M., Lendon, CL, Rizzu, P, Baker, M, Froelich, S, Houlden, H et al. (1998) Association of missense and 5'-splice-site mutations in tau with the inherited dementia FTDP-17. *Nature* **393**:702-705.

Jacobsen, J. S., Wu, CC, Redwine, JM, Comery, TA, Arias, R, Bowlby, M et al. (2006) Early-onset behavioral and synaptic deficits in a mouse model of Alzheimer's disease. *Proc Natl Acad Sci U S A* **103**:5161-5166.

Jiang, Q., Lee, CY, Mandrekar, S, Wilkinson, B, Cramer, P, Zelcer, N et al. (2008) ApoE promotes the proteolytic degradation of Abeta. *Neuron* **58**:681-693.

Jolas, T., Zhang, XS, Zhang, Q, Wong, G, Del Vecchio, R, Gold, L et al. (2002) Long-term potentiation is increased in the CA1 area of the hippocampus of APP(swe/ind) CRND8 mice. *Neurobiol Dis* **11**:394-409.

Julien, C., Tremblay, C, Phivilay, A, Berthiaume, L, Emond, V, Julien, P et al. (2010) High-fat diet aggravates amyloid-beta and tau pathologies in the 3xTg-AD mouse model. *Neurobiol Aging* **31**:1516-1531.

Kamenetz, F., Tomita, T, Hsieh, H, Seabrook, G, Borchelt, D, Iwatsubo, T et al. (2003) APP processing and synaptic function. *Neuron* **37**:925-937.

Kampers, T., Pangalos, M, Geerts, H, Wiech, H, and Mandelkow, E (1999) Assembly of paired helical filaments from mouse tau: implications for the neurofibrillary pathology in transgenic mouse models for Alzheimer's disease. *FEBS Lett* **451**:39-44.

King, D. L., Arendash, GW, Crawford, F, Sterk, T, Menendez, J, and Mullan, MJ (1999) Progressive and gender-dependent cognitive impairment in the APP(SW) transgenic mouse model for Alzheimer's disease. *Behav Brain Res* **103**:145-162.

Kitazawa, M., Oddo, S, Yamasaki, TR, Green, KN, and LaFerla, FM (2005) Lipopolysaccharide-induced inflammation exacerbates tau pathology by a cyclin-

dependent kinase 5-mediated pathway in a transgenic model of Alzheimer's disease. *J Neurosci* **25**:8843-8853.

Knight, E. M., Verkhatsky, A, Luckman, SM, Allan, SM, and Lawrence, CB (2010) Hypermetabolism in a triple-transgenic mouse model of Alzheimer's disease. *Neurobiol Aging*

Koh, S. H., Noh, MY, and Kim, SH (2008) Amyloid-beta-induced neurotoxicity is reduced by inhibition of glycogen synthase kinase-3. *Brain Res* **1188**:254-262.

Konig, G., Monning, U, Czech, C, Prior, R, Banati, R, Schreiter-Gasser, U et al. (1992) Identification and differential expression of a novel alternative splice isoform of the beta A4 amyloid precursor protein (APP) mRNA in leukocytes and brain microglial cells. *J Biol Chem* **267**:10804-10809.

Korogod, N., Lou, X, and Schneggenburger, R (2007) Posttetanic potentiation critically depends on an enhanced Ca(2+) sensitivity of vesicle fusion mediated by presynaptic PKC. *Proc Natl Acad Sci U S A* **104**:15923-15928.

Kullmann, D. M. (2003) Silent synapses: what are they telling us about long-term potentiation? *Philos Trans R Soc Lond B Biol Sci* **358**:727-733.

Kumar, A., Bodhinathan, K, and Foster, TC (2009) Susceptibility to Calcium Dysregulation during Brain Aging. *Front Aging Neurosci* **1**:2

Kuwako, K., Nishimura, I, Uetsuki, T, Saido, TC, and Yoshikawa, K (2002) Activation of calpain in cultured neurons overexpressing Alzheimer amyloid precursor protein. *Brain Res Mol Brain Res* **107**:166-175.

Larson, J., Lynch, G, Games, D, and Seubert, P (1999) Alterations in synaptic transmission and long-term potentiation in hippocampal slices from young and aged PDAPP mice. *Brain Res* **840**:23-35.

Lee, H. G., Perry, G, Moreira, PI, Garrett, MR, Liu, Q, Zhu, X et al. (2005) Tau phosphorylation in Alzheimer's disease: pathogen or protector? *Trends Mol Med* **11**:164-169.

Lee, H. K., Barbarosie, M, Kameyama, K, Bear, MF, and Huganir, RL (2000) Regulation of distinct AMPA receptor phosphorylation sites during bidirectional synaptic plasticity. *Nature* **405**:955-959.

Lee, M. K., Slunt, HH, Martin, LJ, Thinakaran, G, Kim, G, Gandy, SE et al. (1996) Expression of presenilin 1 and 2 (PS1 and PS2) in human and murine tissues. *J Neurosci* **16**:7513-7525.

Lesne, S., Koh, MT, Kotilinek, L, Kaye, R, Glabe, CG, Yang, A et al. (2006) A specific amyloid-beta protein assembly in the brain impairs memory. *Nature* **440**:352-357.

Lewis, J., Dickson, DW, Lin, WL, Chisholm, L, Corral, A, Jones, G et al. (2001) Enhanced neurofibrillary degeneration in transgenic mice expressing mutant tau and APP. *Science* **293**:1487-1491.

- Lewis, J., McGowan, E, Rockwood, J, Melrose, H, Nacharaju, P, Van Slegtenhorst, M et al. (2000) Neurofibrillary tangles, amyotrophy and progressive motor disturbance in mice expressing mutant (P301L) tau protein. *Nat Genet* **25**:402-405.
- Li, F., Calingasan, NY, Yu, F, Mauck, WM, Toidze, M, Almeida, CG et al. (2004) Increased plaque burden in brains of APP mutant MnSOD heterozygous knockout mice. *J Neurochem* **89**:1308-1312.
- Li, S., Hong, S, Shepardson, NE, Walsh, DM, Shankar, GM, and Selkoe, D (2009) Soluble oligomers of amyloid Beta protein facilitate hippocampal long-term depression by disrupting neuronal glutamate uptake. *Neuron* **62**:788-801.
- Liang, M. H. and Chuang, DM (2007) Regulation and function of glycogen synthase kinase-3 isoforms in neuronal survival. *J Biol Chem* **282**:3904-3917.
- Lopez, J. R., Lyckman, A, Oddo, S, LaFerla, FM, Querfurth, HW, and Shtifman, A (2008) Increased intraneuronal resting [Ca<sup>2+</sup>] in adult Alzheimer's disease mice. *J Neurochem* **105**:262-271.
- Lu, M. and Kosik, KS (2001) Competition for microtubule-binding with dual expression of tau missense and splice isoforms. *Mol Biol Cell* **12**:171-184.
- Lucas, J. J., Hernandez, F, Gomez-Ramos, P, Moran, MA, Hen, R, and Avila, J (2001) Decreased nuclear beta-catenin, tau hyperphosphorylation and neurodegeneration in GSK-3beta conditional transgenic mice. *EMBO J* **20**:27-39.
- Maheswaran, S., Barjat, H, Rueckert, D, Bate, ST, Howlett, DR, Tilling, L et al. (2009) Longitudinal regional brain volume changes quantified in normal aging and Alzheimer's APP x PS1 mice using MRI. *Brain Res* **1270**:19-32.
- Makino, H. and Malinow, R (2009) AMPA receptor incorporation into synapses during LTP: the role of lateral movement and exocytosis. *Neuron* **64**:381-390.
- Malenka, R. C., Kauer, JA, Perkel, DJ, Mauk, MD, Kelly, PT, Nicoll, RA et al. (1989) An essential role for postsynaptic calmodulin and protein kinase activity in long-term potentiation. *Nature* **340**:554-557.
- Malinow, R., Schulman, H, and Tsien, RW (1989) Inhibition of postsynaptic PKC or CaMKII blocks induction but not expression of LTP. *Science* **245**:862-866.
- Masliah, E., Terry, RD, Alford, M, DeTeresa, R, and Hansen, LA (1991) Cortical and subcortical patterns of synaptophysinlike immunoreactivity in Alzheimer's disease. *Am J Pathol* **138**:235-246.
- Mastrangelo, M. A. and Bowers, WJ (2008) Detailed immunohistochemical characterization of temporal and spatial progression of Alzheimer's disease-related pathologies in male triple-transgenic mice. *BMC Neurosci* **9**:81

Matsuo, N., Takao, K, Nakanishi, K, Yamasaki, N, Tanda, K, and Miyakawa, T (2010) Behavioral profiles of three C57BL/6 substrains. *Front Behav Neurosci* **4**:29

Mattson, M. P., Cheng, B, Davis, D, Bryant, K, Lieberburg, I, and Rydel, RE (1992) beta-Amyloid peptides destabilize calcium homeostasis and render human cortical neurons vulnerable to excitotoxicity. *J Neurosci* **12**:376-389.

Mawuenyega, K. G., Sigurdson, W, Ovod, V, Munsell, L, Kasten, T, Morris, JC et al. (2010) Decreased clearance of CNS beta-amyloid in Alzheimer's disease. *Science* **330**:1774

McCool, M. F., Varty, GB, Del Vecchio, RA, Kazdoba, TM, Parker, EM, Hunter, JC et al. (2003) Increased auditory startle response and reduced prepulse inhibition of startle in transgenic mice expressing a double mutant form of amyloid precursor protein. *Brain Res* **994**:99-106.

McGowan, E., Sanders, S, Iwatsubo, T, Takeuchi, A, Saido, T, Zehr, C et al. (1999) Amyloid phenotype characterization of transgenic mice overexpressing both mutant amyloid precursor protein and mutant presenilin 1 transgenes. *Neurobiol Dis* **6**:231-244.

Mitchell, J. C., Ariff, BB, Yates, DM, Lau, KF, Perkinson, MS, Rogelj, B et al. (2009) X11beta rescues memory and long-term potentiation deficits in Alzheimer's disease APPswe Tg2576 mice. *Hum Mol Genet* **18**:4492-4500.

Morris, R. G., Schenk, F, Tweedie, F, and Jarrard, LE (1990) Ibotenate Lesions of Hippocampus and/or Subiculum: Dissociating Components of Allocentric Spatial Learning. *Eur J Neurosci* **2**:1016-1028.

Mosconi, L., Pupi, A, and De Leon, MJ (2008) Brain glucose hypometabolism and oxidative stress in preclinical Alzheimer's disease. *Ann N Y Acad Sci* **1147**:180-195.

Mullan, M., Crawford, F, Axelman, K, Houlden, H, Lilius, L, Winblad, B et al. (1992) A pathogenic mutation for probable Alzheimer's disease in the APP gene at the N-terminus of beta-amyloid. *Nat Genet* **1**:345-347.

Munoz, L. and Ammit, AJ (2010) Targeting p38 MAPK pathway for the treatment of Alzheimer's disease. *Neuropharmacology* **58**:561-568.

Murray, I. V., Proza, JF, Sohrabji, F, and Lawler, JM (2011) Vascular and metabolic dysfunction in Alzheimer's disease: a review. *Exp Biol Med (Maywood)* **236**:772-782.

Murrell, J. R., Hake, AM, Quaid, KA, Farlow, MR, and Ghetti, B (2000) Early-onset Alzheimer disease caused by a new mutation (V717L) in the amyloid precursor protein gene. *Arch Neurol* **57**:885-887.

Nathan, T., Jensen, MS, and Lambert, JD (1990) GABAB receptors play a major role in paired-pulse facilitation in area CA1 of the rat hippocampus. *Brain Res* **531**:55-65.

- Nguyen, P. V. (2006) Comparative plasticity of brain synapses in inbred mouse strains. *J Exp Biol* **209**:2293-2303.
- Nguyen, P. V., Abel, T, and Kandel, ER (1994) Requirement of a critical period of transcription for induction of a late phase of LTP. *Science* **265**:1104-1107.
- Noble, W., Planel, E, Zehr, C, Olm, V, Meyerson, J, Suleman, F et al. (2005) Inhibition of glycogen synthase kinase-3 by lithium correlates with reduced tauopathy and degeneration in vivo. *Proc Natl Acad Sci U S A* **102**:6990-6995.
- Noh, K. M., Lee, JC, Ahn, YH, Hong, SH, and Koh, JY (1999) Insulin-induced oxidative neuronal injury in cortical culture: mediation by induced N-methyl-D-aspartate receptors. *IUBMB Life* **48**:263-269.
- Noristani, H. N., Olabarria, M, Verkhatsky, A, and Rodriguez, JJ (2010) Serotonin fibre sprouting and increase in serotonin transporter immunoreactivity in the CA1 area of hippocampus in a triple transgenic mouse model of Alzheimer's disease. *Eur J Neurosci* **32**:71-79.
- Oddo, S., Caccamo, A, Cheng, D, Juleh, B, Torp, R, and LaFerla, FM (2007) Genetically augmenting tau levels does not modulate the onset or progression of Abeta pathology in transgenic mice. *J Neurochem* **102**:1053-1063.
- Oddo, S., Caccamo, A, Shepherd, JD, Murphy, MP, Golde, TE, Kaye, R et al. (2003) Triple-transgenic model of Alzheimer's disease with plaques and tangles: intracellular Abeta and synaptic dysfunction. *Neuron* **39**:409-421.
- Oddo, S., Caccamo, A, Smith, IF, Green, KN, and LaFerla, FM (2006a) A dynamic relationship between intracellular and extracellular pools of Abeta. *Am J Pathol* **168**:184-194.
- Oddo, S., Vasilevko, V, Caccamo, A, Kitazawa, M, Cribbs, DH, and LaFerla, FM (2006b) Reduction of soluble Abeta and tau, but not soluble Abeta alone, ameliorates cognitive decline in transgenic mice with plaques and tangles. *J Biol Chem* **281**:39413-39423.
- Oh, K. J., Perez, SE, Lagalwar, S, Vana, L, Binder, L, and Mufson, EJ (2010) Staging of Alzheimer's pathology in triple transgenic mice: a light and electron microscopic analysis. *Int J Alzheimers Dis* **2010**:
- Okuno, H. (2011) Regulation and function of immediate-early genes in the brain: beyond neuronal activity markers. *Neurosci Res* **69**:175-186.
- Otto, T., Eichenbaum, H, Wiener, SI, and Wible, CG (1991) Learning-related patterns of CA1 spike trains parallel stimulation parameters optimal for inducing hippocampal long-term potentiation. *Hippocampus* **1**:181-192.
- Overk, C. R., Kelley, CM, and Mufson, EJ (2009) Brainstem Alzheimer's-like pathology in the triple transgenic mouse model of Alzheimer's disease. *Neurobiol Dis* **35**:415-425.

Pagani, L. and Eckert, A (2011) Amyloid-Beta interaction with mitochondria. *Int J Alzheimers Dis* **2011**:925050

Palop, J. J., Chin, J, Roberson, ED, Wang, J, Thwin, MT, Bien-Ly, N et al. (2007) Aberrant excitatory neuronal activity and compensatory remodeling of inhibitory hippocampal circuits in mouse models of Alzheimer's disease. *Neuron* **55**:697-711.

Panda, D., Samuel, JC, Massie, M, Feinstein, SC, and Wilson, L (2003) Differential regulation of microtubule dynamics by three- and four-repeat tau: implications for the onset of neurodegenerative disease. *Proc Natl Acad Sci U S A* **100**:9548-9553.

Parent, A., Linden, DJ, Sisodia, SS, and Borchelt, DR (1999) Synaptic transmission and hippocampal long-term potentiation in transgenic mice expressing FAD-linked presenilin 1. *Neurobiol Dis* **6**:56-62.

Pastalkova, E., Serrano, P, Pinkhasova, D, Wallace, E, Fenton, AA, and Sacktor, TC (2006) Storage of spatial information by the maintenance mechanism of LTP. *Science* **313**:1141-1144.

Patrick, G. N., Zukerberg, L, Nikolic, M, de la, MS, Dikkes, P, and Tsai, LH (1999) Conversion of p35 to p25 deregulates Cdk5 activity and promotes neurodegeneration. *Nature* **402**:615-622.

Peineau, S., Taghibiglou, C, Bradley, C, Wong, TP, Liu, L, Lu, J et al. (2007) LTP inhibits LTD in the hippocampus via regulation of GSK3beta. *Neuron* **53**:703-717.

Penet, M. F., Laigle, C, Fur, YL, Confort-Gouny, S, Heurteaux, C, Cozzone, PJ et al. (2006) In vivo characterization of brain morphometric and metabolic endophenotypes in three inbred strains of mice using magnetic resonance techniques. *Behav Genet* **36**:732-744.

Perez, S. E., Dar, S, Ikonomovic, MD, DeKosky, ST, and Mufson, EJ (2007) Cholinergic forebrain degeneration in the APP<sup>swe</sup>/PS1<sup>DeltaE9</sup> transgenic mouse. *Neurobiol Dis* **28**:3-15.

Perkinton, M. S., Ip, JK, Wood, GL, Crossthwaite, AJ, and Williams, RJ (2002) Phosphatidylinositol 3-kinase is a central mediator of NMDA receptor signalling to MAP kinase (Erk1/2), Akt/PKB and CREB in striatal neurones. *J Neurochem* **80**:239-254.

Phiel, C. J., Wilson, CA, Lee, VM, and Klein, PS (2003) GSK-3alpha regulates production of Alzheimer's disease amyloid-beta peptides. *Nature* **423**:435-439.

Piert, M., Koeppe, RA, Giordani, B, Berent, S, and Kuhl, DE (1996) Diminished glucose transport and phosphorylation in Alzheimer's disease determined by dynamic FDG-PET. *J Nucl Med* **37**:201-208.

- Planel, E., Richter, KE, Nolan, CE, Finley, JE, Liu, L, Wen, Y et al. (2007) Anesthesia leads to tau hyperphosphorylation through inhibition of phosphatase activity by hypothermia. *J Neurosci* **27**:3090-3097.
- Plant, K., Pelkey, KA, Bortolotto, ZA, Morita, D, Terashima, A, McBain, CJ et al. (2006) Transient incorporation of native GluR2-lacking AMPA receptors during hippocampal long-term potentiation. *Nat Neurosci* **9**:602-604.
- Pratico, D. (2008) Oxidative stress hypothesis in Alzheimer's disease: a reappraisal. *Trends Pharmacol Sci* **29**:609-615.
- Pugh, P. L., Richardson, JC, Bate, ST, Upton, N, and Sunter, D (2007) Non-cognitive behaviours in an APP/PS1 transgenic model of Alzheimer's disease. *Behav Brain Res* **178**:18-28.
- Qiu, W. Q., Ferreira, A, Miller, C, Koo, EH, and Selkoe, DJ (1995) Cell-surface beta-amyloid precursor protein stimulates neurite outgrowth of hippocampal neurons in an isoform-dependent manner. *J Neurosci* **15**:2157-2167.
- Rempel-Clower, N. L., Zola, SM, Squire, LR, and Amaral, DG (1996) Three cases of enduring memory impairment after bilateral damage limited to the hippocampal formation. *J Neurosci* **16**:5233-5255.
- Resende, R., Moreira, PI, Proenca, T, Deshpande, A, Busciglio, J, Pereira, C et al. (2008) Brain oxidative stress in a triple-transgenic mouse model of Alzheimer disease. *Free Radic Biol Med* **44**:2051-2057.
- Richardson, J. C., Kendal, CE, Anderson, R, Priest, F, Gower, E, Soden, P et al. (2003) Ultrastructural and behavioural changes precede amyloid deposition in a transgenic model of Alzheimer's disease. *Neuroscience* **122**:213-228.
- Richerson, G. B. and Messer, C (1995) Effect of composition of experimental solutions on neuronal survival during rat brain slicing. *Exp Neurol* **131**:133-143.
- Riout-Pedotti, M. S., Friedman, D, and Donoghue, JP (2000) Learning-induced LTP in neocortex. *Science* **290**:533-536.
- Ris, L., Angelo, M, Plattner, F, Capron, B, Errington, ML, Bliss, TV et al. (2005) Sexual dimorphisms in the effect of low-level p25 expression on synaptic plasticity and memory. *Eur J Neurosci* **21**:3023-3033.
- Roberson, E. D., Scarce-Levie, K, Palop, JJ, Yan, F, Cheng, IH, Wu, T et al. (2007) Reducing endogenous tau ameliorates amyloid beta-induced deficits in an Alzheimer's disease mouse model. *Science* **316**:750-754.
- Rockwood, K., Black, SE, Robillard, A, and Lussier, I (2004) Potential treatment effects of donepezil not detected in Alzheimer's disease clinical trials: a physician survey. *Int J Geriatr Psychiatry* **19**:954-960.
- Rodriguez, J. J., Jones, VC, Tabuchi, M, Allan, SM, Knight, EM, LaFerla, FM et al. (2008) Impaired adult neurogenesis in the dentate gyrus of a triple transgenic mouse model of Alzheimer's disease. *PLoS ONE* **3**:e2935

Roettger, V. and Lipton, P (1996) Mechanism of glutamate release from rat hippocampal slices during in vitro ischemia. *Neuroscience* **75**:677-685.

Romberg, C., Mattson, MP, Mughal, MR, Bussey, TJ, and Saksida, LM (2011) Impaired attention in the 3xTgAD mouse model of Alzheimer's disease: rescue by donepezil (Aricept). *J Neurosci* **31**:3500-3507.

Sahara, N., Lewis, J, DeTure, M, McGowan, E, Dickson, DW, Hutton, M et al. (2002) Assembly of tau in transgenic animals expressing P301L tau: alteration of phosphorylation and solubility. *J Neurochem* **83**:1498-1508.

Sandler, V. M. and Barbara, JG (1999) Calcium-induced calcium release contributes to action potential-evoked calcium transients in hippocampal CA1 pyramidal neurons. *J Neurosci* **19**:4325-4336.

Schauwecker, P. E. and Steward, O (1997) Genetic determinants of susceptibility to excitotoxic cell death: implications for gene targeting approaches. *Proc Natl Acad Sci U S A* **94**:4103-4108.

Scheff, S. W., Price, DA, Schmitt, FA, and Mufson, EJ (2006) Hippocampal synaptic loss in early Alzheimer's disease and mild cognitive impairment. *Neurobiol Aging* **27**:1372-1384.

Schenk, D., Barbour, R, Dunn, W, Gordon, G, Grajeda, H, Guido, T et al. (1999) Immunization with amyloid-beta attenuates Alzheimer-disease-like pathology in the PDAPP mouse. *Nature* **400**:173-177.

Schneider, I., Reverse, D, Dewachter, I, Ris, L, Caluwaerts, N, Kuiperi, C et al. (2001) Mutant presenilins disturb neuronal calcium homeostasis in the brain of transgenic mice, decreasing the threshold for excitotoxicity and facilitating long-term potentiation. *J Biol Chem* **276**:11539-11544.

Seabrook, G. R., Smith, DW, Bowery, BJ, Easter, A, Reynolds, T, Fitzjohn, SM et al. (1999) Mechanisms contributing to the deficits in hippocampal synaptic plasticity in mice lacking amyloid precursor protein. *Neuropharmacology* **38**:349-359.

Seki, M., Nawa, H, Morioka, T, Fukuchi, T, Oite, T, Abe, H et al. (2002) Establishment of a novel enzyme-linked immunosorbent assay for Thy-1; quantitative assessment of neuronal degeneration. *Neurosci Lett* **329**:185-188.

Shankar, G. M., Bloodgood, BL, Townsend, M, Walsh, DM, Selkoe, DJ, and Sabatini, BL (2007) Natural oligomers of the Alzheimer amyloid-beta protein induce reversible synapse loss by modulating an NMDA-type glutamate receptor-dependent signaling pathway. *J Neurosci* **27**:2866-2875.

Shankar, G. M., Li, S, Mehta, TH, Garcia-Munoz, A, Shepardson, NE, Smith, I et al. (2008) Amyloid-beta protein dimers isolated directly from Alzheimer's brains impair synaptic plasticity and memory. *Nat Med*

Shen, J., Bronson, RT, Chen, DF, Xia, W, Selkoe, DJ, and Tonegawa, S (1997) Skeletal and CNS defects in Presenilin-1-deficient mice. *Cell* **89**:629-639.

Shen, J. and Kelleher, RJ, III (2007) The presenilin hypothesis of Alzheimer's disease: evidence for a loss-of-function pathogenic mechanism. *Proc Natl Acad Sci U S A* **104**:403-409.

Shi, S., Hayashi, Y, Esteban, JA, and Malinow, R (2001) Subunit-specific rules governing AMPA receptor trafficking to synapses in hippocampal pyramidal neurons. *Cell* **105**:331-343.

Shipton, O. A., Leitz, JR, Dworzak, J, Acton, CE, Tunbridge, EM, Denk, F et al. (2011) Tau protein is required for amyloid {beta}-induced impairment of hippocampal long-term potentiation. *J Neurosci* **31**:1688-1692.

Siklos, L., Kuhnt, U, Parducz, A, and Szerdahelyi, P (1997) Intracellular calcium redistribution accompanies changes in total tissue Na<sup>+</sup>, K<sup>+</sup> and water during the first two hours of in vitro incubation of hippocampal slices. *Neuroscience* **79**:1013-1022.

Silverman, D. H., Small, GW, Chang, CY, Lu, CS, Kung De Aburto, MA, Chen, W et al. (2001) Positron emission tomography in evaluation of dementia: Regional brain metabolism and long-term outcome. *JAMA* **286**:2120-2127.

Small, D. H., Nurcombe, V, Reed, G, Clarris, H, Moir, R, Beyreuther, K et al. (1994) A heparin-binding domain in the amyloid protein precursor of Alzheimer's disease is involved in the regulation of neurite outgrowth. *J Neurosci* **14**:2117-2127.

Smith, J. P., Lal, V, Bowser, D, Cappai, R, Masters, CL, and Ciccotosto, GD (2009) Stimulus pattern dependence of the Alzheimer's disease amyloid-beta 42 peptide's inhibition of long term potentiation in mouse hippocampal slices. *Brain Res* **1269**:176-184.

Snyder, E. M., Nong, Y, Almeida, CG, Paul, S, Moran, T, Choi, EY et al. (2005) Regulation of NMDA receptor trafficking by amyloid-beta. *Nat Neurosci* **8**:1051-1058.

Soutar, M. P., Thornhill, P, Cole, AR, and Sutherland, C (2009) Increased CRMP2 phosphorylation is observed in Alzheimer's disease; does this tell us anything about disease development? *Curr Alzheimer Res* **6**:269-278.

Spencer, J. P., Brown, JT, Richardson, JC, Medhurst, AD, Sehmi, SS, Calver, AR et al. (2004) Modulation of hippocampal excitability by 5-HT<sub>4</sub> receptor agonists persists in a transgenic model of Alzheimer's disease. *Neuroscience* **129**:49-54.

Spillantini, M. G. and Goedert, M (2000) Tau mutations in familial frontotemporal dementia. *Brain* **123** ( Pt 5):857-859.

Squire, L. R. and Zola-Morgan, S (1991) The medial temporal lobe memory system. *Science* **253**:1380-1386.

Steen, E., Terry, BM, Rivera, EJ, Cannon, JL, Neely, TR, Tavares, R et al. (2005) Impaired insulin and insulin-like growth factor expression and signaling

mechanisms in Alzheimer's disease--is this type 3 diabetes? *J Alzheimers Dis* **7**:63-80.

Sterniczuk, R., Antle, MC, LaFerla, FM, and Dyck, RH (2010a) Characterization of the 3xTg-AD mouse model of Alzheimer's disease: part 2. Behavioral and cognitive changes. *Brain Res* **1348**:149-155.

Sterniczuk, R., Dyck, RH, LaFerla, FM, and Antle, MC (2010b) Characterization of the 3xTg-AD mouse model of Alzheimer's disease: part 1. Circadian changes. *Brain Res* **1348**:139-148.

Sturchler-Pierrat, C., Abramowski, D, Duke, M, Wiederhold, KH, Mistl, C, Rothacher, S et al. (1997) Two amyloid precursor protein transgenic mouse models with Alzheimer disease-like pathology. *Proc Natl Acad Sci U S A* **94**:13287-13292.

Stutzmann, G. E., Caccamo, A, LaFerla, FM, and Parker, I (2004) Dysregulated IP3 signaling in cortical neurons of knock-in mice expressing an Alzheimer's-linked mutation in presenilin1 results in exaggerated Ca<sup>2+</sup> signals and altered membrane excitability. *J Neurosci* **24**:508-513.

Stutzmann, G. E., Smith, I, Caccamo, A, Oddo, S, LaFerla, FM, and Parker, I (2006) Enhanced ryanodine receptor recruitment contributes to Ca<sup>2+</sup> disruptions in young, adult, and aged Alzheimer's disease mice. *J Neurosci* **26**:5180-5189.

Sudoh, S., Kawamura, Y, Sato, S, Wang, R, Saido, TC, Oyama, F et al. (1998) Presenilin 1 mutations linked to familial Alzheimer's disease increase the intracellular levels of amyloid beta-protein 1-42 and its N-terminally truncated variant(s) which are generated at distinct sites. *J Neurochem* **71**:1535-1543.

Sun, X., Yao, H, Douglas, RM, Gu, XQ, Wang, J, and Haddad, GG (2010) Insulin/PI3K signaling protects dentate neurons from oxygen-glucose deprivation in organotypic slice cultures. *J Neurochem* **112**:377-388.

Sung, J. Y., Goo, JS, Lee, DE, Jin, DQ, Bizon, JL, Gallagher, M et al. (2008) Learning strategy selection in the water maze and hippocampal CREB phosphorylation differ in two inbred strains of mice. *Learn Mem* **15**:183-188.

Sydow, A. and Mandelkow, EM (2010) 'Prion-like' propagation of mouse and human tau aggregates in an inducible mouse model of tauopathy. *Neurodegener Dis* **7**:28-31.

Takuma, H., Arawaka, S, and Mori, H (2003) Isoforms changes of tau protein during development in various species. *Brain Res Dev Brain Res* **142**:121-127.

Tandon, A., Yu, H, Wang, L, Rogaeva, E, Sato, C, Chishti, MA et al. (2003) Brain levels of CDK5 activator p25 are not increased in Alzheimer's or other neurodegenerative diseases with neurofibrillary tangles. *J Neurochem* **86**:572-581.

Taubenfeld, S. M., Stevens, KA, Pollonini, G, Ruggiero, J, and Alberini, CM (2002) Profound molecular changes following hippocampal slice preparation:

loss of AMPA receptor subunits and uncoupled mRNA/protein expression. *J Neurochem* **81**:1348-1360.

Terry, R. D., Peck, A, DeTeresa, R, Schechter, R, and Horoupian, DS (1981) Some morphometric aspects of the brain in senile dementia of the Alzheimer type. *Ann Neurol* **10**:184-192.

Thomas, G. M. and Huganir, RL (2004) MAPK cascade signalling and synaptic plasticity. *Nat Rev Neurosci* **5**:173-183.

Townsend, M., Mehta, T, and Selkoe, DJ (2007) Soluble Abeta inhibits specific signal transduction cascades common to the insulin receptor pathway. *J Biol Chem* **282**:33305-33312.

Townsend, M., Shankar, GM, Mehta, T, Walsh, DM, and Selkoe, DJ (2006) Effects of secreted oligomers of amyloid beta-protein on hippocampal synaptic plasticity: a potent role for trimers. *J Physiol* **572**:477-492.

Trinchese, F., Liu, S, Battaglia, F, Walter, S, Mathews, PM, and Arancio, O (2004) Progressive age-related development of Alzheimer-like pathology in APP/PS1 mice. *Ann Neurol* **55**:801-814.

Tseng, H. C., Zhou, Y, Shen, Y, and Tsai, LH (2002) A survey of Cdk5 activator p35 and p25 levels in Alzheimer's disease brains. *FEBS Lett* **523**:58-62.

Tsubuki, S., Takaki, Y, and Saido, TC (2003) Dutch, Flemish, Italian, and Arctic mutations of APP and resistance of Abeta to physiologically relevant proteolytic degradation. *Lancet* **361**:1957-1958.

Urayama, A. and Banks, WA (2008) Starvation and triglycerides reverse the obesity-induced impairment of insulin transport at the blood-brain barrier. *Endocrinology* **149**:3592-3597.

Usdin, M. T., Shelbourne, PF, Myers, RM, and Madison, DV (1999) Impaired synaptic plasticity in mice carrying the Huntington's disease mutation. *Hum Mol Genet* **8**:839-846.

Vellas, B., Black, R, Thal, LJ, Fox, NC, Daniels, M, McLennan, G et al. (2009) Long-term follow-up of patients immunized with AN1792: reduced functional decline in antibody responders. *Curr Alzheimer Res* **6**:144-151.

Volianskis, A. and Jensen, MS (2003) Transient and sustained types of long-term potentiation in the CA1 area of the rat hippocampus. *J Physiol* **550**:459-492.

vonBergem, M., Barghorn, S, Li, L, Marx, A, Biernat, J, Mandelkow, EM et al. (2001) Mutations of tau protein in frontotemporal dementia promote aggregation of paired helical filaments by enhancing local beta-structure. *J Biol Chem* **276**:48165-48174.

Walker, E. S., Martinez, M, Brunkan, AL, and Goate, A (2005) Presenilin 2 familial Alzheimer's disease mutations result in partial loss of function and dramatic changes in Abeta 42/40 ratios. *J Neurochem* **92**:294-301.

- Walsh, D. M., Hartley, DM, Condron, MM, Selkoe, DJ, and Teplow, DB (2001) In vitro studies of amyloid beta-protein fibril assembly and toxicity provide clues to the aetiology of Flemish variant (Ala692-->Gly) Alzheimer's disease. *Biochem J* **355**:869-877.
- Walsh, D. M., Klyubin, I, Fadeeva, JV, Cullen, WK, Anwyl, R, Wolfe, MS et al. (2002) Naturally secreted oligomers of amyloid beta protein potently inhibit hippocampal long-term potentiation in vivo. *Nature* **416**:535-539.
- Wang, J. H. and Feng, DP (1992) Postsynaptic protein kinase C essential to induction and maintenance of long-term potentiation in the hippocampal CA1 region. *Proc Natl Acad Sci U S A* **89**:2576-2580.
- Wang, R., Dineley, KT, Sweatt, JD, and Zheng, H (2004) Presenilin 1 familial Alzheimer's disease mutation leads to defective associative learning and impaired adult neurogenesis. *Neuroscience* **126**:305-312.
- Wang, Z., Wang, B, Yang, L, Guo, Q, Aithmitti, N, Songyang, Z et al. (2009) Presynaptic and postsynaptic interaction of the amyloid precursor protein promotes peripheral and central synaptogenesis. *J Neurosci* **29**:10788-10801.
- Waters, J. (2010) The concentration of soluble extracellular amyloid-beta protein in acute brain slices from CRND8 mice. *PLoS ONE* **5**:e15709
- Watson, P. L., Weiner, JL, and Carlen, PL (1997) Effects of variations in hippocampal slice preparation protocol on the electrophysiological stability, epileptogenicity and graded hypoxia responses of CA1 neurons. *Brain Res* **775**:134-143.
- Wei, W., Nguyen, LN, Kessels, HW, Hagiwara, H, Sisodia, S, and Malinow, R (2010) Amyloid beta from axons and dendrites reduces local spine number and plasticity. *Nat Neurosci* **13**:190-196.
- Westerman, M. A., Cooper-Blacketer, D, Mariash, A, Kotilinek, L, Kawarabayashi, T, Younkin, LH et al. (2002) The relationship between Abeta and memory in the Tg2576 mouse model of Alzheimer's disease. *J Neurosci* **22**:1858-1867.
- Winton, M. J., Lee, EB, Sun, E, Wong, MM, Leight, S, Zhang, B et al. (2011) Intraneuronal APP, Not Free A{beta} Peptides in 3xTg-AD Mice: Implications for Tau versus A{beta}-Mediated Alzheimer Neurodegeneration. *J Neurosci* **31**:7691-7699.
- Wszolek, Z. K., Tsuboi, Y, Ghetti, B, Pickering-Brown, S, Baba, Y, and Cheshire, WP (2006) Frontotemporal dementia and parkinsonism linked to chromosome 17 (FTDP-17). *Orphanet J Rare Dis* **1**:30
- Wu, D. C., Yu, YP, Lee, NT, Yu, AC, Wang, JH, and Han, YF (2000) The expression of Cdk5, p35, p39, and Cdk5 kinase activity in developing, adult, and aged rat brains. *Neurochem Res* **25**:923-929.

Wu, L. G. and Saggau, P (1994) Presynaptic calcium is increased during normal synaptic transmission and paired-pulse facilitation, but not in long-term potentiation in area CA1 of hippocampus. *J Neurosci* **14**:645-654.

Yang, L., Wang, Z, Wang, B, Justice, NJ, and Zheng, H (2009) Amyloid precursor protein regulates Cav1.2 L-type calcium channel levels and function to influence GABAergic short-term plasticity. *J Neurosci* **29**:15660-15668.

Yao, M., Nguyen, TV, and Pike, CJ (2005a) Beta-amyloid-induced neuronal apoptosis involves c-Jun N-terminal kinase-dependent downregulation of Bcl-w. *J Neurosci* **25**:1149-1158.

Yao, P. J., Bushlin, I, and Furukawa, K (2005b) Preserved synaptic vesicle recycling in hippocampal neurons in a mouse Alzheimer's disease model. *Biochem Biophys Res Commun* **330**:34-38.

Yu, H., Saura, CA, Choi, SY, Sun, LD, Yang, X, Handler, M et al. (2001) APP processing and synaptic plasticity in presenilin-1 conditional knockout mice. *Neuron* **31**:713-726.

Zaman, S. H., Parent, A, Laskey, A, Lee, MK, Borchelt, DR, Sisodia, SS et al. (2000) Enhanced synaptic potentiation in transgenic mice expressing presenilin 1 familial Alzheimer's disease mutation is normalized with a benzodiazepine. *Neurobiol Dis* **7**:54-63.

Zhang, H., Sun, S, Herreman, A, De Strooper, B, and Bezprozvanny, I (2010a) Role of presenilins in neuronal calcium homeostasis. *J Neurosci* **30**:8566-8580.

Zhang, Y., Kurup, P, Xu, J, Carty, N, Fernandez, SM, Nygaard, HB et al. (2010b) Genetic reduction of striatal-enriched tyrosine phosphatase (STEP) reverses cognitive and cellular deficits in an Alzheimer's disease mouse model. *Proc Natl Acad Sci U S A* **107**:19014-19019.

Zheng, H., Jiang, M, Trumbauer, ME, Sirinathsinghji, DJ, Hopkins, R, Smith, DW et al. (1995) beta-Amyloid precursor protein-deficient mice show reactive gliosis and decreased locomotor activity. *Cell* **81**:525-531.